SOCIETATEA
DE CATALIZA
DIN ROMANIA

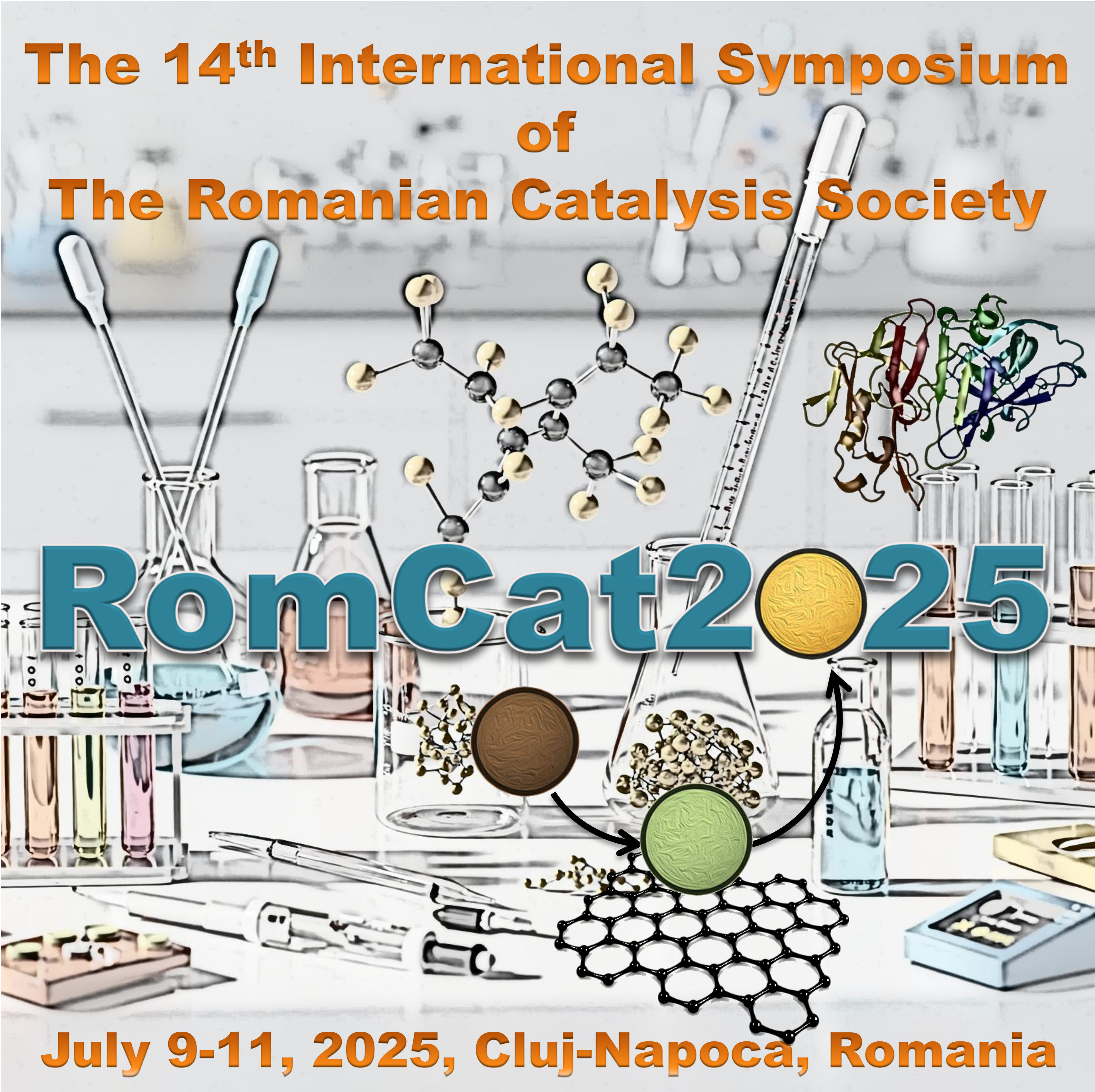

The 14th International Symposium of The Romanian Catalysis Society

RomCat2025

July 9-11, 2025, Cluj-Napoca, Romania

Summer School
"Catalysis at the crossroads between biology and chemistry"
06-08 July 2025

https://www.chimie.unibuc.ro/romcat/

14th International Symposium of The Romanian Catalysis Society RomCat 2025

Book of Abstracts

July 09-11, 2025, Cluj-Napoca, Romania

ORGANIZING COMMITTEE

CHAIR

Prof. Dr. Vasile PÂRVULESCU Corresponding member of Romanian Academy	University of Bucharest (RO)

President of the Romanian Catalysis Society

ORGANIZING COMMITTEE

Prof. Dr. Csaba PAIZS	Babes Bolyai Unversity, Cluj-Napoca (RO)
Dr. Diana LAZĂR	National Institute for R&D of Isotopic and Molecular Technologies, Cluj-Napoca (RO)
Prof. Dr. Eng. Francisc PÉTER	Politehnica University Timişoara, Timişoara (RO)
Dr. Cristian M. TEODORESCU	National Institute of Materials Physics, Bucharest (RO)
Dr. Violeta NICULESCU	National Research and Development Institute for Cryogenic and Isotopic Technologies, Rm. Vâlcea (RO)
Prof. Dr. Simona M. COMAN	University of Bucharest, Bucharest (RO)
Dr. Maria CAZACU Corresponding member of Romanian Academy	“Petru Poni” Institute of Macromolecular Chemistry, Iaşi (RO)
Dr. Viorica PÂRVULESCU	“Ilie Murgulescu” Institute of Physical Chemistry, Bucharest (RO)

SECRETARIAT

Mădălina TUDORACHE
Bogdan COJOCARU
Octavian D. PAVEL
Natalia CANDU
Iunia PODOLEAN
Judith - Hajnal BARTHA-VARI
Contact: romcat@chimie.unibuc.ro

SPONSORS

NANOTEAM

Str. Capitan Grigore Ignat, nr. 26
Cluj-Napoca, 400401, Jud. Cluj,
România
Tel: +40.721.221.781
Fax: +40.364.101.506
email:
mircea_armenean@nanoteam.ro

muso

Bd. Lacul Tei nr. 1-3, Cladirea ISPE,
etj. 2, cam. 209-210, Bucuresti,
020371, Romania
Tel: +40.374.059.393
Fax: +40.213.151.144
email: office@muso.ro

HISTERESIS
TECHNOLOGY FOR THE FUTURE
SPECSGROUP

EVO Business Center Et.1-06, Sos. Pacurari Nr.127, Iaşi, 700545, Jud. Iaşi, Romania
Tel: +40.761.103.687
email: office@histeresis.ro

PureWATER

Pure Water, Str. Constantin Brancuşi,
Nr. 135, Cluj-Napoca, 400458, Jud.
Cluj, Romania
Tel: +40.723.960.102
email: office@pure-water.ro

RomCat2025

PROGRAMME

09.07.2025		10.07.2025		11.07.2025	
8:00	**Registration**				
8:30	**Opening Ceremony**				
9:00	**PL1 R. Craciun**	9:00	**PL3 P. Granger**	9:00	**PL4 A. Primo**
9:40	**K1 C. Teodorescu**	9:40	**K4 C. Boeriu**	9:40	**K8 M. Anghel**
10:10	**O1 E. Talas**	10:10	**O9 F. Peter**	10:10	**O15 A. Silvestru**
10:30	**O2 I. Borbath**	10:30	**O10 N. Deak**	10:30	**O16 M. Bordeiasu**
10:50	**Coffee Break**	10:50	**Coffee Break**	10:50	**Coffee Break**
11:20	**K2 M. Cazacu**	11:20	**K5 S.M. Coman**	11:20	**PL5 H. Garcia**
11:50	**O3 O.D. Pavel**	11:50	**O11 M. Coros**	12:00	**O17 V. Niculescu**
12:10	**O4 M. El Fergani**	12:10	**O12 C. Socaci**	12:20	**O18 V. Diculescu**
12:30	**Lunch Break**	12:30	**Lunch Break**	12:40	**Conclusions & Remarks**
14:00	**PL2 T. Salmi**	14:00	**K6 A. Tompos**	13:00	**Lunch Break**
14:40	**K3 L. Poppe**	14:30	**K7 M. Mihet**	14:00	**SCR Meeting**
15:10	**O5 G. Tasnádi**	15:00	**O13 J. Brem**	15:00	**Goodbye**
15:30	**O6 B. Cojocaru**	15:20	**O14 R. Fontana**		
15:50	**Coffee Break**	15:40	**I2. G. Birda**		
16:20	**O7 O. Petcuta**	**16:00**	**Social events**		
16:40	**O8 L.C. Bencze**				
17:00	**I1. V. Cânpean**				
17:20	**Poster Session +** **Coffee Break**				

PL – Plenary; K – Key note; O – Oral presentation; I - Industry

Summary

PLENARIES

KEY NOTE

ORAL COMMUNICATIONS

POSTER COMMUNICATIONS

INDUSTRY

Plenaries

Novelty and Challenges in Catalysis for Bio-renewables BASF Corp. – Toward a CO_2 Neutral Chemical Industry

Radu Crăciun*
Technology Manager Americas/BASF Corp. Iselin, NJ- USA
Honorary Consul of Romania in NJ-USA
**Corresponding author: rcraciun.honoraryconsul@gmail.com*

Introduction

The “***verbund***” concept, where a side product from the main process becomes the feed for another process, minimizing overall waste generation and optimizing overall process, has been applied with success at BASF for more than 150 years and helped shape the success for a global company. As a responsible chemical company, BASF goal is to become CO_2-neutral by 2050. This challenging goal brought significant strategic decisions toward more sustainable resources. Bio-renewable raw materials and their industries are key components in this strategy. This new direction, has led to the development of many new, novel technologies inside BASF groups, including catalysts. The complexity of an industrial process, the challenges under current geo-political landscape in terms of raw material availability, the importance of reducing CO_2 footprint in chemical industry in general, require flexibility in terms of process design implying fast and efficiently developing new, novel, robust and unique catalysts.

As it is defined, bio-renewables are raw materials which can provide a sustainable growth for chemical industry reaching CO_2 neutrality. The concept of “bio-based platform chemicals” such as bio-ethanol, furfuryl aldehyde, lactic acid, just to mention some, have become key raw materials for new technologies and sustainable chemical technologies. The GreenMap below shows chemical routes for industrial bio-ethanol conversion as platform chemical” to generate value added, novel chemicals/polymers.

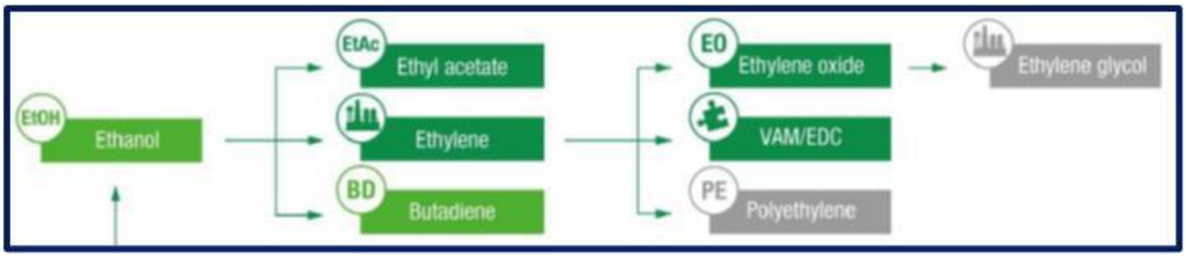

BASF’s new, novel GREEn precious metals catalyst technology platform based on the “***edge-coated***” preparation technique to produced industrial precious metal/PM catalysts, the innovative alumina shape-extrudate technologies employed in converting efficiently bio-alcohols into added value polymers or intermediates via dehydration and the unique Cu-based Cr-free catalysts capable of converting efficiently bioethanol in other valuable chemicals such as ethyl-acetate, will be presented and briefly discussed.

Materials and Methods

The supported precious metal catalysts presented in this work were prepared with BASF’s proprietary technology. The catalysts analyzed and characterized with various techniques, e.g., XPS, HAADF-STEM, FIB-SEM, μ-XRF-CT, etc. The catalysts were evaluated in various chemical reactions such as selective hydrogenation, condensation and efficient bio-alcohols dehydration to alkene industrial scale process.

Results and Discussion

The new GREEn catalysts show improved performance, specifically conversion and selectivity to the desired product in various catalytic reactions. Examples presented, include a case study on the impacts of particle morphology on catalytic performance as well as a demonstration of the impact of precious metal distribution and accessibility in catalyst activity and selectivity. For example, a new group of edge-coated Pt catalysts will be presented. The STEM micrographs of these catalysts shown in Fig. 1, indicate the key difference between how the Pt particulates are being distributed on the porous, high surface area carbon support. While for the "edge-coated" catalyst the Pt particulates are located mainly on the outer shell of a carbon particle support, on the catalyst produced via the regular "well-disperse" method, the particulates are dispersed also inside even the smallest pores of the carbon support.

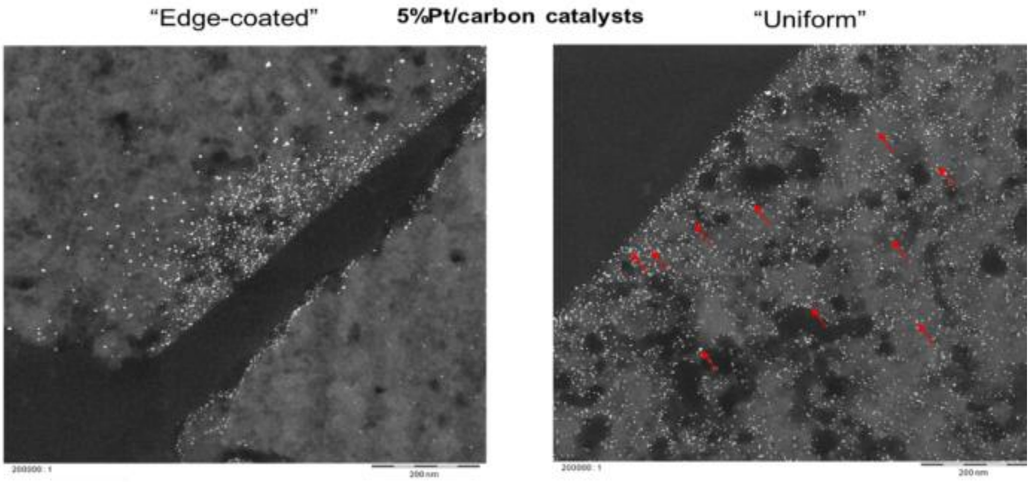

Fig. 1. HAADF-STEM dot map micrograph for Pt/carbon powder catalyst; *i)* left, an edge-coated *vs.* *ii)* conventional, uniform (right) Pt/carbon powder catalyst.

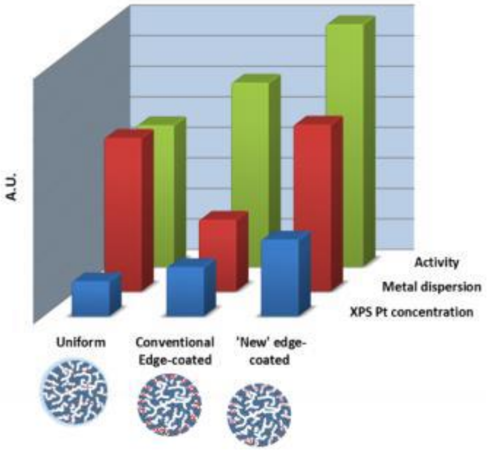

In certain applications, the "edge-coating" technology, will provide a key benefit to the overall process. The figure on the right nicely indicates the effect on the overall performance defined as activity of the catalyst. Other examples will also be highlighted including low-metal containing catalysts and leaching resistant catalysts.

Conclusions

The new GREEn technology-based catalysts, provide advantages over conventional catalysts like for example higher activity and hence improved metal efficiency, higher selectivity for reactions involving bulky substrate molecules, and higher metal leaching resistance. Details about alumina and Cu-catalyst applications will be reviewed in detailed and presented as well.

Low-Temperature Conversion of Biomass to Useful Molecules – Liaison of Catalysis and Reaction Engineering

Tapio Salmi*
Åbo Akademi, Industrial chemistry and reaction engineering, FI-20500 Turku-Åbo Finland
Università di Napoli 'Federico II', Chimica Industriale, IT-80125 Napoli Italy
**Corresponding author: tapio.salmi@abo.fi*

The great and demanding shift from fossil resources to renewable raw materials and sustainable products has been a massive vitamin injection for chemistry and chemical engineering. New catalysts have been discovered, characterized and tested. The trinity for a good heterogeneous catalyst is activity, selectivity and durability. Besides the conventional structures of heterogeneous catalysts, new structures have been developed, such as monoliths, fibres, microreactors, solid foams and 3D printed elements.

The goal is to combine the benefits of traditional powder catalysts and catalyst pellets, i.e., to minimize the diffusion resistance in the catalyst pores by applying very thin catalyst layers but preserving the open structure in order to minimize the pressure drop. Application of new structures is particularly attractive for new chemical applications appearing in the valorization of biomass components to valuable chemicals, food ingredients, pharmaceuticals and fuel components.

Qualitative approach is, however, not sufficient, since the ultimate goal is to gain deep knowledge of the reaction mechanisms and to progress from laboratory to industrial scale. In situ spectroscopic methods and experiments under transient conditions give a strong impact on the understanding of the behavior of complex molecules appearing in biomass. Chemical reaction engineering plays a key role in reaching the ambitious goal. Understanding and modelling the interplay of thermodynamics, kinetics, transport phenomena and fluid dynamics is the way to breakthrough.

The modern trend is to shift from batch and semibatch processes to safe and efficient continuous operation. The systematic approach is illustrated in the lecture with several real-life examples, such as hydrolysis of biopolymers, hydrogenation and oxidation of mono- and oligosaccharides, epoxidation and carbonation of alkenes and carboxylic acids. Examples of the approach are shown in Fig. 1.

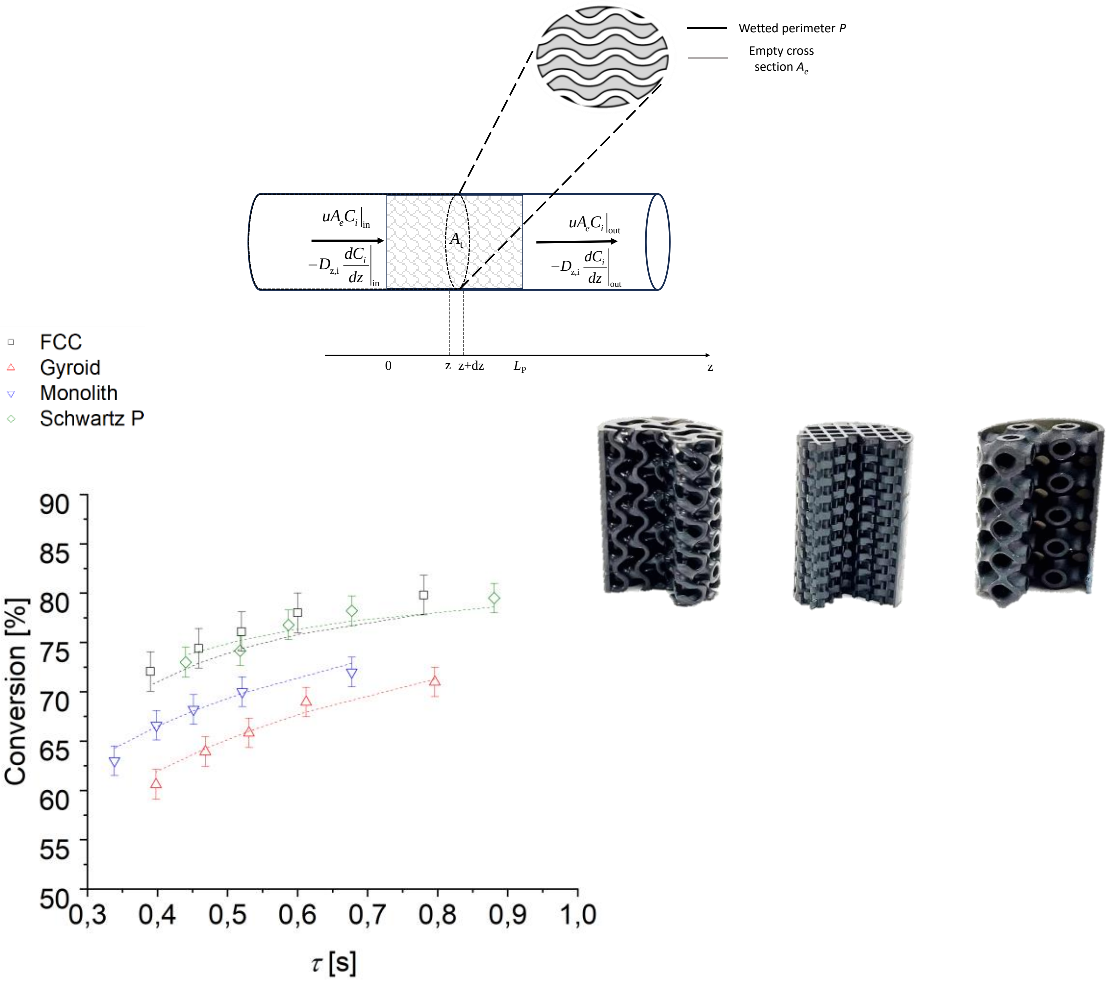

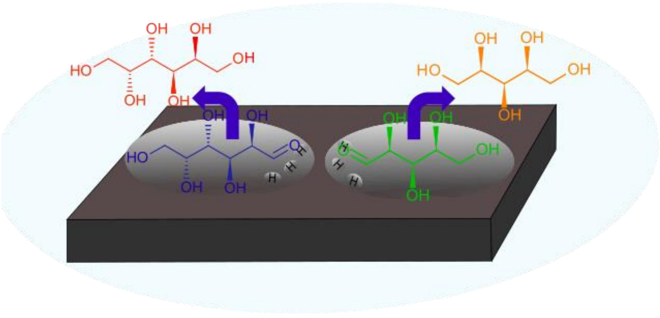

$$r_X = \frac{\kappa_X \cdot \boldsymbol{\alpha} \cdot (1 + (1 - \boldsymbol{\alpha}) \cdot K_X \cdot C_X)^2 \cdot C_X \cdot P_{H_2}}{\left(1 + \sqrt{K_{H_2} \cdot P_{H_2}} + K_X \cdot C_X + (1 - \boldsymbol{\alpha}) \cdot \sqrt{K_{H_2} \cdot P_{H_2}} \cdot K_X \cdot C_X\right)^3}$$

Fig. 1. Continuous operation and modelling of 3D-printed reactor structures in the synthesis of diethyl ether from ethanol (upper); semi-competitive adsorption model in the hydrogenation of sugars to sugar alcohols on solid foams (lower).

References

[1] G. Araujo-Barahona, A. Goicoechea-Torres, K. Eränen, R.-M. Latonen, T. Tirri, A. Smeds, D. Murzin, J. García-Serna, T. Salmi, Chem. Eng. Sci. 281 (2023) 119130.
[2] L. Mastroianni, A. De Jesus Medina Ferrer, A.M. De Domenico, K. Eränen, M. Di Serio, D. Murzin, V. Russo, T. Salmi, Chem. Eng. J. 501 (2024) 157691.

Insights Into the Development of Post-Combustion-Catalysts: How to Manage the Construction of PGM-Support Interface and Related Synergistic Effects

Yuanshuang Zheng, Pascal Granger*
Univ. Lille, CNRS, Centrale Lille, Univ. Artois, UMR 8181 - UCCS - Unité de Catalyse et Chimie du Solide, F-59000 Lille, France
**Corresponding author: pascal.granger@univ-lille.fr*

Nowadays, end-of-pipe catalytic technologies are widespread worldwide. However important challenges are coming across associated to the transition from liquid powered engines to gas powered engines which should lead to further technical adaptations to improve the efficiency of the existing catalytic end-of-pipe technologies [1,2].

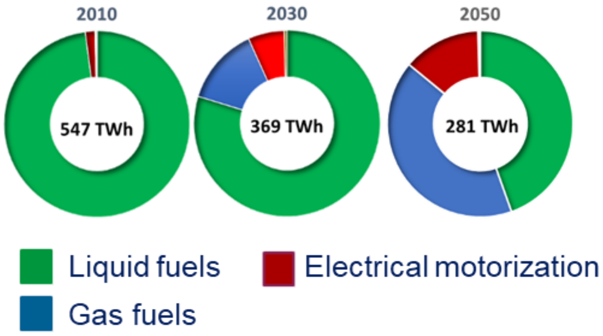

Fig. 1. Scenarios concerning the transition from liquid to gas fuelled engines in France [2].

In the frame of this transition, natural gas and hydrogen can be considered much more attractive than diesel and gasoline fueled-engines in terms of reduction of atmospheric pollutant emissions. Presently catalytic after-treatment technologies are intimately related to an extensive use of platinum group metal (PGM) as well as rare earths which have been classified by the European community as strategically important materials for which a reduction in the use is strongly advised. On this basis, new conceptual ideas should emerge that guide innovation in the development of new generations of post-combustion catalysts.

Possible alternatives integrating reduction in the use of PGM should obey to specific prerequisites such as: *i)* the promotion of the dispersion of PGM avoiding strong ignition effects and structural instabilities; *ii)* the magnification of their intrinsic catalytic properties thanks to support effects.

The use of perovskite type structure is a suitable option to promote the catalytic activity of PGMs especially to improve their thermal stability [3-5]. This lecture will address the importance of the methodology developed to integrate PGMs according to a classic sequential ($Pd/LaMnO_3$) or one-pot method ($LaMn_{0.98}Pd_{0.02}O_3$). Pd-doped $LaMnO_3$ catalysts have been study with palladium stabilized in the perovskite lattice occupying preferential interstitial sites or simply deposited by wet inpregnation onto the perovskite support. As illustrated in Fig. 2 the behaviour to thermal ageing differ from the selected protocol as the Pd-$LaMnO_3$ will grow during ageing on $LaMn_{0.98}Pd_{0.02}O_3$. However, the sintering of Pd particles is rather limited for the impregnated sample and the deterioration of the Pd-$LaMnO_3$

interface was preferentially attributed to segregation processes on the support, rather than to the sintering of palladium particles, leading to an enrichment of the surface in lathane which alters its oxygen storage capacity. The consequence on the kinetics of the methane oxidation has been studied with repect to these structural changes. The differences observed on the kinetic behabiour notably after thermal aging will be discussed based on the coexistence of two different reaction mechanisms involving solely Pd particles or alternately the Pd-$LaMnO_3$ interface, their contribution varying according to the extent of surface changes during thermal aging.

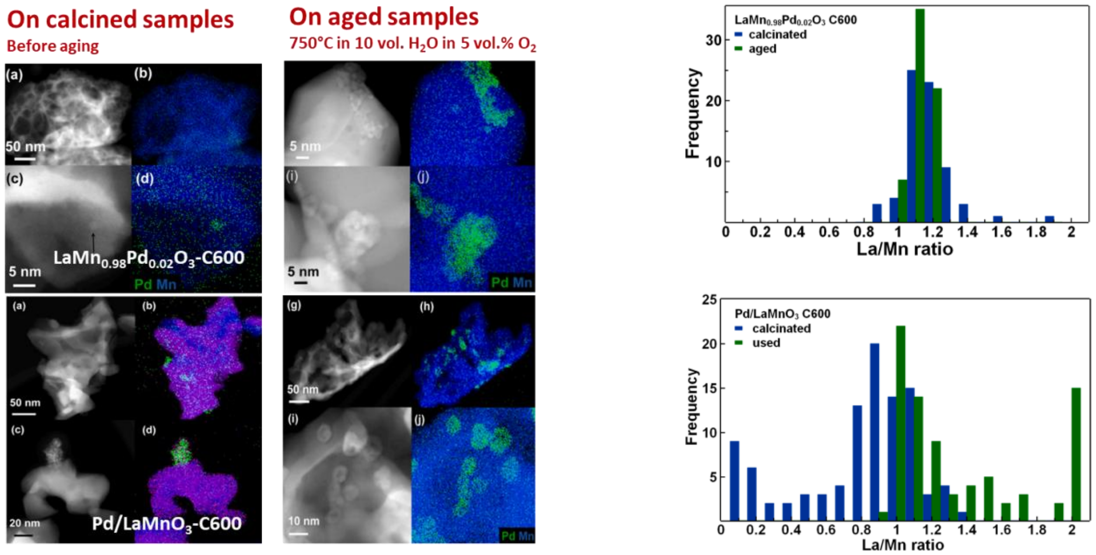

Fig. 2. Impact of the method for palladium incorporation to $LaMnO_3$ on the extent of structural changes under severe operating conditions.

References

[1] Y. Zheng, A. Decoster, V. Parvulescu, P. Granger, Catal. Sci. Technol. 14 (2024) 4106.
[2] http://www.grdf.fr/dossiers/gnv-biognv/vehicules-gnv-france-europe
[3] Y. Zheng, A. Decoster, F. Dhainaut, S. Heyte, M. Marinova, P. Granger, J. Catal. 430 (2024) 115353.
[4] Y. Zheng, M. Marinova, P. Granger, Chem. Eng. J. 475 (2023) 143389.
[5] Y. Renème, A. Lahougue, C. Hamon, F. Dhainaut, Top. Catal. 63 (2020) 1474.

MXenes as Photocatalysts for Solar Fuel Production

Ana Primo*
Instituto de Tecnología Química (UPV-CSIC), Av. dels Tarongers s/n, 46022 València, España
**Corresponding author: aprimoar@itq.upv.es*

Recent advances in two-dimensional transition-metal carbides (MXenes) reveal that shrinking these materials down to quantum-dot dimensions unlocks a genuine semiconductor-like behaviour that can be harnessed for solar-fuel production. In this lecture I will present a coherent story built on our latest publications, highlighting both the how and the why of MXene quantum-dot (MxQD) photocatalysis.

First, I will describe an environmentally benign, HF-free protocol that converts MAX phases directly into highly crystalline Ti_3C_2, Ti_2C, Nb_2C and V_2C dots (≈ 5 nm laterally; 1-4 nm thick) via liquid-phase laser ablation. The one-step process achieves >20 wt.% yield, furnishes oxygen-terminated surfaces, and induces a controllable band-gap opening (≈ 1.9–2.2 eV) responsible for strong photoluminescence and visible-light absorption. Under simulated sunlight these MxQDs evolve H_2 from water with rates up to 2.02 mmol g^{-1} h^{-1} matching noble metal benchmarks while remaining noble metal free.

Building on this platform, we have now demonstrated that the same family of dots catalyses CO_2 hydrogenation to CH_4 (selectivity >80 %) at 200–300 °C under UV-vis irradiation. Ti_3C_2 and Nb_2C dots lead the series, delivering up to 891 µmol CH_4 g^{-1} h^{-1} at 300 °C, with isotopic labelling and electron/hole scavenger studies confirming a genuine photocatalytic pathway. Metal and metal-oxide photodeposition experiments further evidence efficient charge separation at the dot surface, while temperature-controlled runs prove that light lowers the energetic threshold compared with purely thermal routes.

Taken together, these results establish laser-engineered MXene dots as a versatile, tunable and scalable photocatalyst class capable of driving both H_2 evolution and CO_2 valorisation. The lecture will discuss structure–property correlations, stability challenges and opportunities to engineer solid-solution MXenes toward next-generation solar-fuel devices.

References

[1] R. Ramirez et al., Small Methods (2023) 2300063.
[2] R. Ramirez et al., Appl. Catal. B: Environ. 34 (2024) 123316.

MXenes as New Solid Catalysts for Organic Reactions

Hermenegildo García[1]*, Vasile I. Parvulescu[2], Ana Primo[1]
[1]Instituto de Tecnología Química, Consejo Superior de Investigaciones Científicas-Universitat Politécnica de Valencia, Av. De los Naranjos s/n, 46022 Valencia, Spain.
[2]Department of Organic Chemistry, Biochemistry and Catalysis, Faculty of Chemistry, University of Bucharest, Bdul Regina Elisabeta 4-12, Bucharest 030016, Romania
**Corresponding author: hgarcia@itq.upv.es*

Introduction

MXenes are a novel class of two-dimensional (2D) nanomaterials characterized by alternating layers of single atom-thick early transition metals and single atom-thick carbide or nitride layers [1]. The outermost layers are always composed of the transition metal, giving MXenes their general chemical formula, $M_{n+1}X_n$, where ***M*** represents an early transition metal, and ***X*** corresponds to carbon, nitrogen, or a combination of both. These structures typically consist of 3, 5, 7, or 9 layers.

MXenes are commonly synthesized through selective etching of the corresponding **MAX phase**, which has the formula ***M-A-X***, where ***M*** is the early transition metal, ***A*** is a main group metal, and ***X*** is carbon or nitrogen. MAX phases can be produced in bulk via metallurgical synthesis from the corresponding metallic elements and graphite at temperatures around 1500 °C. Subseqeuntly, a etching process removes the ***A*** layers, leaving behind the 2D MXene structure. During this process, terminal groups are introduced onto the surface of the external transition metal layers [2]. Typical etching methods use NH_4F/HCl mixtures in water, introducing functional groups such as -F, -Cl, -O, and -OH onto the MXene surface. The type and proportion of these groups can be determined through XPS or EDX mapping in electron microscopy. MXenes were first discovered in 2011 by Gogotsi, Barsoum, and Naguib [3]. Over the past decade, they have gained attention for their applications, particularly as ***electrocatalysts***, becoming one of the most active materials in this field [4].

The research concept to be presented presents the potential of MXenes as highly efficient and stable thermal catalysts for organic reactions. The active sites in MXenes include M–O and M–OH groups, which are analogous to those found on the surfaces of transition metal oxides. Additionally, MXenes feature unique surface terminations resembling those in molecular complexes, further broadening their catalytic versatility. Additionally, MXenes can also be supports of metal overlays and single metal atoms. Based on this concept of the presentation will show some of the results obtained by the group on the use of MXenes as thermal catalysts.

Experimental

The MXenes used as catalysts are primarily synthesized through HF etching of commercially available $M_{n+1}AlX_n$ precursors. Their crystallinity is analyzed using XRD and selected area electron diffraction. The particle morphology is examined via FESEM while HR-TEM reveals the multilayered structure characteristic of these 2D materials, Fig. 1. The nanometric thickness of the individual

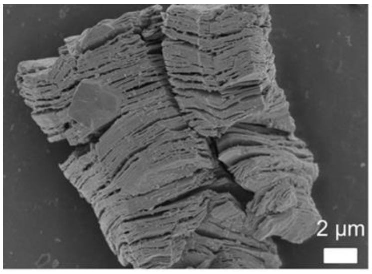

Fig. 1. Accordion-form of Nb_2C MXene.

layers is measured using AFM. Catalytic reactions are conducted in either the gas or liquid phase, and the resulting products are characterized through GC, GC-MS, and NMR spectroscopy. Products were isolated by chromatography.

Results and Discussion

The presentation will highlight the new results of MXenes as materials with intrinsic catalytic activity for a wide range of organic reactions. These include aerobic oxidations, oxidative dehydrogenation of hydrocarbons and other functional groups, hydrogenation of unsaturated C-X multiple bonds, aldol condensations, hydroamination of C ≡ C triple bonds, guanylation of amines, among others. The study focuses on a series of MXenes, including Ti_3C_2, Nb_2C, and V_2C, synthesized from commercial MAX phase precursors. The catalytic activity of single atom site on MXene will also be presented.

Characterization of Brønsted and Lewis acid/base sites using NH_3-TPD, CO_2-TPD, and pyridine adsorption/desorption monitored by IR spectroscopy reveals a low density of active sites 10-30 mmol·g^{-1}. These sites are likely associated with structural defects, atomic vacancies, and surface terminations produced in the harsh etching process. Despite their low abundance, these defects are primarily responsible for the observed catalytic activity. Additionally, the morphology of the MXene samples - whether multilayered accordion-like, expanded layered, or exfoliated - significantly influences catalytic performance. Post-synthesis surface functionalization further modifies catalytic activity, with certain modifications positioning MXenes among the most active solid catalysts in terms of TOF.

DFT calculations on models give insights on the possible reaction mechanisms and the active sites that apparently correspond to two or more neighbor metal atoms cooperating to the reaction, Fig. 2.

Beyond their intrinsic catalytic properties, MXenes are particularly effective as supports for single-atom catalysis. Single atoms can be incorporated into MXenes directly during their synthesis via the molten salt method. These single atoms occupy vacant sites in the metal layer, enabling catalytic activity in specific reactions, such as hydrogenations. This dual functionality - intrinsic activity and support for single-atom catalysis - illustrates the versatility and potential of MXenes in advanced catalytic applications.

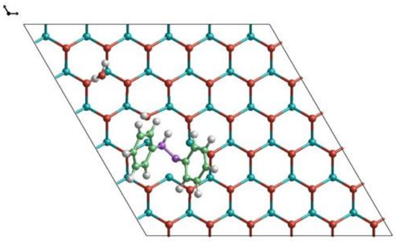

Fig. 2. Model showing the transition state of aniline coupling on two neighbour Nb atoms on a defective site of Nb_2C Mxene.

Conclusions

The catalytic activity of metal oxides, carbides, and related compounds is well established. In this context, MXenes offer distinct advantages as catalysts due to their unique 2D morphology, which provides highly accessible active sites and improved atom utilization. The tunable chemical composition of MXenes opens up an expansive chemical space, with over 70 materials reported to date. Moreover, their catalytic activity can be further optimized through precise control of surface termination groups, enhancing their performance. These features make MXenes highly promising catalysts for a wide range of organic reactions, combining structural efficiency with chemical versatility.

References

[1] K.R.G. Lim, M. Shekhirev, B.C. Wyatt, B. Anasori, Y. Gogotsi, Z.W. Seh, Nat. Synth. 1 (2022) 601.
[2] M. Tang, J. Li, Y. Wang, W. Han, S. Xu, M. Lu, W. Zhang, H. Li, Symmetry 14 (2022) 2232.
[3] M. Naguib, V.N. Mochalin, M.W. Barsoum, Y. Gogotsi, Adv. Mater. 26 (2014) 992.
[4] Y. Wang, Y. Nian, et al., Adv. Energy Mater. 11 (2021) 2002967.

Key notes

Interplay Between Ferroelectricity and Molecular Adsorptions on (*001*) Barium Titanate: Perspectives for Carbon Capture, Utilization and Storage

Alexandru-Cristi Iancu[1,2], Nicoleta G. Apostol[1], Adela Nicolaev[1], Laura E. Abramiuc[1], Cristina F. Chirilă[1], Dana G. Popescu[1], George A. Lungu[1], Cristian A. Tache[1], Cristian M. Teodorescu[1]*
[1]*National Institute of Materials Physics, Atomiștilor 405A, 077125 Măgurele, Romania*
[2]*Faculty of Physics, University of Bucharest, Atomiștilor 405, 077125 Măgurele, Romania*
**Corresponding author:* *teodorescu@infim.ro*

Although in the last years there was increasing evidence of the remarking catalytic properties of ferroelectric materials, the fundamental processes involved are still under debate. Since an essential step of these processes consists in molecular adsorption, the studies presented in this contribution concentrate on the influence of the ferroelectric state of the adsorption processes. A pre-requisite for such studies is the cleanness of the sample surface, together with its good crystallinity, in order to work on a system as close as possible on the ones supposed by theoretical modelling. This was achieved for the first time almost one decade ago, on lead zirconate titanate (PZT) thin films, where a cleaning procedure involving extended annealing in oxygen allowed one to synthesize surfaces with no carbon contamination as investigated by synchrotron radiation X-ray photoelectron spectroscopy (SRXPS) in an enhanced surface sensitivity regime and crystallinity revealed by low energy electron diffraction (LEED) [1]. This film was in a well-defined polarization state oriented inwards and it was found that carbon monoxide is adsorbed and partly dissociated on this surface. Carbon is then desorbed in form of carbon dioxide when the substrate is heated above the Curie temperature. Therefore, these experiments indicate the clear interplay between the polarization state and adsorption/desorption processes. Since carbon monoxide has a very low dipole moment (about 0.1 Debye), a mechanism involving the polarizability of the molecule by the field generated by the ferroelectric surface was established, yielding a binding energy proportional to the square of the substrate polarization [2]. The drawback of these processes is that when one tries to get rid of the adsorbate by heating the substrate above the Curie temperature, carbon uptakes oxygen from the substrate. Therefore, the surface is depleted in oxygen and is not stable upon several cycles of adsorption/desorption. On the contrary, for a substrate with lower polarization, such as barium titanate (BTO) with about one quarter of the polarization of PZT, the interaction energy is lower than the dissociation energy and therefore molecules are adsorbed without dissociation. Upon heating the substrate, molecules are adsorbed without affecting the substrate. All these processes are schematized for both carbon monoxide and carbon dioxide in Fig. 1. It is shown in which cases the molecules are adsorbed and dissociated (as observed on PZT [1]) or not (as observed on BTO [2-4]), how for dissociated molecules some atoms/ions are ejected or attracted to the surface, and how molecules adsorbed in non-dissociated states form additional bonds with atoms from the first layer of the ferroelectric surface. It follows that exploring the use of barium titanate is highly desirable, since this material is abundant, non toxic, relatively cheap, and can provide the ability of reversible molecular adsorption/desorption of carbon-containing molecules from the ambient atmosphere.

A first study involved a similar experiment with carbon monoxide on a 12.5 nm thick BTO film with outwards polarization and BaO termination [2]. The clean substrate was characterized by LEED and SRXPS, then adsorption and desorption processes were followed-up by ultrafast SRXPS. The complete XPS characterization allowed one to propose adsorption mechanisms and sites, while the carbon monoxide was completely desorbed upon heating above the Curie temperature, with full recovery of the barium titanate substrate. The next step was to investigate by the same methods a molecule without permanent dipole moment in the gas phase, ethylene [3]. The results were consistent with the findings for carbon monoxide, i.e., a clear influence of the ferroelectric state on molecular adsorption. Moreover, the molecule is oxidized in its last adsorption steps and, upon heating at moderate temperatures (since the Curie temperature of the BTO(*001*) thin film is about 420 K), the oxidation process is reversed and ethylene is desorbed in its reduced state, while the substrate is recovered.

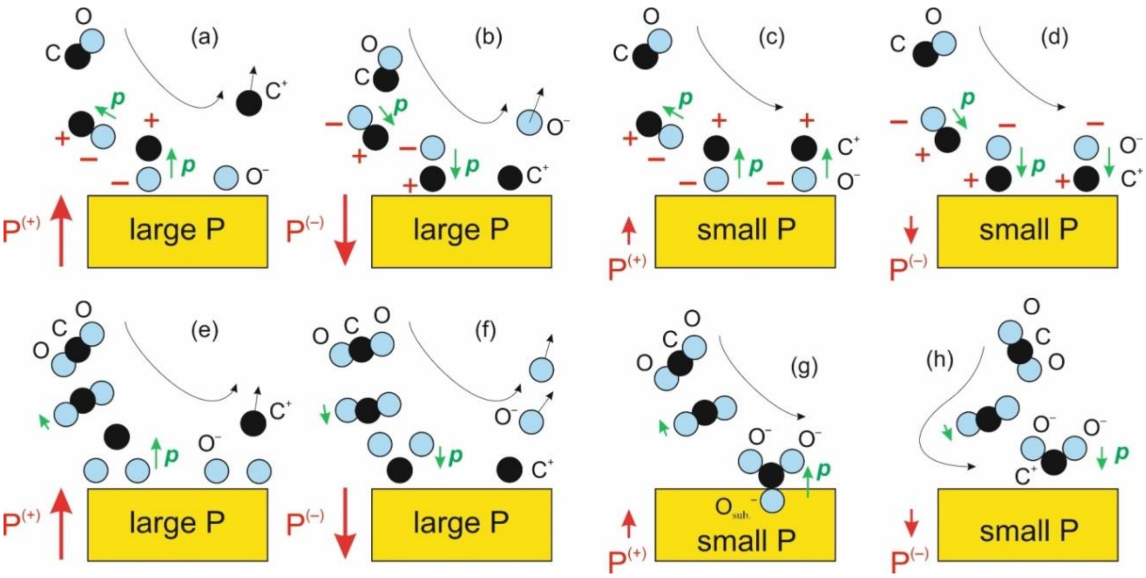

Fig. 1. Interplay between the substrate polarization and molecular adsorption processes for carbon monoxide (a–d) and carbon dioxide (e–h). For large polarization oriented outwards (a, e) the molecule is dissociated and carbon is ejected from the surface. If the large polarization is oriented inwards (b, e), then carbon is attracted to the surface and oxygen is released. In the case of low polarization, such that the stored elastic energy in the polarized molecule is lower than the dissociation energy (c, d, g, h) the molecules are adsorbed non-dissociatively and eventually form additional bonds on the surface.

The last and most important study from this contribution is the adsorption of carbon dioxide by the polarized BTO(*001*) substrate with Ba termination. Adsorption geometries are again determined, together with a clear interplay of the substrate polarization on the adsorption processes. The unexpected and encouraging result was that the amount of adsorbed carbon approaches one monolayer (one carbon atom for a surface BaO unit cell) at room temperature. This promotes barium titanate as a valid candidate for decarbonization. In Ref. [4] where this work was presented, an estimate of carbon dioxide adsorption ability based on this experiment yielded a capacity of about 8 mg per g of material for 20 nm sized barium titanate powder, by supposing that the ferroelectric properties are similar to the bulk. A scale-up of this finding yields a necessary of about 1.2 million tons BTO with an initial price of 2-3 billion USD to remove 10 billion tons carbon dioxide per year, by using a total power of about 40 GW (30 billion USD per year). Complete decarbonization could then be achieved in about 20 years.

References

[1] L.C. Tănase, N.G. Apostol, L.E. Abramiuc, C.A. Tache, L. Hrib, L. Trupină, L. Pintilie, C.M. Teodorescu, Sci. Rep. 6 (216) 35301.

[2] A.-C. Iancu, N.G. Apostol, A. Nicolaev, L.E. Abramiuc, C.F. Chirilă, D.G. Popescu, C.M. Teodorescu, Mater. Adv. 5 (2024) 5709.
[3] A.-C. Iancu, A. Nicolaev, N.G. Apostol, L.E. Abramiuc, C.M. Teodorescu, Heliyon 10 (2024) e35072.
[4] A.-C. Iancu, G.A. Lungu, C.A. Tache, C.M. Teodorescu, Mater. Adv. 5 (2024) 8798.

Silicones – from Conventional Materials to Solutions for Today's Challenges

Maria Cazacu*
Department of Inorganic Chemistry, "Petru Poni" Institute of Macromolecular Chemistry, Iasi, Aleea Gr. Ghica Voda 41A, 700487, Romania
**Corresponding author: mcazacu@icmpp.ro*

Organosilicones, with their unique hybrid nature combining organic and inorganic components, represent a class of materials that is constantly evolving and diversifying to meet the ever-changing demands of a wide range of fields. From the synthesis of polysiloxanes, the most representative compounds of the class, which contain chained siloxane units, –[Si–O]–, with organic groups (generally methyl) attached to silicon atoms, and the production of specialized elastomers, to emerging applications in soft robotics, energy generation, sensing, and self-healing materials, silicon-based compounds have been constantly expanding their functional boundaries.

Results obtained in the development of advanced and adaptable silicone-based compounds and materials, from the perspective of fundamental chemistry, materials engineering and high-tech applications, will be reviewed here. Recent advances in the preparation and functionalization of silicone elastomers will be highlighted, including the development of materials with the ability to respond to various external stimuli (electrical, mechanical, thermal, optical) and self-healing capacity, manufacturing by additive technologies, as well as efforts aimed at recycling and sustainability in this field, Fig. 1 [1,2]. In the case of silicones, this means a paradigm shift, moving from classic silicones for passive applications to active, "smart" ones and from thermosets to thermoplastics. Approaches to this, generally involve the chemical insertion of polar organic moieties into the diorganosiloxane backbone, adjustment of the crosslinking pattern and density, or the physical incorporation of various fillers into the silicone matrix to impart new functionalities.

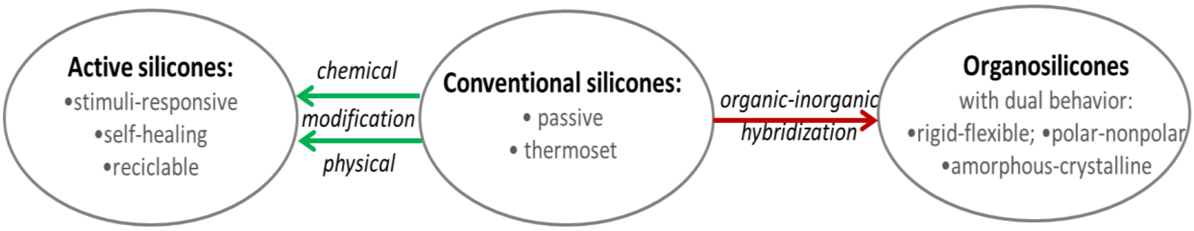

Fig. 1. Two main directions in diversifying silicon-based products and properties.

There is also a growing interest in the introduction of short silane or siloxane structural motifs into organic or organic-inorganic structures, which significantly modify their properties and even induce new behaviors. Examples would include surfactants or pharmaceuticals containing silicon as an isosteric carbon substitute, and a developing direction involving organosilicone proligands, in which passive siloxane/silane moieties are functionalized with chelating groups able to form metal complexes of various dimensionalities (from 0D to 3D). Such compounds can exhibit dual behavior (rigid-flexible, crystalline-amorphous, polar-nonpolar) as well as phase separation phenomena, and exhibit a wide range of electrical, magnetic, thermal, and biological properties, Fig. 1. These properties make them of interest in fields ranging from medicinal chemistry to catalysis and electronics [3,4].

Despite the great potential of organosilicones, their continued development faces significant challenges, including the precise control of structure and molecular weight, the integration of multiple functionalities, and alignment with sustainability requirements.

Acknowledgements

This work was financially supported by a grant from the Ministry of Research, Innovation and Digitization, project no. PNRR-III-C9-2023-I8-99 within the National Recovery and Resilience Plan.

References

[1] M. Cazacu, M. Dascalu, G. Stiubianu, A. Bele, C. Tugui, C. Racles, Rev. Chem. Eng. 39(6) (2023) 941.
[2] C. Tugui, M. Cazacu, D.M. Manoli, A. Stefan, M. Duduta, ACS Appl. Polym. Mater. 5(10) (2023) 7936.
[3] M.-F. Zaltariov, M. Cazacu, Adv. Inorg. Chem. 76 (2020) 155.
[4] M. Cazacu, C. Racles, M.-F. Zaltariov, M. Dascalu, A. Bele, C. Tugui, A. Bargan, G. Stiubianu, Polymers 13 (2021) 1605.

Understanding the Molecular Mechanism of Fumonisin Esterase-Catalysis by Kinetic and Structural Studies

Dániel J. Incze[1,2], Zsófia Molnár[1,3], Gergely N. Nagy[3,4], Ibolya Leveles[3,4], Beáta G. Vértessy[3,4], Zsófia Bata*[2], László Poppe*[1,5]

[1]Department of Organic Chemistry and Technology, Faculty of Chemical Technology and Biotechnology, Budapest University of Technology and Economics, Budapest, Hungary

[2] Dr. Bata Ltd., Research and Development Laboratory, Ócsa, Hungary

[3] Institute of Molecular Life Sciences, HUN-REN, Research Centre for Natural Sciences, Budapest, Hungary

[4] Department of Applied Biotechnology and Food Science, Faculty of Chemical Technology and Biotechnology, Budapest University of Technology and Economics, Budapest, Hungary

[5] Biocatalysis and Biotransformation Research Center, Faculty of Chemistry and Chemical Engineering, Babeş-Bolyai University of Cluj-Napoca, Cluj-Napoca, Romania

**Corresponding authors: sbata@drbata.com; poppe.laszlo@vbk.bme.hu*

Introduction

Fumonisins are sphingolipid-like mycotoxins that cause serious concerns when they contaminate food and feed products [1]. Fumonisin B_1 esterase (FE, EC 3.1.1.87) can cleave the tricarballylic acid (TCA) moieties of fumonisin B_1, FB_1; Fig. 1, accounting for 70% of fumonisin contamination; thereby representing a biotechnological tool for detoxification of FB_1 [2].

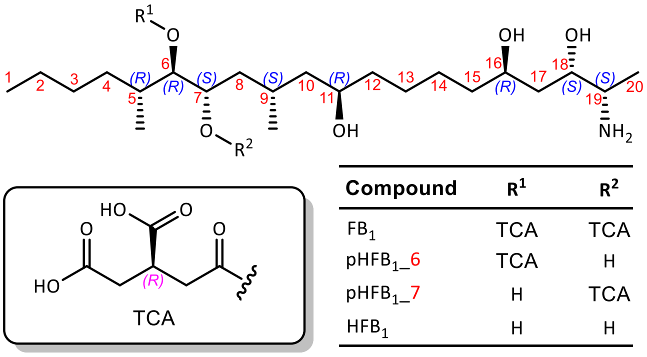

Compound	R¹	R²
FB_1	TCA	TCA
$pHFB_1$_6	TCA	H
$pHFB_1$_7	H	TCA
HFB_1	H	H

Fig. 1. Fumonisin B_1 and its degradation products by fumonisin B_1 esterase. FB_1.

Results and discussion

Recently, we reported the regioselective cleavage of the TCA ester at C6 in the first step of FB_1 hydrolysis and kinetic characterization for two FEs [3]. The low K_M values (4.76-44.3 µM) are comparable to concentrations of environmental contaminations, and the high catalytic efficiencies are promising for practical applications. One of the FEs (FE2) showed a high potential to eliminate FB_1 at the beginning of the corn refining process, during the soaking step. The X-ray structure of FE2 enabled the understanding of FB_1 hydrolysis at the molecular level, Fig. 2A [3]. It revealed an arginine binding pocket and the catalytic role of the glutamate preceding the catalytic serine. Computations, Fig. 2B, showed that FE2 can accommodate FB_1 within the active site of FE2 [3].

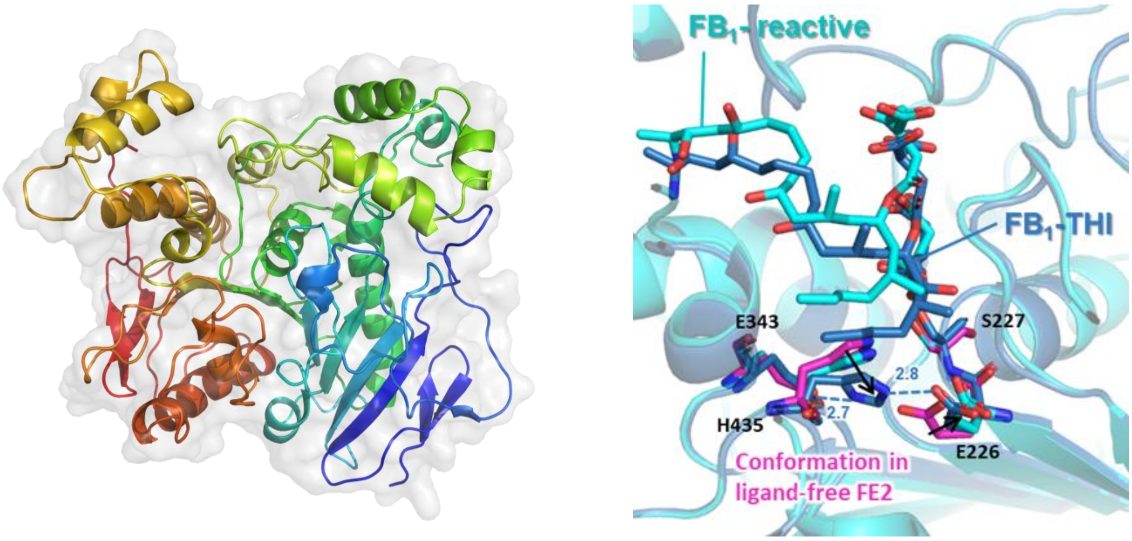

(A) (B)

Fig. 2. X-ray structure of FE2 (A) and computed arrangement of fumonisin B1 and the reaction intermediate forming from it within the active site of FE2 (B).

Further x-ray structures of S227A mutant of FE2 with and without fumonisin B_1 related ligands confirmed the calculated arrangements of the substrates.

Conclusions

Computations with representatives of other fumonisins showed that FE2 can likely detoxify all fumonisins, indicating its potential applicability in food and feed products.

Acknowledgements

The authors would like to thank Diamond Light Source for beamtime (proposal mx34263), and the staff of beamline I03 for assistance with crystal testing and data collection.

References

[1] R.T. Riley, A.H. Merrill, J. Lipid Res. 60 (2019) 1183.
[2] S. Heinl, R. Grabherr, J. Biotechnol. 145 (2010) 120.
[3] D.J. Incze, Z. Molnár, G.N. Nagy, I. Leveles, B.G. Vértessy, L. Poppe, Z. Bata, Food Chem. 473 (2025) 143110.

Multifunctional Deep Eutectic Mixtures as Green Reactive Solvents for Chemical and Enzymatic Catalytic Reactions

Carmen Gabriela Boeriu*
Politehnica University of Timisoara, Romania
**Corresponding author: carmengabriela.boeriu@upt.ro*

The past decades witnessed the revolutionary transition for the chemical industry towards sustainable technologies, to reshaping the chemical processes to make them safer, less polluting, more efficient, and greener, using preferably renewable resources as substrates. Collaborative actions from industry with academic and research communities fulfilled significant steps towards greener processes, corroborating the green chemistry concept proposed by Paul Anastas [1].

Deep eutectic solvents (DESs) advanced as the new generation of green and sustainable extraction and reaction media in biorefineries and in a multitude of chemical and biotechnological processes, surpassing both supercritical carbon dioxide (sCO_2) and ionic liquids (ILs) in performance and green print. Type I and type II DESs, formed of quaternary ammonium salts and metal halides [2], are the first developed eutectic solvents, and are applied as extraction media and reaction solvents. Type III DESs contain choline chloride or betaine hydrogen-bond acceptors (HBAs), and a variety of hydrogen-bond donors (HBDs), including polyols, carbohydrates, carboxylic acids, amines or amides, linked via hydrogen bonding. Natural deep eutectic solvents (NADESs), made exclusively of natural, non-toxic, and biodegradable components, are a tailor-made subclass of type III DESs, and are ideal solvents for chemo-catalytic and biocatalytic transformations. Recent studies by our group and others showed that DESs can have multiple functions, acting simultaneously as extraction solvent, reaction medium, source of substrate and source as catalyst [3-6]. The novel approach for the utilization of multifunctional reactive deep eutectic solvents (R-DES) and reactive natural deep eutectic solvents (R-NADESs) in catalytic conversions illustrated in Fig. 1 opens the way to the development of greener biocatalytic and chemo-catalytic processes, with simpler downstream processing and minimal discarded wastes, which will speed up their durable implementation in industry.

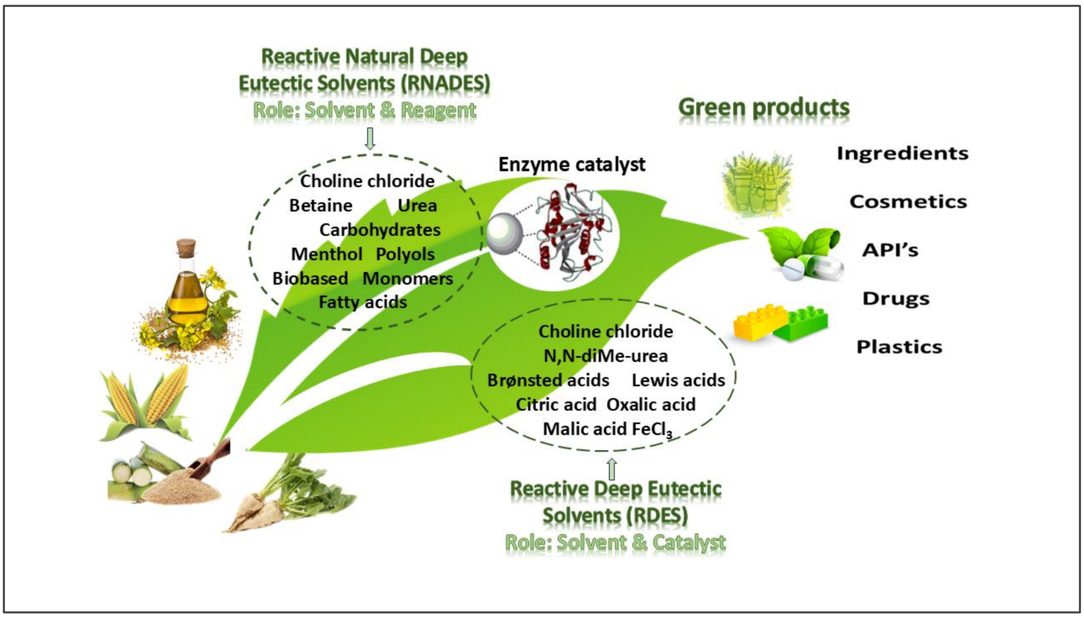

Fig. 1. Graphic representation of synthetic processes using reactive deep eutectic solvents.

This paper discusses the innovative applications of reactive deep eutectic solvents, i.e. R-DES and R-NADES, in chemo-catalytic and biocatalytic reactions for the synthesis of a large diversity of high value chemicals and materials, including biosurfactants, flavours, biobased building blocks and biobased polymers, with highlights on esterification, transesterification, glycerolysis, polymerization, and redox reactions. It will also discuss critically the advantages and disadvantages of DESs' utilisation, as well as the intrinsic relationship between the physical and chemical properties on their performance.

Acknowledgements

This work was supported by a grant of the Romanian Ministry of Education and Research, CCCDI-UEFISCDI, project number PN-III-P4-ID-PCE-2020-2177, within PNCDI III, contract number PCE 157/2021.

References

[1] P. Anastas, N. Eghbali, Chem. Soc. Rev. 39 (2010) 301.
[2] E.L. Smith, A.P. Abbott, K.S. Ryder, Chem. Rev. 114 (2014) 11060.
[3] A.R. Buzatu, M.A. Soler, S. Fortuna, O. Ozkilinc, D.M. Dreavă, I. Bîtcan, V. Badea, P. Giannozzi, F. Fogolari, L. Gardossi, F. Peter, A. Todea, C.G. Boeriu, Catal. Today 426 (2024) 114373.
[4] A.R. Buzatu, A. Todea, F. Peter, C.G. Boeriu, ChemCatChem 16(13) (2024) e202301597.
[5] A.R. Buzatu, A. Todea, R. Pop, D.M. Dreavă, C. Paul, I. Bîtcan, M. Motoc, F. Peter, C.G. Boeriu, Molecules 30 (2025) 778.
[6] R. Amoroso, F. Hollmann, C. Maccallini, Molecules 26 (2021) 6286.
[7] J.A. Sirvio, J. Ukkola, H. Liimatainen, Cellulose 26 (2019) 2303.

Heterogeneous Catalyzed Valorization of Furanics: A Sustainable Bridge to Fuels and Chemicals

Simona M. Coman*, Mihai Bordeiasu, Calin Licu, Magdi El Fergani, Natalia Candu, Vasile I. Parvulescu
Department of Inorganic Chemistry, Organic Chemistry, Biochemistry and Catalysts, Faculty of Chemistry, University of Bucharest, Regina Elisabeta Blvd., no. 4-12, Bucharest 030018, Romania
**Corresponding author: simona.coman@chimie.unibuc.ro*

While the world is facing the challenges of climate change and pollution, significant research and development efforts have focused on the use of biomass as an alternative to fossil resources. Its use in biorefineries represents a sustainable solution for producing chemicals, materials, and energy [1,2]. The biomass used is mainly lignocellulosic, derived from agricultural residues and waste. Algal biomass is also increasingly recognized as a versatile feedstock for producing renewable chemicals, various high-value products, fuels and commodities [3,4]. These approaches avoid competition between food and chemicals and have the potential to significantly reduce CO_2 emissions [4,5].

Furanics (i.e. 5-hydroxymethylfurfural (HMF) and furfural), derived from biomass dehydration process, act as versatile platform molecules that can be catalytically transformed into a diverse array of valuable products, offering a pathway to reduce dependence on fossil resources and mitigate environmental impacts. These catalytic processes frequently involve reactions such as hydrogenation, oxidation, and ring-opening, which can be tailored to yield specific target compounds, Scheme 1. For instance, hydrogenation of furanics can lead to the production of valuable chemicals like tetrahydrofuran derivatives, which find applications in the pharmaceutical and polymer industries. Oxidation reactions can generate dicarboxylic acids, important precursors for biodegradable polymers while ring-opening processes can result in the formation of linear aldehydes and ketones, which serve as building blocks for various chemical syntheses.

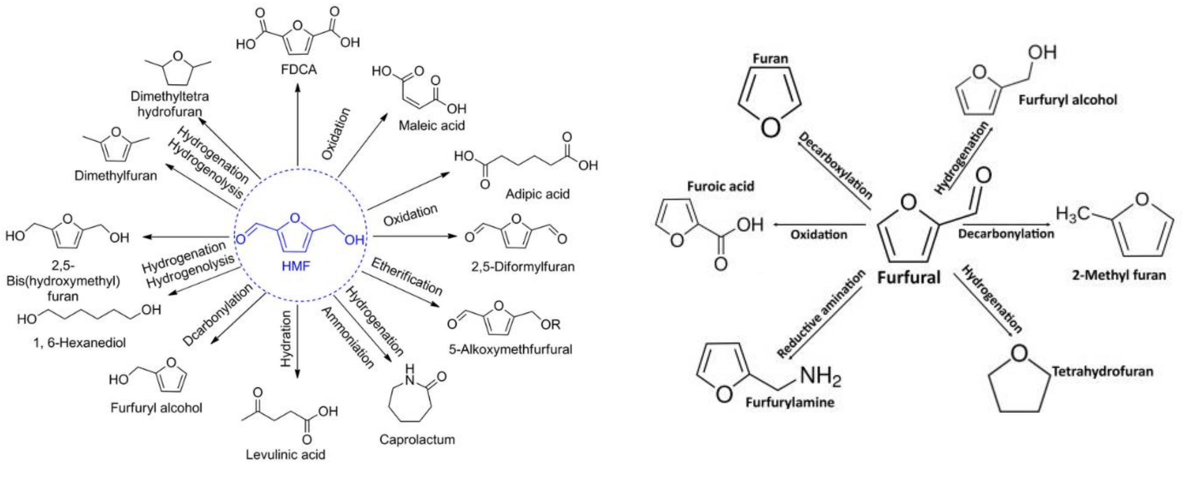

Scheme 1. Conversion of HMF and furfural into bio-chemical compounds [6,7].

The valorization of furanics through heterogeneous catalysis not only contributes to the production of renewable fuels and chemicals but also promotes the utilization of agricultural, forestry and algae biomass residues, creating new value chains in the bioeconomy.

The development of efficient and selective heterogeneous catalysts for furanics oxidation will be discussed. Challenges such as catalyst stability, resistance to deactivation, and scalability of processes will be also addressed. All the catalysts which will be presented were comprehensively characterized by BET, XRD, SEM-EDX, XPS, ICP-OES, FTIR- and Raman spectroscopy, CO_2- and NH_3-TPD measurements.

Acknowledgements

This research was partly funded by the Romanian Ministry Research and Digitalization, grant number PNRR-III-C9-2022-I5-18, ResPonSE, Project, No. 760010/2022.

References

[1] D.M. Alonso, J.Q. Bond, J.A. Dumesic, Green Chem. 12(9) (2010) 1493.
[2] J.H. Clark, V. Budarin, F.E.I. Deswarte, J.J.E. Hardy, F.M. Kerton, A.J. Hunt, R. Luque, D.J. Macquarrie, K. Milkowski, A. Rodriguez, O. Samuel, S.J. Tavener, R.J. White, A.J. Wilson, Green Chem. 8(10) (2006) 853.
[3] S. Chakraborty, N.T. Dunford, Biomass 4(2) (2024) 329.
[4] R. Katiyar, S. Banerjee, A. Arora, Biofuel Bioprod. Bior. 15(3) (2021) 879.
[5] X. Yan, O.R. Inderwildi, D.A. King, Energy Environ. Sci. 3(2) (2010) 190.
[6] P. Pal, S. Shunmugavel, ChemSusChem 12 (2018) 145.
[7] N. Ayoub, Z. Hamie, J. Toufaily, E. Guenin, G. Enderlin, ACS Sustainable Chem. Eng. 12 (2024) 9568.

Effect of Strong Metal-Support Interaction on the Improvement of Mo-Doped Titania-Carbon Composite Supported Pt Electrocatalysts Performance

András Tompos[1]*, Cristina Silva[1], Irina Borbáth[1]*, Gábor P. Szijjártó[1], Erzsébet Dodony[2], Dániel Olasz[2], György Sáfrán[2], Kristóf Zelenka[1], Ágnes Szegedi[1], Zoltán Pászti[1]
[1]Institute of Materials and Environmental Chemistry, HUN-REN Research Centre for Natural Sciences, Magyar Tudósok körútja 2, H-1117 Budapest, Hungary
[2]Institute for Technical Physics and Materials Science, HUN-REN Centre for Energy Research, Konkoly-Thege M. út 29-33, H-1121 Budapest, Hungary
**Corresponding authors: borbath.irina@ttk.hu, tompos.andras@ttk.hu*

Introduction

Recent studies demonstrated that the strong metal-support interaction (SMSI) phenomenon offers possibilities for enhancing stability and functionality of catalysts. SMSI can occur in reducible oxide supported catalysts, usually resulting in electron transfer between the metal and the oxide, accompanied by the decoration of the metal particles with ultra-thin layers of the support material upon annealing under reductive conditions [1].

Composites of transitional metal doped TiO_2 and carbon represent an emerging class of multifunctional supports proposed for Pt electrocatalysts in polymer electrolyte membrane fuel cells (PEMFCs). This work focuses on the development of SMSI and its influence on the catalytic performance of the $Pt/Ti_{0.8}Mo_{0.2}O_2$-C system, a representative of the mixed oxide-carbon composite supported Pt electrocatalyst family. Beneficial metal-support interactions developing at the Pt-oxide-carbon junctions contribute to higher activity and better stability of the catalysts, which may allow design of effective electrodes with decreased Pt content. Since the ultimate goal of this study is to propose an improved family of catalysts for PEMFCs, testing the most promising electrocatalysts under PEMFC operating conditions is a realistic step after laboratory materials science/electrochemistry studies.

Experimental

A catalyst prepared using HNO_3-glucose-functionalized Black Pearls 2000 carbon with $Ti_{0.8}Mo_{0.2}O_2/C$ mass ratio of 50/50 offering optimal balance between oxide-Pt interactions and longevity was investigated [2]. To induce SMSI, $Pt/Ti_{0.8}Mo_{0.2}O_2$-C electrocatalysts with 20 and 40 wt.% Pt content were treated at 350 °C in H_2 stream (denoted as 20Pt/50FC-350H and 40Pt/50FC-350H). Structural and surface chemical properties of the resulting catalysts were studied by N_2 physisorption, XRD, TEM, STEM/EDS and XPS completed with in situ H_2 exposure experiments. Catalytic activity was assessed by cyclic voltammetry and CO_{ad} stripping voltammetry combined with 500- and 10,000-cycle stability tests measurements. Fuel cell polarization measurements were carried out on the 40Pt/50FC-350H as described in our previous study [3]. Polarization measurements were performed at 80 °C under pure H_2 and 100 ppm CO/H_2 fuel on the anode and O_2 on the cathode. Similar measurements on the 40 wt.% Pt/C (40Pt/C, QuinTech) reference catalyst were done for comparison.

Results and discussion

XPS combined with in situ H_2 exposition clearly demonstrated appearance of very easily reducible Mo species after the reductive pretreatment, which evidences transport of Mo species to the surface of the Pt particles, as shown schematically in Fig. 1A. Semiquantitative analysis of the exposed/buried nature of Pt using the intensity ratio of low and high kinetic energy Pt features conducted on the 20Pt/50FC-350H catalyst indicated that Pt started to be somewhat buried after reductive pretreatment, which is consistent with migration of Mo species to Pt surface. At the same time, the latter result also indicates that the decoration layer on Pt is discontinuous or very thin, in contrast with the Pt particles alloyed with tin after reductive pretreatment of the Pt/$Ti_{0.8}Sn_{0.2}O_2$-C system, where relatively thick tin oxide overlayer forms under oxidative conditions [4].

Presence of 100 ppm CO negatively impacts both catalysts due to the blocking of active sites on the Pt surface, Fig. 1B. However, the CO tolerance of the 40Pt/50FC-350H results in a much smaller voltage loss (~ 80 mV) compared to pure H_2 fuel, while on the 40Pt/C, this voltage loss is 370 mV. Better CO tolerance of 40Pt/50FC-350H can be attributed to SMSI effect, which reduce CO adsorption on the active catalytic sites due to the electronic ligand effect and improve surface cleaning, presumably due to the bifunctionality of adjacent, Mo^{n+} and Pt containing, surface sites.

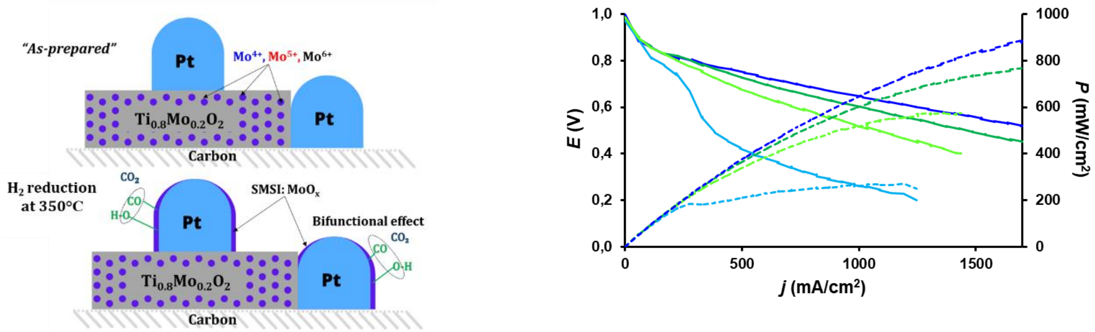

Fig. 1. (a) Proposed model of transformation in Pt/$Ti_{0.8}Mo_{0.2}O_2$-C catalysts after reductive pre-treatment; Polarization responses (b) for the 40Pt/50FC-350H and the 40Pt/C catalysts under pure H_2 and 100 ppm CO/H_2 fuel. The Pt loading in both electrodes was 0.6 mg_{Pt}/cm^2.

Conclusions

Based on the experiment in a single cell test device using 100 ppm CO/H_2 fuel, the 40 wt.% Pt/$Ti_{0.8}Mo_{0.2}O_2$-C catalyst demonstrates a clear advantage over the conventional 40 wt.% Pt/C catalyst in terms of CO tolerance, highlighting the effectiveness of the advanced $Ti_{0.8}Mo_{0.2}O_2$-C support structure, together with SMSI induction, in improving PEM fuel cell performance.

Acknowledgements

This research was funded by Project no. RRF-2.3.1-21-2022-00009, titled National Laboratory for Renewable Energy has been implemented with the support provided by the Recovery and Resilience Facility of the European Union within the framework of Programme Széchenyi Plan Plus.

References

[1] I. Jiménez-Morales, S. Cavaliere, D. Jones, Rozière, Phys. Chem. Chem. Phys. 20 (2018) 8765.

[2] I. Borbáth, E. Tálas, Z. Pászti, K. Zelenka, I. Ayyubov, K. Salmanzade, I.E. Sajó, G. Sáfrán, A. Tompos, Appl. Catal. A: Gen. 620 (2021) 118155.

[3] D. Gubán, A. Tompos, I. Bakos, Á. Vass, Z. Pászti, E.G. Szabó, I.E. Sajó, I. Borbáth, Int. J. Hydrog. Energy. 42 (2017) 13741.

[4] C. Silva, K. Salmanzade, I. Borbáth, E. Dódony, D. Olasz, G. Sáfrán, A. Kuncser, E. Pászti-Gere, A. Tompos, Z. Pászti, Nanomaterials 13 (2023) 2245.

On the Role of MOF-Derived Carbon Type as Promoter for CO_2 Hydrogenation to Methanol

Angela M. Kasza[1,2], Mihaela D. Lazar[1], Maria Mihet[1]*
[1]*National Institute for Research & Development of Isotopic and Molecular Technologies - INCDTIM, 67–103 Donat Str., 400293 Cluj–Napoca, Romania*
[2]*Babes-Bolyai University, Faculty of Chemistry and Chemical Engineering, 11 Arany Janos Str., 400028, Cluj–Napoca, Romania*
**Corresponding author: maria.mihet@itim-cj.ro*

Introduction

Although methanol (MeOH) synthesis from syngas (CO and H_2) containing small amounts of CO_2 is a well-established industrial process, methanol synthesis by CO_2 hydrogenation is receiving great attention, especially in the context of tremendous interest in CO_2 valorization pathways. Not only is methanol an important chemical feedstock and a platform intermediate to produce a large variety of bulk commodities [1], but MeOH might be an alternative for the chemical storage of energy (*the power-to-liquid concept, P2L*) [1-3]. However, hydrogenation of CO_2 to methanol is a challenging process considering the thermodynamics of the reaction, the stability of the CO_2 molecule, the possible side reactions (*RWGS*, reaction 2), and catalyst deactivation problems due to water formation. All these issues are closely interconnected and point out to on the importance of designing highly efficient, selective, and stable catalysts for CO_2–MeOH.

$$CO_2 + 3H_2 \leftrightarrow CH_3OH + H_2O \quad \Delta H_{298K} = -49.5\ \text{kJ/mol} \qquad (1)$$

$$CO_2 + H_2 \leftrightarrow CO + H_2O \quad \Delta H_{298K} = 41.2\ \text{kJ/mol (RWGS)} \qquad (2)$$

Among the various strategies to improve the catalytic performance of CO_2–MeOH catalysts, one is to use high surface area carbon materials, allowing in this way an enhanced dispersion of the catalytic components, as well as improved water resistance as a consequence of the hydrophobic character of the added carbon. Herein, we report the modification of typical Cu-ZnO-Al_2O_3 (CZA) catalysts by promotion with two types of MOF-derived carbon structures, obtained from the flexible, microporous Al-based metal-organic framework (MOF), that is MIL-53(Al). The influence of these two types of MOF-derived carbon structures on the physico-chemical properties and the catalytic performance of the modified CZA catalysts was investigated.

Experimental

MOF-derived nanoporous carbon was obtained by thermal treatment in an inert atmosphere (Ar flow, 600 °C for 5 h) of MIL-53(Al) obtained by an optimized hydrothermal synthesis method previously established by our group [4]. In this way, an alumina-doped carbon (C_{as}) was obtained, with Al_2O_3 particles uniformly distributed within the carbonaceous structure, as a consequence of the Al presence in the pristine MOF. The alumina-free MOF-derived carbon structure (*C*) was obtained by 10% HCl treatment at 80 °C for 5 h. Both carbon structures were further used to modify the typical Cu-ZnO-Al_2O_3 catalysts, with a carbon loading of 6 wt.%. Thus, an appropriate amount of alumina-free carbon (*C*) was dispersed into a 1 M metal salt solution with Cu:Zn:Al = 6:3:1, followed by precipitation with 1 M Na_2CO_3 or $NaHCO_3$ at pH=7, and 70 °C. On the other hand, since the alumina-doped carbon structure (C_{as}) already contains Al_2O_3, the second series of carbon-modified CZA catalysts was prepared starting from Cas dispersed in a metal salt solution containing only Cu and Zn, followed by precipitation under the same conditions. The CZA-C and CZA-Cas materials were calcined in air at 300 °C, and then characterized by XRD, BET, SEM/TEM/EDX, TPR, H_2/CO_2-TPD, FT-IR, DRIFTS, and the active copper surface area was estimated by the N_2O oxidation method followed by TPR. Additionally, thermodynamic analysis was performed in ChemCAD using a Gibbs reactor, under different reaction conditions (temperature, pressure, and reactants ratio), while catalytic performance was investigated using a plug-flow reactor, and reaction products analyzed by gas-chromatography.

Results and discussion

XRD analysis revealed the presence of CuO, with no evident diffraction lines corresponding to ZnO or Al_2O_3, suggesting an amorphous state thereof, alongside a uniform distribution along the matrix. Indeed, EDX mapping evidences a uniform distribution of all the components, Fig. 1(b). In terms of surface area, all MOF-derived carbon promoted materials show an increase of S_{BET}, irrespective of the carbon type. On the other hand, pore size distribution shifts from a broader one in the case of CZA alone, to a bimodal porosity as a consequence of the carbon presence, with a larger proportion of smaller pores for the CZA-C_{as} series, Fig. 1(a). Reducibility of materials is also influenced by the type of added MOF-derived carbon. Thus, CZA-Cas samples are more reducible than their homologues, exhibiting only one reduction peak at lower temperatures, Fig. 1(c). Both carbon-modified series show modified hydrogen adsorption capacities, the CZA-Cas samples exhibiting larger values, alongside a different distribution of the hydrogen activation sites. On the other hand, the CO_2 adsorption capacity is lower for the carbon-modified samples, however with a larger contribution of the medium strength basic sites in the case of CZA-Cas, known for their important role in CO_2–MeOH, Fig. 1(d). Both FTIR and DRIFTS reveal structural differences depending on the added carbon type. CO_2 hydrogenation to MeOH is mostly influenced by the operating pressure (linear dependence), while temperature window is quite narrow due to the competing RWGS reaction.

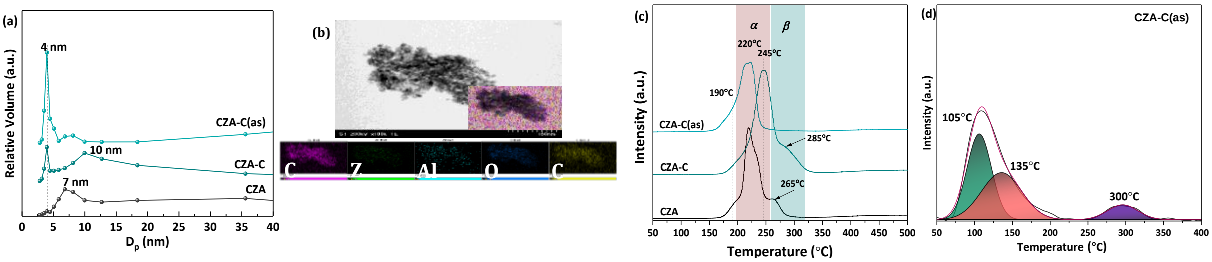

Fig. 1. Characterization of CZA modified by different types of MOF-derived carbon: a) pore size distribution; b) electron microscopy; c) TPR profiles; d) CO_2-TPD profiles.

Conclusions

Two types of MOF-derived carbon structures were employed two modify CZA catalysts for CO_2–MeOH. Thus, materials modified with alumina-doped carbon, C_{as}, revealed different structural and functional properties as compared to their counterparts modified with alumina-free carbon, C, with subsequent differences in catalytic performance in CO_2–MeOH process.

Acknowledgements

This work was supported through the “Nucleu” Program within the National Research Development and Innovation Plan 2022–2027, Romania, carried out with the support of MEC, project no. 27N/03.01.2023, component project code [PN 23 24 01 01].

References

[1] I. Abbas, H. Kim, C.-H. Shin, S. Yoon, K.-D. Jung, Appl. Catal. B Environ. 258 (2019) 117971.
[2] U.I. Din, M.S. Shaharun, M.A. Alotaibi, A.I. Alharthi, J. CO_2 Util. 34 (2019) 20.
[3] A. Velty, A. Corma, Chem. Soc. Rev. 52 (2023) 1773.
[4] O. Grad, A.M. Kasza, A. Turza, M. Dan, L. Barbu-Tudoran, M.D. Lazar, M. Mihet, J. Environ. Chem. Eng. 11 (2023) 109456.

UV-Raman Spectroscopic Characterization of the Modified TiO_2-Based Materials with Photocatalytic and Catalytic Activity

Elena Maria Anghel[1]*, Gabriela Petcu[1], Florica Papa[1], Irina Atkinson[1], Madalina Ciobanu[1], Nicoleta Apostol[2], Elena Buixaderas[3], Viorica Parvulescu[1]

[1]*Institute of Physical Chemistry-Ilie Murgulescu, Spl. Independentei 202, 060021, Bucharest Romania*

[2]*National Institute of Materials Physics, Atomiştilor 405A, 077125 Măgurele – Ilfov, Romania*

[3]*Institute of Physics, Czech Academy of Sciences, Na Slovance 2, 18200 Prague, Czech Republic*

**Corresponding author: manghel@icf.ro*

Introduction

UV-Raman spectroscopy is a powerful technique for characterizing TiO_2-based photocatalysts and their mesoporous silica supports, enabling fluorescence interference avoidance and Raman intensity enhancement due to the short wavelength of the excitation laser [1]. This method is useful for identifying active sites, framework titania, and monitoring phase transformations in metal oxide photocatalysts such as anatase to rutile, since this technique is more sensitive to surface regions than visible-Raman spectroscopy and X-ray diffraction [1,2]. TiO_2-zeolite, MCM48, KIT-6, and SBA-supported catalysts with Au and Pt exhibit strong metal-support interactions, which can significantly enhance their photocatalytic and catalytic properties [3-5]. Recent studies have explored the synthesis and photocatalytic applications of TiO_2-based composites, particularly in environmental applications and hydrogen production [1-5].

Experimental

Some catalytic TiO_2-based materials and their preparation methods (sol-gel, direct synthesis, hydrothermal, and impregnation) are listed in Table 1.

The UV resonance Raman spectra of the catalysts before and after the temperature programmed oxidation (TPO) and reduction (TPR) tests were obtained using a LABRAM HR800 spectrometer equipped with a He-Cd laser (λ_L=325 nm), a microscope objective of 40×NUV/0.47, and a 2400-groove grating.

Table 1. TiO_2-containing systems with or without supports and their preparation methods.

Catalyst system	**Type of support**	**Photo/catalytic active sites Concentration/Immobilization method**		
		TiO_2	**Au**	
Au-TiO_2	Zeolite Y, MCM-48, KIT-6	10 %, i	1 % , i	
Au-CeO_2-TiO_2	Zeolite Y	**TiO_2**	**CeO_2**	**Au**
		0.7-3.5 %, ds	1 %, i	0.1-0.3 %, i
Au-TiO_2		0.7-3.5 %, ds	-	0.1-0.3 %, i
FeO_x, CoO_x, NiO_x/TiO_2		**TiO_2**	**Fe/Co/Ni oxide**	
		1/2 %, ds	5 %, i	
W-TiO_2-CeO_2	-	TiO_2	CeO_2	W
		h, sg	6-35 %, ds	0.7-1 %, i
Pt-TiO_2-CeO_2	SBA-15	**TiO_2**	**CeO_2**	**Pt**
		10 %, ds	1 %, i	0.2, 0.5, 1 %, i

**ds-direct synthesis, i-impregnation, h-hydrothermal, sg-sol-gel*

Results and discussion

Influence of the preparation methods, such as sol-gel, hydrothermal, direct synthesis, and impregnation methods, and compositional aspect can be investigated by UV-Raman spectroscopy as illustrated in Fig. 1. The Y zeolite support can be easily depicted in the 5TY(-/Ce/CeAu) spectra in Fig. 1a, even in the gold-containing material where a decrease in the intensity of the Raman bands occurs. Framework titania seems to exist in the 5TY spectrum. According to the UV-VIS spectra in the inset of Fig. 1a, nearly resonant Raman spectra were collected for the 5TY(Ce/CeAu) materials. Anatase polymorph (~400, 512, and ~637 cm^{-1}) seems to exist in the sol-gel prepared samples with and without tungsten oxide. The band at ~760 cm^{-1} might be originating from peroxo-species, O_2^{2-} [1] on the sample surface, Fig. 1b. This band is rather enhanced for the samples which underwent TPO tests and vanishes by TPR processes, Fig. 1b. Moreover, during TPO tests with rich oxygen supply, the oxygen vacancies diffusion towards surface occurs for the ceria component [1]. Hence, the 2LO band increases as noticed in the TiO_2-CeO_2 sg600-TPO spectrum in Fig. 1 b. Conversely, no 2LO band is detectable in the TiO_2-CeO_2 sg600-TPR spectrum. Thus, the UV-Raman spectroscopy is very helpful in studying the oxidation and reduction processes involving catalytic materials.

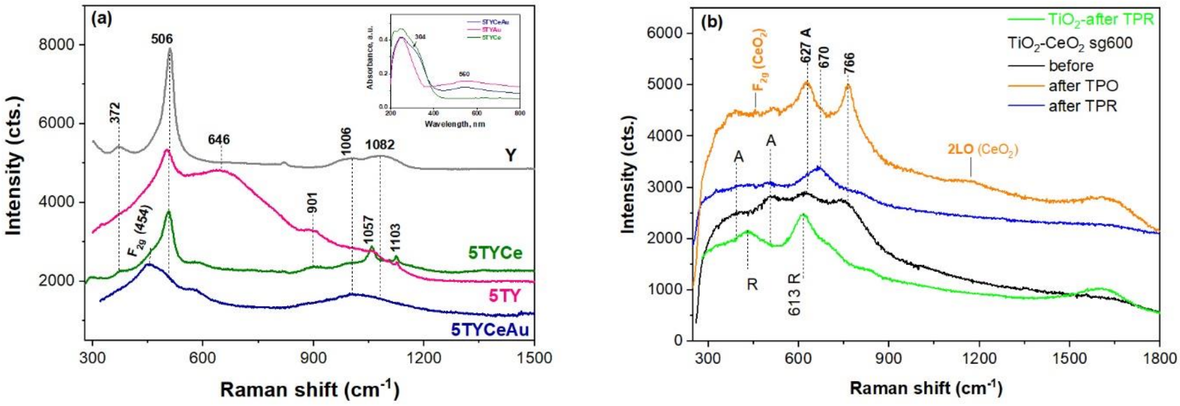

Fig. 1. UV-Raman spectra of the TiO_2-based materials: (a) 5TY(-/Ce/CeAu) (Inset represents the UV-VIS spectra) and (b) before and after TPO and TPR tests. (A and R stand for framework anatase and rutile).

Conclusions

UV-Raman spectroscopy has enabled identification of the framework and/or extraframework TiO_2 in the catalytic systems in Table 1. While porous silica-based supports are easily detectable in UV-Raman spectroscopy regardless of titania's strong scattering ability, the vibrational modes of ceria, especially its oxygen vacancies, are sometimes masked by extraframework TiO_2.

References

[1] C. Hess, Chem. Soc. Rev. 50 (2021) 3519.

[2] S. Jin, Z. Feng, F. Fan, C. Li, Catal. Lett. 145 (2015) 468.

[3] G. Petcu, F. Papa, E.M. Anghel, I. Atkinson, S. Preda, S. Somacescu, D.C. Culita, A. Baran, E.M. Ciobanu, L.M. Jecu, M. Constantin, V. Parvulescu, Gels 9 (2023) 503.

[4] G. Petcu, E.M. Anghel, E. Buixaderas, I. Atkinson, S. Somacescu, A. Baran, D.C. Culita, B. Trica, C. Bradu, M. Ciobanu, V. Parvulescu, Catalysts 12 (2022) 1129.

[5] T. Tabakova, D. Nikolova, I. Ivanov, E.M. Anghel, D. Karashanova, Y. Karakirova, A.M. Venezia, J. Vakros, M. Crisan, K. Tenchev, M. Gabrovska, Int. J. Hydrog. Energy. 70 (2024) 389.

Oral Presentations

Mixed Oxide-Carbon Composite Supported Platinum Electrocatalysts for Polymer Electrolyte Membrane Fuel Cells by Use of Graphene Derivatives

Emília Tálas[1]*, Ilgar Ayyubov[1], Irina Borbáth[1], Zoltán Pászti[1], László Trif[1], Ágnes Szegedi[1], Tamás Szabó[2], Erzsébet Dodony[3], András Tompos[1]

[1]Renewable Energy Research Group, Institute of Materials and Environmental Chemistry, HUN-REN Research Centre for Natural Sciences, Magyar Tudósok körútja 2, H-1117 Budapest, Hungary

[2]Department of Physical Chemistry and Materials Science, University of Szeged, Rerrich Béla tér 1, H-6720 Szeged, Hungary

[3]Institute for Technical Physics and Materials Science, HUN-REN Centre for Energy Research, Konkoly-Thege M. út 29-33, H-1121 Budapest, Hungary

**Corresponding author: talas.emilia@ttk.hu*

Introduction

Polymer electrolyte membrane fuel cells (PEMFCs) convert chemical energy into electricity efficiently and in an environmentally friendly way. The lifetime of PEMFCs is significantly influenced by the stability of the catalyst used in them. In our previous works we found that composite type supports with the formula of $Ti_{(1-x)}Mo_xO_2$-C (x: 0-0.2, C: Black Pearls, Vulcan-XC (Cabot)) provided higher stability for the Pt active metal compared to simple conductive carbon supports [1]. Every component of above composite has important function; TiO_2 skeleton being strongly resistant to electrocorrosion increases the stability and hinders the dissolution of the incorporated Mo dopant; the Mo doping metal acts as a co-catalyst providing enhanced CO oxidation activity and CO tolerance; the carbon material provides appropriate specific surface area (SSA_{BET}) and electrical conductivity [1,2]. Non-traditional carbon materials as graphene nanosheets offer new possibilities for electrocatalyst support but certain functionalization is inevitable for their use [3]. A widely studied group of "graphene" materials is the graphene nanoplatelets (GNP) [4]. Due to its relatively extensive condensed aromatic ring system, electric conductivity of GNP is excellent. However, the amount of its O- containing functional groups (O-fg) is insufficient as they are situated only on the edges of the nanoparticles [4]. In contrast, graphite oxide (GO) is rich in O-fgs. In addition, the appearance of π-π interaction between the two graphene derivatives is assumed [4]. The aim of this work was to explore the effect of combining GNP and GO on the behavior of a mixed oxide-carbon composite supported electrocatalyst.

Experimental

GNP (Aldrich; SSABET: $750 m^2 \cdot g^{-1}$) and GO (from Hummers-Offeman method) were used as starting carbon materials. Composites of 75 wt.% $Ti_{(1-x)}Mo_xO_2$-25 wt.% C were prepared via multistep sol-gel method followed by high-temperature heat treatment (HTT) [1]. Due to the highly apolar nature of GNP intense ultrasound treatment was used [2]. 20 wt.% Pt was loaded on the supports by ethylene glycol-$NaBH_4$-assisted reduction [1]. Metal content was measured by ICP. SSA_{BET} and pore volume values were obtained from N_2 physisorption. The structural and surface chemical properties were characterized by use of XRD, TG-MS, TEM and XPS. Electrical conductivity of the powdery catalysts was obtained by impedance spectroscopy in two-probe method [2]. The electrochemical performance was evaluated by cyclic voltammetry, rotating disc electrode measurements and long term stability tests. Electrochemical surface areas (ECSAs) were calculated from cyclic voltammograms [2].

Results and discussion

Table 1 shows that SSA_{BET} values large enough (>100 $m^2 \cdot g^{-1}$), and element contents slightly different from the nominal value were achieved. The mixed oxide existed only in the rutile phase, Mo only existed in the incorporated form, and the O-fgs of C were lost after HTT. Pt on the surface was in finely dispersed form. The preparation was well reproducible.

Table 1. Denomination and results of characterization of the Pt/$Ti_{(1-x)}Mo_xO_2$-C catalysts (nominal Pt: 20 wt%; nominal $Ti_{(1-x)}Mo_xO_2$/C=75 wt%/25 wt%; nominal Ti/Mo=4/1).

Sample	GNP/GO ratio	Support		Catalyst			
					ICP-OES		
		SSA_{BET} ($m^2 \cdot g^{-1}$)	Pore volume ($cm^3 \cdot g^{-1}$)	XRD $Pt_{average}$ particle size (nm)	Pt (wt.%)	(Ti+Mo+O)/C (wt.%/wt.%)	Ti/Mo (mol/mol)
Pt/100GNP	100	136	0.14	3.7	17.7	58.3/41.7	4.8/1
Pt/75GNP	75/25	128	0.31	3.0	16.5	59.2/40.8	5.1/1
Pt/50GNP	50/50	105	0.33	2.6	18.6	60.0/40.0	5.2/1
Pt/50GNP*	50/50	130	0.44	2.3	n.d.	n.d.	n.d.
Pt/25GNP	25/75	125	0.45	2.5	17.4	58.1/41.9	4.8/1

**sample from repeated preparation; n.d.: no data*

Electrical conductivity of the composite supported catalysts was obviously smaller than that of reference 20 wt.% Pt/C (Quintech), but it increased by use of GNP-GO mixtures, Fig. 1A. Long term stability of the new type of catalysts expressed in $ECSA_N/ECSA_1$ x 100 % (N: number of cycles) was more favorable compared to that of Pt/C, Fig. 1B.

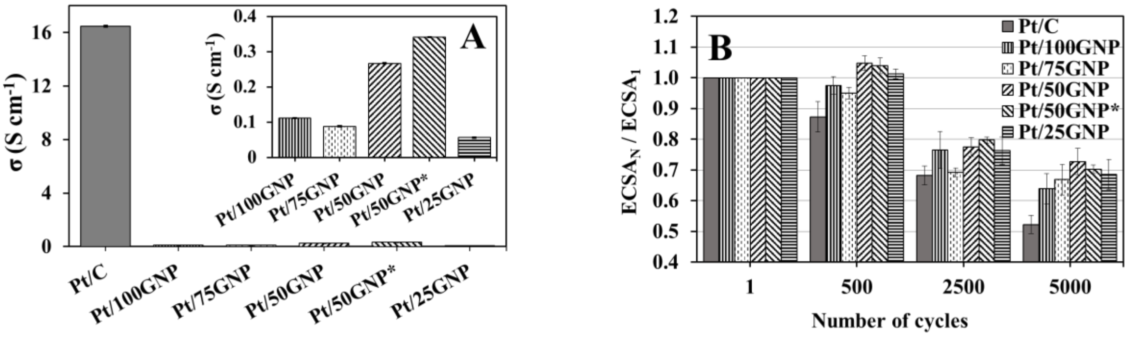

Fig. 1. (A) Conductivity and (B) long term stability of the electrocatalysts investigated.

Conclusions

Use of GNP-GO increased the long term stability of the composite supported Pt catalysts. Adding GO is supposed to act as non-covalent functionalization of GNP. The GO/GNP ratio was also influencing factor. The details will be given in the presentation.

Acknowledgements

a) Project no. RRF-2.3.1-21-2022-00009, titled the National Laboratory for Renewable Energy, b) Hungarian innovation project VEKOP-2.3.3.15-2016-00002 (THEMIS microscope).

References

[1] I. Borbáth, E. Tálas, Z. Pászti, K. Zelenka et al, Appl. Catal. A: Gen. 620 (2021) 118155.
[2] I. Ayyubov, E. Tálas, I. Borbáth, Z. Pászti, et al, Nanomaterials 14 (2024) 1053.
[3] E. Antolini, Appl. Catal. B: Environ. 123-124 (2012) 52.
[4] N.S. Kazi, A. Badarudin, N.M.N. Zubir, Nanoscale Res. Lett. 10 (2015) 16.

Strategies to Improve Stability of Sn-Containing Composite Supported Pt Electrocatalysts for Sustainable Energy Conversion Technologies

Irina Borbáth[1]*, Zoltán Pászti[1], Cristina Silva[1], Erzsébet Dodony[2], Dániel Olasz[2], György Sáfrán[2], Ágnes Szegedi[1], Zoltán Sebestyén[1], András Tompos[1]
[1]Institute of Materials and Environmental Chemistry, HUN-REN Research Centre for Natural Sciences, Magyar Tudósok körútja 2, H-1117 Budapest, Hungary
[2]Institute for Technical Physics and Materials Science, HUN-REN Centre for Energy Research, Konkoly-Thege M. út 29-33, H-1121 Budapest, Hungary
**Corresponding author: borbath.irina@ttk.hu*

Introduction

Electrocatalysts are key components of polymer electrolyte membrane fuel cells (PEMFCs), which largely determine the performance, active lifespan and cost of the cell. Our recent findings have demonstrated the attractiveness of oxophilic metal-doped TiO_2-rutile-based mixed oxide–carbon composite supported Pt catalysts, in which strong metal-support interactions (SMSI) at the Pt-oxide-carbon triple junctions ensure high stability for the Pt nanoparticles [1,2]. Among other transition metals, Sn was found to be a valuable modifier providing enhanced CO tolerance and activity in the oxygen reduction reaction (ORR) [3].

In this contribution, various approaches such as the use of functionalized carbon, reductive treatment and electrochemical oxidation were applied to improve the stability of $Pt/Ti_{(1-x)}Sn_xO_2$–C composite supported electrocatalysts. The effect of these experimental variables on the catalyst properties was systematically explored, along with the development of the SMSI.

Experimental

Based on our previous results on the structure and performance of Sn-containing catalysts, the 20 wt.% $Pt/Ti_{0.9}Sn_{0.1}O_2$–C sample was selected as the best [3]. The functionalization of commercial carbon (Black Pearls 2000) pre-treated in N_2 at 1000 °C was carried out by a two-step treatment with HNO_3 and glucose [4]. Using unmodified and functionalized carbon (FC) materials the synthesis of composites with $Ti_{0.9}Sn_{0.1}O_2/C$ ratio of 50/50 and 25/75 was done as described earlier [3,5]. The effect of carbon functionalization and reductive pre-treatments on the structure of the catalysts (denoted as Pt/50C, Pt/50FC and Pt/75FC) was investigated by N_2 physisorption, XRD, TEM, STEM/EDS and XPS completed with in situ H_2 and air exposure experiments. The electrocatalytic performance of the catalysts in their initial, as-prepared state and after reductive pre-treatment was measured by cyclic voltammetry (CV) and COad stripping voltammetry. Stability was investigated by short- (500-cycle) and long-term (10,000-cycle) tests between 50 and 1000 mV potential limits, which were performed on the as-prepared samples as well as on those previously subjected to the ORR measurements.

Results and discussion

Structural analysis of the *as-prepared* and reduced catalysts confirmed the homogeneous coverage of the carbon backbone by the oxide phase, which facilitated strong interactions between Pt particles and the oxide crystallites. The XPS analysis revealed a tin oxide-rich overlayer, emphasizing a significant coupling between surface tin species and Pt. The structural advantages of this system were evident in the formation of Pt-oxide-carbon triple junctions, which are key for achieving high dispersion and catalytic activity. XPS studies, consistently with electrochemical investigations, revealed that formation of metallic tin under reductive conditions was accompanied by Sn-Pt alloying. The alloying process, schematically shown in Fig. 1A, was identified as the most critical structural change induced by the reductive pre-treatment. As a result of the very strong Pt-support interaction, reversible encapsulation of Pt by tin oxide was observed under oxidizing conditions, highlighting the dynamic nature of the Sn-Pt interaction.

Electrochemical stability tests confirmed that carbon functionalization and reductive pre-treatment improved long-term stability, suggesting that it is a viable approach for optimizing performance. As shown in Fig. 1B, further improvement in stability was observed for catalysts used after ORR measurements: the decrease of the electrochemical active Pt surface area loss after 10,000-cycle stability tests (decreases of $\Delta ECSA_{10,000}$) is consistently 6-8 %.

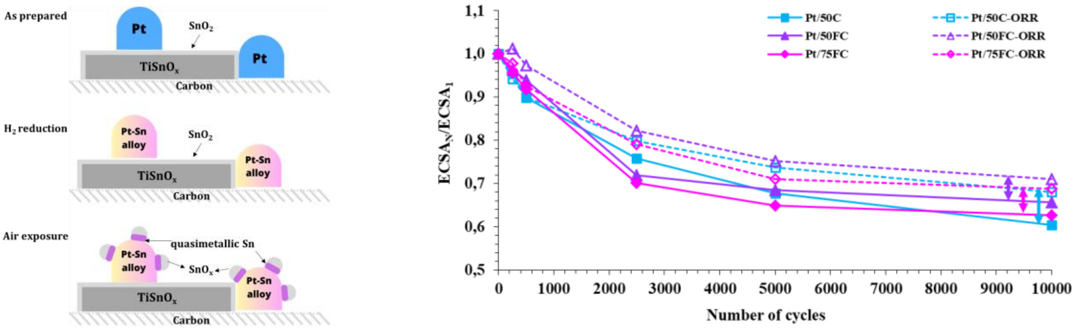

Fig. 1. (A) Proposed model of transformation in $Pt/Ti_{(1-x)}Sn_xO_2$–C catalysts after reductive and oxidative pre-treatments. (B) Change of ECSA during 10,000 CV cycles for the Pt/50C (■), Pt/50FC (▲) and Pt/75FC (♦) electrocatalysts obtained on the *as-prepared* samples (filled symbols) and after ORR measurements (open symbols). $ECSA_N/ECSA_1$ values are compared as a function of the cycles number.

Conclusions

The obtained results confirm that carbon functionalization, reductive pre-treatment and mild electrochemical oxidation are means of fine-tuning the metal-support interaction in the $Ti_{(1-x)}Sn_xO_2$–C composite supported electrocatalyst family, offering a strategy to improve the catalytic properties of the systems.

Acknowledgements

This research was funded by Project no. RRF-2.3.1-21-2022-00009, titled National Laboratory for Renewable Energy has been implemented with the support provided by the Recovery and Resilience Facility of the European Union within the framework of Programme Széchenyi Plan Plus.

References

[1] I. Borbáth, E. Tálas, Z. Pászti, K. Zelenka, I. Ayyubov, K. Salmanzade, I.E. Sajó, G. Sáfrán, A. Tompos, Appl. Catal. A: Gen. 620 (2021) 118155.
[2] C. Silva, I. Borbáth, E. Dodony, D. Olasz, G. Sáfrán, Á. Szegedi, K. Zelenka, A. Tompos, Z. Pászti, Mater. Res. Bull. 182 (2025) 113114.
[3] I. Borbáth, K. Salmanzade, Z. Pászti, A. Kuncser, D. Radu, Ş. Neaţu, E. Tálas, I.E. Sajó, D. Olasz, G. Sáfrán, Á. Szegedi, M. Florea, A. Tompos, Catal. Today 438 (2024) 114788.
[4] I. Borbáth, K. Zelenka, Á. Vass, Z. Pászti, G.P. Szijjártó, Z. Sebestyén, G. Sáfrán, A. Tompos, Int. J. Hydrog. Energy. 46 (2021) 13534.
[6] C. Silva, K. Salmanzade, I. Borbáth, E. Dódony, D. Olasz, G. Sáfrán, A. Kuncser, E. Pászti-Gere, A. Tompos, Z. Pászti, Nanomaterials 13 (2023) 2245.

LDH-Type Catalysts Tailored by Organic Alkaline: A New Approach in Synthesis

Octavian D. Pavel, Bogdan Cojocaru, Rodica Zăvoianu, Vasile I. Pârvulescu*
University of Bucharest, Faculty of Chemistry, Bucharest, 050663, Romania
Research Center for Catalysts & Catalytic Processes, Faculty of Chemistry, University of Bucharest, 030018, Romania
**Corresponding author: vasile.parvulescu@chimie.unibuc.ro*

Introduction

The traditional synthesis of Layered Double Hydroxides (LDH) materials is often accompanied by some disadvantages in terms of energy, contamination possibility with alkaline cations, the number of tools used as well as number of steps involved, generation of wastewater, [1] etc. A new approach in terms of synthesis that tends to eliminate these disadvantages considers the use of organic alkalis that present a dual role: synthesis agent from a structural point of view, as well as template molecule from a textural point of view respectively. This approach can be considered a key in tailoring the predetermined physicochemical properties required by the various processes that involve them.

Experimental

Several LDH-type materials involving monovalent cations, e.g. Li, bivalent cations, e.g., Mg; Zn; Cu; Fe, but also trivalent cations, e.g., Al; Y, have been synthesized using both traditional methods, i.e. co-precipitation, and non-traditional methods, i.e. mechanochemical. The syntheses were performed in the presence of quaternary ammonium salts as organic alkalis as well as traditional alkalis, i.e., $NaOH/Na_2CO_3$, for comparison. The obtained LDHs were calcined at 460 °C and subsequently hydrated to reconstruct the initial layered structure manipulating the memory effect exhibited by these solids. The influences of the physicochemical properties of these materials on their catalytic activities were evaluated in three different reactions: the cyanoethylation of ethanol with acrylonitrile, the Claisen-Schmidt condensation between cyclohexanone and benzaldehyde, and the cycloxenanone self-condensation.

Results and discussion

X-ray patterns of the synthesized LDH solids confirmed the pure layered structure for materials involving di- and tri-valent cations, Fig. 1. Despite the fact that Y^{3+} was partially placed in octahedral positions, the use of organic alkalis created a uniform texture with a narrow pore distribution around 35-60 Å. The presence of a surfactant, e.g. cetyltrimethylammonium bromide, also led to a more advanced texture ordering when organic alkali was used compared to the case of inorganic alkalis. Li_4Al LDH was successfully synthesized by the traditional co-precipitation method, using inorganic alkalis, while the organic alkali led to the generation of gibbsite like contaminant, in a more significant amount, as the hydrocarbon chain of the quaternary salt was larger, Fig. 2.

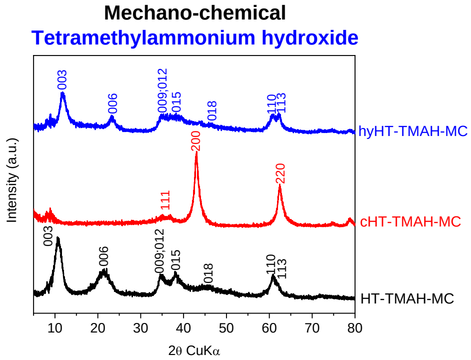

Fig. 1. The XRD patterns of Mg_3Al synthesized by mechanochemical method with tetramethylammonium hydroxide (black line - LDH; red line - mixed oxides; blue line - reconstructed layer structure).

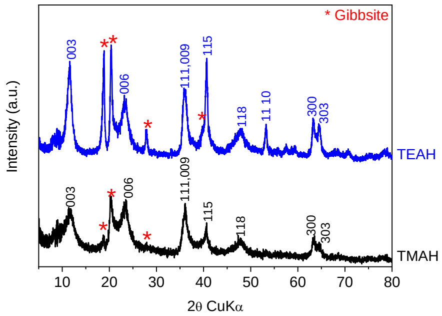

Fig. 2. The XRD patterns of Li_4Al-LDH synthesized in presence of tetramethyl and tetraethylammonium hydroxides.

The involvement of the different precursors of the cation salts considered played a key role not only in generating the layered structure but also in preserving the memory effect, the optimal order being nitrates > chlorides > sulfates. Regardless of precursors type used, the textural properties followed the trend depending on the type of synthesis agent used, e.g., organic – narrow pore distribution up to 100Å, inorganic - large pore distribution up to 2000Å. TEM images confirmed the typical hexagonal shapes of LDH materials which were obviously compacted in the case of organic alkalis using. The use of quaternary salts did not prevent the oxidation of Fe^{2+} to Fe^{3+} under atmospheric working conditions.

The catalytic activities for the cyanoethylation between ethanol and acrylonitrile showed a linear variation with the basicity values presented by the solids (mixed oxides > reconstructed structure > parent LDH) [2]. The Claisen-Schmidt condensation between cyclohexanone and benzaldehyde led totally to the di-condensed product due to the ability of the single bond of the mono-condensed compound between cyclic fragments to twist inside the pores for a subsequent condensation with another aldehyde molecule. In the case of cyclohexanone self-condensation, the presence of the double bond between the cyclic fragments of the mono-condensed compound immobilizes the molecule so that the available space in the pores does not allow further condensation towards the di-condensed product, and thus the selectivity to the mono-condensate prevails.

Conclusions

Organic alkalis are a viable alternative to traditional inorganic ones, both for the co-precipitation method and for the non-traditional one, e.g. mechanochemical.

Acknowledgements

Funding from the Romanian Ministry of Research, Innovation and Digitalization is acknowledged within the project PNRR-III-C9-2022-I5-18 (contract 760010/2022).

References

[1] R. Zavoianu S.E. Taha, B.E. Cojocaru, V.I. Pârvulescu, O.D. Pavel, Catal. Today 435 (2024) 114693.
[2] B. Cojocaru, B.C. Jurca, R. Zavoianu, R. Birjega, V.I. Pârvulescu, O.D. Pavel, Catal. Commun. 170 (2022) 106485.

Catalytic Upgrading of Ulvan to Biochemicals Using Nb@Zeolites

Magdi El Fergani*, Natalia Candu, Iunia Podolean, Simona M. Coman
Department of Inorganic Chemistry, Organic Chemistry, Biochemistry and Catalysis, Faculty of Chemistry, University of Bucharest, 4-12 Regina Elisabeta Av., 030018 Bucharest, Romania
**Corresponding author: magdi.belkassim@chimie.unibuc.ro*

Introduction

There is a growing recognition of the need to develop innovative biomass-based processes for sustainable bioproduction in the chemical industry. These processes are considered carbon-neutral, as they do not introduce additional carbon dioxide into the atmosphere, making them an environmentally viable alternative to conventional methods [1]. In this context, green algae of the order ulvales frequently contribute to algal blooms in nutrient-rich coastal waters, leading to the accumulation of significant biomass that remains largely underutilized. Nevertheless, the sulfated polysaccharides known as ulvans, which form a major structural component of their cell walls, possess a unique chemical composition and structural properties. These characteristics make ulvans a promising raw material for the synthesis of high-value biomolecules [2].

This study aims to promote the marine bio-economy by exploring the potential of Ulva lactuca and its polysaccharide ulvan for biochemical production. To achieve this, novel and efficient Nb@zeolite catalysts were developed and applied in a one-pot conversion process, enabling the transformation of ulvan extracted from Ulva lactuca into rhamnose (Rha) and hydroxymethylfurfural (HMF) within mono/biphasic solvent systems. The integration of these catalysts offers a promising strategy for enhancing the valorization of marine biomass, contributing to the advancement of sustainable biochemical production.

Experimental

All the synthesis reagents were of analytic purity (Sigma-Aldrich). The zeolite-based catalysts were synthesized through a two-step post synthesis methodology, involving a dealumination of H-Beta and H-USY (CBV-720) zeolites (different Si/Al ratios) with nitric acid followed by its impregnation with Nb ethoxide (0.05 mol% Nb), then calcined in static air [3]. The synthesized Nb@Beta18 and Nb@Y30 nanostructured catalysts were comprehensively characterized using XRD, BET, DRIFT, NH_3, CO_2-TPD, and XPS techniques. The catalytic tests were conducted in a stainless steel autoclave as follows: 0.06 g of catalyst was added to 0.05 g of Ulvan in water. After sealing, the reactor was heated to 140-180 °C, under stirring for 6-24 h. Under comparable conditions, additional catalytic tests were performed in a biphasic solvent consisting of an aqueous solution of 20% NaCl and organic solvents (methyl isobutyl ketone (MIBK) and methyl isopropyl ketone (MIPK)). After the reaction, the catalyst was separated from the reaction and the products were identified by GC-MS and quantitatively analyzed by GC-FID chromatography.

Results and discussion

The prepared catalysts Nb@Beta18 and Nb@Y30 displayed a mono-modal mesoporosity and contain residual framework Al-acid sites, extra framework isolated Nb(V)O-H and Nb_2O_5 pore-encapsulated clusters, in which Nb(V)O-H (DRIFT and XPS analysis) exhibit moderate strength Brønsted acidity. The former species (Al extra-framework) preventing the solubilization of the zeolite framework in hot water. Also, the acidity of the zeolites improved and in association to the mesoporous texture generates an efficient environment for the hydrolysis/dehydration of Ulvan.

In the preliminary catalytic results, the Nb@Y30 catalyst demonstrated the highest selectivity of 51.8% for Rha at a conversion of 87.5% ulvan in the aqueous monophase system, under the conditions of 12 h and 180 °C. On the other hand, when the reaction was conducted in a biphasic system, the catalyst achieved a lower conversion of 46.7% ulvan, with a selectivity of 25.5% for HMF under identical reaction parameters.

Conclusions

These experimental results demonstrate that Nb@zeolite catalysts exhibit high activity in the hydrolysis of ulvan to Rha and FUR biomolecules. Moreover, zeolites, some of the most widely used catalysts in petrochemicals, can be modified in such a way as to become efficient catalysts for marine bio-economy.

A comprehensive analysis of the optimal catalytic features and reaction conditions, as well as the correlation between the catalytic performance and properties, will be provided.

Acknowledgements

The Romanian Ministry Research and Digitalization is acknowledged for funding within the grant PNRR-III-C9-2022-I5-18, ResPonSE, Project, No. 760010/2022.

References

[1] P. Sudarsanam, R. Zhong, S.V.D. Bosch, S.M. Coman, V.I. Parvulescu, B.F. Sels, Chem. Soc. Rev. 47 (2018) 8349.

[2] A. Robic, D. Bertrand, J.-F. Sassi, Y. Lerat, M. Lahaye. J. Appl. Phycol. 21 (2009) 451.

[3] M.E. Fergani, N. Candu, M. Tudorache, P. Granger, V.I. Parvulescu, S.M. Coman, Molecules 25(21) (2020) 4885.

Cell-Free Enzyme Engineering for Biocatalysis

András Telek[1,2], Viktor Gaják[2,3], Gergő Dargó[2], Jan Mican[4,5], David Bednar[4,5], Beáta G. Vértessy[1,6], Gábor Tasnádi[2]*
[1]*Department of Applied Biotechnology, Budapest University of Technology and Economics, Budapest, Hungary*
[2]*Servier Research Institute of Medicinal Chemistry, Budapest, Hungary*
[3]*Eötvös Loránd University, Institute of Chemistry, Budapest, Hungary*
[4]*Loschmidt Laboratories, Department of Experimental Biology and RECETOX, Masaryk University, Brno, Czech Republic*
[5]*International Clinical Research Center, St. Anne's University Hospital, Brno, Czech Republic*
[6]*Institute of Molecular Life Sciences, Research Centre for Natural Sciences, HUN-REN, Budapest, Hungary*
**Corresponding author: gabor.tasnadi@servier.com*

Despite the numerous advantages provided by enzymes and advancements witnessed in the related fields, the implementation of biocatalysis in the chemical and pharma industries has been slow [1]. This can be associated with technological, cultural, and financial reasons [2].

Two main obstacles of widespread adoption are the need for specialized facility and staff, and the long timelines of biocatalytic process development, especially that of enzyme engineering. The former could be addressed by using cell-free protein synthesis (CFPS) which enables the production of enzymes from an appropriate DNA template without bacterial manipulation [3]. The time needed to obtain an enzyme which can effectively be used for early chemical development of an API can be shortened by using semi-rational library design [4].

In this presentation, an innovative fully cell-free workflow will be highlighted which combines PCR-based synthesis of linear DNA fragments with CFPS providing activity information from an enzyme variant library within 2 days. Importantly, the cell-free nature of the protocol makes enzyme engineering accessible to organic chemistry labs without large investment into specialized laboratories. The simplicity of the protocol and the short turnaround time enable the demonstration of the synthetic utility of an enzyme in early phase of chemical development at Servier, a mid-sized pharma company. This could potentially bridge the gap between low-performing wild-type enzymes and expensive directed evolution campaigns, and ultimately could lead to the industrialization of more biocatalytic reactions in the future.

References

[1] E.O. Romero, A.T. Saucedo, J.R. Hernández-Meléndez, D. Yang, S. Chakrabarty, A.R.H. Narayan, JACS Au 3 (2023) 2073.
[2] F. Gallou, H. Gröger, B.H. Lipshutz, Green Chem. 25 (2023) 6092.
[3] J. Rolf, K. Rosenthal, S. Lütz, Catalysts 9 (2019) 190.
[4] Y. Bao, Y. Xu, X. Huang, Mol. Catal. 553 (2024) 113755.

LDH-Organic Sensitizer Composites for Decontamination of Water

Bogdan Cojocaru[1,2]*, Qays Al Hasnawi[1], Sabina Gabriela Ion[1,2], Mădălina Tudorache[1,2], Rodica Zăvoianu[1,2], Octavian Dumitru Pavel[1,2], Vasile I. Parvulescu[1,2]*
[1]University of Bucharest, Faculty of Chemistry, Departrment of Inorganic Chemistry, Organic Chemistry, Biochemistry and Catalysis, 4-12 Regina Elisabeta Blv, 030018 Bucharest, Romania;
[2]Research Center for Catalysts & Catalytic Processes, Faculty of Chemistry, University of Bucharest, 4-12 Regina Elisabeta Blv., Bucharest 030018, Romania
**Corresponding authors: vasile.parvulescu@chimie.unibuc.ro*
bogdan.cojocaru@chimie.unibuc.ro

Introduction

Photocatalytic degradation of the antibiotics is still an efficient method used to remove them from the water systems. The photocatalytic systems which involve supramolecular chemistry concepts use chromophores as photosensitizers, avoiding the limitations of the "classical" systems as TiO_2 related mostly to their large band-gap. Metallo-phthalocyanines (MPc) are electron donors that play the role of a substrate that can absorb the radiation in the visible range. This research aimed to synthesis of different magnetic-LDH systems incorporating metallo-phthalocyanines (Pc) and their application in to the removal through a simple and environmentally friendly method of β-lactams antibiotics from water.

Experimental

$Mg_{0.325}Fe_{0.325}Al_{0.25}$-LDH was synthesized using co-precipitation by inorganic ($NaOH/Na_2CO_3$) or organic alkali (TMAH). For the insertion of phthalocyanine (Fe, Cu or Ni-Pc) in the LDH structure, the latter's memory effect was exploited. The magnetic nanoparticles were attached to the LDH@MPc. Te samples were characterized by XRD, DRIFT, DR-UV-Vis, textural and elemental analysis.

Results and discussion

X-ray patterns are typical to LDH-type layered materials and magnetite. Lines corresponding to Fe_3O_4 can also be observed, which highlight the partial oxidation of Fe^{2+} to Fe^{3+}. Due to the presence of Fe^{3+} species, the samples exhibited a strong absorption around 500 nm (underlining their absorption capabilities in the visible domain) together with the characteristic bands of the metallo-phthalocyanines. The presence of the photosensitizers was also evidenced by DRIFT. Although TMAH can act also as a template molecule, besides being a synthesis agent, the surface area of the composites based on LDH-TMAH is smaller than the one of the composites starting from the LDH-NaOH. Also, the amount of sensitizer, determined by elemental analysis, is smaller for the LDH-TMAH based composites.

The composites were more active towards amoxicillin removal compared with ampicillin, Fig. 1.

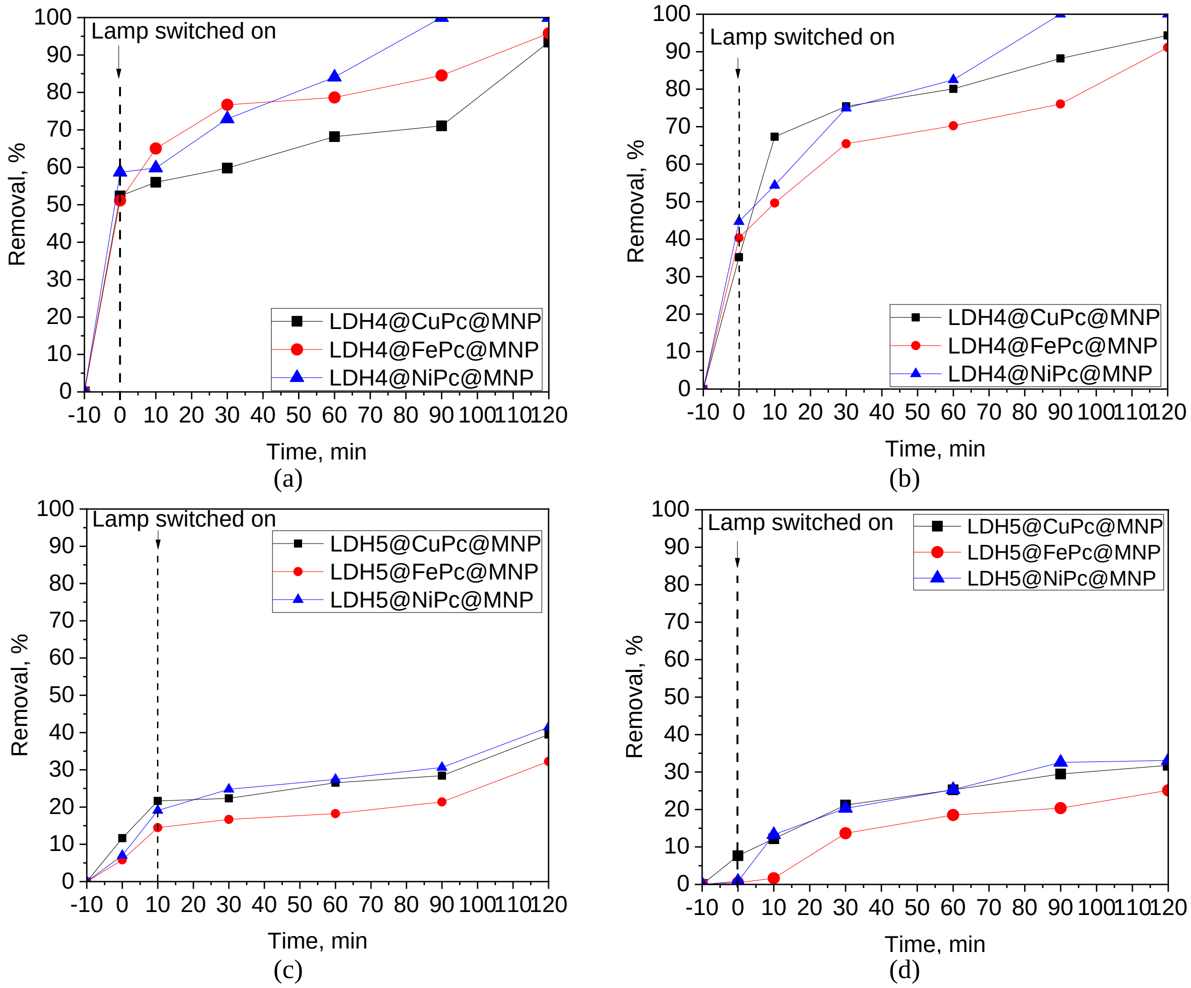

(a) (b) (c) (d)

Fig. 1. Removal % of amoxicillin using (a) LDH-NaOH; (c) LDH-TMAH and ampicillin using (b) LDH-NaOH; (d) LDH-based composites using a sunlight simulator.

The nature of the phthalocyanine did not have such a great influence, although some differences in the activity were observed. The removal was a combination between adsorption and photocatalytic degradation. The best composites for this application were those based on LDH-NaOH. They presented high adsorption capacity in 10 min and, in the same time, high photocatalytic activity for both amoxicillin and ampicillin

Conclusions

The magnetic-LDH-MPc systems can easely remove antibiotics by a synergetic effect between adsorption and photodegradation.

Acknowledgements

Funding from the Romanian Ministry of Research, Innovation and Digitalization is acknowledged within the project PNRR-III-C9-2022-I5-18 (contract 760010/2022).

References

[1] S.G. Ion, M. Tudorache, O.-D. Pavel, B. Cojocaru, Catalysts 14 (2024) 668.

Hierarchical Zeolite-Based Catalysts for Glycerol Acetalization

Oana Adriana Petcuta, Maria Balan, Vasile I. Parvulescu, Simona M. Coman*
Department of Inorganic Chemistry, Organic Chemistry, Biochemistry and Catalysis, Faculty of Chemistry, University of Bucharest, Regina Elisabeta Blvd., no. 4-12, Bucharest 030018, Romania
**Corresponding author: simona.coman@chimie.unibuc.ro*

Introduction

Glycerol is an important biorenewable feedstock which provide various opportunities for chemoselective transformation into other high value chemicals. In order to scale up the biodiesel industry to replace fossil fuels, glycerol valorization must be employed, as it has been found that resulting glycerol quantities could surpass current demand. In order to resolve the accumulation of glycerol as a waste, the catalytic valorisation of glycerol into value-added products (i.e. bio-polymers, polyunsaturated fatty acids, ethanol, hydrogen, n-butanol, glycerol carbonate, glycerol acetyl esters, etc.) is needed [1-3]. Acetalization is one of the many reactions that transform glycerol into useful products. When acetone is used as reactant, two glycerol ketals can be formed as reaction products, namely solketal (2,2-dimethyl-[1,3]-dioxane-4-yl-methanol) and 2,2-dimethyl-[1,3]-dioxane-5-ol. Glycerol acetals and ketals are good additives for diesel or biodiesel fuels, improving the octane number, cold flow properties, and reducing particle emissions [4].

Experimental

Starting from five different pristine zeolites fourteen different hierarchical micro-/mesoporous zeolite catalysts were prepared by various top-down methods (i.e., dealumininination, desilication and dealumination/desilication) either in conventional or microwave conditions. Obtained materials were characterized through XRD diffraction, liquid nitrogen adsorption-desorption isotherms at -196 °C, DRIFT spectroscopy and CO_2-/NH_3-TPD analysis. The catalytic experiments were carried out in closed glass vials in following conditions: 100 mg of catalyst, 1/3 glycerol/acetone molar ratio (1.56 g glycerol, 2.96 g acetone), and 40 °C. The resulted mixture was stirred at 700-1000 rpm for 1-6 h. After reaction, the products were separated by gravitational filtering into two phases: a clear aqueous phase and another phase that contains the catalyst and unreacted glycerol. The clear aqueous phase was silylated, diluted with ethyl acetate and analyzed with a GC-MS Carlo Erba Instruments (Waltham, MA, USA) QMD 1000 equipped with Factor Four VF-5HT column (30 m × 0.25 mm × 0.25 μm) and flame ionization detector (GC-MS-FID).

Results and discussion

The characterization methods showed a change in the framework molar Si/Al ratio and, therefore, a modification of their acidic/basic properties. However, the crystallinity of the zeolites after the structural modification was maintained in most of the cases. For exemplification the DRIFT spectra, XRD patterns and CO_2-TPD profiles of BEA 12.5 samples obtained by dealumininination or desilication are given in Fig. 1. Preliminary catalytic results showed that the most efficient material in terms of glycerol conversion (81%) and solketal selectivity (100%) was desilicated BEA12.5 and dealuminated BEA12.5 under MW irradiation. The structure of solketal was confirmed by ATR-FTIR spectroscopy and 1H, ^{13}C-NMR analysis. The screening of the catalysts is shown in Fig. 2.

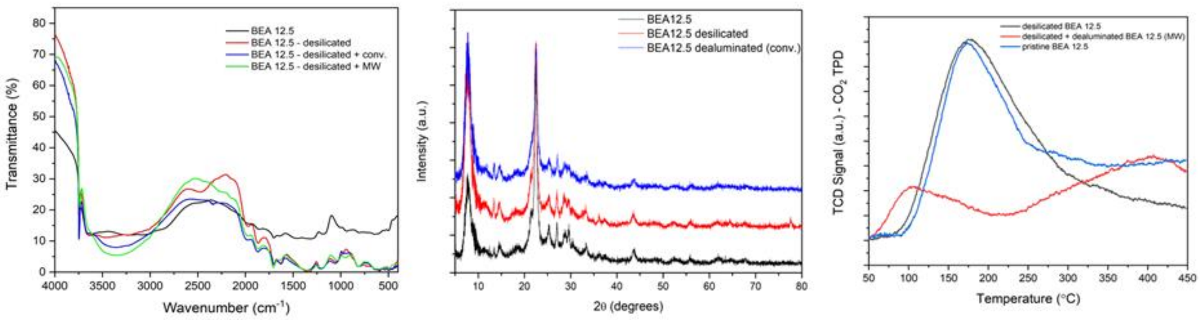

Fig. 1. DRIFT spectra for BEA 12.5 zeolite samples (left), XRD pattern for beta zeolite samples (middle), CO_2 TPD profiles of BEA 12.5 samples (right).

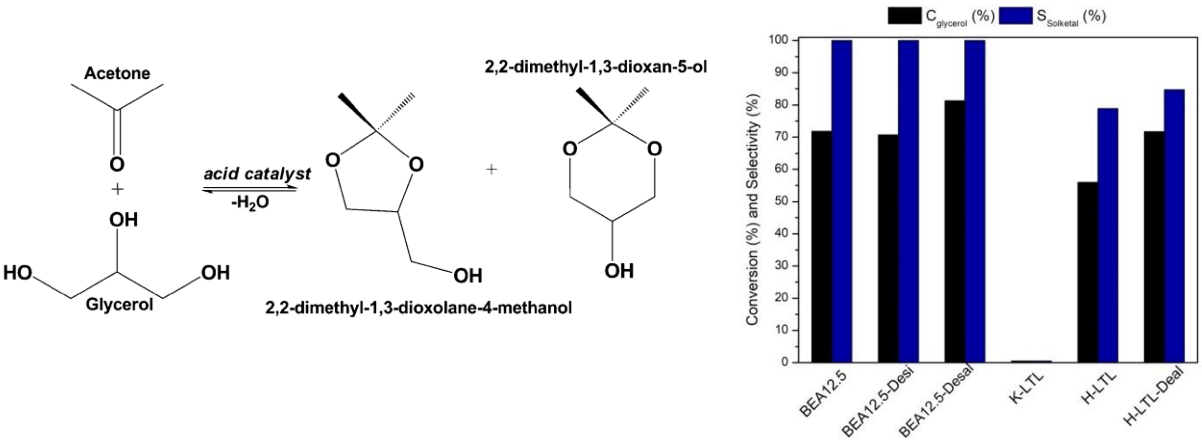

Fig. 2. Glycerol conversion and selectivity to Solketal in the presence of hierarchical zeolite-based catalysts. *Reaction conditions:100 mg catalyst, 1/3 glycerol to acetone molar ratio, 40 °C, 900 rpm, 6 h*.

Conclusions

A range of hierarchical micro-/mesoporous zeolite were successfully prepared, characterized and demonstrated to be efficient for glycerol acetalization to solketal. The best catalytic results and the catalytic features – catalytic efficiency correlation will be discussed.

References

[1] C. Bornes, I.C.M.S. Santos-Vieira, R. Vieira, L. Mafra, M.M.Q. Simões, J. Rocha, Catal. Today 419 (2023) 114159.
[2] J. Pradima, M.R. Kulkarni, A. Archna, Resource-Efficient Technologies 3 (2017) 394.
[3] A. Sandid, V. Spallina, J. Esteban, Fuel Process. Technol. 253 (2024) 108008.
[4] A.R. Trifoi, P.Ş. Agachi, T. Pap, Renew. Sustain. Energy Rev. 62 (2016) 804.

Biocatalytic Toolbox for the Synthesis of L- and D-Phenylalanines

László Csaba Bencze*, Raluca Bianca Tomoiaga, Krisztina Kelemen, Souad Diana Tork, Levente Csaba Nagy
Enzymology and Applied Biocatalysis Research Center, Babeș Bolyai University, Arany János Street 11, 400028 Cluj-Napoca, Romania
**Corresponding author: laszlo.bencze@ubbcluj.ro*

Introduction

Due to increasing emphasis on enantiopure chiral starting materials, enantiopure l- and d-phenylalanines have emerged as valuable building blocks. Since biocatalytic approaches provide an eco-friendly, stereoselective alternative to traditional chemical routes, we explored several L- and D-amino acid producing enzymes for the production of these highly valuable enantiopure phenylalanines. Thus, our focus targeted phenylalanine ammonia-lyases (PALs, EC 4.3.1.24/25), which catalyze the ammonia addition onto *trans*-cinnamic acids providing optically pure l-phenylalanine**s**. Their applicability on industrial scale has been demonstrated by the multi-ton scale production of (*S*)-2,3-dihydro-1*H*-indole-2-carboxylic acid by DSM [1] or by the synthesis of (3*S*)-5-(benzyloxy)-2-(diphenylacetyl)-6-methoxy-1,2,3,4-tetrahydro-isoquinoline-3-carboxylate (Olodanrigan, also known as EMA 401) by Novartis [2]. However, the limited substrate tolerance of the *wild-type* PALs from various sources still hinders their wider synthetic applications [3] recent protein engineering studies focusing on extending the substrate scope of PALs [4-6]. For the synthesis of D-Phes we targeted and explored the reductive amination of phenylpyruvated catalyzed by engineered D-amino acid dehydrogenases (DAADHs), while also attempting the stereoselectivity reversal of PALs within the ammonia addition reaction.

Results and discussion

Using rational design we developed several engineered PALs with enhanced activity toward high-value substrates [6,7]. Further, we combined our rational design approach with an extensive saturation mutagenesis strategy, both procedures unveiling variants of improved activity towards the targeted 3,4-dimethoxy-phenylalanine [8]. Using data mining as alternative strategy for identifying novel PALs with activity toward challenging substrates, we explored several bacterial aromatic ammonia-lyases that exhibit unique selectivity-modulating residues and distinct substrate specificity compared to currently explored AALs [9]. Further, using the in-house engineered PALs, we optimized and provided efficient gram-scale synthetic procedure for several L-phenylalanine analogues [10]. Our recent attempts have been focused on the stereoselectivity reversal of PALs.

The stereoselective synthesis of d-phenylalanines we approached through a chemoenzymatic cascade, combining the Knoevenagel-Doebner condensation, yielding *trans*-cinnamic acids from benzaldehydes, with the PAL-catalysed ammonia addition reaction, providing the corresponding L-Phes. The sequential oxidation by L-amino acid deaminase (LAAD) leads to phenylpyruvic acids, which upon reductive amination by DAADH whole-cell biocatalysts produces the desired D-phenylalanines. After optimizing key process parameters, we successfully obtained several D-phenylalanines on a 500 mg-preparative-scale. In another attempt we focus on the development of an alternative procedure using immobilized chemo-and biocatalyst within a continuous-flow procedure [11].

Acknowledgements

This work was financed by the project “Advanced (multi)-enzymatic synthesis and purification processes for biobased furan derivatives – ASPIRE” funded by European Union – Nextgeneration EU and Romanian Government, under National Recovery and Resilience Plan for Romania, contract no. 760042/23.05.2023, cod PNRR-III-C9-2022-I8-ASPIRE/PNRR2022, through the Romanian Ministry of Research, Innovation and Digitalization, within Component 9, Investment I8.

References

[1] B. de Lange et al. ChemCatChem 3 (2011) 289.
[2] L. Hardegger et al. Org. Process Res. Dev. 24 (2020) 1763.
[3] F. Parmeggiani, et al. Chem. Rev. 118 (2018) 73.
[4] L.C. Bencze, A. Filip et. al. Org. Biomol. Chem. 15 (2017) 3717.
[5] S.T. Ahmed et al. ACS Catal. 8 (2018) 3129.
[6] E.Z.A. Nagy, S.D. Tork et al. ACS Catal. 9 (2019) 8825.
[7] S.D. Tork, M.E. Moisă, L. Cserepes, A. Filip, L.C. Nagy, F.D. Irimie, L.C. Bencze, Sci. Rep. 12(1) (2022) 10606.
[8] R.B. Tomoiagă, S.D. Tork, A. Filip, L.C. Nagy, L.B. Bencze, Appl. Microbiol. Biotechnol. 107 (2023) 3507.
[9] R.B. Tomoiagă, G. Ágoston, K. Boros, L.C. Nagy, M.I. Toşa, C. Paizs, L.C. Bencze, ChemBioChem (2024) e202400011.
[10] S.D. Tork, E.Z.A. Nagy, R.B. Tomoiagă, L. Bencze, J. Org. Chem. 88 (2023) 852.
[11] K. Boros, L. Gal, C.A. Gal, M. Wäscher, R.B. Tomoiagă, M.I. Toşa, J. Pietruszka, L.C.Bencze, Proc. Biochem. 140 (2024) 45.

Synthesis of Polyesteramides Using Innovative Biocatalytic Pathways

Ioana Cristina Benea[1], Anamaria Todea[1], Alessandro Pellis[2], Ioan Bîtcan[1], Diana Maria Dreavă[1], Francisc Péter[1]*

[1]University Politehnica Timişoara, Faculty of Chemical Engineering, Biotechnology and Environmental Protection, Blvd. V. Pârvan 6, Timişoara, Romania

[2]Università degli Studi di Genova, Dipartimento di Chimica e Chimica Industriale, Via Dodecaneso 31, 16146, Genova, Italy

**Corresponding author: francisc.peter@upt.ro*

Introduction

Lipases are enzymes well known for their versatility to catalyze a variety of synthetic reactions alongside hydrolysis, including esterification, transesterification, amidation, and even epoxidation, polycondensation and ring-opening polymerization. The utilization of lipases for *in vitro* synthesis of oligomers and polymers with defined structures came to the forefront of biocatalysis in the last decades, when numerous polyesters and polyamides were synthesized using biocatalytic pathways [1]. Recently, polyesteramides had also received increasing interest due to the presence of both ester and amide bonds in their backbone resulting in better robustness and improved mechanical and thermal properties compared to polyesters, together with the preservation of the biodegradability and biocompatibility. Such improved properties can allow extended applicability, particularly in the biomedical domain, e.g., as nanosized drug carriers [2,3]. Moreover, if the monomers are from renewable biomass sources, the whole process becomes sustainable and green, as illustrated in Fig. 1. Nevertheless, the biocatalytic synthesis of copolymers or terpolymers with alternating ester and amide bonds is not an easy task, needing a suitable approach concerning the selection of the biocatalyst, reaction system, reaction conditions and work-up procedure. In this presentation, our recent results concerning the lipase-catalyzed synthesis of new polyesteramides by various biocatalytic pathways will be summarized.

Experimental

Polyesteramides from ε-caprolactam and hydroxy acids were synthesized in solventless or organic media using 2 mL Eppendorf tubes and a Thermomixer Comfort heating shaker. Immobilized *Candida antarctica* B lipase (Novozyme 435) was the biocatalyst, and the reactions were typically carried out for 24 h at 80 °C. The product was isolated by extraction with THF and evaporation of the solvent. Random and block terpolyesteramides from ε-caprolactone, (CL) 1,8-octanediamine (ODA) and either dimethyl itaconate (DMI) or dimethyl adipate (DMA) were obtained using the same biocatalyst at 85 °C in 10 mL round-bottom flasks connected to a rotary evaporator, at 80 °C and 1000 mbar pressure for 6 h, and subsequent for 42 h at 12 mbar vacuum. The monomer conversions and average molecular weights were determined by GPC, while MALDI-TOF MS was used for identification of the molecular species and estimation of the relative composition of the products.

Results and discussion

The synthesis of polyesteramides from ε-caprolactam and a hydroxy acid (L-malic, 3-hydroxybutyric, 12-hydroxystearic, or 16-hydroxyhexadecanoic acid) using Novozyme 435 as catalyst, Fig. 1, yielded oligoesteramides with average molecular weights depending on the structure of the co-monomer. Using short chain hydroxy acids holding secondary hydroxyl groups (L-malic and 3-hydroxybutyric acid) the average degree of polymerization (DP) was no higher than 4, while in the case of 12-hydroxystearic acid the longer hydrocarbon chain between the reactive groups led to DP value increased to 7. The best results were obtained for the long-chain hydroxy acid with primary hydroxyl group, 16-hydroxyhexadecanoic acid, yielding a product with 75% copolymer content and Mw higher than 3000 Da [3].

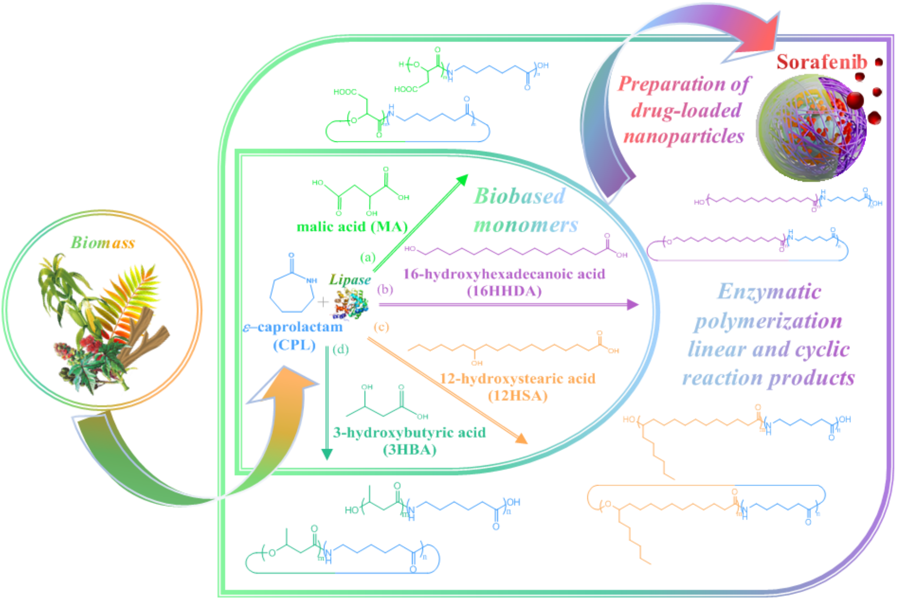

Fig. 1. Synthetic strategy for biocatalytic synthesis of polyesteramides from ε-caprolactam and hydroxy acids.

Considering the CL:DMA:ODA terpolyesteramides, lower molecular weights were obtained for the random copolymers (M_w 4360 Da) compared to the block copolymers (M_w 5160 Da). An increase in the degree of polymerization was also observed, from 7.3 in the case of random copolymers to 9.9 for the block copolymers [4]. This innovative approach of enzymatic block copolymerization could allow further developments for new speciality biobased polymers.

Acknowledgements

This work was partially supported by a grant of the Romanian Ministry of Education and Research, CCCDI - UEFISCDI, project number PN-III-P2-2.1-PED-2019-2638, within PNCDI III, contract number 272PED.

References

[1] Y. Jiang, K. Loos, Polymers 8 (2016) 243.
[2] A. Todea, D.M. Dreavă, I.C. Benea, I. Bîtcan, F. Peter, C.G. Boeriu, Processes 9 (2021) 646.
[3] I.C. Benea, I. Kántor, A. Todea, A. Pellis, I. Bîtcan, L. Nagy, S. Kéki, D.M. Dreavă, F. Péter, T. Feczkó, React. Funct. Polym. 191 (2023) 105702.
[4] I.C. Benea, D. Dăescu, A. Todea, L. Nagy, S. Keki, I. Păuşescu, A. Pellis, F. Peter, Int. J. Biol. Macromol. 282 (2025) 137046.

Synthesis and Applications of Sulfonyl and Sulfinyl Containing Compounds

Noemi Deak[1]*, David Madec[2], Gabriela Nemes[1]
[1]Babeş-Bolyai University, Faculty of Chemistry and Chemical Engineering, Arany János street, no.11, 400028, Cluj-Napoca
[2]Université de Toulouse, UPS, LHFA, UMR-CNRS 5069, 118 Route de Narbonne, F-31062 Toulouse, France
**Corresponding author: noemi.deak@ubbcluj.ro*

Introduction

Sulfinyl and sulfonyl containing compounds are proven to have multiple applications, for example as biologically active derivatives, fine chemicals, pharmaceuticals, ligands in catalyst structures, material chemistry, etc. [1] For this reason, their synthesis presents an interest in the scientific community [1].

The significance of compounds containing sulfoxide and/or sulfone groups was highlighted by our research group as well [2,3] in the design and application of novel pincer type ligands. These O,C,O-chelating pincer ligands, Fig. 1, with sulfonyl or sulfinyl moieties as ortho substituents, can be used for obtaining transition metal complexes and *p* block element containing derivatives [2]. These remarkable results made us work on continuously improving the processes for the synthesis of sulfoxides and sulfones employing different strategies.

Results and discussion

Among the synthetic pathways we investigated for the synthesis of the sulfonyl and sulfinyl containing compounds, Fig. 1, we would like to mention the cross coupling reactions between 1,3-dibromo-5-tert-butylbenzene and the corresponding sulfinate or thiol. These reactions were tested with either palladium or copper catalyst.

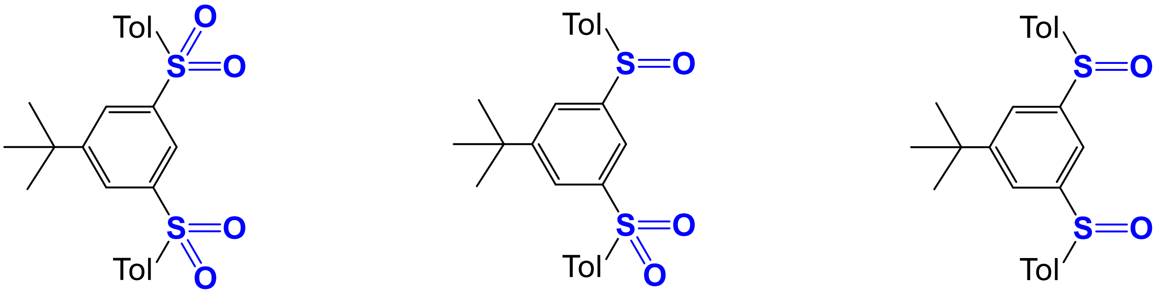

Fig. 1. Sulfonyl and sulfinyl containing compounds obtained in the presented work.

Another approach for obtaining the target compounds shown in Figure 1, was the oxidation of the bis-thioethers. For this, different conditions were evaluated, particularly vanadium catalyzed sulfoxidations [4].

Conclusions

In conclusion, different synthetic strategies were employed for the synthesis of sulfonyl and sulfinyl containing compounds, among which palladium or copper catalyzed cross coupling reactions and vanadium catalyzed sulfoxidation reactions.

References

[1] I. Fernández, N. Khiar, Chem. Rev. 103 (2003) 3651.
[2] N. Deak, D. Madec, G. Nemes, Eur. J. Inorg. Chem. 29 (2020) 2769.
[3] N. Deak, O. Thillaye du Boullay, S. Mallet-Ladeira, I.-T. Moraru, D. Madec, G. Nemes, Eur. J. Inorg. Chem. 2020(39) (2020) 3729.
[4] N. Deak, M. Idboumlik, A. Soran, M. Lachkar, B. El Bali, G.Nemes, Studia UBB Chemia LXIX 3 (2024) 7.

Cold Plasma Treatment of Liquid Phase Glycerol at Atmospheric Pressure

Cristian Tudoran, Gabriela Blăniţă, Maria Coroş*
National Institute for Research and Development of Isotopic and Molecular Technologies,
67-103 Donat Street, Cluj-Napoca 400293, Romania
**Corresponding author: maria.coros@itim-cj.ro*

Introduction

Glycerol, a tribasic alcohol, is the major by-product of biodiesel production - approximately 10% of overall production [1]. Recently, extensive numbers of literature papers have been reported on glycerol transformation to more profitable products using various methods [2]. Among them, plasma treatment showed promising results [3]. Plasma, the fourth state of matter, is an ionized gas containing a multitude of active species: electrons, free radicals, ions, etc.

In this paper we present the design, construction, assembly and laboratory testing of a portable reactor for the reconversion of glycerol using cold plasma [4].

Experimental

The experiments were performed using 5 mL of sample, air was used as plasmogenic gas, at a discharge supply voltage of 10 V and a discharge frequency of 100 kHz. The investigated reaction parameters were: reaction time (3, 5 and 7 min) and concentration of the reaction mixture (aqueous solutions of glycerol 0.1 M, 0.5 M, 1 M, 3 M and 5 M. The input power was 20 W. The reactions were monitored using UV-Vis spectrometry. The portable microreactor described here has been designed and built for chemical reactions assisted by cold plasma. Its purpose is to provide users with a versatile, simple, and robust device. The reaction cell of the microreactor consists of a coaxial arrangement of two tubes, positioned vertically, Fig 1. The liquid sample, in the form of a film, passes through an electrical discharge (plasma).

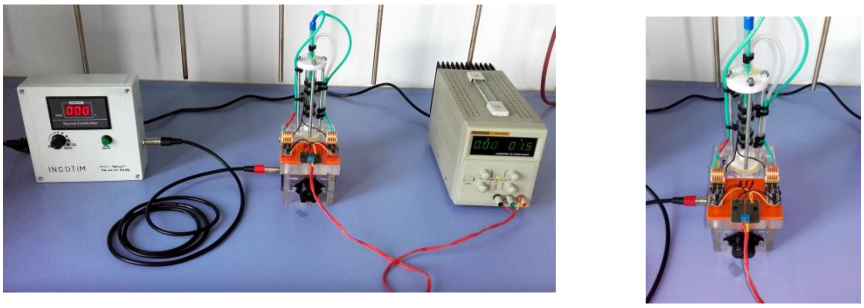

Fig. 1. Cold plasma microreactor (left); cold plasma reaction cell (right).

Results and discussion

The tests performed in the cold plasma reactor, with a dielectric barrier discharge cell, consisted of *i)* plasma diagnosis, *ii)* flow regulation of the reaction mixture through the cold plasma reactor, *iii)* investigation of the reaction parameters (reaction time, reaction mixture concentration) and *iv)* investigation of the discharge parameters (input power). Plasma diagnosis study was performed at different power levels: 1, 2, 5, 6, and 10 W. In the recorded spectra of the electric discharge emission generated inside the reaction chamber, the emission lines of O_2, H_2 as well as the molecular bands of NO, and OH, Fig. 2, were observed.

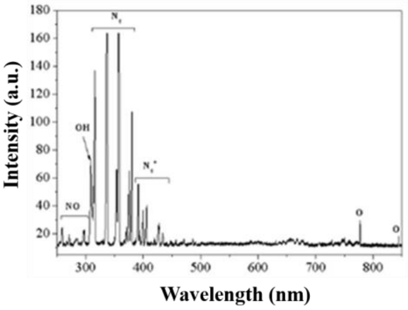

Fig. 2. UV-Vis emission spectrum of the electrical discharge in the reaction chamber.

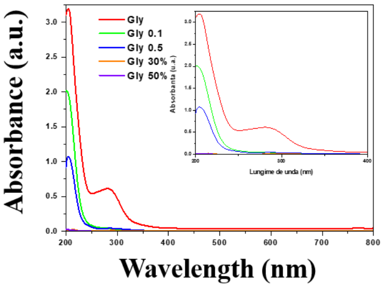

Fig. 3. UV-Vis spectra of the glycerol solutions treated for 5 minutes with cold plasma.

In all cases, the decrease until the disappearance of the signal at ~280 nm, specific to glycerol, was observed, which implies its transformation into other products. Fig. 3 shows the evolution of the absorption spectra for the 5-minute exposure time.

Conclusions

The tests performed for the glycerol oxidation in the cold plasma reactor consisted of *i)* plasma diagnosis, *ii)* flow of the reaction mixture through the cold plasma reaction chamber, *iii)* investigation of the reaction parameters (reaction time, reaction mixture concentration) and *iv)* investigation of the discharge parameters (input power), with the aim of optimizing the operating conditions.

Acknowledgements

This work was supported through the “Nucleu” Program within the National Research Development and Innovation Plan 2022–2027, Romania, carried out with the support of MEC, project no. 27N/03.01.2023, component project code PN 23 24 01 01.

References

[1] R.L. Naylor, M.M. Higgins, Glob. Food Sec. 16 (2018) 75.
[2] J. Prasad, B. Modhera, Int. J. Hydrogen Energy 109 (2025) 823.
[3] S. Bang, R. Snoeckx, M.S.Cha, ChemSusChem 17 (2024) e202300925
[4] M. Coroş, C. Tudoran, G. Blăniță, D. Lazăr, Inventors, INCDTIM assignee, Romanian patent application 00712/18.11.2024

Graphene Derivatives as Cocatalysts in the Photodegradation of Organic Pollutants with Titania Nanotubes

Crina Socaci*, Marcela C. Rosu, Alexandra Urda, Dragos Cosma, Diana Lazar, Maria Mihet, Teodora Radu
National Institute for Research and Development of Isotopic and Molecular Technologies, 67-103 Donat, 400293 Cluj-Napoca, Romania
**Corresponding author: crina.socaci@itim-cj.ro*

Introduction

Photocatalysis is a promising oxidation technique capable of degrading organic contaminants using UV and visible light exposure [1]. The photonic efficiency of the most common photocatalyst, titanium dioxide, is under 10% for most of the degradation processes due to its restricted sensitivity to UV light. In order to improve the photocatalytic efficiency, several methods have been developed: doping with 3d transition metals like Co, Ni, Mn, Fe or noble metals, mainly silver or gold and lately, the preparation of hybrids with other nanomaterials. Among nanomaterials, graphene showed their potential as electron cocatalyst to enhance the photocatalytic efficiency of semiconductors. Starting from the common agreement regarding the positive impact of the graphene-based material on the photocatalytic activity of TiO_2 containing composites, we prepared, characterized and tested a series of composites containing metal or metal oxides nanoparticles, graphene oxide, reduced graphene oxide or nitrogen-doped graphene and titania nanotubes for the degradation of some model emerging pollutants. [2,3].

Experimental

The surface morphology and structural aspects of the prepared nanocomposites were assessed by SEM/TEM microscopy, powder X-Ray diffraction measurements and XPS spectroscopy, while the optical characteristics by measuring the DR UV-Vis spectra and calculating the bandgap energies. The photocatalytic performance was evaluated using a visible light LED source and the time evolution of degradation by high-performance liquid chromatography. The influence of the graphene derivative in the composite was evaluated in terms of its role in the adsorption process, in the charge separation or band alignments associated with the photocatalytic processes.

Results and discussion

The DR UV-Vis spectra of Au and NiO nanoparticles decorated titania nanotubes with graphene derivatives are presented in Fig. 1. A small shift of the maximum optical absorption of TiO_2 is observed for both type of composites. In addition, the presence of Au nanoparticles is further extending the absorption to the visible light domain.

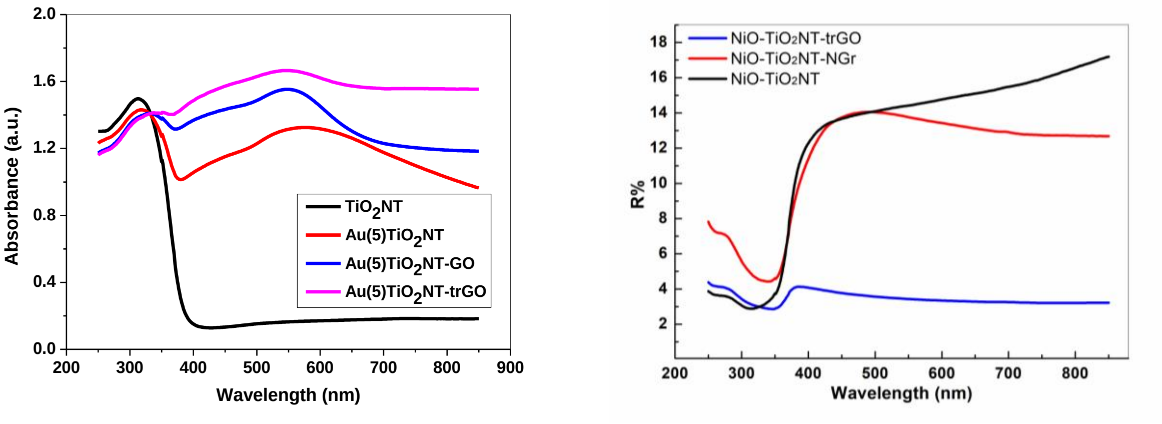

Fig. 1. UV-Vis absorption spectra of Au and NiO-TiO_2NT-graphene composites.

The photocatalytic activity experiments on the NiO-TiO_2NT composites showed that reduced graphene oxide (trGO) was having a better influence as compared to the nitrogen-doped graphene (NGr) - 20% to 55% for amoxicillin; 24% to 50% for acetaminophen and 8 to 74% for estradiol visible light photodegradation. Similarly, the photocatalytic efficiency of Au-TiO_2NTs was considerably improved by addition of graphene oxide (GO) or reduced graphene oxide (trGO) - from 20% or less β-estradiol degradation to 100% (for GO) or 50% (for trGO).

The obtained data were correlated with the XPS spectra and valence band determinations and the mechanisms behind the graphene derivatives presence was explored.

Conclusions

When the proper band alignment exists, the enhancement in the photocatalytic behavior of the decorated titania nanotubes and graphene derivatives was due either to an electron transfer from titania to the graphene derivative in case of NiO-containing composite, or to the clearly improved absorption step in case of the Au-containing composites.

Acknowledgements

This work was supported by the Ministry of Education and Research, under Romania’s National Recovery and Resilience Plan PNRR-III-C9-2022-I8 program with Project code 167/15.11.22.

References

[1] S.C. Ameta, R. Ameta, Advanced oxidation processes for waste water treatment-emerging green chemical technology, Chapter 6 – Photocatalysis, Academic Press (2018) 135-175.

[2] A. Urda, T. Radu, K.R. Gustavsen, D. Cosma, M. Mihet, M.C. Rosu, A. Ciorîța, A. Vulcu, K. Wang, C. Socaci, J. Phys. D: Appl. Phys. 58 (2025) 015103.

[3] D. Cosma, M.-C. Roşu, C. Socaci, A. Urda, T. Radu, A. Turza, M. Dan, R. M. Costescu, K. R. Gustavsen, O. Dobroliubov, K. Wang, J. Environ. Chem. Eng. 12(3) (2024) 112885.

Development of Beta-Lactamase Inhibitors

Jürgen Brem[1,]*, Christopher J. Schofield[2]
[1]Enzymology and Applied Biocatalysis Research Center, Faculty of Chemistry and Chemical Engineering, Babes-Bolyai University, Cluj-Napoca, Roman
[2]Department of Chemistry, Chemistry Research Laboratory and the Ineos Oxford Institute for Antimicrobial Research, University of Oxford, Oxford, United Kingdom
**Corresponding author: jurgen.brem@ubbcluj.ro*

Introduction

Antibiotic resistance is arguably one of the biggest public health threats. β-Lactam antibiotics are the most important class of antibacterials, but their use is increasingly compromised by resistance, most importantly via serine- and or metallo-β-lactamase (SBL & MBL) catalyzed hydrolysis. Carbapenems, known as ‘drugs of last resort’, manifest improved stability to extended-spectrum SBLs, although they are hydrolyzed by SBLs with carbapenemase activities and all MBLs. Hence the development of MBL inhibitor(s), especially to protect carbapenems, is thus an unmet clinical need, in particularly in the developing world, where MBL-producing bacteria are widely disseminated.

Results and discussion

Considering that the β-lactam-mediated SBL inhibition by clavulanic acid has been successfully employed in the clinic via imitating the initial substrate binding mode and that β-lactam antibiotics are mimics of the substrates of their transpeptidase targets (penicillin-binding proteins), we proposed that an analogous ‘substrate/intermediate-mimic focused’ approach may enable the identification of broad-spectrum MBL inhibitors (MBLIs).

We conducted various high throughput screenings as an effort of public–private partnerships that led to the identification and optimization of cyclic boronates and indole carboxylates as broad-spectrum carbapenemase/MBLIs [1,2].

These compounds have an unprecedented MBL (in some cases SBL) binding mode, which is different with regards to those of both carbapenem substrates and their hydrolysis products. They protect carbapenems minimum from MBL activity in multidrug-resistant (MDR) and extensively drug-resistant (XDR) Gram-negative pathogens, and one of the series shown activity in multiple *in vivo* mouse infection models.

Conclusions

Overall, we discovered and/or further developed & characterized these new classes of inhibitors. They represent new types of metalloenzyme inhibitors that works via unprecedented mechanism of actions. These mechanism may be of utility not only for MBLs, but also in the inhibition of other classes of MBL fold hydrolases that are medicinal chemistry targets and more generally for the inhibition of metallohydrolases.

Acknowledgements

We thank the ELF Screening partners for efforts leading to the initial hits, the ENABLE Portfolio Management Committee (PMC) members and EFPIA partners for guidance, and the Diamond Light Source synchrotron for access to the IO3, IO4 and IO4-1 beamlines.

The Oxford work was also supported by Cancer Research UK, the Medical Research Council, the Biotechnology and Biological Research Council and the Ineos Oxford Institute for Antimicrobial Research (C.J.S.).

J.B. thanks the BACPROBIO project, funded by European Union – NextGenerationEU and the Romanian Government, under National Recovery and Resilience Plan for Romania, contract no

760251./28.12.2023, code PNRR-C9-I8-CF92/31.07.2023 through the Romanian Ministry of Research, Innovation and Digitalization.

References

[1] J. Brem, T. Panduwawala, J.U. Hansen et al., Nature Chem. 1 (2022) 15.
[2] J. Brem, R. Cain, S. Cahill, M. A. McDonough, I. J. Clifton, J.-C. Jiménez-Castellanos, M. B. Avison, J. Spencer, C. W. G. Fishwick, C. J. Schofield, Nature Commun. 7 (2016) 12406.

Phosphine- and Stibine- Ligated Cyclometalated Palladium Complexes: Synthesis, Characterization and Evaluation of the Catalytical Properties

Raffaele Fontana*, Levente Kiss, Lucian C. Pop, Cristian Silvestru

Babeș-Bolyai University, Faculty of Chemistry and Chemical Engineering, Department of Chemistry, Supramolecular Organic and Organometallic Chemistry Centre, 11 Arany Janos Street, RO-400028, Cluj-Napoca, Romania

**Corresponding author: raffaele.fontana@stud.ubbcluj.ro*

Introduction

Cyclometalated palladium(II) compounds have attracted increasing attention in organometallic chemistry, finding applications in organic synthesis and in catalysis. Several groups have focused their research in this area, enhancing and tuning the palladacycles catalytic capabilities, by modifying their electronic and steric properties [1]. On this basis many efforts were made to develop highly effective catalysts for reactions such as Suzuki cross-coupling and homocoupling of phenylboronic acids to obtain nonsymmetric and symmetric compounds, respectively [2,3].

Experimental

General Suzuki cross-coupling reaction: an aryl halide was mixed with phenylboronic acid, potassium carbonate and a palladium-based catalyst in methanol. The reaction mixture was stirred at room temperature for 30 min under aerobic conditions. After the reaction mixture was dried under reduced pressure and the crude solid was extracted with hexane, the product was purified through flash chromatography on silica gel to afford the product. The yields were determined by ^{1}H NMR spectroscopy.

Results and discussion

The main objectives of this research work concern (*i*) the design and synthesis of a new series of neutral and ionic compounds containing the five-membered palladacycle fragment $[2\text{-}\{O(CH_2CH_2)NCH_2\}C_6H_4]Pd(II)$ in which the palladium is coordinated to by different donor atoms (P and Sb) in the ancillary ligand, Scheme 1, (*ii*) their structural characterization by multinuclear NMR spectroscopy in solution and single-crystal X-ray diffraction, and (*iii*) evaluation of their catalytic properties towards homocoupling and Suzuki cross-coupling reactions

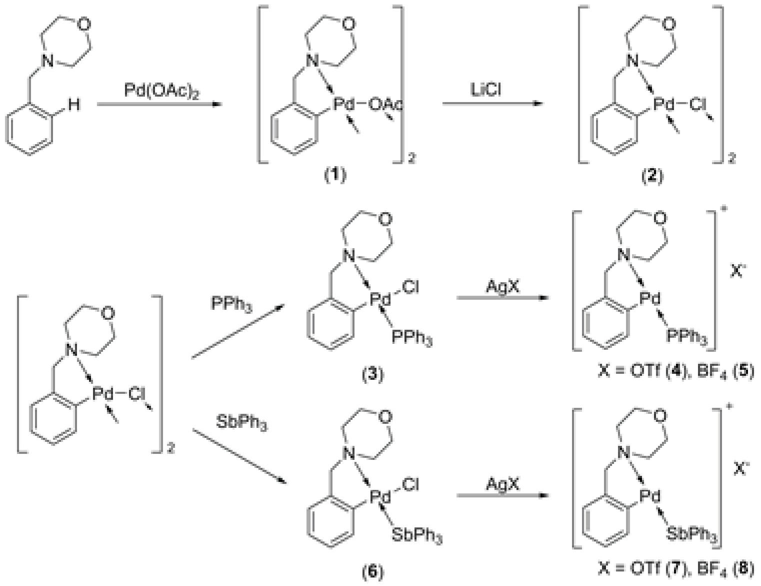

Scheme 1. Synthesized palladium complexes.

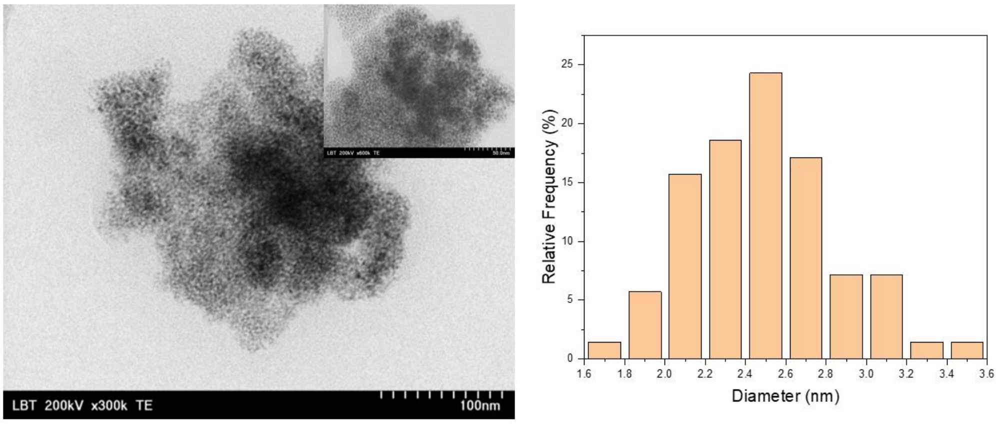

Fig. 1. TEM image (a) and Pd nanoparticle size distribution histogram (b). Inset shows a zoomed image of the Pd nanoparticle from the first cycle.

Conclusions

The obtained compounds act as efficient precatalyst leading to the formation of the active Pd(0) catalytic species. The implemented catalytic system allowed us to successfully catalyse Suzuki cross-coupling and homocoupling reactions at room temperature, using low catalyst loading and short reaction times without negatively affecting the reaction yield. The obtained Pd(0) nanoparticles were also morphologically characterized through TEM, and they were further used in catalytic tries showing the possibility of easily recovering of the catalyst (Fig. 1).

References

[1] H. Wang, J. Yang, Appl. Organometal. Chem. 30 (2016) 262.
[2] K; Karami, N. Rahimi, M.B. Shehni, Tetrahedron Lett. 53 (2012) 2428.
[3] D.A. Kader, M.K. Sidiq, S.G. Taher, D.M. Aziz, J. Organomet. Chem. (2025) 1030.

Organoselenium Compounds as Antioxidants and Catalysts

Anca Silvestru*
Supramolecular Organic and Organometallic Chemistry Centre, Chemistry Department, Faculty of Chemistry and Chemical Engineering, Babes-Bolyai University, 11 Arany János Street, 400028 Cluj-Napoca
**Corresponding author: anca.silvestru@ubbcluj.ro*

Organoselenium chemistry emerged a continuously increased interest during last years based on their importance in fundamental and applied research. Diorganoselenides proved to be valuable candidates as catalysts in organic synthesis [1], precursors for nanomaterials [2] or agents with a significant antioxidant, antiproliferative, anti-inflammatory or antidepressant activity [3]. It was observed that the presence of additional nitrogen donor atoms capable for intramolecular coordination has a significant influence not only on the structure and stability of the organoselenium species, but also on their reactivity and specific properties [4].

Recently we were interested on new homo- and heteroleptic diorganoselenium(II) compounds bearing aryl groups decorated with pendant arms capable for C,N coordination, and/or alkyl groups bearing various functionalities, e.g., OH, pyrazole, pyridine, etc., as depicted in Scheme 1.

The antioxidant behavior and catalytic activity of several diorganoselenides bearing pyrazole or pyridine functionalities was investigated on the oxidation reaction of PhSH with H_2O_2 by a combination of analytical methods (^{1}H and ^{77}Se NMR, UV-Vis spectroscopy).

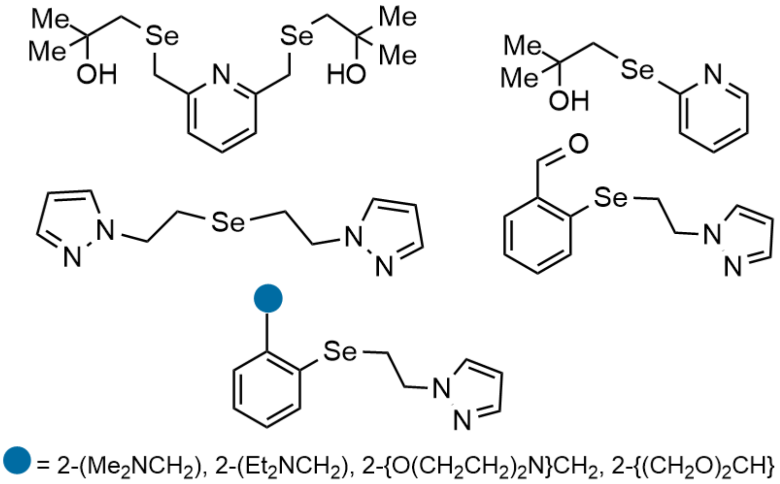

● = 2-(Me_2NCH_2), 2-(Et_2NCH_2), 2-{O(CH_2CH_2)$_2$N}CH_2, 2-{(CH_2O)$_2$CH}

Scheme 1. Organic groups in the homo- and the heteroleptic diorganoselenium(II) compounds.

References

[1] A. Kumar, G.K. Rao, A.K. Singh, Dalton Trans. 41 (2012) 11949.
[2] R. Gui, H. Jin, Z. Wang, L. Tan, Coord. Chem. Rev. 296 (2015) 91.
[3] B. Banerjee, M. Koketsu, Coord. Chem. Rev. 339 (2017) 104.
[4] A.J. Mukherjee, S.S. Zade, H.B. Singh, R.B. Sunoj, Chem. Rev. 110 (2010) 4357.

Design of Fe-Doped ZIF-67 Derived Carbon Catalysts for HMF Oxidation

Mihai Bordeiasu[1,2], Joanna Goscianska[2], Vasile I. Parvulescu[1], Simona M. Coman[1]*
[1]*Department of Inorganic Chemistry, Organic Chemistry, Biochemistry and Catalysts, Faculty of Chemistry, University of Bucharest, Regina Elisabeta Blvd., no. 4-12, Bucharest 030018, Romania*
[2]*Department of Chemical Technology, Faculty of Chemistry, Adam Mickiewicz University in Poznań, Uniwersytetu Poznańskiego 8, Poznań, 61-614, Poland*
**Corresponding author: simona.coman@chimie.unibuc.ro*

Introduction

5-Hydroxymethylfurfural (HMF), a furanic compound derived from the dehydration of hexose sugars, is a promising platform chemical for the production of various biofuels and biochemicals [1]. 2,5-Furandicarboxylic acid (FDCA), for instance, is an important chemical employed as an alternative monomer to terephthalic acid (TPA) for the production of polyethylene 2,5 furandicarboxylate (PEF). Most of the studies have concentrated on noble metal-based catalysts, molecular oxygen as the oxidant, and aqueous alkaline solutions to ensure the basic environment [2]. However, despite their notable efficiency, these catalytic systems have several drawbacks such as the presence of an inorganic base in the homogeneous phase and neutralization steps to obtain a pure product.

The zeolitic imidazolate framework (ZIFs) subfamily of MOFs is frequently used as precursors in synthesizing heteroatom-doped nanocarbon materials for electrochemical and chemical processes [3,4]. However, developing efficient and scalable processes remains challenging since ZIFs often suffer from uneven decomposition during pyrolysis, causing metal-based nanoparticle agglomeration, low N-doping, and decreased surface area [5]. To address these issues, strategies using silica (SiO_2), polymers, or surfactant protective layers for pyrolysis have emerged [6].

The present study aimed to design bimetallic Fe_xCo_y-ZIF-derived N-nanocarbon frameworks (Fe_xCo_y-NCF) capable of selectively oxidizing HMF to FDCA under base-free conditions. To ensure a high dispersion of the metal species, a large surface area, and hierarchical mesopores the bimetallic Fe_xCo_y-ZIF precursors were coated with a silica shell before carbonization.

Experimental

Bimetallic Fe, Co carbon materials (NPC – Nanoporous carbon and NCF – Nanocarbon Framework) were prepared by carbonization of Fe_xCo_y-ZIF (where x = 0.05, 0.1 and 0.15, and y = 0.95, 0.90 and 0.85) precursors at 700 °C for 2 h under a constant Ar flow. The materials were characterized with BET, XRD, TG-DTA, XPS, SEM-EDX, elemental analysis, CO_2-/NH_3-TPD, FT-IR and Raman spectroscopy, and ICP-OES. The catalytic experiments were carried out in a stainless-steel autoclave in acetonitrile (ACN) as solvent and TBHP (t-BuOOH, 70 wt.% aqueous solution) as oxidation agent. The experiments were carried out under autogenic pressure, at 70–110 °C for 0.5-24 h. The recovered products were analyzed by GC-FID (GC-Shimadzu apparatus) while the identification of the products was made by a GC-MS Carlo Erba Instruments (Waltham, MA, USA) QMD 1000.

Results and discussion

The XRD patterns of Fe_xCo_y-NCF catalysts, Fig. 1A, presents a broadening diffraction line at 25.8°, indexed to the (*002*) plane of graphite-type carbon as well as broad and low intensity of the diffraction lines at 44.2, 51.5, and 75.9° indicating tiny sized cobalt particles of Co^0 and Co-N_x species. The porosity of Fe_xCo_y-NPC and Fe_xCo_y-NCF materials was investigated by N_2 adsorption-desorption measurements at -196 ºC. As Fig. 1B shows all materials exhibit a hysteresis loop characteristic to abundant, random, bumpy, and non-uniform mesopores. SEM images revealed the dodecahedral shape of the particles, inherited from the ZIF precursors, but with more concave and rougher surfaces in the Co-NCF samples, Fig. 1C, attributable to the formation of larger pores.

All prepared catalyst exhibits high activity in HMF oxidation, affording conversions of more than 86%, Fig. 1D. The presence of iron in the bimetallic samples have an unexpected effect, even at very low dosage, promoting the oxidation pathway to FDCA. As such, the Fe_xCo_y-NCF achieved almost full conversion and selectivity to FDCA in the range of 50.0-82.4% as a function of the iron content.

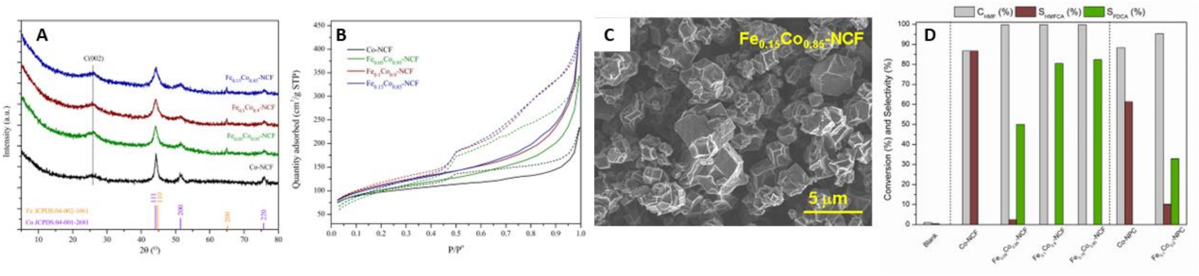

Fig. 1. (A) XRD pattern of Fe_xCo_y-NCF, (B) adsorption-desorption isotherms of Fe_xCo_y-NCF, (C) SEM image of $Fe_{0.15}Co_{0.85}$-NCF and (D) catalytic activity of Fe_xCo_y-NCF and Fe_xCo_y-NPC (*reaction conditions: 1 mmol HMF, 7.26 mmoles TBHP, 25 mg catalyst, 5 mL ACN, 80 ºC, 6h*).

Conclusions

The catalytic HMF oxidation to FDCA was significantly enhanced by the incorporation of iron. High catalytic performance was obtained for the NCF samples, which were synthesized using SiO_2 protective shell during carbonization. The $Fe_{0.15}Co_{0.85}$-NCF catalyst exhibited the highest efficiency (99.9% HMF conversion and 82.4% FDCA selectivity) under mild conditions (80 °C, 6 h) using tert-butyl hydroperoxide (TBHP) as the oxidant.

Acknowledgements

This research was funded by the Romanian Ministry Research and Digitalization, grant number PNRR-III-C9-2022-I5-18, ResPonSE - Project, No. 760010/2022.

References

[1] L. Hu, L. Lin, Z. Wu, S. Zhou, S. Liu, Renew. Sustain. Energy Rev. 74 (2017) 230.
[2] W. Guan, Y. Zhang, Y. Chen, J. Wu, Y. Cao, W. Wei, P. Huo, J. Catal. 396 (2021) 40.
[3] K.S. Park, Z. Ni, A.P. Côté, J.Y. Choi, R. Huang, F.J. Uribe-Romo, H.K. Chae, M. O'Keeffe, O.M. Yaghi, Proc. Natl. Acad. Sci. U.S.A. 103 (2006) 10186.
[4] A. Ejsmont, T. Darvishzad, G. Slowik, P. Stelmachowski, J. Goscianska, J. Colloid Interface Sci. 653 (2024) 1326.
[5] R. Kumar, P. Wang, W. Xue, Y. Jia, Z. Zhu, L. Luo, J. W.-C. Wong, J. Zhao, Next Materials 5 (2024) 100227.
[6] C. Wang, J. Kim, J. Tang, M. Kim, H. Lim, V. Malgras, J. You, Q. Xu, J. Li, Y. Yamauchi, Chem 6 (2020) 19.

Synthesis of Ti-SBA-15 from Rice Husk Ash: An Efficient and Robust Lewis Solid Catalyst for Organic Dyes Degradation

Violeta-Carolina Niculescu[1]*, Silviu-Laurentiu Badea[1], Ramona-Raluca Handolescu[1,2], Amalia Soare[1], Nadia Paun[1]

[1]National Research and Development Institute for Cryogenic and Isotopic Technologies-ICSI Rm. Valcea, 4th Uzinei Street, 240050 Rm. Valcea, Romania.

[2]Doctoral School of Engineering of Animal and Plant Resources, Faculty of Horticulture, University of Craiova, 13 A.I. Cuza Street, 200585 Craiova, Romania

**Corresponding author: violeta.niculescu@icsi.ro*

Introduction

Titanium-incorporated mesoporous silica materials have emerged as efficient heterogeneous catalysts in advanced oxidation processes, particularly in the photo-Fenton reaction [1]. These materials combine the high surface area and uniform pore structure of mesoporous silica with the photoactive properties of Ti^{4+} ions. In the photo-Fenton process, hydrogen peroxide (H_2O_2) and UV or visible light are used to generate highly reactive hydroxyl radicals (•OH) that degrade organic pollutants in water. When titanium is dispersed within the silica framework, it can act as a Lewis acid centre and promote the activation of H_2O_2 under light irradiation [2]. Key advantages of Ti-mesoporous silica include: high dispersion of Ti^{4+} active sites, ensuring accessibility; improved stability and reusability compared to homogeneous Fenton systems; enhanced mass transfer due to the mesoporous structure; potential for operation at neutral pH, unlike traditional Fenton systems that require acidic conditions [3]. These catalysts have shown promising performance in degrading dyes, pharmaceuticals, and other persistent organic pollutants under mild reaction conditions.

Experimental

Rice husk ash (RHA) was obtained by the thermal treatment of rice husks at 550 °C for 6 h in a calcination furnace. The SBA-15 molecular sieve was synthesized using Pluronic P123 dispersed in ultrapure water. Then, 2M HCl was added under magnetic stirring at 35 °C. Subsequently, RHA was added as a silica source, leading to the formation of a reactive gel composition. This mixture was stirred at 35 °C for 24 h and then conditioned and for 48 h/100 °C in a Teflon autoclave. The resulting material was washed with ultrapure water, dried at 60 °C for 24 h, and then calcined in a furnace. Titanium acetylacetonate was dissolved in methanol acidified with 5 mL HCl. 50 mL titanium acetylacetonate solution was added to SBA-15. The mixture was stirred at 40 °C for 24 h. The resulting mixture was centrifuged for 15 minutes at 4500 rpm, the precipitate was dried under vacuum at 50 °C, then calcined at 550 °C for 6 h, resulting a white powder. The materials were characterized by FTIR, ICP-OES, SEM, specific surface area, pore size distribution and elemental analysis. Photocatalytic activity was studied for removal of neutral red as one of the most widely used dye pollutants, in presence of H_2O_2 and UV irradiation, at 35 °C. The trend of the neutral red degradation was monitored by UV–Vis spectroscopy after dispersed solid catalyst centrifugation.

Results and discussion

Elemental and EDS analysis revealed high Si content, residual amount of C, as well as the incorporation of Ti (1.06%) into the silica matrix. Among the observed mineral elements, Ca and K were prominent. ICP-OES analysis revealed a content of 0.85% Ti. For the SBA-15, the silica matrix structure was preserved after the introduction of Ti particles, while the incorporation of spherical particles can be observed. These particles have sizes ranging between 1.2-1.4 µm, in accordance with data from the literature [2,3]. SEM revealed that all samples had a rod-like topography. BET surfaces and pores distribution were 129.99 $m^2 \cdot g^{-1}$ and 3.71 nm for the support, 118.11 $m^2 \cdot g^{-1}$ and 3.70 nm for the catalyst, respectively. The adsorption isotherms were of type IV and showed that the silica belongs to mesoporous materials [4]. In the FTIR spectrum, the characteristic siloxane (–Si–O–Si–) peak appeared at 1058 cm^{-1}. The stretching vibration of the Si–OH bond was noted at 801 cm^{-1}, and the bending vibration of the Si–O bond was recorded at 490 cm^{-1} [4]. The presence of adsorption peaks at 940-990 cm^{-1} indicated the existence of Si–O–Ti bonds [3].

The presence of catalyst increased the degradation efficiency. Although the high pH is in favour of the formation of hydroxyl radicals, the presence of a metal such as Ti will increase their aggressive nature. Higher amount of oxidant resulted in an increase in dye removal. Nevertheless, considering the principles of green chemistry, efforts were made to use less oxidant. At high pH values, hydrogen peroxide deprotonates to form an H_2O_2/HO_2^- equilibrium. The decrease in absorbance at 530 nm followed a first-order kinetic model, as indicated by the linear relationship between ln(A) and time, with a high correlation coefficient ($R^2 \approx 0.996$). The apparent rate constant (k) was calculated to be 0.0156 min^{-1}, corresponding to a half-life ($t_{1/2}$) of approximately 45 min.

Conclusions

Ti-SBA-15 was synthesized using rice husk ash as sustainable silica source, its properties being systematically characterized. The resulting mesoporous material exhibited structural and textural characteristics comparable to those synthesized from conventional silica sources, underscoring the viability of agricultural waste valorisation in advanced material synthesis. The photocatalytic activity was tested in the degradation of neutral red as a representative dye. Under the optimized conditions, up to 80% of neutral red was degraded after 90 minutes in the presence of Ti-SBA-15. A comparison between Ti-SBA-15 and other titanium-catalysts clearly demonstrated its high performance with a lower amount of catalyst used. The significant advantages include a green chemistry approach, high efficiency at neutral pH, and reduced catalyst and degradation process costs.

Acknowledgements

The work has been funded by the Romanian Ministry of Education and Research, under NUCLEU Program-Financing Contract no. 20N/05.01.2023, Project PN 23150402: "*Laboratory experiments valorisation in the development of technologies for the production of biofuels from agro-industrial waste*" and by the Ministry of Agriculture and Rural Development–Romania, under Sectorial Plan-ADER 2026, Project ADER 6.3.7–"*Applicability measures regarding the investigation of the organochlorine and organophosphorus contaminants distribution on the soil-plant-vegetable/fruit-finished product chain, following different types of soils in various areas*". The authors are grateful to Adriana Marinoiu, and Anca Zaharioiu, from National Research and Development Institute for Cryogenic and Isotopic Technologies-ICSI Rm. Valcea, for specific surface area, pores distribution, and elemental analysis.

References

[1] F. Mahfoozi, A. Mahmoudi, M.R. Sazegar, K. Nazari, J. Sol-Gel Sci. Technol. 100 (2021) 170.
[2] M.V. Zakharova, F. Kleitz, F.-G. Fontaine, Dalton Trans. 46 (2017) 3864.
[3] G. Almohammadi, C. O'Modhrain, S. Kelly, J.A. Sullivan, ACS Omega 5 (2020) 791.
[4] Q.N. Khanh Nguyen, N.T. Yen, N.D. Hau, H.L. Tran, J. Chem. 2020 (2020) e8456194.

Arrays of Electroactive Peptides on Gold for the Assessment of 20S Proteasome Activity and Inhibition

Madalina M. Barsan[1], Ariana Serban[1], Melania Onea[1], Magdalena Wysocka[2], Adam Lesner[2], Victor C. Diculescu[1]*
[1]National Institute of Materials Physics, Atomistilor 405, 077125, Magurele, Romania
[2]Faculty of Chemistry, University of Gdansk, Wita Stwosza 63, 80-308 Gdansk, Poland
**Corresponding author: victor.diculescu@infim.ro*

Introduction

Understanding intracellular protein degradation is a topic of huge interest because of the need to monitor, control and develop new pathways against several mortal diseases. Among the proteases, 20S proteasome was first localized in the nucleus and in the cytoplasm of all eukaryotic cell, cell membrane and in human alveolar space. The recently discovered 20S proteasome secreted outside the cell, circulating proteasome, has the most significant diagnostic value, its presence and high enzymatic activity being observed in several types of cancer. In this context, there is considerable interest in developing sensitive and selective assays and sensors that monitor protease activity [1,2]. This work comes as a response to the need of having highly sensitive, low cost, performant tools to determine the specific catalytic activity and inhibition of 20S proteasome using synthetic peptides with high specificity and sensitivity, Fig. 1. The peptide sequence used in this work is ABZ-VVSYAMG-(O2Oc)2-OH (the VVSYAMG is the amino acid sequence, and O2Oc is 8-amino-3,6-dioxooctanoic acid, which acts as a linker), which targets the chymotrypsin-like activity of the 20S proteasome releasing the ABZ-VVSY-OH fragment, and where the ABZ (2-aminobezoic acid) is electroactive.

Experimental

A Au bulk electrode was chemically modified with a self-assembled monolayer of 4-aminothiophenol (PATP) by immersing the Au electrode in a 10 mM solution PATP in ethanol for 24 h. The synthetic peptide was then immobilized on Au/PATP by using the free amino group of PATP and the carboxylic group of the synthetic peptide, activated by EDC and NHS. The Au/PATP/peptide modified electrode was allowed to dry in air for 4 h, and the reagents excess washed by immersion in water. For the assessment of the 20S proteasome activity, the Au/PATP/peptide sensor was immersed for increasing incubation times in solutions of 20S proteasome of 1, 5 or 10 ng·mL^{-1} in a total volume of 50 µL, with 15, 30 or 60 s steps. A similar procedure was used for the inhibition studies.

Results and discussion

The immobilization of the peptide and its interaction with 20S proteasome was investigated by SEM, QCM, SPR, ATR-FTIR (not shown). The activity of 20S proteasome was assessed electrochemically by cyclic voltammetry (CV) and electrochemical impedance spectra (EIS) after the immersion Au/PATP/peptide in 20S proteasome solution, Fig. 2. CV study showed a decrease in both capacitive and faradaic currents corresponding to the ABZ-VVSY-OH removal, allowing the quantification of the 20S proteasome activity (not shown). The EIS study revealed that the processes tacking place at the peptide/solution interface has a linear dependence with the incubation time in the 20S proteasome solution, Fig. 2. A gradual increase of the R_3 and decrease of the CPE_3 values with increasing incubation time in the 20S solution was observed for all concentrations. The R_3 value corresponds to the charge transfer reaction at the peptide/solution interface and correlates with to the ABZ-VVSY-OH fragment redox reaction. The R_3 value is strongly affected by the ABZ-VVSY-OH fragment concentration at the electrode surface, which decrease in time under the action of the 20S proteasome. Therefore, the increase in the incubation time leads to the increase in the R_3 value due to ABZ-VVSY-OH fragment removal from the peptide by the proteolysis performed by the 20S proteasome. The dependence is linear and the slope of R_3 variation with time can therefore be used as a measure of proteasome activity. The perfected assay was applied for the investigation of the inhibitory effect of one synthetic, bortezomib, and two naturally occurring, epoxomicin, and lactacystin inhibitors.

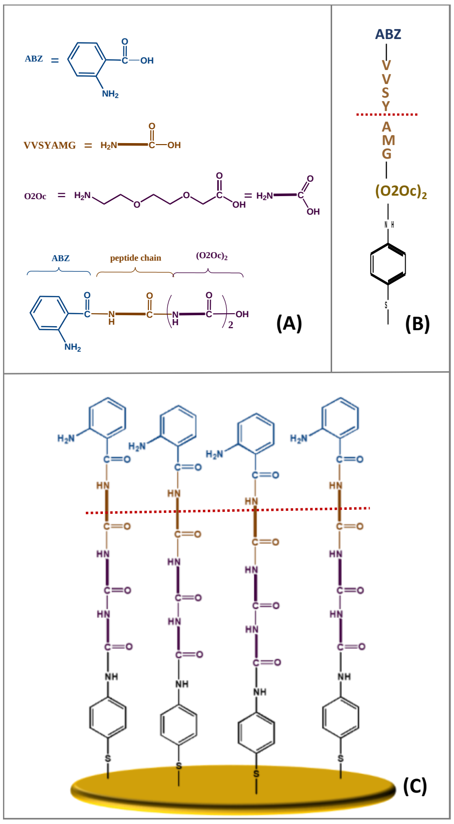

Fig. 1. Schematic representation of (A) the synthetic peptide, (B) peptide modified Au/PATP electrode and (C) proteolysis action of the proteasome on the synthetic peptide.

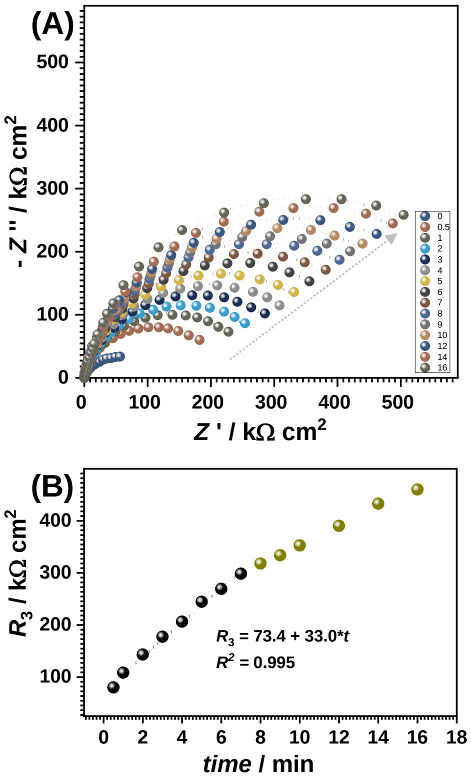

Fig. 2. (A) EIS spectra recorded at Au/PATP/peptide electrode for increasing incubation times in 5 ng/mL 20S proteasome; E_{app} = +0.68 V. (B) Plot of charge transfer resistance values *vs.* incubation time

Conclusions

The proposed electrochemical assay based on the immobilized synthetic peptide offers a sensitive, reliable, fast and cost effective route for the detection of enzyme activities of interest with application in inhibition studies and drug therapy development.

Acknowledgements

Financial support from the Romanian Ministry of Research, Innovation and Digitalization, through Projects: NANOBIOSURF-SMIS 103528, and Core Program of the National Institute of Materials Physics under the Project PC1-PN23080101.

References

[1] M.M. Barsan, A. Serban, M. Onea, M. Wysocka, A. Lesner, V.C. Diculescu, Appl. Surf. Sci. 610 (2023) 155620.
[2] M.M. Barsan, V.C. Diculescu, Analyst 146 (2021) 3216.

Poster Presentations

Functional and Phylogenetic Characterization of Novel Aromatic Ammonia-Lyases

Gyopárka Ágoston*; Raluca Bianca Tomoiagă; Csaba Levente Nagy; László Csaba Bencze*
Enzymology and Applied Biocatalysis Research Center, Faculty of Chemistry and Chemical Engineering, Babeș-Bolyai University, 11 Arany János Str., RO-400028 Cluj-Napoca, Romania
**Corresponding authors:* gyoparka.agoston@stud.ubbcluj.ro, laszlo.bencze@ubbcluj.ro

Introduction

Phenylalanine ammonia-lyases (PALs) have become valuable biocatalysts for the synthesis of several APIs [1]. Alongside histidine and tyrosine ammonia-lyases (HALs and TALs), they contain the catalytically essential 3,5-dihydro-5-methylidene-4H-imidazole-4-one prosthetic group (MIO group), forming the MIO enzyme family. A significant limitation of PALs shows in their low activity towards poly-substituted substrates with electron donating substituents – a challenge which has not been yet solved by the means of protein engineering [2].

A novel representative of this enzyme family, the aromatic ammonia-lyase from *Loktanella atrilutea* (*La*AAL), shows high activity in the production of the commercially important l-3,4-dimethoxy-phenylalanine, a key intermediate in the production of anti-Parkinson drug l-DOPA [3]. The present study focuses on the characterization of *La*AAL, including the determination of its optimal working conditions in the reversible ammonia addition reaction between *trans*-3,4-dimethoxy-cinnamic acid and l-3,4-dimethoxy-phenylalanine and the exploration of its substrate domain in the ammonia addition reaction route. In addition, new AALs similar to *La*AAL were identified and the evolutionary relationships within the MIO enzyme family were investigated.

Experimental

The thermal denaturation profile of the enzyme in buffer solutions of different pH (between 6 and 12) was measured with differential scanning fluorometry, while in the specific activity and enzyme kinetic measurements the production of the given *trans*-cinnamic acid derivate was followed using UV-VIS spectrophotometry. The enzyme's conversion-based activity was determined using RP-HPLC.

Similarity study was executed with the Basic Local Alignment Tool (BLAST), with the selection of sequences with high coverage and identity values above 60%. Multiple sequence alignment of the selected amino acid sequences was conducted using MUltiple Sequence Comparison by Log-Expectation (MUSCLE), and the phylogenetic analysis was performed in MEGA11.

Results and discussion

The optimal working conditions of *La*AAL were determined in the reversible ammonia addition reaction between *trans*-3,4-dimethoxy-cinnamic acid and l-3,4-dimethoxy-phenylalanine. The enzyme showed the highest activity at 30 °C, using 4 M $[NH_4][H_2NCO_2]$ (pH~9.5) as ammonia source, Fig. 1. Under these conditions, the substrate scope of *La*AAL was mapped, following the conversions of the ammonia addition reactions of several mono-, di- and poly-substituted *trans*-cinnamic acids. *La*AAL showed high conversion rates towards *meta*- and di-/poly-substituted substrates. Among these, enzyme kinetic measurements were conducted for the best-performing compounds. Of the natural AAL substrates *La*AAL showed the greatest specificity for l-tyrosine (3.62 $\mathbf{s}^{-1}\cdot mM^{-1}$), while the highest overall specificity constants were observed for l-2-naphtylalanine (6.43 $\mathbf{s}^{-1}\cdot\mathrm{mM}^{-1}$) and l-3-methoxyphenylalanine (6.42 $\mathbf{s}^{-1}\cdot\mathrm{mM}^{-1}$).

Through data-mining tools, homologues of *La*AAL were retrieved and their evolutionary relationships with PALs, TALs and HALs of different origins were assessed via phylogenetic analysis. The resulting phylogenetic diagram revealed that the newly identified AALs form a distinct cluster, having common ancestors with PALs of bacterial origin, while their unique substrate scope and catalytic site fingerprint a distinct role of this subclass of the aromatic ammonia-lyase family.

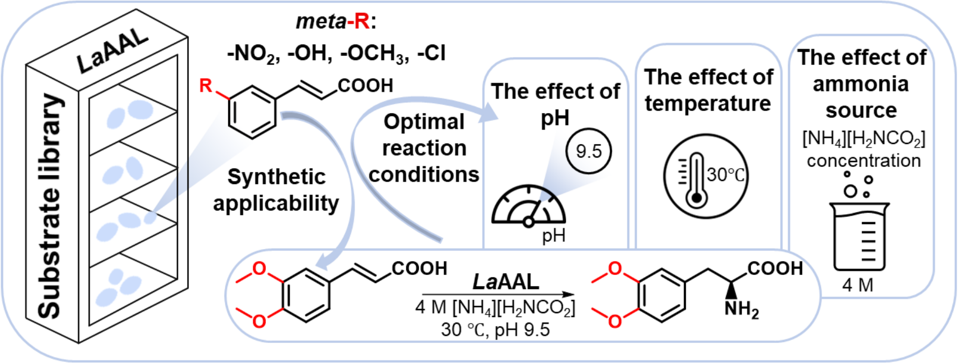

Fig. 1. General scheme of the characterization of *La*AAL.

Conclusions

*La*AAL displays promising catalytic properties toward substituted *trans*-cinnamic acid derivatives. The discovery of closely related AAL homologues with distinct active site features and evolutionary separation from known PALs, TALs, and HALs provides valuable insights for future enzyme engineering aimed at expanding the substrate scope of MIO-dependent ammonia-lyases.

Acknowledgements

This work was supported by the National Authority for Scientific Research and Innovation (ANCSI), PNRR-III-C9-2022-I8, Project code: 760042/23.05.2023. Gy. Á. thanks to the Collegium Talentum Programme of Hungary and the STAR-Institute of the Babeş-Bolyai University for the provided student-research fellowship.

References

[1] F. Parmeggiani, N. J. Weise, S.T. Ahmed, N.J. Turner, Chem. Rev. 118 (2018) 73.
[2] S.D. Tork, M.E. Moisa, L. Cserepes, A. Filip, L C. Nagy, F.D. Irimie, L.C. Bencze, Sci. Rep. 12 (2022) 10606.
[3] R.B. Tomoiaga, S.D. Tork, A. Filip, L.C. Nagy, L.C. Bencze, Appl. Microbiol. Biotechnol. 107 (2023) 1243.

Furfural Valorization *via* a One-Pot Chemoenzymatic Cascade to L-3-(2-Furyl)alanine

Anca-Elena Anghel, Souad-Diana Tork, Laura Barabas, Laszlo Csaba Bencze*, Csaba Paizs, Monica Ioana Toșa*
Enzymology and Applied Biocatalysis Research Center, Faculty of Chemistry and Chemical Engineering, Babeș-Bolyai University, Cluj-Napoca, Romania
**Corresponding authors:* laszlo.bencze@ubbcluj.ro, monica.tosa@ubbcluj.ro

Introduction

Furfural is a platform chemical that, due to its conjugated double bond system and aldehyde functional group, holds potential for conversion into a diverse array of value-added compounds (such as furfurylalcohol, methyl tetrahydrofuran or tetrahydrofurfurylalcohol), with applications in agriculture, biofuel and polymer production, as well as in the pharmaceutical industry [1]. Since it can be obtained from the hydrolysis of lignin-derived hemicellulose (a biorefinery carbohydrate), under acidic conditions, furfural has also been described as a biobased compound [2]. Turning to biocatalysis as a more sustainable, and environmentally-benign approach to obtain valuable compounds from biomass, various strategies to enzymatically transform furfural have been described, leading to maleic acid, fumaric acid [3], furfuryl alcohol [4] or furfurylamine [5]. However, the target compound of these approaches is rarely a non-proteinogenic amino acid.

In this work, a one-pot chemoenzymatic approach towards the synthesis of L-3-(2-furyl)alanine starting from furfural is proposed. The cascade involves two steps: a chemical step, the synthesis of 3-(2-furyl)acrylic acid through the Knoevenagel-Doebner condensation of furfural and malonic acid, and an enzymatic, phenylalanine ammonia lyase (PAL) - catalysed step, the ammonia addition onto 3-(2-furyl)acrylic acid, yielding L-3-(2-furyl)alanine. While the chemical step has been optimized within our group, the present work focuses on maximizing the yield of L-3-(2-furyl)alanine in the enzymatic step, and on coupling the two steps in a one-pot setup, thus enabling the synthesis of this non-proteinogenic amino acid on preparative scale.

Experimental

The *At*PAL-catalysed ammonia addition onto furylacrylic acid has been optimized in terms of choosing the best-suited type of biocatalyst (isolated enzyme, wet or lyophilized whole cells), identifying the optimal substrate concentration to biocatalyst ratio (mM:OD_{600}), and the maximum substrate concentration that can be quantitatively converted into the desired amino acid. Additionally, the effect of temperature and concentration of the ammonia source on the stationary conversion in the hydroamination reaction have also been investigated.

Since a chemoenzymatic cascade approach needs to take into account the possible incompatibilities between the optimal reaction conditions of the chemical and enzymatic steps, the inhibitory effect of DMSO and residual furfural (from the Knoevenagel-Doebner condensation step) on the enzymatic reaction conversion has also been studied on analytical scale. This was a prerequisite to check the feasibility of the preparative-scale coupling of the two reactions.

Having in hand the optimal conditions for both reactions, their preparative scale coupling was also performed, starting from 500 mg furfural. The desired L-amino acid was successfully isolated (72.3% conversion) *via* ion exchange chromatography, and its identity was confirmed using NMR spectroscopy, mass spectrometry and HPLC.

Results and discussion

Since significant substrate inhibition at high substrate concentrations (above 50 mM) was observed when performing the biotransformation using the isolated enzyme, the whole cell biocatalyst was chosen for further investigations. While no significant changes in conversion could be observed when using the wet or lyophilized *E. coli* cells expressing *At*PAL, for ease of manipulation, the lyophilized biocatalyst was chosen. The maximum substrate concentration that could be used to ensure quantitative conversion into the desired amino acid in 24 h was 200 mM 3-(2-furyl)acrylic acid. When optimizing the substrate to biocatalyst ratio (mM:OD_{600}), the optimal biocatalyst amount corresponded to an OD_{600} value of 100. The optimal temperature for the biotransformation was 30 °C, while the optimal concentration of the ammonia source (ammonium carbamate) was 3 M. When attempting to couple the chemical and enzymatic step on analytical scale, final DMSO concentrations higher than 20% (v/v) proved to be strongly inhibitory for the enzyme-catalyzed reaction, while furfural proved to be an even more potent inhibitor, with a furfural content of above 4% leading to a significant drop in the hydroamination reaction conversion (c=55%). Using the optimal enzymatic reaction conditions (200 mM furylacrylic acid, OD_{600}=100 for lyophilized *At*PAL biocatalyst, at 30 °C, with 3 M ammonium carbamate as the ammonia source), the chemical and enzymatic step were successfully coupled on preparative scale, starting from 500 mg furfural, yielding the desired L-3-(2-furyl)alanine with 72.3% overall conversion. The non-proteinogenic amino acid was isolated using ion exchange chromatography and its identity was confirmed *via* NMR spectroscopy, MS and HPLC.

Conclusions

This work focuses on optimizing the reaction parameters for the *At*PAL-mediated hydroamination of furylacrylic acid, to obtain an enantiomerically enriched non-proteinogenic amino acid, L-3-(2-furyl)alanine. The optimized enzymatic reaction is then coupled with the chemical synthesis of furylacrylic acid, *via* the Knoevenagel-Doebner condensation of furfural with malonic acid. After checking the compatibility of the two steps on analytical scale, the procedure is scaled up to a gram-level synthesis, enabling the production of L-3-(2-furyl)alanine from a biobased resource (furfural), with an overall 72.3% conversion into the desired product.

Abbreviations

*At*PAL – phenylalanine ammonia lyase from *Arabidopsis thaliana*

Acknowledgements

This work was supported by the project "Advanced (multi)-enzymatic synthesis and purification processes for bio-based furan derivatives – ASPIRE" funded by European Union – NextGenerationEU and the Romanian Government, under National Recovery and Resilience Plan for Romania, contract no 760042/23.05.2023, cod PNRR-C9-I8-CF25/14.11.2022, through the Romanian Ministry of Research, Innovation and Digitalization, within Component 9, Investment I8".

References

[1] K.J. Yong, T.Y. Wu, C.B.T.L. Lee, Z.J. Lee, Q. Liu, J.M. Jahim, Q. Zhou, L. Zhang, Biomass Bioenergy, 161 (2022) 106458.
[2] J.J. Bozell, G.R. Petersen, Technology development for the production of biobased products from biorefinery carbohydrates—the US Department of Energy's "Top 10" revisited, Green Chem.12 (2010) 539.
[3] Y.M. Huang, G.H. Lu, M.H. Zong, W.J. Cui, N. Li, Green Chem. 23 (2021) 8604.
[4] X.Y. Zhang, Z.H. Xu, M.H. Zong, C.F. Wang, N. Li, Catalysts 9 (2019) 70.
[5] A. Dunbabin, F. Subrizi, J.M. Ward, T.D. Sheppard, H.C. Hailes, Furfurylamines from biomass: transaminase catalysed upgrading of furfurals, Green Chem. 19 (2017) 397.

Green and Sustainable Ruthenium on Biochar Catalyst for Efficient Deuteration of α-Protons in Amino Acids

Ancuţa Balla, Claudia Lar, Cristina Marcu, József-Zsolt Szücs-Balázs, Maria Miheţ, Septimiu Tripon, Alexandru Turza

National Institute for Research and Development of Isotopic and Molecular Technologies, 67-103 Donat, 400293, Cluj-Napoca, Romania

Introduction

The deuteration of organic molecules, particularly those containing C–H bonds, plays a crucial role in organic synthesis and the development of isotopically labeled compounds. Amino acids are fundamental building blocks in biological systems, and the selective deuteration of α-protons in their structure can provide valuable insights into metabolic pathways and mechanisms. Ruthenium, known for its robustness and effectiveness in C–H activation, has emerged as a promising catalyst for these transformations. In this study, we report the synthesis of ruthenium (Ru) catalysts supported on biochar and their application in the deuteration of α-protons adjacent to amino groups in Glycine and L-Alanine. The incorporation of Ru onto biochar not only enhances the catalytic activity but also utilizes a sustainable support material, presenting a greener approach to catalyst design.

Experimental

Biochar (BCK) was prepared from spent coffee zest through pyrolysis under oxygen-free conditions at 850 °C, afterwards activated, chemical with KOH (BCK-KOH), and physically with CO_2 (BCK-CO2) to enhance surface area and functional groups. Ruthenium was introduced onto the biochar surface by wet impregnation method starting from $RuCl_3 \cdot 3H_2O$, resulting in a catalyst designated as Ru7.5/BCK-KOH, and Ru7.5/BCK-CO2. The experimental conditions are listed in Table 1. The catalyst characterization was performed using techniques such as BET surface area analysis, SEM. The deuteration procedure follow the literature protocol [1] and involves a mixture of the target Glycine or L-Alanine, the catalyst, a base (NaOH) and deuterated water (≥ 99% at D) as a deuterium source. The reaction medium is maintained in a H_2 atmosphere ($pH_2 \approx 2.5$ bar), under thermal conditions (70 °C) and continuous stirring for 3 days. The extent of deuteration was monitored using ^{1}H- and ^{13}C-NMR.

Table 1. Experimental conditions for catalyst preparation.

Biochar/Calalysts	**Pyrolysis**	**Activation**
BCK-KOH	850 °C, 2 h, He 100 mL·min^{-1}	BCK:KOH = 1:2; Calcination 850 °C, 1 h, He 100 mL·min^{-1}; Washing deionized water until pH 7; Drying 8 h at 110 °C
BCK-CO2		BCK – CO_2 200 mL·min^{-1}, 850 °C, 1.5 h
Ru7.5/BCK-KOH **Ru7.5/BCK-CO2**	Activated BCK in *contact* with a solution of $RuCl_3 \cdot 3H_2O$, 24 h, ultrasonication. *Drying* 12 h, 110 °C. *Calcination* 4 h, 400 °C, Ar 100 mL·min^{-1}. *Reduction* 4 h, 650 °C, H_2 100 mL·min^{-1}	

Results and discussion

In ^{1}H NMR spectrum of Glycine, Fig. 1a, a signal is observed at 3.478 ppm which corresponds to the methylene protons; while in the spectrum of selective deuterated Glycine this signal is missing, Fig. 1b, which proves the total deuteration of the methylene protons. The standard BET method revealed a specific surface area of 1046.6 $m^2 \cdot g^{-1}$ for Ru7.5/BCK-KOH, and 6012.6 $m^2 \cdot g^{-1}$ for Ru7.5/BCK-CO2. The results are displayed in Fig. 1.

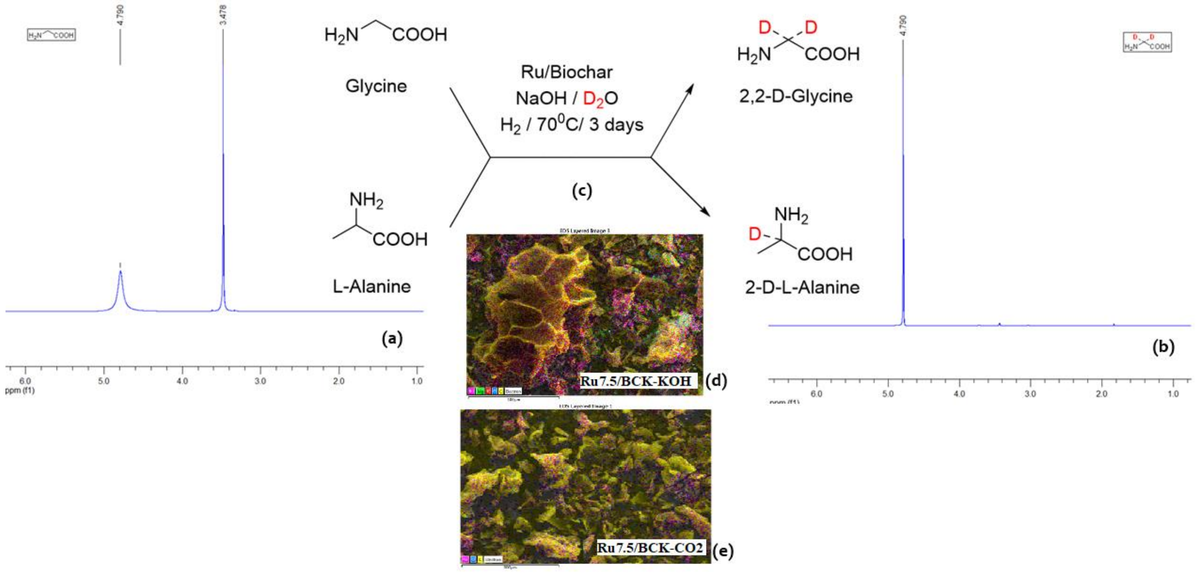

Fig. 1. Experimental data.

Conclusions

Ru/activated BCK is a promising catalyst deuteration of α-protons adjacent to amino groups in Glycine and L-Alanine.

Acknowledgements

This work was supported through the “Nucleu” Program within the National Research Development and Innovation Plan 2022–2027, Romania, carried out with the support of MEC, project no. 27N/03.01.2023, component project code PN 23 24 01 05, and through the Installations and Special Objectives of National Interest (IOSIN), IZOSTAB.

References

[1] A. Michelotti, F. Rodrigues, M. Roche, Org. Process Res. Dev. 21 (2017) 1741.

The Impact of the Layered Materials Synthesis Method Type on the Photodegradation of the Recalcitrant Dye Orange G

Dragoș-Sebastian Baltag[1,2], Adina Răducan[1], Petruța Oancea[1], Bogdan Cojocaru[1,3], Rodica Zăvoianu[1,3], Vasile I. Pârvulescu[1,3], Octavian D. Pavel[1,3]*
[1]University of Bucharest, Faculty of Chemistry, 4-12 Regina Elisabeta Av., 030018 Bucharest, Romania
[2]National Institute for Research and Development in Chemistry and Petrochemistry ICECHIM, Splaiul Independenței 202, 060021, Bucharest, Romania
[3]Research Center for Catalysts & Catalytic Processes, Faculty of Chemistry, University of Bucharest, 4-12 Regina Elisabeta Blv., 030018 Bucharest, Romania
**Corresponding author: octavian.pavel@chimie.unibuc.ro*

Introduction

Azo dyes represent about 60-70 % of all synthetic dyes produced worldwide being resistant to biodegradation, under aerobic conditions. Actually, advanced oxidation processes (AOPs) (e.g. Fenton oxidation, ozonation, direct and indirect photolysis, etc.) were applied for decomposing of these toxic and non-biodegradable azo dyes [1]. More recently, layered materials such as layered double hydroxides (LDH) as well as mixed oxides resulting from their calcination represent a viable class of photocatalysts. Furthermore, the textural properties of these solids can be tailored by different synthesis approaches using both traditional and non-traditional hydrolysis agents. The aim of this work was to evaluate the photodegradation properties of binary and ternary LDHs (e.g. M^{2+} (Co, Zn, Cd) and M^{3+} (Fe)) in the decomposition of a recalcitrant dye such as Orange G.

Experimental

Both, traditional (co-precipitation CP) and non-traditional (mechano-chemical MC) methods were considered for the synthesis of LDH-type materials using tetramethylammonium hydroxide (TMAH) as organic alkali. The nitrate solutions of considered cations (M^{2+}=Zn; Co, Cd and M^{3+}=Fe at a molar ratio $M^{2+}/M^{3+}=3$) were contacted with TMAH at 600 rpm and pH=10. For comparison inorganic alkali were also considered (Na_2CO_3 and NaOH at 1 M of Na_2CO_3). All synthesized samples were washed up to pH=7, dried at 120 °C, 24 h, and further calcined at 600 °C, 18 h. The catalysts were characterized by XRD, DRIFT, DR-UV-Vis, etc. The photocatalytic properties of the synthesized photocatalysts were determined for a solution of $4\cdot10^{-5}$ M Orange G using UV light radiation (using a low-pressure mercury lamp with wavelength of 254 nm radiation) in the 1 cm optical path thickness cuvette. The incident photon intensity was calculated as $1.62\cdot10^{-5}$ E/s, determined by the actinometric study of ferrioxalate. The catalysts had a fixed concentration of 1mg/mL for all degradation test.

Results and discussion

The presence of Fe cation in the Zn_3Fe system conducts the synthesis to mixed oxides, both for using inorganic (Na_2CO_3/NaOH) and organic (TMAH) precipitating agents, Fig. 1. No corresponding LDH diffraction lines are present. In contrast, the replacement of Fe by Al leads in presence of TMAH to the transformation of nitrate precursors through the LDH phase, along with of a ZnO phase, its presence being also supported by literature data [2]. Meanwhile, the spinel phase $ZnFe_2O_4$ is not present for calcined samples.

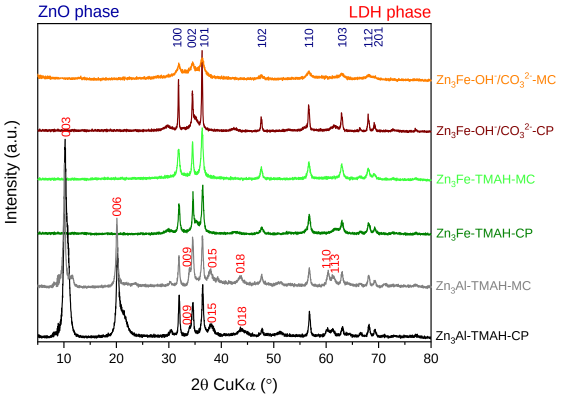

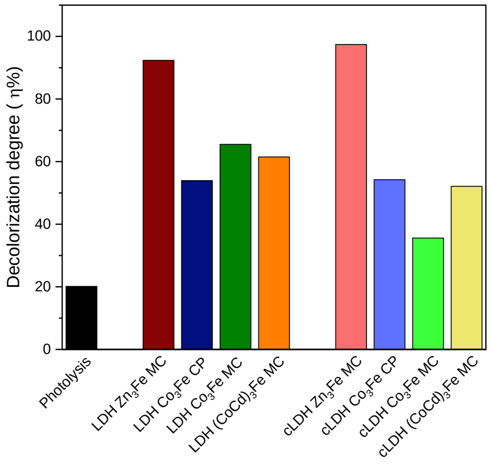

Fig. 1. XRD patterns of LDH samples synthesied by CP and MC

Fig. 2. The comparative decolorization degree of Orange G solution after 120 min of irradiation

The photocatalytic activity of solid catalysts was appreciated based on the decolorization degree of the initial solution after 120 minutes. The best catalytic systems were Zn_3Fe, both for initial sample (92.37%) and calcined at 600 °C (97.43%), Fig. 2. This optimal behavior is due to the synergistic effect of the two contributions presented by both samples: *i)* for the initial sample, intense contribution at 3.21 eV and weak at 2.11 eV; *ii)* for the calcined sample, intense contribution at 3.20 eV and weak at 2.16 eV. These values are smaller compared to the band gaps of the simple oxides: ZnO of 3.44 eV and Fe_2O_3 of 2.2 eV. However, in the presence of UV light, holes (hvb) are produced, which can oxidize pollutant molecule

Conclusions

Zn_3Fe system is a viable photocatalyst for the degradation of Orange G using UV light radiation due to the synergy of the two contributions from the initial and mixed oxide obtained at 600 °C and evidenced by DR-UV-Vis techniques.

Acknowledgements

This work is supported by Doctoral School on Chemistry from the University of Bucharest.

References

[1] A. Islam, S.H. Teo, Y.H. Taufiq-Yap, C.H. Ng, M L. Ibrahim, Resour. Conserv. Recycl. 175 (2021) 105849.
[2] F. Teodorescu, A.I. Slabu, O.D. Pavel, R. Zăvoianu, Catal. Commun. 133 (2020) 105829.

New Tricks for an Old Enzyme: Furan-, Thiophene-, and Phenyl-Based 1,2-Diketones Meet Carbonic Anhydrase

Laura E. Barabás*, Bence Tőkés, Monica I. Toşa, Csaba Paizs
Babeş-Bolyai University, Faculty of Chemistry and Chemical Engineering, Enzymology and Applied Biocatalysis Research Center, Arany János 11, 400028, Cluj-Napoca, Romania
**Corresponding author: laura.barabas@ubbcluj.ro*

Introduction

In recent decades, numerous research works have therefore been carried out to develop various stereoselective methods for the preparation of 1,2-diols with different diastereomeric and enantiomeric compositions. Several methods based on either carbon-oxygen or carbon-carbon bond formation are known for the preparation of these compounds. One of the best known of these asymmetric syntheses is the dihydroxylation of alkenes catalysed by OsO_4 [1], or the other well-known method, pinacol coupling [2], which involves a reductive process with the coupling of an aldehyde or ketone molecule. All these methods have been shown to be suitable for the preparation of 1,2-diols, but in many cases it is difficult to control their cross/homo-selectivity.

We present here a new enzymatic procedure for the synthesis of enantiopure *erythro*- and *threo*-1,2-diols from 1-phenylpropane-1,2-diones; 1-(furan-2-yl)propane-1,2-dione and 1-(thiophen-2-yl)propane-1,2-dione mediated by human carbonic anhydrase II in the presence of phenylsilane as hydride donor.

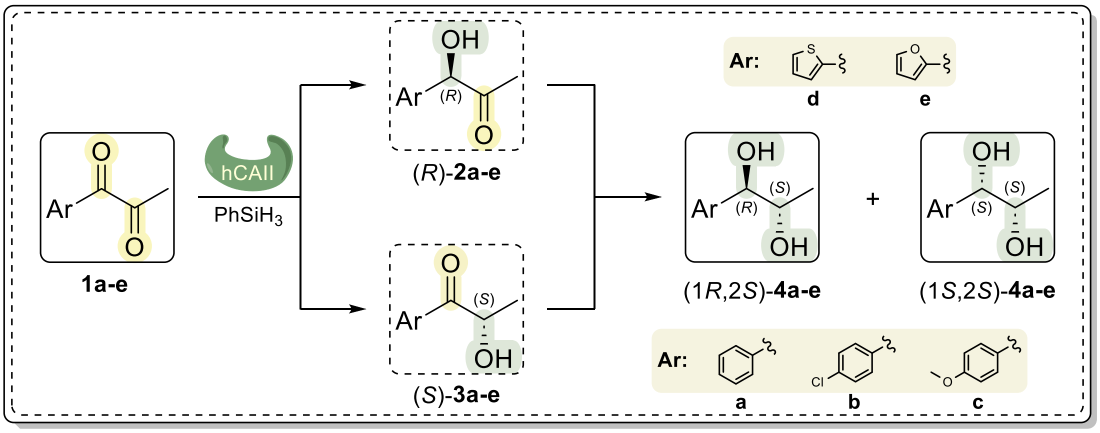

Fig. 1. Enzymatic reduction of 1,2-propandiones catalysed by human carbonic anhydrase II in the presence of phenylsilane.

Experimental

In Tris buffer solution (50 mM, pH=8.0) - DMSO (70:30%, v/v) 10-500 mM substrate was dissolved and then lyophilized cell powder was added to this solution (5 $mg{\cdot}mL^{-1}$ lyophilized cell powder). This suspension was incubated at 20 °C for a few minutes, then the reaction was initiated by adding phenylsilane (6 equiv.). The reaction mixture was incubated for 4 h at 20 °C and 1000 rpm on an orbital shaker.

Results and discussion

The figure below presents the conversion profiles obtained at various concentrations of 1,2-diketone substrates. These data clearly demonstrate the exceptional catalytic activity of human carbonic anhydrase II under the applied reaction conditions. Notably, the enzyme maintains high efficiency even at elevated substrate loadings, which is particularly remarkable for a native enzyme displaying a novel enzymatic activity. This highlights the robustness and versatility of carbonic anhydrase II in promoting diol formation in the presence of phenylsilane.

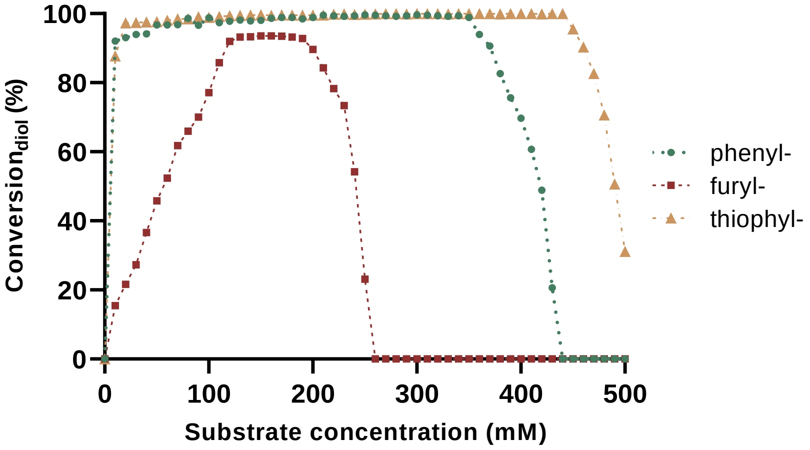

Fig. 2. Conversions of 1,2-diketones mediated by carbonic anhydrase II in the presence of phenylsilane at varying substrate concentrations.

Conclusions

In the presence of phenylsilane, human carbonic anhydrase II exhibits remarkably high catalytic efficiency in the transformation of 1,2-diketones, even at exceptionally high substrate concentrations. This represents an outstanding result for a native enzyme, especially given the discovery of a previously unrecognized catalytic activity. The reaction proceeds with notable stereoselectivity, yielding exclusively (1*R*,2*S*)- and (1*S*,2*S*)-1,2-diols, indicating that the enzyme's active site exerts precise stereochemical control. These findings highlight an unexpected catalytic versatility of carbonic anhydrase II and open new avenues for its application in biocatalysis.

Acknowledgements

The present work has received financial support through the Proiect PNRR, contract nr. 760042/23.05.2023, Advanced (multi)-enzymatic synthesis and purification processes for biobased furan derivatives – ASPIRE.

References

[1] A. J. DelMonte, J. Haller, K.N. Houk, K.B. Sharpless, D.A. Singleton, T. Strassner, A.A. Thomas, J. Am. Chem. Soc. 119 (1997) 9907.
[2] H.C. Aspinall, N. Greeves, C. Valla, Org. Lett. 7 (2005) 1919.

Metal-Affinity-Based Immobilization of Enzymes on Carbon Nanotubes

Judith-Hajnal Bartha-Vari[1,]*, Monica Ioana Toșa[1], László Poppe[1,2], Csaba Paizs[1]
[1]*Enzymology and Applied Biocatalysis Research Center, Babeș-Bolyai University, Faculty of Chemistry and Chemical Engineering, Arany János Street no.11, 400028 Cluj-Napoca, Romania*
[2]*Department of Organic Chemistry and Technology, Budapest University of Technology and Economics, Rakpart street no.3, 1111 Budapest, Hungary*
**Corresponding author: judith.vari@ubbcluj.ro*

Introduction

Novel biocatalytic methods are often used in organic synthesis both on the laboratory and industrial scale since biocatalysts are selective, easy-to-handle and environmentally friendly [1].

Immobilization can often modify and improve the key properties of enzymes and may also enable their recovery and reuse [2].

For the covalent immobilization the use of purified enzyme is mandatory, the purification step can be costly and laborious. The metal-affinity immobilization can overcome these drawbacks and enable the simultaneous purification and immobilization of the enzyme [3]. Moreover, using affinity-based immobilization methods, the recovery and reuse of the carrier material can also be achieved.

The use of nanomaterials as carrier for enzyme immobilization has numerous advantages, including high specific surface area, tunable morphology and abundant chemically active sites [4].

Experimental

Several support materials were tested starting from carboxy and amino functionalized carbon nanotubes (SwCNT-COOH and SwCNT-NH_2). SwCNT-NH_2 was derivatized with bisepoxy linkers with different length (glycerol diglycidyl ether, 1,4-butanediol diglycidyl ether, neopentyl glycol diglycidyl ether, 1,4-cyclohexanedimethanol diglycidyl ether).

After the activation of the carboxy groups the functionalization of SwCNT-COOH was also carried out using 1,3-diaminopropane, or 1,3-diaminopropane coupled with glycerol diglycidyl ether and 1,3-diaminopropane. The EDTA chelator was introduced onto the obtained amino-alkylated surfaces, and after the chelator decoration, the support materials were charged with metal ions, Fig. 1.

The poly-His-tagged recombinant *Pc*PAL was immobilized to the previously prepared support materials. The amount of the immobilized enzyme was determined spectrophotometrically using the Bradford method. Immobilization yield: 99.7%, enzyme loading: 0.1 (mgprotein·mg^{-1} immobilized preparate).

The specific activity for each enzyme preparate was measured spectrophotometrically. The biocatalysts activity was measured using RP-HPLC.

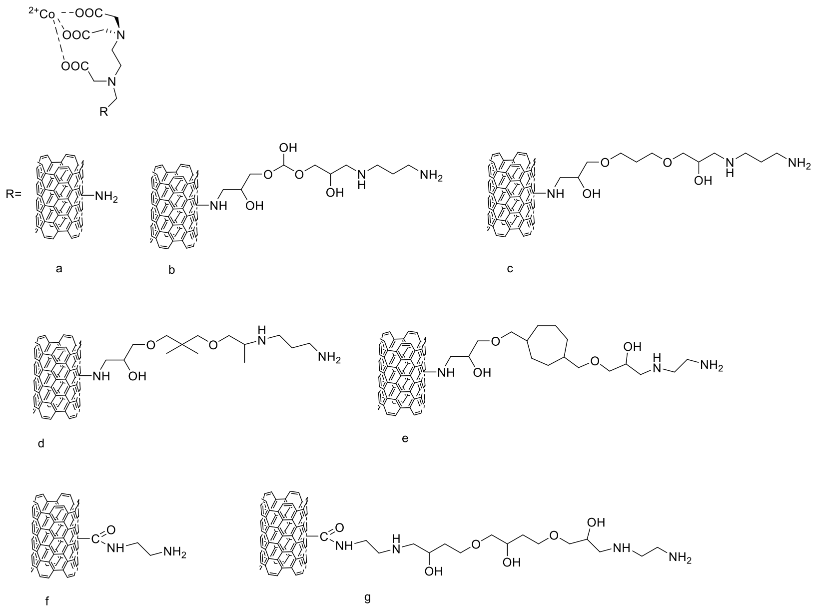

Fig. 1. Affinity-tag decorated support materials.

Results and discussion

Based on the enzymatic activity, the two best-performing preparates (*b* and *g*) were selected and tested for the ammonia elimination from L-phenylalanine and ammonia addition to *trans*-cinnamic acid reactions in batch mode. The biocatalysts were characterized by high activity and selectivity.

The reusability of the biocatalyst was also investigated using repeated batch cycles.

Conclusions

This study demosntrates the usefulness of carbon nanotubes for the IMAC-based immobilization of polyhistidine-tagged phenylalananine ammonia lyase. The enzyme immobilized on the suport materials functionalized with linkers off different lenght proved to be an active and stable biocatalyst in the ammonia addition and elimination reactions.

Acknowledgements

This work was supported by the project “Renewable Enzyme Immobilization - RENZI” funded by European Union – NextGenerationEU and the Romanian Government, under National Recovery and Resilience Plan for Romania, contract no 760241/28.12.2023, cod PNRR-C9-I8-CF87/31.07.2023, through the Romanian Ministry of Research, Innovation and Digitalization, within Component 9, Investment I8”

References

[ ] L. Poppe, L. Novák, Selective Biocatalysis: A Synthetic Approach, VCH, Weinheim, (1992).
[2] R.A. Sheldon, S. van Pelt, Chem. Soc. Rev. 42 (2013) 6223.
[3] B. Alács, A. Zrinyi, G. Hornyánszky, L. Poppe, E. Bell, Catalysts 14 (2024) 14.
[4] Y.-P. Sun, K. Fu, Y. Lin, W. Huang, Acc. Chem. Res. 35 (2002) 1096.

Toward a Heterocyclic Schiff Base and Its Cu(II) Complex with Anticancer Potential

Alexandra Bîrzu*, Mihaela Dascalu, Gheorghe Roman, Vladimir Arion
”Petru Poni” Institute of Macromolecular Chemistry of Iasi, 41A Grigore Ghica Vodă Alley, 700487, Iasi, Romania
**Corresponding author: birzu.alexandra@icmpp.ro*

Introduction

Schiff bases, discovered over 150 years ago, have emerged as key compounds in medicinal chemistry due to their remarkable biological activities and structural versatility. Defined by the presence of an imine group (−CH=N− or >C=N−), Schiff bases are synthesized through the condensation of primary amines with aldehydes or ketones. Their ability to form stable complexes with metal ions-by coordinating through donor atoms such as nitrogen, oxygen, and sulfur-greatly enhances their pharmacological potential. Notably, heterocyclic Schiff bases, especially those incorporating nitrogen-containing frameworks like benzimidazole and indole, have demonstrated a wide spectrum of biological properties including anticancer, antimicrobial, antitumor, antioxidant, anti-inflammatory, and antiproliferative effects, while complex formation with metal ions further enhances this activity [1,2].

Part of a multi-step synthesis strategy, starting from 4-methoxy-1H-indole-2-carboxylic acid, the preliminary steps for obtaining the Schiff base of 3-methoxy-8-oxo-5,6,8,9-tetrahydro-7H-benzo[5,6]azocino[3,4-b]indole-indole(i) with 2-pyridinecarboxaldehyde for subsequent coordination to Cu(II), to obtain complexes with anticancer potential, are presented.

Experimental

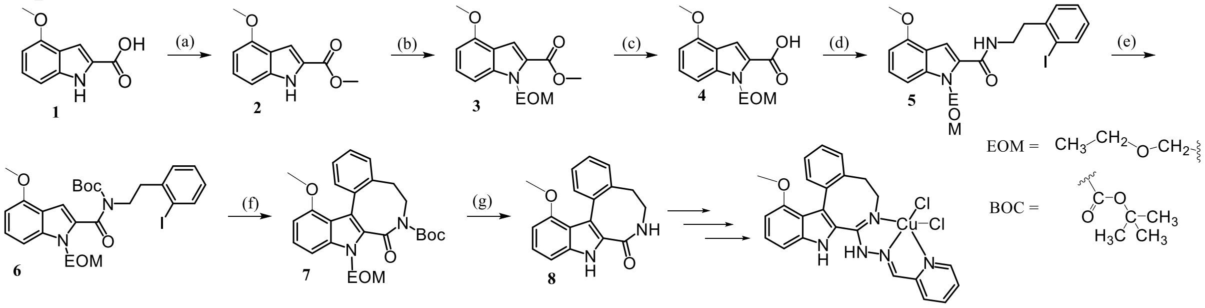

Scheme 1. Synthetic pathway toward a new methoxy-substituted indolobenzazocine-based ligand. Reaction conditions: (a) H_2SO_{4c}, methanol, reflux overnight; (b) chloromethyl ethyl ether, DMF, rt, overnight; (c) $LiOH \cdot H_2O$, ethanol–water, reflux, 2 h; (d) 2-iodophenylethanamine, EDCI·HCl, DMAP, DCM, 0 °C→ rt, 18 h; (e) Boc2O, DMAP, MeCNdry, RT, 18 h (f) PPh_3, Ag_2CO_3, $Pd(CH_3COO)_2$, DMF, argon atmosphere, 110 °C, 2 h, (g) HCl, dioxane, 80 °C, 2 h.

Results and discussion

Preliminary modeling studies suggested that introducing methoxy substituents on either the indole moiety or the benzene ring could enhance the biological activity of second-generation indolobenzazocine-based complexes [3]. The synthesis of one such ligand, up to the construction of the indolobenzazocine scaffold [4], is outlined in Scheme 1. The synthesis started with esterification of a commercially available carboxylic acid with methanol in the presence of sulfuric acid as catalyst under reflux to give the methyl ester. This product was then alkylated with chloromethyl ethyl ether in DMF at room temperature to introduce the ethoxymethyl (EOM) protecting group. Hydrolysis of the ester under basic conditions with lithium hydroxide in an ethanol-water mixture yielded the corresponding acid, which was then coupled with 2-iodophenylethanamine by using 1-ethyl-3-(3-dimethyllaminopropyl)carbodiimide hydrochloride (EDCI·HCl) and 4-dimethylaminopyridine (DMAP) in dichloromethane at 0 °C to afford a secondary amide. Protection of the amide nitrogen with a tert-butoxycarbonyl (Boc) afforded the precursor 6 for the key ring-closing step. The tetracyclic indolobenzazocine core 7 was assembled via a Pd(II)-catalyzed intramolecular Heck-type cyclization using $Pd(OAc)_2$, Ag_2CO_3, and PPh_3 in DMF under an argon atmosphere at 110 °C. Deprotection of both Boc and EOM groups was then performed with hydrochloric acid in dioxane under heating. Further functionalization steps required to complete the synthesis of the target ligand are currently ongoing in our group. All intermediates synthesized to date have been purified by column chromatography or recrystallization, and their structures were confirmed by NMR spectroscopy.

Conclusions

In summary, a synthetic route toward a methoxy-substituted indolobenzazocine-based ligand has been successfully developed up to the formation of the tetracyclic core structure. The approach incorporates strategic functional group transformations, protective group manipulations, and a key Pd-catalyzed intramolecular Heck cyclization to construct the required scaffold. Although the subsequent steps needed to complete the synthesis of a Schiff basae are underway, the intermediates obtained thus far have been purified and characterized. This work lays a solid foundation for the preparation of a new generation of indolobenzazocine-based ligands with potentially enhanced biological properties.

Acknowledgements

This work was financially supported by a grant from the Ministry of Research, Innovation and Digitization, project no. PNRR-III-C9-2023-I8-99 within the National Recovery and Resilience Plan.

References

[1] N. Behera, T. Behera, J. Rout, S. Moharana, (2024). Significant Aspects of Heterocyclic Schiff Bases and Their Metal Complexes. IntechOpen. doi: 10.5772/intechopen.115087

[2] A.A. Shanty, J.E. Philip, E. J. Sneha, M.R. Prathapachandra Kurup, S. Balachandran, P.V. Mohanan, Bioorg. Chem. 70 (2017) 67.

[3] C. Wittmann, O. Dömötör, I. Kuznetcova, G. Spengler, J. Reynisson, L. Holder, G.J. Miller, E.A. Enyedy, R. Bai, E. Hamel, V.B. Arion, Dalton Trans. 52 (2023) 9964.

[4] I. Kuznetcova, M. Ostojić, N. Gligorijević, S. Aranđelović, V.B. Arion, Drugs. Inorg. Chem. 61 (2022) 20445.

High-Throughput Assay for Screening Engineered Phenylalanine Ammonia-Lyase Libraries

Naomi Bondilă*, Raluca Bianca Tomoiagă, Krisztina Kelemen, László-Csaba Bencze*
Enzymology and Applied Biocatalysis Research Center, Faculty of Chemistry and Chemical Engineering Babeș-Bolyai University, Cluj-Napoca, Romania
**Corresponding authors: naomi.bondila@stud.ubbcluj.ro, laszlo.bencze@ubbcluj.ro*

Introduction

Phenylalanine ammonia-lyases (PALs) are highly efficient and selective biocatalysts used to produce optically pure L-phenylalanines (L-Phes) by the hydroamination of *trans*-cinnamic acid. Despite the increased synthetic interest for D-amino acids [1,2] to the engineering of PALs for the synthesis of D-phenylalanine (D-Phe) still remains challenging. Directed evolution might stimulate the development of D-selective PALs, however a key obstacle is the lack of high-throughput screening systems affording reliably identification of active D-PAL variants.

The aim of our research was to develop and optimize a solid-phase high-throughput screening assay based on a coupled enzymatic system involving D-amino acid oxidase (DAAO), enabling the efficient detection of D-selective PAL mutants generated through directed evolution processes.

Results and discussion

The recombinant form of DAAO was succesfully expressed and isolated, while their activity was assessed in different buffers, follwed by the set-up of the coupled enzyme system.

Within this system, the FAD-dependent DAAO selectively oxidizes D-phenylalanine, reducing molecular oxygen to hydrogen peroxide (H_2O_2), whilehorse radish preoxidase (HRP) further reduces H_2O_2 to water, simultaneously oxidizing 4-AA. The oxidized 4-AA then condenses with vanillic acid (VA), resulting in the formation of a red quinonimine dye, as illustrated in Fig. 1. The color intensity varies with the reaction yield and can be detected on a nitrocellulose membrane containing the cellular biocatalysts incorporating the plasmid, harbouring the gene of a particular PAL variant.

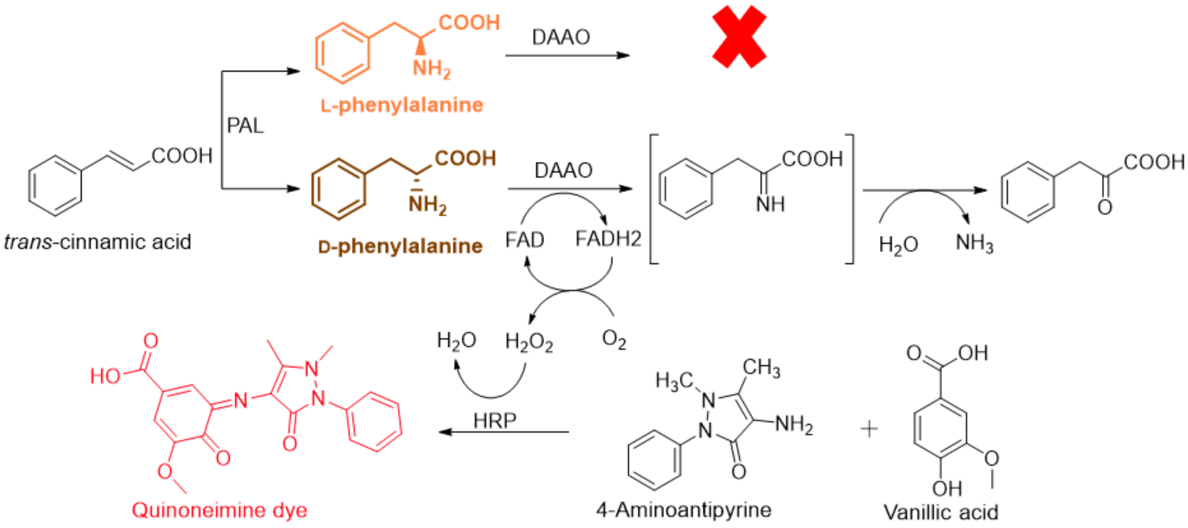

Fig. 1. The DAAO-coupled high-throughput solid-phase assay for detection of PALs with D-selectivity.

Conclusions

After the successful set-up, the limit of the detection in case of the assay was determined to be equivalency to 5% conversion within the PAL mediated hydroamination reaction, which, corresponded to 0.5 mM D-Phe. Pre-treatment of the membrane, containing the colonies of whole-cell PAL library, with HRP was found to be crucial for eliminating the background coloring.

Acknowledgements

This work was supported by the project “Advanced (multi)-enzymatic synthesis and purification processes for biobased furan derivatives – ASPIRE” funded by European Union – Nextgeneration EU and Romanian Government, under National Recovery and Resilience Plan for Romania, contract no. 760042/23.05.2023, cod PNRR-III-C9-2022-I8-ASPIRE/PNRR2022, through the Romanian Ministry of Research, Innovation and Digitalization, within Component 9, Investment I8.

References

[1] N. Zashikhina, V. Sharoyko, M. Antipchik, I. Tarasenko, Y. Anufrikov, A. Lavrentieva, T. Tennikova, E. Korzhikova-Vlakh, Pharmaceutics 11 (2019) 27.
[2] F. Parmeggiani, N.J. Weise, S.T. Ahmed, N.J. Turner, Chem. Rev. 118 (2018) 73.
[3] M. Chachin, M. Yamada, A. Fujita, T. Matsuoka, K. Matsushita, Y.N. Kurachi, J. Pharmacol. Exp. Ther. 304 (2003) 1025.

Selective Oxidation of HMF to FDCA Over Transitional Metal Oxides Based Magnetic Nanoparticles

Natalia Candu, Mihai Bordeiasu, Magdi El Fergani, Vasile I. Parvulescu, Simona M. Coman*
Faculty of Chemistry, University of Bucharest, Regina Elisabeta Blvd., no. 4–12, Bucharest 030018, Romania
**Corresponding author:* simona.coman@chimie.unibuc.ro

Introduction

Environmental pollution and fossil resource depletion are among humanity's greatest challenges. In connection with this, the green chemistry movement offers solutions like eco-friendly reagents, shorter reaction pathways, and sustainable raw materials such as biomass [1]. Furan-derived compounds from biomass, like 5-hydroxymethylfurfural (HMF) and 2,5-furandicarboxylic acid (FDCA), have been used in sustainable energy and platform molecules. FDCA, one of essential priority chemicals, is widely used in polyester, polyurethane, and polyamide synthesis [2] and is an attractive feedstock for "green" polymers. FDCA is typically synthesized from HMF through oxidation over heterogeneous catalysts, such as MnO_2 [3] Pd-Bi-Te/C[4], Pt/CeO_2 [5] or cationic Ru(4 wt.%)-$Fe_3O_4@SiO_2$ [6] using oxygen or peroxide as the oxidizing agent. Heterogeneous catalysis has limitations due to reliance on precious metals and challenges like leaching and poor recyclability. Therefore, there is growing demand for innovative strategies to develop solid catalytic systems using cost-effective transition metals. Our study aimed to design efficient monometallic magnetic catalysts like $Fe_3O_4@SiO_2$-MOx, with 1, 5 or 10 wt.% active phase (i.e. MOx = MnOx, CoOx, and FeOx) and bimetallic ones, combining active phases of monometallic magnetic catalysts for selective oxidation of HMF to FDCA. These materials offer enhanced oxidation properties and practical separation advantages.

Experimental

Magnetic core (Fe_3O_4) was synthesized via a co-precipitation method. Further the shell was deposed starting from TEOS (tetraethyl orthosilicate) solution. Finally, 1, 5 or 10 wt.%, of Co, Mn or Fe were deposited-precipitated under basic pH. The prepared magnetic catalysts samples were denoted as xMe@MNP (where MNP=$Fe_3O_4@SiO_2$, x=5 or 10 wt.% and Me=CoOx, FeOx or MnOx), Scheme 1. The prepared catalysts were characterized by XRD and DRIFT. The catalytic oxidation tests were carried out in 10 mL glass vials. Generally, 0.025 g of catalyst were added to a solution of 4 mmoles HMF in 4.4 mL of acetonitrile, and 2.17-4.34 mmol of t-BuOOH (70 wt.% in H_2O) or H_2O_2 (30%) oxidant. After sealing, vials were heated up to a temperature of 80-120 °C for 6-24 h. The resulted reaction mixture was distilled under vacuum, at 50 °C, and the dried residue was silylated. The analysis and identification of the reaction products has been performed by GC-FID and GC-MS chromatography.

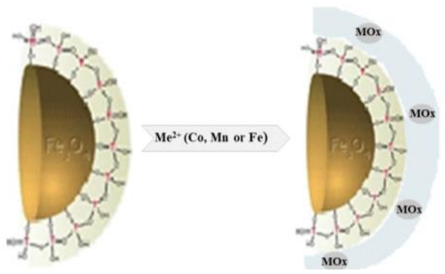

Scheme 1. General preparation procedure of xMe@MNP catalysts.

Results and discussion

The XRD patterns, Fig. 1, of the prepared catalyst display the diffraction lines characteristic to magnetite (2θ = 30.1, 35.4, 43.1, 53.4, 57.1, and 62.6°) and a broad diffraction line (2θ = 20°), due to the amorphous silica which coats the magnetic nanoparticles surface. No additional diffraction lines corresponding to crystalline MnO_x, FeO_x or CoO_x were evidenced, indicating the incorporated oxides are homogeneously highly dispersed on the silica shell.

In the presence of monometallic catalysts the oxidation of HMF proceeded to HMFCA with selectivities of 84.4-98.2% for conversions of HMF in a range of 71.7-87.8%, at 100 °C and 6 h and irrespective of the active phase nature. However, the bimetallic catalysts exhibited superior catalytic performance at a lower catalyst loading with FDCA as the main reaction product. Therefore, in the presence of Fe5@Co5@MNP catalyst FDCA was obtained with a selectivity of 86.7% for a total conversion of HMF. These performances are attributed to the synergistic interactions between Fe and Co.

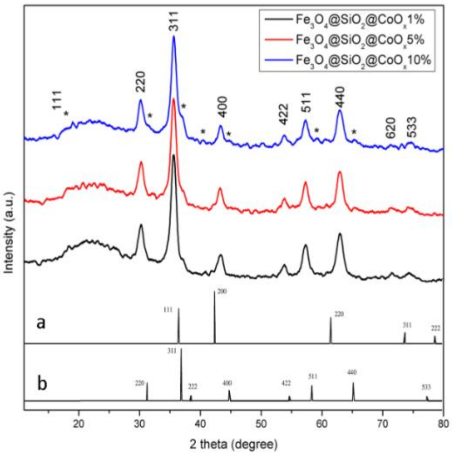

Fig. 1. XRD patterns of the catalysts.

Conclusions

In summary, this study demonstrates the successful synthesis of mono- and bimetallic magnetic based catalysts with enhanced efficiency in the HMF oxidation. While the monometallic catalysts lead to HMFCA as main reaction product the bimetallic samples preponderately lead to FDCA. Their better performance is attributed to the synergistic interactions between the two supported transitional metal oxide phases. The presence of magnetite core ensures a straightforward magnetic separation of the catalysts at the end of the reaction. The potential of such catalysts serves as a promising approach for advancing marine biomass valorization and fostering the sustainable production of biopolymers.

Acknowledgements

The Romanian Ministry Research and Digitalization is acknowledged for funding within the grant PNRR-III-C9-2022-I5-18, ResPonSE - Project, No. 760010/2022.

References

[1] K. Sudesh, T. Iwata, Clean 36 (2008) 433.
[2] M. Gomes, A. Gandini, A.J.D. Silvestre, B. Reis, J. Polym. Sci. Part A: Polym. Chem. 49 (2011) 3759.
[3] E. Hayashi, T. Komanoya, K. Kamata, M. Hara, ChemSusChem 10 (2017) 654.
[4] M.S. Ahmed, D.S. Mannel, T.W. Root, S.S. Stahl, Org. Process Res. Dev. 21 (2017) 1388.
[5] W. Gong, K. Zheng, P. Ji, RSC Adv. 7 (2017) 34776.
[6] A. Tarsoaga, M. El Fergani, V.I.,Parvulescu, S.M. Coman, ACS Sustain. Chem. Eng. 6 (2018) 14292.

NiAl-Ti_3C_2 MXene as an Efficient Catalyst for Fine Chemicals Synthesis

Bogdan Cojocaru[1,2], Octavian D. Pavel[1,2]*, Liang Tian[3], Dana G. Popescu[4], Vasile I. Parvulescu[1,2]*, Hermenegildo Garcia[3]*

[1]*University of Bucharest, Faculty of Chemistry, Departrment of Inorganic Chemistry, Organic Chemistry, Biochemistry and Catalysis, 4-12 Regina Elisabeta Blv, 030018 Bucharest, Romania;*

[2]*Research Center for Catalysts & Catalytic Processes, Faculty of Chemistry, University of Bucharest, 4-12 Regina Elisabeta Blv., Bucharest 030018, Romania*

[3]*Instituto Universitario de Tecnología Química, Consejo Superior de Investigaciones Científicas-Universitat Politecnica de Valencia, Universitat Politecnica de Valencia, Av. De los Naranjos s/n, 46022 Valencia, Spain*

[4]*National Institute of Materials Physics, Atomistilor 405A, 077125 Magurele, Romania*

**Corresponding author: vasile.parvulescu@chimie.unibuc.ro, hgarcia@qim.upv.es, octavian.pavel@chimie.unibuc.ro*

Introduction

Since fine chemicals are considered the pure molecules useful as synthesis intermediates as well as final products, there has been an accelerated growth in this field in the last decade [1]. The Biginelli and the Claisen-Schmidt condensation are two important reactions for generating new C-C bonds. Both reactions require the presence of base sites. MXenes, a class of two-dimensional inorganic compounds incorporating thin layers of transition metal carbides, nitrides or carbonitrides, may be an optimal alternative for promoting the considered reactions. The aim of this work involved the synthesis of catalytic solids of the Ni-Al MXenes type and the evaluation of catalytic activities in the Biginelli reaction as well as the Claisen-Schmidt condensation of cyclohexanone with benzaldehyde.

Experimental

NiAl-MXene was prepared by hydrothermal aluminum etching starting from a commercial nickel aluminum carbide MAX phase powder involving a step of delamination by ultrasound with a 700 W type sonication system. The physicochemical properties were evaluated by XRD, XPS, CO_2/NH_3-TPD, Raman, etc. Both condensation reaction were carried out in batch conditions. Biginelli reaction considered benzaldehyde/ethylacetoacetate/urea (thiourea) in molar ratios of 1/1/1.5 in the presence of 3 mL of ethanol and 0.082 g catalyst for 4 h at reflux to synthesize ethyl 4-(4-formylphenyl)-6-methyl-2-oxo-3,4-dihydro-1H-pyrimidine-5-carboxylate or ethyl 4-(4-formylphenyl)-6-methyl-2-thioxo-3,4-dihydro-1H-pyrimidine-5-carboxylate synthesis. The Claisen-Schmidt condensation considered cyclohexanone/benzaldehyde of 1/2 as molar ratio, 20 mg of catalyst under solvent-free conditions for 2h at 120 °C for 2-benzyliden cyclohexanone (mono-condensed product) or 2,6-dibenzylidene cyclohexanone (di-condensed product).

Results and discussion

XRD patterns confirm the nickel uniform dispersion on the catalyst surface, a fact also confirmed by XPS measurements, Fig. 1. The MXene structure has been preserved regardless the time and type of reaction considered. The slight broadening of the line at 25.4° is assigned to adsorbed condensed product, also highlighted by the DRIFT spectra.

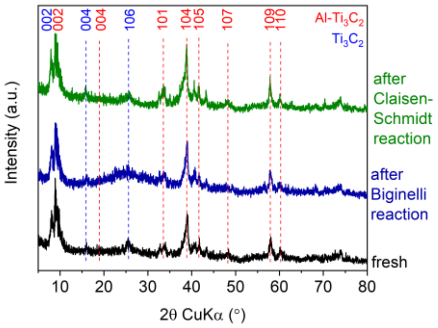

Fig.1. The XRD patterns of NiAl-Ti_3C_2.

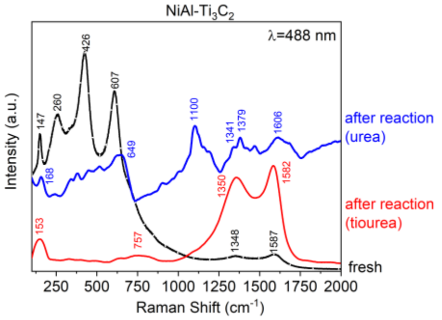

Fig. 2. Raman shift of NiAl-Ti_3C_2 after Biginelli reaction.

^{1}H- and ^{13}C-NMR analysis for ethyl 4-(4-formylphenyl)-6-methyl-2-oxo-3,4-dihydro-1H-pyrimidine-5-carboxylate and ethyl 4-(4-formylphenyl)-6-methyl-2-thioxo-3,4-dihydro-1H-pyrimidine-5-carboxylate confirmed the synthesis of these molecules whit TON between 193.3-361.2 and 189.4-371.9. On surface are present both acid and base site (i.e. 0.03 versus 0.02 mmol/g), but more than 95% of the CO_2 was desorbed at a higher temperature as 206 °C, while desorption of NH_3 occurred at a lower temperature, as 74 °C. Also, the solid chemisorbed an important amount of hydrogen (e.g. 3.53 mmol/g) confirming the metallic character as well. The presence of base site led to 24.7% of cyclohexanone conversion, while the acid sites directed the selectivity to the 2-benzyliden cyclohexanone product of 91.30%. The blank reaction does not lead to values in 2-benzyliden cyclohexanone greater than 6.71%. The literature data confirms that in the presence of base solid the conversion is much higher while the selectivity to the di-condensed product is almost total [2].

Conclusions

Ni-Al-Ti_3C_2 Mxene is a viable candidate for the Biginelli reaction with 92.1% yield in ethyl 4-(4-formylphenyl)-6-methyl-2-oxo-3,4-dihydro-1H-pyrimidine-5-carboxylate and 94.8% yield in ethyl 4-(4-formylphenyl)-6-methyl-2-thioxo-3,4-dihydro-1H-pyrimidine-5-carboxylate. Also, the presence of acid-base sites facilitates a discretionary targeting to the mono-condensed product for Claisen-Schmidt condensation.

Acknowledgements

Funding from the Romanian Ministry of Research, Innovation and Digitalization is acknowledged within the project PNRR-III-C9-2022-I5-18 (contract 760010/2022).

References

[1] R. Ciriminna, C. Della Pina, R. Luque, M. Pagliaro, Org. Process. Res. Dev. 29 (2025) 1191.
[2] B. Cojocaru, B.C. Jurca, R. Zăvoianu, R. Bîrjega, V.I. Pârvulescu, O.D. Pavel, Catal. Commun. 170 (2022) 106485.

Noble Metals-Modified ZnAl Mixed Oxides as Efficient Catalysts for the Photodegradation of Bisphenol A

Liuba Cretu[1], Monica Pavel[1], Anca Vasile[1], Razvan State[1], Alexandru Ioan Straca[2], Alexandra Minea[2], Florica Papa[1]*, Ioan Balint[1]
[1] "Ilie Murgulescu" Institute of Physical Chemistry of the Romanian Academy, 202 Spl. Independentei 060021 Bucharest, Romania
[2] Faculty of Chemistry, University of Bucharest, 4-12, Blvd. Regina Elisabeta, 030018 Bucharest, Romania
**Corresponding author: frusu@icf.ro*

Introduction

Layered double hydroxides (LDHs), also known as hydrotalcite-like compounds, constitute an important class of lamellar inorganic materials. Their structure is represented by the general formula of $[M^{2+}_{1-x}M^{3+}_{x}(OH)_2]^{x+}(A^{n-})_{x/n}\cdot mH_2O$, where M^{2+} and M^{3+} are divalent and trivalent metal cations and A^{n-} is a charge-balancing anion located in the interlayer space [1]. These compounds are very attractive due to their robust structure, flexible physicochemical properties, environmentally friendly preparation, and nontoxicity. After calcination, these LDHs yield mixed oxides with unique features, such as high specific surface area, good stability, and homogeneity of cations. One facile and effective route to enhance the photocatalytic activity of mixed oxides derived from LDH precursors is to decorate their surfaces with well-controlled nanoparticles (NPs). This study focuses on the development of mono- (Au, Ni) and bimetallic (Ni-Au) NPs supported on ZnAl mixed oxides issued from LDH precursors and their detailed characterization. The obtained materials were investigated as efficient catalysts for the photocatalytic degradation of Bisphenol A (BPA).

Experimental

In the first stage, ZnAl LDH precursor was synthesized using the coprecipitation method at a constant pH of 9.5. This involved metal nitrates in a ratio of $M^{2+}/M^{3+} = 3/1$, combined with an aqueous precipitation solution containing 1 M NaOH and 0.2 M Na_2CO_3. The precipitate was stirred and aged at 75 °C for 12 h. The resulting solid was washed with deionized water and dried at 110 °C overnight. The zinc-aluminium mixed oxide was obtained by thermal decomposition of ZnAl-type LDH precursor at 650 °C for 6 h in an air atmosphere. Mono- (Ni, Au) and bimetallic (Ni-Au) NPs protected by PVP (polyvinylpyrrolidone) were prepared by the alkaline polyol method. The preparation protocol is described in detail in a previous publication [2]. Well-dispersed nanoparticles (NPs) were deposited on ZnAl oxides derived from the LDH precursors by dispersing the colloidal nanoparticles onto the $ZnAlO_x$ support. The catalytic materials were then dried at 100 °C for 4 h and subsequently calcined at 350 °C for 1 h.

The photocatalytic degradation of Bisphenol A (BPA) was conducted under simulated solar irradiation in a quartz photoreactor maintained at 20 °C. The light source was a solar simulator (AM 1.5 Peccell-L01, Yokohama, Japan) equipped with a 150 W Xe short-arc lamp, producing 1000 $W\cdot m^{-2}$ intensity.

Results and discussion

The LDH structure was confirmed by X-ray diffraction (XRD) analysis. Calcining the ZnAl LDH at 650 °C resulted in a pure ZnO crystalline phase. The deposition of the nanoparticles onto the ZnAlO matrix was also verified using XRD tool. The optical features of unmodified ZnAlO and those of NPs-containing ZnAlO mixed oxides are displayed in Fig.

1 . The time-dependent concentration of BPA over ZnAlO, Ni@ZnAlO, Au@ZnAlO and Ni-Au@ZnAlO are given in Fig. 2.

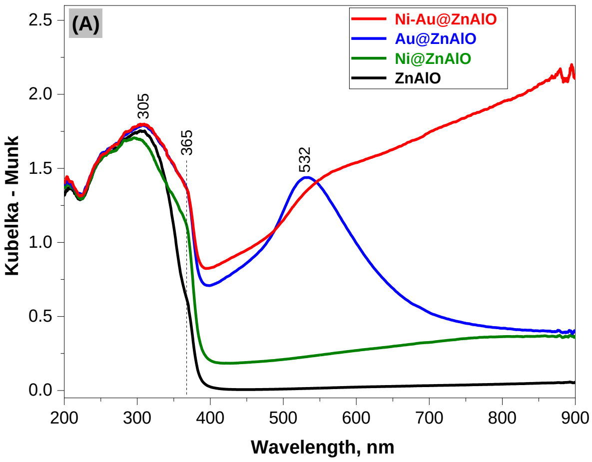

Fig. 1. The UV-Vis absorption spectra of ZnAlO, Ni@ZnAlO, Au@ZnAlO, and Ni-Au@ZnAlO photocatalysts.

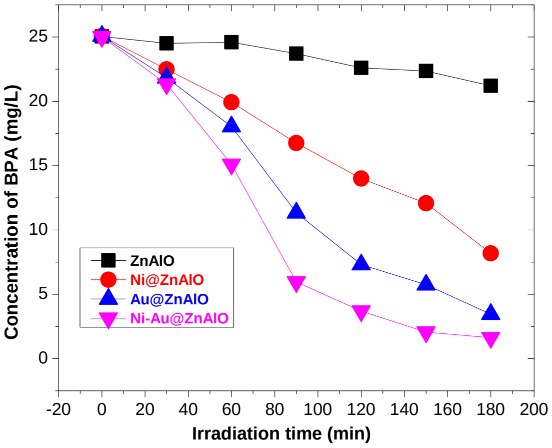

Fig. 2. Time-dependent concentration of BPA.

Conclusions

The Ni-Au@ZnAlO catalytic systems demonstrated superior photocatalytic efficiency in eliminating BPA from wastewater compared to the NP-free ZnAlO catalyst. The photocatalytic activity order towards BPA degradation evolved as follows: Ni-Au@ZnAlO > Au@ZnAlO > Ni@ZnAlO > ZnAlO. The results suggest that these materials could facilitate the development of effective compounds for plastic waste removal and may have other environmental applications.

References

[1] A. Sharma, S. Kumari, S. Sharma, T. Singh, S. Kumar, A. Thakur, S.K. Bhatia, A.K. Sharma. Mater. Tod. Sustain. 22 (2023) 100399.
[2] F. Papa, C. Negrila, M. Miyazaki, I. Balint, J. Nanopart. Res. 13(10) (2010) 5057.

Design of Bi-Enzymatic Cascade System for Converting Benzaldehydes into Value-Added Products

Laura Barabás, Tímea Csete, Csaba Paizs*
Enzymology and Applied Biocatalysis Research Center, Babeș-Bolyai University, Cluj-Napoca, Romania
**Corresponding author: csaba.paizs@ubbcluj.ro*

Introduction

Over the past decade, transaminase (TA) catalysis has emerged as a highly active area of research, driven by the growing demand for chiral amine pharmaceuticals. TAs are pyridoxal 5'-phosphate-dependent enzymes that facilitate the transfer of amino groups from donor molecules to acceptor molecules [1-5].

Pyruvate decarboxylase (PDC), particularly from *Zymomonas mobilis*, is recognized as an industrially valuable biocatalyst and a promising target for metabolic engineering aimed at producing high-value compounds [6].

A synergistic combination of TA and PDC offers a promising approach for the synthesis of biogenic products [9]. In particular, PDC is employed to shift the equilibrium of the TA-catalyzed reductive amination towards amine product formation by removing pyruvate, a byproduct, from the reaction mixture.

In this study, the (*S*)-selective TA from *Pseudomonas psychrotolerans* was utilized to synthesize a range of benzylic amines. To shift the equilibrium towards amine production, PDC from *Zymomonas mobilis* was employed to catalyze the condensation of unreacted aldehydes into enantiopure α-hydroxy ketones, thereby converting the starting materials into valuable products: benzylic amines and acyloins. Additionally, to improve cost-efficiency, the reactions were also performed using whole-cell biocatalysts

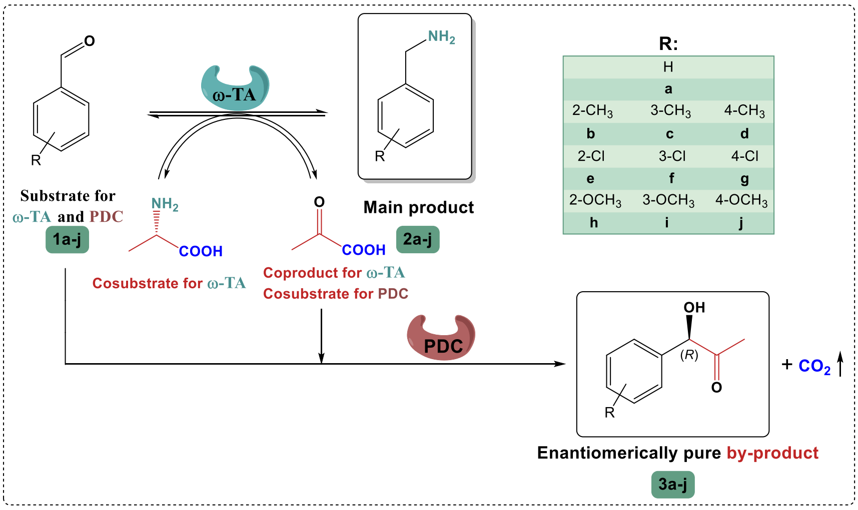

Fig. 1. Bi-enzymatic cascade for the conversion of benzaldehydes to benzylamines and enantiopure α-hydroxy ketones catalyzed by *PpS*-TA and *Zm*PDC.

Experimental

A series of experiments was carried out to optimize a cascade system using (*S*)-selective transaminase from *Pseudomonas psychrotolerans* (*PpS*-TA) and pyruvate decarboxylase from *Zymomonas mobilis* (*Zm*PDC) for the synthesis of benzylic amines and acyloins. Key factors such as pH, substrate concentration, and enzyme loading were systematically investigated. The role of *Zm*PDC in shifting the transamination equilibrium toward product formation was also assessed. HPLC-MS/MS and preparative HPLC methods were developed for reaction monitoring and product purification.

Results and discussion

A biocatalytic cascade with (*S*)-selective *PpS*-TA and *Zm*PDC was optimized using benzaldehyde as a model substrate. Key factors such as pH, enzyme and substrate concentrations, and enzyme addition timing were evaluated, with pH 7.0 and 100 $\mu g \cdot mL^{-1}$ enzyme loading identified as optimal. Simultaneous enzyme addition gave the highest overall conversions. *Zm*PDC effectively shifted the transamination equilibrium, doubling benzylamine yield. Substituted benzaldehydes showed structure-dependent efficiencies, with chlorinated derivatives giving the highest acyloin conversion.

Conclusions

We optimized a two-enzyme cascade using *PpS*-TA and *Zm*PDC for the efficient conversion of benzaldehydes to benzylic amines and acyloins. This system offers a mild and efficient route for dual biocatalytic synthesis.

These studies collectively enabled a detailed understanding and fine-tuning of the biocatalytic cascade, laying the groundwork for scalable synthesis of valuable amines and α-hydroxy ketones.

Acknowledgements

The present work has received financial support through the Proiect PNRR, contract nr. 760042/23.05.2023, Advanced (multi)-enzymatic synthesis and purification processes for biobased furan derivatives – ASPIRE.

References

[1] E.E. Ferrandi, D. Monti, World J. Microbiol. Biotechnol. 34 (2018) 1.
[2] A. Gomm, E. O'Reilly, Curr. Opin. Chem. Biol. 43 (2018) 106.
[3] S.A. Kelly, S. Pohle, S. Wharry, S. Mix, C.C.R. Allen, T.S. Moody, B.F. Gilmore, Chem. Rev. 118 (2018) 349.
[4] S.A. Kelly, S. Mix, T.S. Moody, B.F. Gilmore, Appl. Microbiol. Biotechnol. 104 (2020) 4781.
[5] I. Slabu, J. Galman, R. Lloyd, N. Turner, ACS Catal. 7 (2017) 8263.
[6] D. Dobritzsch, S. König, G. Schneider, G. Lu, J. Biol. Chem. 273 (1998) 20196.
[7] L. Quinn, P. Armshaw, T. Soulimane, C. Sheehan, M.P. Ryan, J.T. Pembroke, Microorganisms. 7 (2019) 494.
[8] Y. Zhang, P. Yao, Y. Cui, Q. Wu, D. Zhu, Adv. Synth. Catal. 360 (2018) 4191.
[9] N. Alcover, G. Álvaro, M. Guillén, Catalysts 11 (2021) 973.

Pt-3D Graphene Nanocomposite for Enhanced Glycerol Oxidation

Monica Dan*, Oana Grad, Angela Kasza, Maria Mihet, Alexandru Turza, Septimiu Tripon, Diana Lazar
National Institute for R&D for Isotopic and Molecular Technologies, Cluj Napoca, Romania
**Corresponding author:* monica.dan@itim-cj.ro

Introduction

Using partial oxidation to turn waste materials like glycerol into useful compounds such as aldehydes, ketones, and carboxylic acids could be regarded as an example of circular economy in action [1]. To achieve high yield and selectivity in partial oxidation of glycerol, many factors (temperature, oxygen concentration, pH, reactor pressure, catalyst) have to be very carefully considered [2,3]. We have developed a series of catalysts that might have the potential to enhance the partial oxidation of glycerol. The prepared catalysts are based on 3D graphene with controlled mesoporous-macroporous structure decorated with monometallic (Pt).

Experimental

The 3D graphene support has been synthetized from graphene oxide through assembly via the hydrothermal method by regulating temperature and pressure conditions. The metallic nanoparticles (2%) have been incorporated into the 3D graphene support by employing the wet impregnation method using as precursor H_2PtCl_6 followed by reduction in Ar + H_2 (10% vol.) at 250 °C for 1 h. Different characterization methods were used to analyze the 3D graphene metallic nanocomposites, such as X-ray diffraction to examine the crystalline structure of the nanocomposite before and after the metal nanoparticles deposition, the thermogravimetric analysis (TGA) to evaluate the thermal stability, and electron microscopy (including both TEM and SEM) to highlight the presence and distribution of the metallic nanoparticles. The catalytic activity tests were performed in a glass reactor in liquid state, applying mild reaction conditions (2 bar, 40 °C, with a reaction time of 3, 6, 9 h).

Results and discussion

Fig. 1a shows the XRD pattern of the prepared nanocomposite material, confirming the presence of a 3D structure with 3-4 layers of graphene, indicated by the large broad peak at $2\theta=24°$. The addition of platinum (Pt) nanoparticles does not alter the 3D structure of the nanocomposite. The lines corresponding to Pt do not appear indicating very small Pt crystallites. The surface morphologies of the 3D-graphene/Pt nanocomposites were examined by SEM and TEM (Fig. 1b and 1c). The SEM investigation confirms the 3D porous structure with open pores in the range of hundreds of nanometers to several micrometers [4]. From the TEM image analysis we can conclude that the Pt nanoparticles are of small size (up to 5 nm) and homogenously distributed on the surface of the 3D-graphene nanocomposites Fig. 1c.

From the structural and morphological characterization, we can conclude that it exists a strong interaction between the Pt nanoparticles and the 3D-graphene support, which could enhance the nanocomposite's catalytic proprieties.

The catalytic activity function of reaction time on is presented in Fig. 2a. We observe that an increase in reaction time leads to a higher catalytic conversion of glycerol. Product analysis shown in Fig. 2b reveals the formation of glyceric acid, glyceraldehyde and dihydroxyacetone suggesting thus that Pt-nanocomposite promotes both oxidation and isomerization pathways.

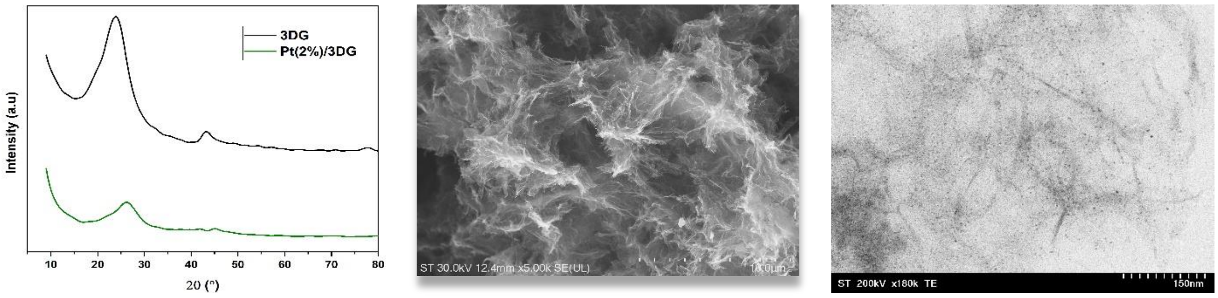

(a) (b) (c)

Fig. 1. (a) XRD recorded spectra; (b) SEM of 3DG composites; (c) TEM images of Pt (2%)/3DG

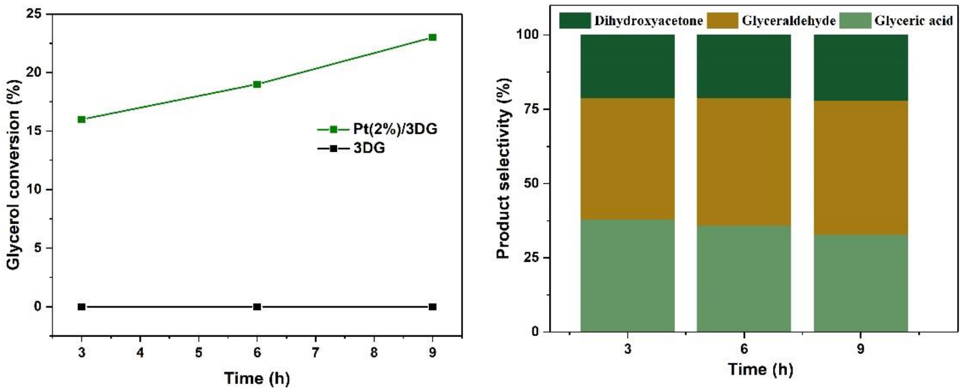

(a) (b)

Fig. 2. (a) Glycerol conversion vs time and (b) selectivity to reaction products.
(*Reaction conditions: 4 mL 1wt.% glycerol, 2 bar* O_2*, Pt: glycerol ratio = 1:440*).

Conclusions

We have developed a method of synthesis for metallic nanocomposites with high porosity and a good dispersion of metallic nanoparticle. This method ensures a homogeneous incorporation of Pt metal nanoparticles onto the 3D-graphene structure. The prepared Pt-nanocomposite has proven to be a good catalytic material in the partial oxidation of glycerol, with great potential for green chemistry.

Acknowledgements

The research leading to these results has received funding from the PNRR-III-C9-2022-I8, Project no. CF 167/15.11.2023, Molecular Carbon Nanostructures: Establishing a Green Synthesis, Studying Properties, and Examining Potential Applications.

References

[1] S. Verma, S. Lu, P.J.A. Kenis, Nature Energy 4 (2019) 466.
[2] X. Hu, J. Lu, C. Liu, L. Chen, X. Zhang, H. Wang, Environ. Chem. Lett. 21 (2023) 2825.
[3] S. Sattayasamitsathit, Y. Gu, K. Kaufmann, W. Jia, X. Xiao, M. Rodriguez, S. Minteer, J. Cha, B. Burckel, S. Wang, R. Polsy, J. Wang, J. Mat. Chem. A 1 (2013) 1639.
[4] M. Zhang, Y. Sun, J. Shi, W. Ning, Z. Hou, Chin. J. Catal. 38 (2017) 537.

Central Composite Model for Parameters Optimization in the Enzyme Catalyzed Esterification

Adrian-Ioan Dudu*, Csaba Paizs, Monica Ioana Toșa
Enzymology and Applied Biocatalysis Research Center, Faculty of Chemistry and Chemical Engineering, Babeș-Bolyai University, Arany Janos 11, 400028, Cluj Napoca, Romania
**Corresponding author: adrian.dudu@ubbcluj.ro*

Introduction

In recent years an increase in the public's demand for bio-products has been observed. This has prompted increased efforts by the food and agricultural industries to develop alternative methods for preparing food ingredients with significantly reduced environmental impact in order to satisfy the general public's needs.

The current work shows the synthesis of seven aroma esters (anisyl propionate and butyrate, cinnamyl propionate and butyrate, benzyl propionate, butyrate and hexanoate) by direct esterification of carboxylic acids with the corresponding alcohols mediated by lipase B from *Candida antarctica* encapsulated in a sol-gel matrix in a solvent-free system using vacuum to remove the resultant water. The reaction parameters were optimized for each reaction system by factorial design experiments considering four factors (acid excess, temperature, applied vacuum and reaction time) on two levels. This study presents an alternative to the currently applied method for obtaining aroma esters which is extraction from natural sources.

Experimental

Lipase B from *Candida antarctica* (CaL-B) was encapsulated in a tailored sol-gel matrix based on octyltriethoxysilane, *n*-propyltrimethoxysilane and tetramethoxysilane mixture (in a molar *ratio* of 1.6:0.4:1, respectively) using polyvinylic alcohol (as a 4% aqueous solution) as additive. The synthesis of seven aroma esters (anisyl propionate and butyrate, cinnamyl propionate and butyrate, benzyl propionate, butyrate and hexanoate) was performed by direct esterification of aromatic alcohols (anisyl, cinnamyl, benzyl) with short-chained fatty acids (propionic, butyric, hexanoic) in a solvent-free system.

Results and discussion

By applying factorial design method (central composite) for optimization of each reaction the conversions were significantly increased (for example, from an isolation yield of 49.4% to 94.3% for cinnamyl butyrate). A semi-preparative experiment was further set-up for cinnamyl butyrate preparation and green chemistry metrics were determined for the above-mentioned synthesis. A mass intensity of 6.04 and a *E*-factor of 4.76 demonstrated that the newly developed enzymatic process is suitable for industrial application based on the green chemistry principles. The 'heat maps' for the factorial design experiments of 3 selected aroma esters and the green metrics calculation results for the semi-preparative experiment for cinnamyl butyrate synthesis are presented in Fig. 1.

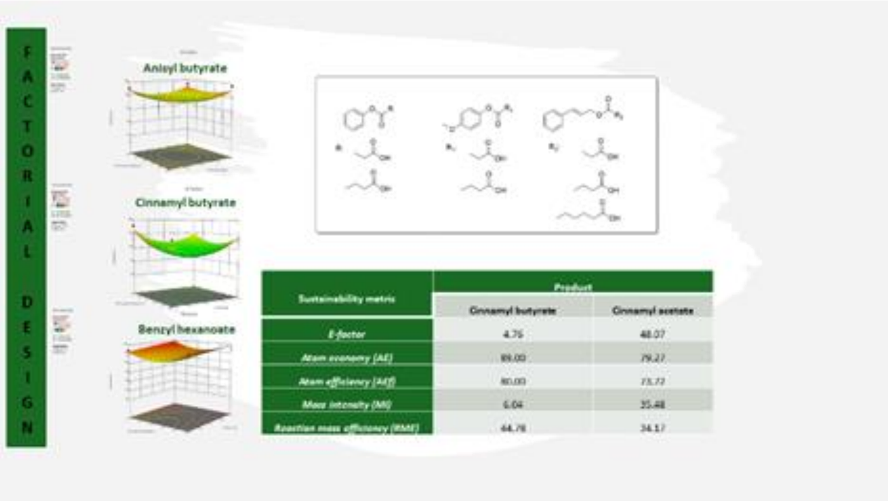

Sustainability metric	Product	
	Cinnamyl butyrate	Cinnamyl acetate
E-factor	4.76	48.07
Atom economy (AE)	89.00	79.27
Atom efficiency (AEf)	80.00	73.72
Mass intensity (MI)	6.04	35.48
Reaction mass efficiency (RME)	44.78	34.17

Fig. 1. Green metrics calculation results and heat maps for the factorial design experiments in the case of anisyl butyrate, cinnamyl butyrate and benzyl hexanoate.

Conclusions

Factorial design experiments were set-up for seven aroma esters of interest and the conversion values were significantly improved using the optimal parameters determined for each aroma ester. These results can be considered a solid base for a potential industrial scale-up of the enzymatic esterification process for aroma ester preparation.

Acknowledgements

This work was supported by the project “Advanced (multi)-enzymatic synthesis and purification processes for bio-based furan derivatives – ASPIRE” funded by European Union – NextGenerationEU and the Romanian Government, under National Recovery and Resilience Plan for Romania, contract no 760042/23.05.2023, cod PNRR-C9-I8-CF25/14.11.2022, through the Romanian Ministry of Research, Innovation and Digitalization, within Component 9, Investment I8.

Hydrothermal Synthesis of 3D Reduced Graphene Oxide as Catalytic Support for Gold Nanoparticles

Oana Grad*, Monica Dan, Angela Kasza, Maria Mihet, Alexandru Turza, Septimiu Tripon, Diana Lazar

National Institute for Research and Development of Isotopic and Molecular Technologies, 67-103 Donat Str. 400293 Cluj-Napoca, Romania

**Corresponding author: oana.grad@itim-cj.ro*

Introduction

The porous 3D graphene-based materials have attracted intense interest due to their unique network structure, high porosity, large surface area, excellent chemical/thermal stabilities, and mechanical properties [1]. For this reason, 3D graphene materials have been extensively studied for various applications in composite materials, catalysis, environmental protection, energy storage, and sensors [2]. The methods reported for preparing 3D graphene architectures have garnered significant attention, primarily focusing on graphene compositions combined with polymers or carbon nanotubes. In contrast, hydro/solvothermal 3D self-assembly synthesis offers a scalable, efficient, and low-temperature approach for producing 3D graphene by reducing graphene oxide [3].

In this study, we report the preparation and characterization of stable supramolecular reduced graphene oxide (3D-rGO) hydrogel, fabricated through hydrothermal self-assembly of graphene oxide (GO) using a one-step method and used as catalytic support in the preparation of gold catalysts. The catalytic activity and selectivity of the resulted catalysts will be investigated for glycerol oxidation in the liquid phase.

Experimental

The hydrothermal synthesis process of 3D-rGO hydrogel was developed and optimized by identifying the optimal reaction conditions (ultrasound time, temperature, autoclave reaction time, and the concentration of graphene oxide in H_2O).

The catalysts prepared on the 3D-rGO support were Au(2%)/3D-rGO ($NaBH_4$) and Au(2%)/3D-rGO (Ar + H_2). The employed preparation methods were impregnation in a solution of 3D-rGO, followed by *i)* chemical reduction with 1M $NaBH_4$ in 0.3M NaOH for 4 h at room temperature or *ii)* thermal reduction in a (H_2+Ar) mixture (10 vol.% H_2) for 1 h at 250 °C. The resulted materials were characterized by X-ray diffraction (XRD) to identify graphene and establish the degree of reduction of GO and scanning electron microscopy (SEM) to visualize the 3D porous structure. Additionally, the thermal stability and textural properties (surface area, porosity) were assessed using thermogravimetric analysis (TGA) and the multipoint Brunauer-Emmet-Teller (BET) method.

Results and discussion

The synthesis parameters which were studied and optimized for the reproducible and efficient preparation of 3D-rGO were: GO concentration in water (2-8 $mg\cdot mL^{-1}$), sonication time (2-4 h), sonication frequency (30 - 35%), reaction time (12-48 h), reaction temperature (100-180 °C). The optimized parameters were: 8 $mg\cdot mL^{-1}$ GO in water, 2 h sonication time, 35% sonication frequency, 24 h reaction time, and 180 °C reaction temperature. The resulted 3D-rGO hydrogel shows a 3D porous network structure and good mechanical and thermal stability, Fig. 1a and Fig. 1b.

After the Au impregnation, the reduction by (H_2+Ar) led to a uniform dispersion of metal nanoparticles on the 3D-rGO support, while the reduction with $NaBH_4$ produced agglomeration of AuNPs (bunch-like appearance). Both methods provide relatively large nanoparticles. The XRD profiles of both catalysts are very similar, indicating the good crystallinity of the carbon and the formation of a few layers of 3D-rGO material. Metal reflexions can also be seen, Fig. 1c. The surface area is lower compared to the support, ranging in the 77-83 $m^2 \cdot g^{-1}$, which is in the same domain as other metal few-layer graphene type materials, Table 1.

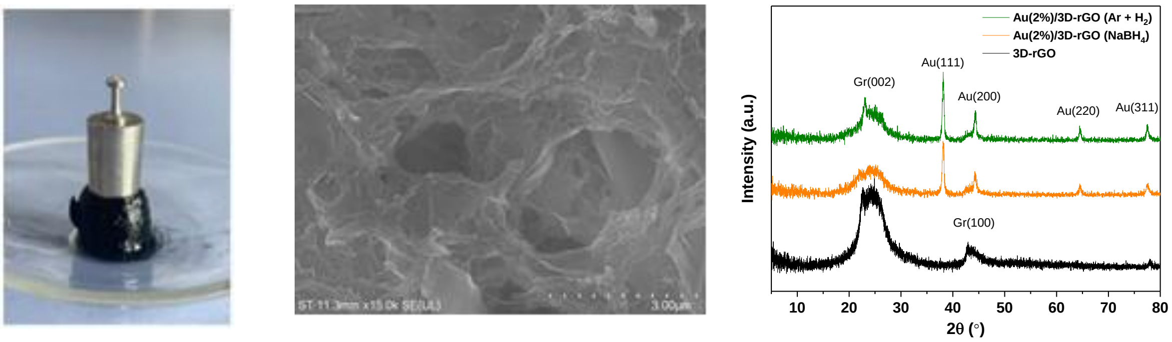

(a) (b) (c)

Fig. 1. (a) Image of a wet 3D-rGO hydrogel demonstrating its mechanical strength; (b) SEM image of 3D-rGO hydrogel; (c) XRD patterns of the Au(2wt.%)/3D-rGO catalysts.

Table 1. Textural properties of the Au(2wt.%)/3D-rGO catalysts.

Catalyst	S_{BET} ($m^2 \cdot g^{-1}$)	V_p ($cm^3 \cdot g^{-1}$)	d_{Gr} (nm)	n
3D-rGO	106	0.47	0.37	4
Au(2wt%)/3D-rGO ($NaBH_4$)	77	0.45	0.36	4.5
Au(2wt%)/3D-rGO ($Ar+H_2$)	83	0.50	0.36	4.5

d_{Gr} graphene interlayer distance calculated from XRD, n average number of carbon layers in 3D-rGO calculated from XRD

Conclusions

The catalytic support, 3D graphene in the form of rGO hydrogel (3DG) with a 3D structure, was prepared for the deposition of gold nanoparticles. Thus, a hydrothermal preparation method was developed and optimized by determining the optimal reaction conditions. By depositing Au NPs on the 3D graphene catalytic support in the form of rGO hydrogel, two new nanocomposite materials Au(2wt%)/3D-rGO ($NaBH_4$) and Au(2wt%)/3D-rGO ($Ar+H_2$) were prepared and characterized. The results obtained from the characterizations proved the achievement of the desired composition, the porous structure, and the uniform distribution of nanoparticles on the surface of the catalytic support. The catalytic performance of both catalysts will be investigated toward glycerol oxidation reaction in the liquid phase.

Acknowledgements

The authors acknowledge the PNRR-III-C9-2022-I8 Project no. 167/15.11.2023, Molecular Carbon Nanostructures: Establishing a Green Synthesis, Studying Properties, and Examining Potential Applications.

References

[1] Z. Chen, L. Jin, W. Hao, W. Ren, H-M. Cheng, Mater. Today Nano 5 (2009) 100027.
[2] Q. Shi, Y. Cha, Y. Song J-I. Lee, C. Zhu, X. Li, M-K. Song, D. Du, Y. Lin, Nanoscale 8 (2016) 15414.
[3] P.S. Sasikala, P. Polin, C. Aymonier, Adv. Mater. 29 (2017) 1605473.

WonderFALL – Chemo-Enzymatic Cascade for D-Phenylalanine Analogues

András Ernő Iszlai, Raluca Bianca Tomoiaga, Anca Elena Anghel, Monica Ioana Toşa, Csaba Paizs, László Csaba Bencze*
Enzymology and Applied Biocatalysis Center, Faculty of Chemistry and Chemical Engineering, Babeş-Bolyai University
**Corresponding author: laszlo.bencze@ubbcluj.ro*

Introduction

Aromatic d-amino acids (d-AAs) have gained increasing attention in the industry, especially in the pharmaceutical field. Recently, biocatalytic procedures for the synthesis of d-AAs emerged as powerful and environmentally friendly methods [1]. Our research group studied a complex chemoenzymatic pathway to obtain d-phenylalanines from benzaldehyde analogous using four different biocatalysts. For the scalable and high-yield production of d-phenylalanine analogues, we adapted a chemo-enzymatic cascade featuring three key enzymes: *wild-type* and engineered phenylalanine ammonia-lyase from *Arabidopsis thaliana* (*At*PAL) variants [2], l-amino acid deaminase from *Proteus mirabilis* (*Pm*LAAD) [3], and an engineered d-amino acid dehydrogenase from *Ureibacillus thermosphaericus* (*Ut*DAADH) [4], while glucose dehydrogenase from *Bacillus subtilis* (*Bs*GDH) handled the continuous NADPH cofactor regeneration (Fig. 1).

Experimental

The preparative-scale synthesis started from 0.5 g of the differently substituted benzaldehydes and two equivalents of malonic acid dissolved in DMSO. The mixture was under reflux at 90 °C for 6 h in the presence of piperidine, yielding the corresponding *trans*-cinnamic acid. The resulting *trans*-cinnamic acid was diluted in 4 M NH_4OH (pH 8.5) and up to 5% DMSO, to ensure complete solubilisation. Next, the biocatalytic cascade was caried out using *E. coli* whole cells individually expressing *At*PAL, for 18 h, followed by the simultaneous addition of *Pm*LAAD, and *Ut*DAADH together with *Bs*GDH, for other 18 h at 35 °C and 200 rpm. The obtained d-phenylalanine was purified using an ion exchange resin.

Results and discussion

To maximise the productivity across the whole cascade depicted in Fig. 1, we fine-tuned one variable at a time (ammonia level, pH, NADPH supply, and the whole-cell-to-substrate ratio) for every enzyme involved. In the opening step, a modified Knoevenagel–Doebner condensation converts a benzaldehyde derivative (1) and malonic acid into the corresponding *trans*-cinnamic acid (2). *At*PAL then performs a hydroamination in the presence of excess ammonia to furnish the l-amino acid (3). Introducing *Pm*LAAD selectively triggers the oxidative deamination of the l-Phe analogue, giving the α-keto acid (4); *Ut*DAADH subsequently reduces the α-keto acid to the corresponding d-amino acid (5) while *Bs*GDH continuously regenerates NADPH by converting d-glucose into gluconic acid. Ammonia proved to be a double-edged sword; high levels needed for the PAL step strongly suppressed the LAAD module, yet a 4 M NH_4OH buffer at pH 8.5 delivered 70-100% conversion at every stage. These optimizations were performed on different substrates and validated both at analytical scale for rapid screening and at preparative scale to confirm synthetic utility.

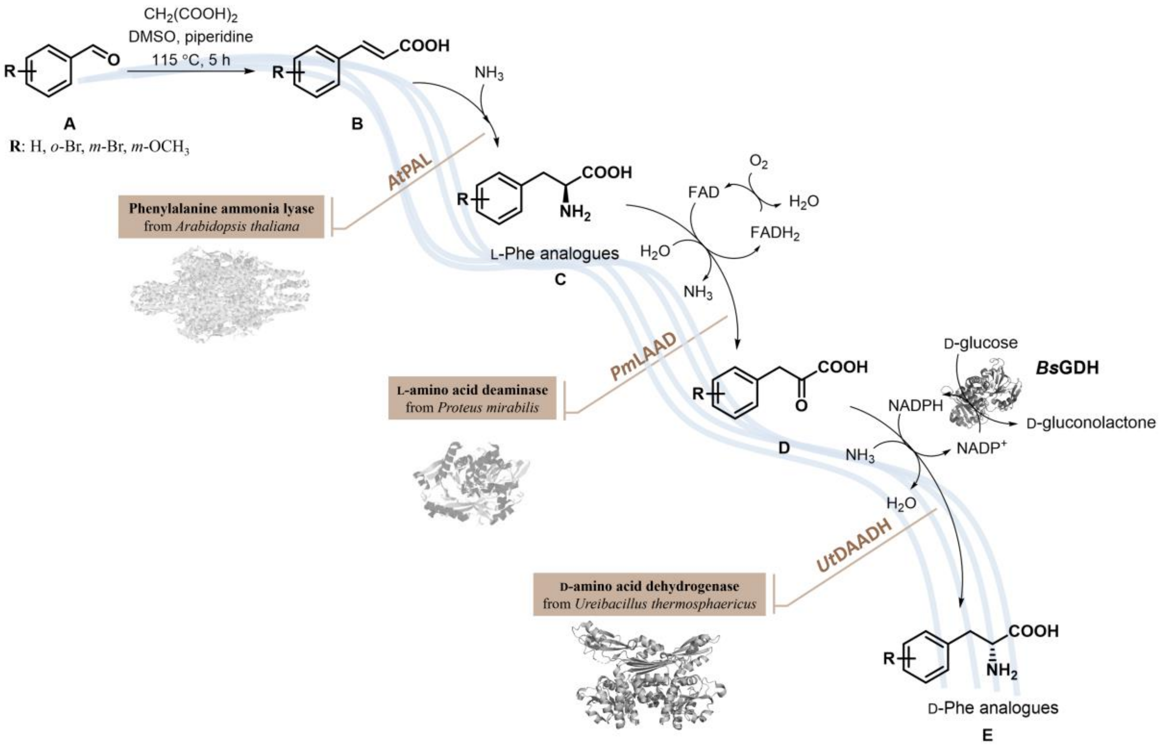

Fig. 1. General overview of the chemo-enzymatic synthesis of D-phenylalanine analogues.

Conclusions

A novel chemo-enzymatic protocol employing engineered PAL and DAADHs has been developed to access high-value d-phenylalanine intermediates. Relying on whole-cell biocatalysts, the cascade is inherently eco-friendly, and its optimised conditions supply preparative-scale quantities of several d-phenylalanine analogues.

Acknowledgements

This work was financed by the National Research Council-UEFISCDI, project nr. PNRR-III-C9-2023 – I8, project code 760241/28.12.2023.

References

[1] F. Parmeggiani, N.J. Weise, S.T. Ahmed, N.J. Turner, Chem. Rev. 118 (2018) 73.
[2] A. Dreßen, T. Hilberath, U. Mackfeld, A. Billmeier, J. Rudat, M. Pohl, J. Biotech. 258 (2017) 148.
[3] L. Zhu, G. Feng, F. Ge, P. Song, T. Wang, Y. Liu, Z. Zhou, Appl. Biochem. Biotechnol. 187 (2019) 75.
[4] H. Akita, J. Hayashi, H. Sakuraba, T. Ohshima, Front. Microbiol. 9 (2018) 1760.

Mechanistic Investigations of CO_2 Reduction on bi-Dimension Metal-Carbon Catalysts: Experimental Kinetics and Theoretical Modelling

Raluca-Ioana Jalbă[1,2], Bogdan Jurca[1], Isabela Man[2], Vasile Pârvulescu[1]*
[1]*Faculty of Chemistry, University of Bucharest, 4-12 Regina Elisabeta Av., Bucharest, Romania*
[2]*"C. D. Nenițescu" Institute of Organic and Supramolecular Chemistry*
**Corresponding author: vasile.parvulescu@chimie.unibuc.ro*

Introduction

The effects of the CO_2 emissions in terms of global warming and climate change are well known. In this context, using the natural gas distribution network, the Sabatier methanation can provide a potential mitigation of pollution. Thus, the selective CO_2 conversion to CO via Reverse Water Gas Shift (RWGS) offers a clean energy promising route. Further, it can provide a raw source in the Fischer-Tropsch process leading to synthetic fuels [1].

Meanwhile, the methanol has attracted much attention as an important chemical intermediate and molecules platform for the synthesis of important commodities and products such as a wide range of bulk chemicals including DME, formaldehyde, acetic acid, light olefins, aromatics, also serving as an excellent solvent and energy source [2].

On the other side, as metal nanoparticles, the support plays a key role on the catalytic behaviour. Also, single metal atoms could be stabilized via strong metal-support interactions through the charge transfer processes [3] where the metals could be packed into a honeycomb-like 2D lattice. Both carbon and/or nitrogen layers may occupy the octahedral sites through surface terminal groups which largely dictate the properties of MXenes [4]. In this context scattered experimental studies corroborated to theoretical calculations demonstrated MXenes could serve as efficient thermal catalysts for particular reactions [5]. Moreover, tuning the resistance to deactivation by controlling the catalytic activity offers additional advantages, such as the catalysts stability [6].

Experimental

The present study investigated the kinetics of the CO_2 reduction onto bi-dimensional metal-carbon catalysts based on the experimental results and theoretical modelling. With this scope, a matrix of experiments using a packed bed continuous flow reactor, on-line coupled to a gas chromatograph, by varying H_2:CO_2 molar ratio (7, 4, 2, 1), pressure (1, 5, 10, 20, 40 bar) and temperature (150-500 °C) was established while keeping constant the reactants flow. All the investigated catalysts were fully characterized. The theoretical modelling of the support, the metal cluster and the catalyst assembly was performed using a GPAW ab-initio simulation software in the framework of DFT.

Results and discussion

The experimental runs were carried out in a differential conversion regime. Then, the reaction rate and the penta-component real gas mixture diffusion coefficients have been calculated; the mass transfer limitations were excluded based on the Weisz-Prater criterion values. The global activation energies were determined from the Arrhenius plots, Fig. 1a,b. Further, the values of the unit cell parameters and size of the metallic clusters were determined by a Rietveld refinement of the high-resolution XRD patterns and served as experimental input values in the DFT theoretical modelling. Furthermore, to determine the energetics of the catalyst surface intermediates, theoretical investigations concerning CO_2 dissociative chemisorption were performed. As an example, from the DFT theoretical calculations, the surface shown to be very reactive towards the hydrogen chemisorption. However, CO_2 still requires an enough large surface area to be chemisorbed and to undergo a superficial reduction. Therefore, from the theoretical description of a *p(4 x 4)* supercell and 4 atomic slabs used in the modelling of the Co(*111*) FCC with one Fe atom replaced on the surface exposed to reactants, a maximum hydrogen coverage (73.33%) has been provided as an activated surface, Fig. 2.

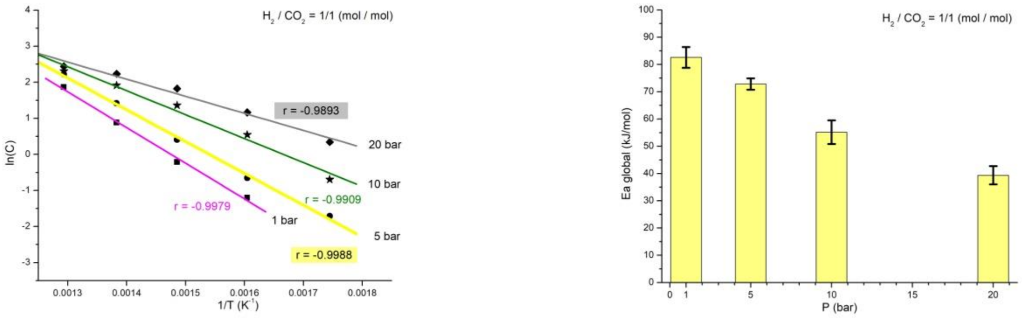

Fig. 1. (a) Arrhenius lines plotted at different pressures for molar ratio H_2/CO_2 = 1/1; (b) Global activation energies determined from slopes of Arrhenius representations H_2/CO_2 = 1/1.

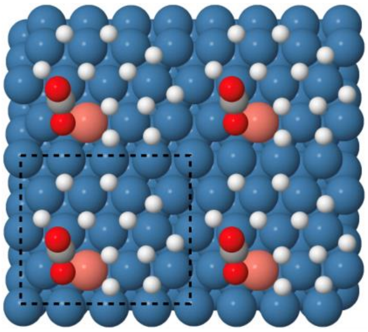

Fig. 2. The maximum hydrogen coverage of 73.33% needed to adsorb and to be activated on the surface for CO_2 chemisorption. The unit cell is marked with dashed line.

Conclusions

The present investigation provided catalytic data related to the behaviour of the metal-carbon-based catalysts, thus affording selectivity to CO, CH_4 or CH_3OH..

Acknowledgements

This work is supported by Doctoral School on Chemistry from the University of Bucharest.

References

[1] J. Wei, Q. Ge, R. Yao, Z. Wen, C. Fang, L. Guo, H. Xu, J. Sun, Nature Commun. 8 (2017) 15174.
[2] H. Zhao, X. Liu, C. Zeng W. Liu, L. Tan, J. Am. Chem. Soc. 146 (2024) 23649.
[3] L. Peng, B. Jurca, A. Primo, A. Gordillo, V.I. Parvulescu, H. García, ACS Sustainable Chem. Eng. 9 (2021) 9264.
[4] V. Mohammadi, J. Rosen, Y. Gogotsi, Science 372 (2021) 1165.
[5] R.R. Grau, P.G. Aznar, G. Sastre, S. Goberna-Ferrón, O. Pavel, A. Tirsoaga, B. Cojocaru, D.G. Popescu, V.I. Parvulescu, A. Primo, H. García, J. Am. Chem. Soc. 147 (2025) 3315.
[6] B. Jurca, L. Peng, A. Primo, A. Gordillo, V.I. Parvulescu, H. García, ACS Appl. Mater. Interfaces 13 (2021) 36976.

MOF-Derived Carbon Modified $CuO/ZnO/Al_2O_3$ Catalysts for CO_2 Hydrogenation to Methanol

Angela M. Kasza[1,2]*, Mihaela D. Lazar[1], Maria Mihet[1]
[1]*National Institute for Research & Development of Isotopic and Molecular Technologies - INCDTIM, 67–103 Donat Str., 400293 Cluj–Napoca, Romania*
[2]*Babes-Bolyai University, Faculty of Chemistry and Chemical Engineering, 11 Arany Janos Str., 400028, Cluj–Napoca, Romania*
**Corresponding author: angela.kasza@itim-cj.ro*

Introduction

In light of the growing scientific and technological interest in converting CO_2 into valuable chemicals, the hydrogenation of CO_2 to methanol (CO_2-to-MeOH) has recently gained significant momentum. This process is seen not only as a promising pathway for reducing CO_2 emissions, but also as an alternative method for energy storage in chemical form, within the framework of the "*power-to-liquid*" (*P2L*) concept [1], as well as a complementary route to the traditional methanol production from syngas. However, the CO_2-to-MeOH process presents several complex challenges due to its thermodynamic constraints – being a highly exothermic reaction, proceeding with decreasing number of moles – as well as the inherent stability of the CO_2 molecule, potential side reactions, and catalyst deactivation, all of which are intricately linked. Recent research efforts have largely centered on catalyst optimization to enhance methanol yield, and the most extensively studied catalyst is the commercial $Cu/ZnO/Al_2O_3$ (CZA), composed of 50-70% Cu, 20-50% ZnO and 5-20% Al_2O_3, an untypical catalyst since the metal oxides do not play the role of supports for Cu [2].

Among the various strategies targeting enhanced catalytic performance, the use of carbon materials emerges as a particularly versatile approach. In the present study, MOF-derived carbon (C_{MOF}) was used to modify CZA catalysts, as it can simultaneously contribute to increasing the specific surface area, improve copper dispersion, and increase water resistance due to the hydrophobic character of the added carbon.

Experimental

C_{MOF} was obtained by thermal treatment at 600 °C (at a rate of 0.5 $°C \cdot min^{-1}$) for 5 h, under an inert atmosphere of MIL-53(Al) synthesized by a cost-effective hydrothermal procedure [3], leading to a carbon structure with channel-like porosity, and high surface area (~1500 $m^2 \cdot g^{-1}$), after the complete removal of alumina, which was carried out by leaching in 10% hydrochloric acid at 80 °C for 5 h (as confirmed by TGA measurements).

The C_{MOF}-CZA catalysts were prepared by precipitating 1 M Cu-Zn-Al salt solutions (Cu:Zn:Al = 6:3:1) with 1 M $NaHCO_3$ at pH=7, with the addition of varying amounts of C_{MOF} (0/3/12 wt.%). Materials were characterized by XRD, BET, SEM/TEM/EDX, FT-IR, TPR, CO_2 & H_2-TPD techniques, and the active copper surface area was also determined by the N_2O oxidation method.

Furthermore, thermodynamic equilibrium was investigated under different conditions of temperature, pressure, and reactants mole ratio by thermodynamic simulations in ChemCAD using a Gibbs reactor, with Soave-Redlich-Kwong (SRK) equation of state model.

Results and discussion

X-ray diffraction analysis of CZA catalysts, Fig. 1, indicates the presence of CuO crystallites, with slightly larger crystal sizes observed in the C_{MOF}-modified samples. The absence of distinct ZnO and Al_2O_3 diffraction lines suggests that these components are present in an amorphous state and are highly dispersed within the material. According to BET measurements, both the surface area and pore volume of MOF-derived carbon modified CZA catalysts exhibited a noticeable proportional rise upon increasing the C_{MOF} loading, accompanied by a narrowing of the pore size distribution, Fig. 2.

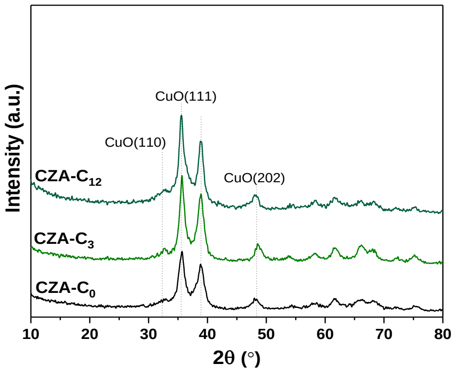

Fig. 1. XRD patterns of CZA catalysts.

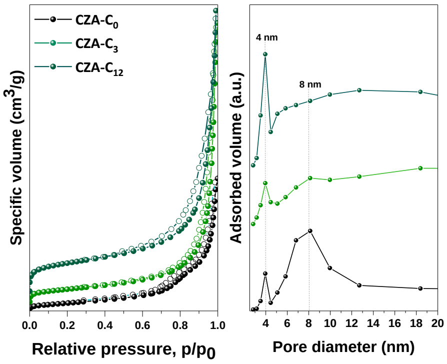

Fig. 2. N_2 sorption isotherms and pore size distribution of CZA catalysts.

Based on the TEM/SEM/EDX analyses, the results revealed a uniform distribution of catalyst components within the matrix, while a slight increase in CuO particle size was observed with higher C_{MOF} content. Furthermore, the reducibility of the catalysts (TPR), as well as their interaction with CO_2 and H_2, were found to be highly dependent by the addition of C_{MOF}; CZA sample with the highest C content, i.e., 12 wt.% desorbs the largest amounts of carbon dioxide and hydrogen (as proved by H_2&CO_2 Temperature Programmed Desorption measurements). Referring to the thermodynamic simulation results, it was found that the operating pressure exerts the most significant impact on the CO_2 hydrogenation process. CO_2 conversion increases almost linearly with rising pressure, while methanol selectivity shows a sharp increase up to a certain pressure threshold, after which the rate of increase becomes more moderate. Additionally, the simulations indicated that CO_2 conversion initially decreases with increasing temperature due to thermodynamic limitations, but begins to rise again beyond a specific temperature point, which can be attributed to the growing contribution of the reverse water-gas shift (RWGS) reaction

Conclusions

Due to the morphological and structural characteristics of these MIL-53(Al)-derived carbon modified CZA catalysts, which exhibit an increased specific surface area, distinct reducibility, altered active copper surface area, and enhanced chemisorption capacity for hydrogen and carbon dioxide, they show promising potential for CO_2 hydrogenation to methanol.

Acknowledgements

This work was supported through the “Nucleu” Program within the National Research Development and Innovation Plan 2022–2027, Romania, carried out with the support of MEC, project no. 27N/03.01.2023, component project code [PN 23 24 01 01].

References

[1] A. Velty, A. Corma, Chem. Soc. Rev. 52 (2023) 1773.
[2] U.J. Etim, Y. Song, Z. Zhong, Front. Energy Res. 8 (2020) 545431.
[3] O. Grad, A.M. Kasza, A. Turza, M. Dan, L. Barbu-Tudoran, M.D. Lazar, M. Mihet, J. Environ. Chem. Eng. 11 (2023) 109456.

Silica-Supported Enzyme Systems for Continuous Flow Kinetic Resolution of Secondary Alcohols

Gabriel Katona[1,]*, Matild Pap[1], Csaba Paizs[1], Melinda-Emese László[1], László Poppe[1,2]
[1]*Enzymology and Applied Biocatalysis Center, Faculty of Chemistry and Chemical Engineering, Babeș-Bolyai University, 400028 Cluj-Napoca, Romania*
[2]*Department of Organic Chemistry and Technology, Budapest University of Technology and Economics, Rakpart street no.3, 1111 Budapest, Hungary*
**Corresponding author:* *gabriel.katona@ubbcluj.ro*

Introduction

Enzyme immobilization through sol-gel techniques is widely regarded as a reliable approach for producing robust biocatalysts. In this study, *Candida antarctica* lipase B (CaL-B) was entrapped within sol-gel matrices synthesized from three different silane-based precursors using mixtures of tetramethoxysilane, triethoxysilanes, and *n*-propyltrimethoxysilane, along with Tween 80 as a modifying agent [1]. The immobilized enzyme's activity was tested within the acylation reaction of 1-phenylethanol with vinyl acetate.

Experimental

Enzymatic kinetic resolution under continuous-flow conditions was performed using a urethane type fotopolimer (BASF Ultracur 3D) based microfluidic reactor equipped with a peristaltic pump, wherein CaL-B lipase immobilized in a sol-gel matrix was packed. The sol-gel biocatalyst was synthesized *via* encapsulation using sodium fluoride (NaF) basic medium, which promoted crosslinking. Tween 80 was incorporated as an additive to enhance enzyme entrapment and stability [2]. The resulting sol-gel material was first ground and fractionated using four molecular sieves (size ranges: >100 µm, 80-100 µm, 80-63 µm, 63-40 µm), and the classified particles were then used to pack the microfluidic reactor. To assess catalytic activity, a solution of racemic 1-phenylethanol and vinyl acetate in hexane was continuously fed into the microfluidic chip. Reaction samples were periodically collected, diluted with hexane, and analyzed using gas chromatography. The enzymatic resolution of *rac*-1 phenylethanol with vinyl acetate in hexane is presented in Fig. 1.

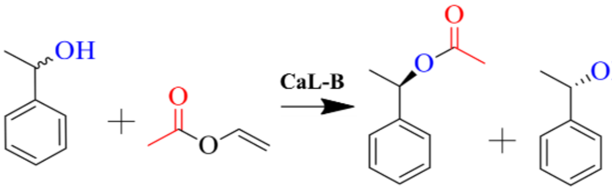

Fig. 1. Enzymatic resolution reaction of *rac*-1 phenylethanol with vinyl acetate.

Results and discussion

Each particle size fraction was tested in the acylation reaction to determine its impact on catalytic performance. Among the tested groups, the 80-63 µm particles exhibited the highest conversion rates, thereby establishing this size range as the most effective for further investigation. Using this optimal particle size fraction, reaction conditions were subsequently optimized, beginning with a temperature range from 25 °C to 60 °C. The optimal temperature was found to be 55 °C, and the best substrate/acylating agent *ratio* was 50 mM PHEETOH: 50 mM VA as demonstrated in Table 1. Time-dependent studies were conducted from 10 to

180 min, and substrate concentration was increased from 50 mM to 300 mM, as detailed in Table 2.

Table 1. Temperature screening of the biocatalyst by substrate concentration ratio changing.

Concentration ratio (mM : mM)	Time (min)	Temperature (°C)	Conversion (C%)
50:50	20	55	40.9
50:37.5			36.7
50:75			38.5
50:100			40.9

Table 1. Temperature screening of the biocatalyst by substrate concentration ratio changing.

Concentration ratio (mM : mM)	Temperature (°C)	Time (min)	Conversion (C%)
50:50	55	180	42.5
60:60			40.2
70:70			37.0
80:80			38.4
90:90			35.0
100:100			32.8
150:150			28.5
200:200			25.0
250:250			21.7
300:300			20.3

Conclusions

In summary, CaL-B was immobilized within silane-based matrices using the sol-gel method with various silane precursors. The resulting biocatalysts were evaluated in the enzymatic esterification of racemic 1-phenylethanol with vinyl acetate under continuous-flow conditions in a microfluidic system. Optimal reaction parameters were determined to be a flow rate of 20 µL·min^{-1}, a substrate concentration/acylating agent *ratio* of 50 mM:50 mM (phenylethanol:vinyl acetate), a reaction temperature of 55 °C, and a residence time of 180 min.

Acknowledgements

This work was supported by the project“Renewable Enzyme Immobilization - RENZI” funded by European Union – Next Generation EU and the Romanian Government, under National Recovery and Resilience Plan for Romania, contract no 760241/28.12.2023, cod PNRR-C9-I8-CF87/31.07.2023, through the Romanian Ministry of Research, Innovation and Digitalization, within Component 9, Investment I8.

References

[1] A. Ursoiu, C, Paul, T. Kurtán, F. Péter, Molecules 17 (2012) 13045.
[2] A.I. Dudu, M.A. Lăcătuș, L.C. Bencze, C. Paizs, M.I. Toșa, ACS Sustainable Chem. Eng. 9 (2021) 5461.

Exploring new yeast strains as whole-cell biocatalysts for the synthesis of (*R*)-phenylacetylcarbinols

Mihai Andrei Lăcătus[1], Monica Ioana Toșa[1], Pál Csuka[2], Viktória Bódai[3], László Poppe[1,2]*, Csaba Paizs[1]*

[1]*Enzymology and Applied Biocatalysis Center, Faculty of Chemistry and Chemical Engineering, Babeș-Bolyai University, Cluj-Napoca, Romania*

[2]*Department for Organic Chemistry and Technology, Budapest University of Technology and Economics, Budapest, Hungary*

[3]*Fermentia Microbiological Ltd, Budapest, Hungary*

**Corresponding authors: csaba.paizs@ubbcluj.ro, poppe.laszlo@vbk.bme.hu*

Introduction

Asymmetric α-hydroxyketones represent important chiral building blocks for the synthesis of many other end-of-the-pipe products, especially in the pharmaceutical industry [1]. As a representative, (*R*)-phenylacetylcarbinol ((*R*)-PAC) is the key precursor for the synthesis of ephedrine and pseudoephedrine [2]. Accordingly, many biocatalytic strategies were developed for the stereoselective synthesis of α-hydroxyketones and the acyloin condensation reaction mediated by employing pyruvate decarboxylase enzymes is by far the most industrially attractive, especially by using whole-cell microorganisms as biocatalysts despite their well know primary disadvantage of by-product formation [2,3]. As such, the discovery of new microorganisms that contain highly active pyruvate decarboxylases, that are also capable of efficiently performing acyloin condensation reactions, is an attractive endeavor.

We explored the potential of 12 newly isolated yeast strains from various genera as whole-cell biocatalysts for acyloin condensation reactions, by screening them for their carboligase activity in the synthesis of (*R*)-phenylacetylcarbinol from benzaldehyde, Fig. 1a. The strains that showed a high carboligase activity were then further investigated and the key reaction conditions were optimized by factorial design experiments, in order to reduce byproduct formation and achieve a high conversion into carboligation product, Fig. 1b. Further, the applicative potential of these yeast strains was emphasized by exploring their native substrate domain, by testing a wide variety of functionalized aromatic aldehydes as substrates, Fig. 1c.

Experimental

Yeasts were received as lyophilized whole cells from Fermentia Microbiological Ltd (Budapest, Hungary). Typical reactions set-up: a suspension of lyophilized yeast cells (150 mg) in 5 mL PBS buffer, containing $MgCl_2$ (0.1 mM) and co-substrate (sodium pyruvate, 0.4 mmol, 2 eq.) was incubated for 0.5 h at room temperature with orbital shaking (1000 rpm), followed by addition of benzaldehyde (0.2 mmol, 1 equiv.) in 100 µL of isopropanol. After addition of the substrate, the reactions were further incubated for 4 h under the same conditions. The reaction outcome was assessed by chiral gas chromatography or by a previously reported proton NMR method/ developed chiral HPLC methods [4].

Results and discussion

In the first stage, the screening of 12 new yeasts revealed four strains with a high carboligase activity (*P. carsonii*, *L. elongisporus*, *C. guilliermondii* and *C. guilliermondii* var) for the synthesis of highly enantiopure (*R*)-phenylacetylcarbinol from benzaldehyde, using sodium pyruvate as substrate. Further, the key reaction conditions (pH, temperature and amount of co-substrate) were optimized using two successive factorial design experiments that assessed the degree of influence for each factor as well as the optimum values for a maximum carboligase activity. In optimum conditions (pH=6, T=20 °C and 2 eq. of pyruvate), the four strains provided quantitative conversions of benzaldehyde and high conversions (80-99%) into the desired (*R*)-PAC product, with excellent optical purities (*ee* > 97%) after just 4 h or reaction. Finally, the preliminary substrate scope of these strains revealed that the native pyruvate decarboxylase enzymes of these yeasts are capable of accepting a wide variety of *meta* and *para* substituted benzaldehydes as substrates, providing conversions of 10-90% into carboligation products with reasonable optical purity (*ee*>90%). Ortho-substituted as well as bulky, sterically hindered aldehydes were no or poor substrates by the PDC enzymes.

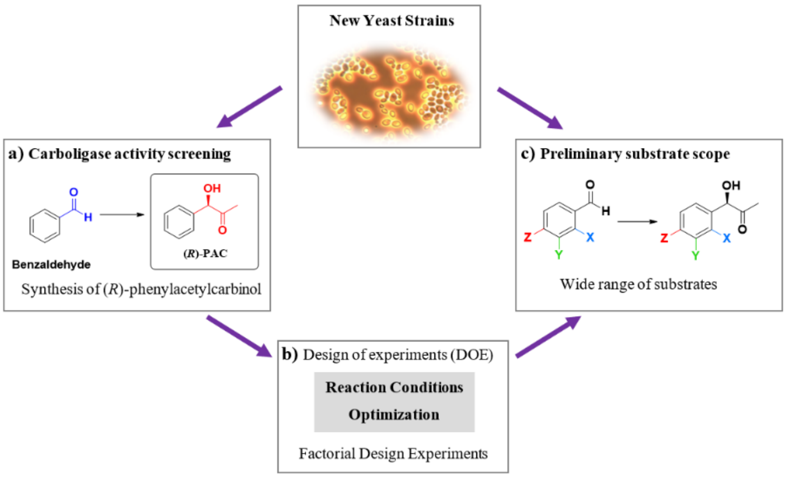

Fig. 1. General overview of investigating the yeast strains as whole-cell biocatalysts for the synthesis of (R)-phenylacetylcarbinol and analogues.

Conclusions

Four new strains of *Pichia carsonii*, *Lodderomyces elongisporus*, *Candida guilliermondii* and *Candida guilliermondii* were identified as potent whole-cell biocatalysts for the synthesis of (*R*)-phenylacetylcarbinol and analogues, with a high PDC enzymatic activity and relatively broad substrate spectrum. Besides the immediate applicability of these yeast strains, they also represent new sources of PDCs for future studies and development.

Acknowledgements

This work was supported by the project "Renewable Enzyme Immobilization - RENZI" funded by European Union – NextGenerationEU and the Romanian Government, under National Recovery and Resilience Plan for Romania, contract no 760241/28.12.2023, cod PNRR-C9-I8-CF87/31.07.2023, through the Romanian Ministry of Research, Innovation and Digitalization, within Component 9, Investment I8".

References

[1] M. Brovetto, D. Gamenara, P. Saenz Méndez, G.A. Seoane, Chem. Rev. 111 (2011) 4346.
[2] C. Andreu, M.L. Del Olmo, Appl. Microbiol. Biotechnol. 98(13) (2014) 5901.
[3] P. Hoyos, J.V. Sinisterra, F. Molinari, A.R. Alcántara, P.D. De María, Acc. Chem. Res. 43 (2010) 288.
[4] C. Andreu, M. lí del Olmo, Appl. Microbiol. Biotechnol. 102 (2018) 4717.

Amino- and Epoxy- Decorated Resin-Based EDTADa-Co^{2+} Chelate Complexes for Enzyme Immobilization

Melinda-Emese László[1,]*, Judith-Hajnal Bartha-Vári[1], Adrian-Ioan Dudu[1], Gabriel Katona[1], Csaba Paizs[1], László Poppe[1,2]
[a]*Enzymology and Applied Biocatalysis Research Center, Babeș-Bolyai University, Faculty of Chemistry and Chemical Engineering, Arany János Street no.11, 400028 Cluj-Napoca, Romania*
[b]*Department of Organic Chemistry and Technology, Budapest University of Technology and Economics, Rakpart street no.3, 1111 Budapest, Hungary*
**Corresponding authors: melinda.laszlo@ubbcluj.ro*

Introduction

In biocatalysis enzyme immobilization has emerged as a powerful strategy to overcome limitations such as low stability, sensitivity to environmental conditions, and difficulty in recovery and reuse of the enzyme in its native form. The choice of the immobilization method depends on the nature of the enzyme, the support material, and the intended application [1]. Immobilized metal-chelate affinity chromatography (IMAC) introduced by Porath *et al.* in 1975 is a widely used chromatographic separation method [2,3,4] based on the specific interaction between electron-donating groups on biomolecules - typically histidine residues - and divalent transition metal ions immobilized on a solid support *via* covalent attachment of a chelating ligand, commonly nitrilotriacetic acid (NTA) or iminodiacetic acid (IDA). This study focuses on the preparation of chelator-type supports charged with Co^{2+} ions, suitable for the immobilization of His-tagged enzymes such as phenylalanine ammonia-lyase from *Petroselinum crispum* (*Pc*PAL) or *Lactobacillus kefir* alcohol dehydrogenase (*Lk*-ADH), starting from two commercially available resin-based supports: SEPLITE LX1000EP with 50 umol epoxy groups/1 g of polymer and SEPLITE LX1000HA with –(CH$_2$)$_6$–NH$_2$ chain, 0.4 mmol amino groups/1 g polymer.

Experimental

Amino-decorated resin-based supports (abbreviated further as AP) were derivatized with four different bisepoxide linkers (GDE: glycerol diglycidyl ether, BDE:1,4-butanediol diglycidyl ether, NDE: neopentyl glycol diglycidyl ether, CDE: 1,4-cyclohexanedimethanol diglycidyl ether) followed by the modification with 1,3-diaminopropane (DPr), while epoxy-decorated resin-based supports (abbreviated further as EP) were functionalized with five different *a,ω*-terminal diamino alkane moieties: 1,3-diaminopropane; 1,4-diaminobutane (DBu); 1,6-diaminohexane (DHx); 1,7-diaminoheptane (DHp) and 1,8-diaminooctane (DOc), before obtaining the ethylenediamine-tetraacetic dianhydride (EDTADa)-derived chelators charged with cobalt ions (Co^{2+}), serving as enzyme carriers. A simplified representation of the prepared support is depicted in Fig. 1.

Purified *Pc*PAL or *Lk*-ADH enzyme solutions of known concentrations were immobilized onto the prepared carriers. The immobilization yield was determined using the Bradford-assay.

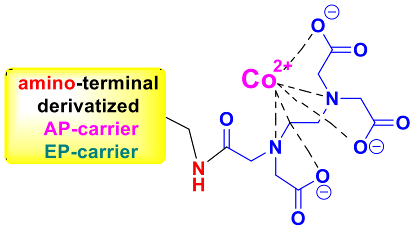

Fig. 1. Resin-based EDTADa-Co^{2+} chelate complex.

Results and discussion

The spectrophotometric determinations revealed that the enzyme immobilization yield varied between 95-100% in all cases. Immobilization was carried out also without the transition metal ion charging. These results are summarized in Table 1.

Table 1. Immobilization yield and enzymatic charge of *Lk*-ADH onto EP-based carrier without metal ion charging.

Biocatalyst code	Immobilization yield (%)	Enzymatic charge (ug enzyme·mg^{-1} support)
EP-DPr-EDTADa-Lk-ADH	97	87
EP-DBu-EDTADa-Lk-ADH	95	84
EP-DHx-EDTADa-Lk-ADH	98	87
EP-DHp-EDTADa-Lk-ADH	97	87
EP-DOc-EDTADa-Lk-ADH	98	88

Specific enzymatic activity of the immobilized *Pc*PAL compared to native enzyme is presented in Table 2.

Table 2. Specific enzymatic activity of native and immobilized *Pc*PAL.

Biocatalyst	Specific enzymatic activity (umol·min^{-1}·mg^{-1})
*Pc*PAL native	0.29470
AP-GDE-DPr-EDTADa-Co^{2+}- *Pc*PAL	0.09825
EP-DPr-EDTADa-Co^{2+}- *Pc*PAL	0.12282

Conclusions

The prepared amino- and epoxy-decorated resin-based EDTADa-Co^{2+} chelate complexes proved to be suitable carriers for the tested purified His-tagged enzymes. Further experiments will be conducted using cell lysate in order to purify and immobilize the target protein in a single step process.

Acknowledgements

This work was supported by the project “Renewable Enzyme Immobilization - RENZI” funded by European Union – NextGenerationEU and the Romanian Government, under National Recovery and Resilience Plan for Romania, contract no 760241/28.12.2023, cod PNRR-C9-I8-CF87/31.07.2023, through the Romanian Ministry of Research, Innovation and Digitalization, within Component 9, Investment I8”

References

[1] S. Datta, L.R. Christena, Y.R.S. Rajaram, Biotech 3 (2013) 1.
[2] H. Block, B. Maertens, A. Spriestersbach, *et al.*, Methods Enzymol. 463 (2009) 439.
[3] F. Nagy, G. Tasnádi, D. Balogh-Weiser, E. Bell, *et al.*, ChemCatChem 10 (2018) 3490.
[4] B. Alács, G. Hornyánszky, L. Poppe E. Bell, Catalysts 14 (2024) 14.

Immobilization of (*S*)-Selective ω-Transaminase from *Pseudomonas Psychrotolerans* for Optically Pure Amine Synthesis

Mădălina Elena Moisă*, Krisztina Kelemen, Aishwarya Singh, Oana Maria Popa, Alina Filip, Csaba Paizs, László Csaba Bencze, Monica Ioana Toșa
Enzymology and Applied Biocatalysis Research Center, Faculty of Chemistry and Chemical Engineering, Babeș-Bolyai University of Cluj-Napoca, Arany János Str. 11, RO-400028 Cluj-Napoca, Romania
**Corresponding authors:* madalina.moisa@ubbcluj.ro

Introduction

Chiral amines are essential structural motifs in a wide range of bioactive molecules, including pharmaceuticals, agrochemicals, and fine chemicals. The demand for optically pure amines continues to grow due to the increasing emphasis on stereoselectivity in drug design and the recognition that enantiomers often exhibit significantly different biological activities. Among the various methods available for synthesizing enantiomerically enriched amines, biocatalysis has gained substantial attention as an environmentally friendly and selective approach. In particular, ω-transaminases (ω-TAs) are valuable biocatalysts known for their ability to transfer amino groups to prochiral ketones or remove them from racemic amines, enabling the synthesis of optically pure amines under mild conditions. These enzymes depend on pyridoxal-5'-phosphate (PLP) as a cofactor and are utilized in two primary types of processes: kinetic resolution and asymmetric synthesis. In kinetic resolution, ω-TAs selectively react with one enantiomer of a racemic amine, converting it into a ketone while leaving the other enantiomer untouched. Although this method is limited to a theoretical maximum yield of 50%, it remains useful for obtaining enantiomerically enriched compounds from readily available racemic mixtures. On the other hand, asymmetric synthesis, particularly through the reductive amination of prochiral ketones, allows for the generation of a single enantiomer in up to 100% theoretical yield, making it a more efficient and scalable strategy [1].

Despite their promising catalytic properties, the practical application of ω-TAs in industrial bioprocesses is often hindered by challenges such as poor stability under process conditions, limited reusability, and difficulties in downstream recovery. Enzyme immobilization offers an effective strategy to address these limitations by enhancing operational stability, enabling catalyst recycling, and facilitating integration into continuous flow systems. Immobilization onto solid supports can also influence enzyme activity and selectivity, making support selection and immobilization method critical to biocatalyst performance [2].

In this study, the newly discovered ω-transaminase from *Pseudomonas psychrotolerans* (*Pp*S-TA) [3] was immobilized onto various solid supports, employing different immobilization methods, to investigate its performance in the synthesis of optically pure (*R*)-phenylethylamine, a chiral amine with wide-ranging industrial significance. By advancing the understanding of enzyme-support interactions and the functional stability of immobilized systems, this work contributes to the development of more robust and efficient biocatalytic processes for chiral amine synthesis.

Experimental

Enzyme expression and purification through Ni-NTA affinity chromatography were performed according to a previously optimized protocol [3] and the enzyme's purity was assessed by SDS-PAGE. Several commercially available supports were tested for the immobilization of *Pp*S-TA by adsorption, covalent and coordinative binding. Carboxy- and amino-functionalized supports were derivatized with glycerol diglycidyl ether (GDE) according to previously described methods [4], while supports bearing epoxy groups and His-binding ability were employed in the enzyme immobilization processes without prior derivatization. The enzyme immobilization yield and enzyme load were determined spectrophotometrically using the Bradford method and the efficiency of the immobilized biocatalysts in the kinetic resolution of *rac*-1-phenyleyhlamine was evaluated by chiral HPLC, employing Crownpak CR-I(+) column (3.0 mm x 150 mm, 5 µm) and ACN: $HClO_4$ solution (pH=1) 40:60 as mobile phase (at 0.4 $mL\cdot min^{-1}$ flow rate, and 25 °C).

Results and discussion

Initially, a wide collection of commercially available supports, including epoxy and amino methacrylate resins, epoxy polyacrylic resins, epoxy-functionalized cellulose and silica, carboxy and amino single-walled carbon nanotubes, partially reduced graphene oxide and Ni-NTA and Ni-IDA functionalized silica, cellulose and polyacrylate, was screened for the immobilization of *Pp*S-TA. Enzyme immobilization was conducted by three methods: covalent (through epoxy groups), coordinative (through Ni-NTA or Ni-IDA) and physical (through adsorption) binding. The newly developed biocatalysts were investigated in the kinetic resolution of *rac*-1-phenylethylamine.

While some of the supports proved to be inefficient for the immobilization of *Pp*S-TA, good conversions of up to 18% were registered in the initial screening. The data revealed that the best performing biocatalysts were obtained by covalently attaching the ω-TA to the amino-functionalized methacrylic supports from Purolite ECR8309F and ECR8415F. Next, using these supports, seven bis-epoxides and glutaraldehyde were tested as linkers. As indicated by our results, the more hydrophobic linkers (glutaraldehyde, neopentyl glycol diglycidyl ether and 1,4-cyclohexanedimethanol diglycidyl ether) provided the best results in the investigated biotransformation with conversions ranging from 35-41% after 120 h reaction time.

Conclusions

The newly developed biocatalysts by the covalent immobilization of *Pp*S-TA onto commercially available supports are promising candidates for establishing efficient processes for the synthesis of optically pure amines.

Acknowledgements

This work was supported by the project "Advanced (multi)-enzymatic synthesis and purification processes for bio-based furan derivatives – ASPIRE" funded by European Union – NextGenerationEU and the Romanian Government, under National Recovery and Resilience Plan for Romania, contract no 760042/23.05.2023, cod PNRR-C9-I8-CF25/14.11.2022, through the Romanian Ministry of Research, Innovation and Digitalization, within Component 9, Investment I8".

References

[1] M.D. Patil, G. Grogan, A. Bommarius, H. Yun, Catalysts 8 (2018) 254.
[2] W. Khanam, N.C. Dubey, Mater. Today Chem. 24 (2022) 100922.
[3] C.A. Gal, M.I. Toșa, L.E. Barabás, L. Poppe, A. Varga, C. Paizs, Mol. Catal. 531 (2022) 112660.
[4] J.H. Bartha-Vári, M.E. Moisă, L.C. Bencze, F.D. Irimie, C. Paizs, M.I. Toșa, Molecules 25 (2020) 651.

Improved Methodologies for Monitoring PETase Activity

Blanka-Eszter Nagy*, Krisztina Kelemen, Raluca Bianca Tomoiagă, Róbert Tőtős, Monica Ioana Toşa, Csaba Paizs, László Csaba Bencze*
Enzymology and Applied Biocatalysis Research Center, Faculty of Chemistry and Chemical Engineering, Babeș-Bolyai University, Cluj-Napoca, Romania
**Corresponding authors:* blanka.nagy@ubbcluj.ro, laszlo.bencze@ubbcluj.ro

Introduction

Polyethylene terephthalate (PET) accumulation presents a serious environmental treat due to its durability and widespread use in consumer products [1]. Enzymatic hydrolysis of PET, via PET degrading enzymes -PETases- particularly by cutinases such as leaf-branch compost cutinase (LCC), offers a green and efficient alternative to conventional plastic recycling, converting PET into its monomers: bis(2-hydroxyethyl) terephthalate (BHET), mono(2-hydroxyethyl) terephthalate (MHET), terephthalic acid (TPA), and ethylene glycol (EG) [2]. However, the development of high-performance PET-degrading enzymes depends not only on protein engineering and expression systems but also on robust and precise analytical tools to assess catalytic efficiency.

Experimental

A recombinant expression system was developed for efficient production of LCC using the pET-21a(+) vector in *E. coli* Rosetta pLysS. To evaluate enzymatic PET hydrolysis, two complementary analytical methods, HPLC and UV-Vis spectroscopy, were optimized. For the HPLC assay, caffeine was introduced as an internal standard, significantly improving quantification accuracy of TPA and related products. Calibration curves were established over a wide concentration range (µM to low mM), enabling sensitive and reproducible detection of PET hydrolysis products.

The UV-Vis assay was refined by adjusting detection wavelengths and recalculating the medium extinction coefficients of the aromatic degradation products. Cross-validation between the two methods ensured consistency and reliability of measurements [3].

Results and discussion

The enhanced HPLC method demonstrated improved sensitivity, precision, and reproducibility compared to traditional setups, with a limit of detection below reported PETase activity thresholds. Product concentration measurements showed low variability and minimal deviation from theoretical values across replicates. The optimized UV-Vis method provided a faster yet reliable alternative, validated against the HPLC results. Using these upgraded analytical tools, time-resolved monitoring of LCC-mediated PET hydrolysis revealed distinct degradation profiles for each monomer, Fig. 1., offering insights into reaction dynamics and enzyme performance under varying conditions.

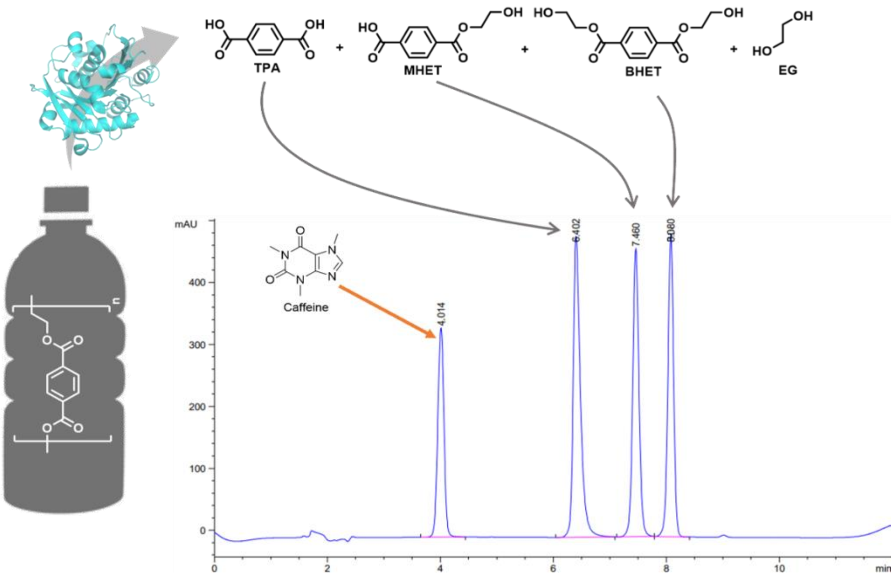

Fig. 1. HPLC analysis of the biodegradation products (TPA at 6.4 min, MHET at 7.8 min and BHET at 8 min) of PET using caffeine (at 4 min) as internal standard.

Conclusions

The refined analytical assays developed in this study enhance the sensitivity, accuracy, and consistency of PETase activity measurements. These improvements are critical for evaluating biocatalyst efficiency and support ongoing efforts to develop enzyme-based solutions for PET biodegradation and sustainable plastic recycling.

Acknowledgements

This work was supported by a grant of the Romanian National Authority for Scientific Research, UEFISCDI: Immobilized PET-degrading enzymes for microplastic control (detection and removal), project number PN-IV-P1-PCE-2023-2007.

References

[1] M. Oliveira, M. Almeida, Trends Anal Chem. 114 (2019) 196.
[2] V. Tournier, C.M. Topham, A. Gilles, B. David, C. Folgoas, E. Moya-Leclair, E. Kamionka, M.L. Desrousseaux, H. Texier, S. Gavalda, M. Cot, E. Guemard, M. Dalibey, J. Nomme, G. Cioci, S. Barbe, M. Chateau, I. Andre, S. Duquesne, A. Marty, Nature 580 (2020) 216.
[3] K. Boros, B.E. Nagy, R.B. Tomoiagă, R. Tőtős, M.I. Toșa, C. Paizs, L.C. Bencze, Sci. Rep. 15 (2025) 1877.

Chemoenzymatic Synthesis of Furan Based Structures Derived from Renewable Resources

Loránd Nagy*, Csaba Paizs
"Babeş-Bolyai" University, Faculty of Chemistry and Chemical Engineering, Enzymology and Applied Biocatalysis Research Center
**Corresponding author: lorand.nagy@ubbcluj.ro*

Introduction

Developing chemoenzymatic routes for converting bio-based molecules is an area of intensive research in green chemistry. In this work, we present our most recent advances in using human carbonic anhydrase II (hCAII), an enzyme with outstanding catalytic activity to reduce furan-based aldehydes and ketones. In organisms hCAII reversibly catalyzes the hydration of carbon dioxide to form bicarbonate anions. Beside this rapid reaction, it can serve as an oxidoreductase in the presence of a proper hydride-ion donor [1].

This work involves the chemical synthesis of various 5-aryl-furan-2carbonyls, which were subsequently converted into the corresponding alcohols. In the case of prochiral ketones, hCAII demonstrated excellent enantioselectivity, yielding enantiopure products.

Our initial goal was to broaden the substrate scope of the enzyme by exploring its activity on larger, structurally complex molecules that had not been previously tested. These bulkier substrates represent a novel class for hCAII, expanding the boundaries of its known catalytic versatility.

Experimental

The synthesis of the substrates was performed in accordance with the chemoenzymatic method developed by Bencze et al. [2]. The heteroaryl ethanones (**1a**,**1b**) were prepared from the corresponding aniline using a modified Meerwein arylation method also used in the synthesis of *Dantrolene* [3]. The carbonyl substrates obtained were further reduced to alcohols (**Scheme 1.**) The reaction conversion and enantiomeric excess of products were investigated.

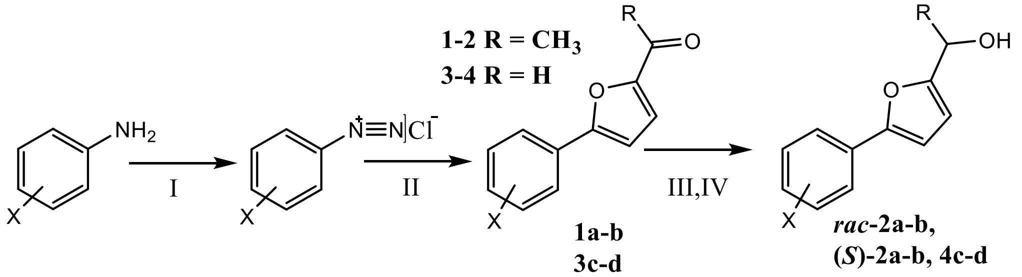

1-4	X
a	2-Cl
b	4-NO$_2$
c	4-Br
d	4-CH$_3$

Scheme 1. Synthetic scheme for phenyl-furan alcohols. Reagents: (I) HCl, NaNO$_3$; (II) furfural (**3-4**)/ 2-acetyl furan, CuCl$_2$ (**1-2**); (III) NaBH$_4$; (IV) hCAII, phenylsilane

Results and discussion

The enzymatic reactions were carried out in TRIS buffer (50 mM, pH=8) with 30% DMSO content, using three equivalents of phenyl silane as hydride ion donor and TWEEN 80 (1%, v/v) to increase the solubility. The investigated substrate concentrations varied between 2.5-10 mM. Samples were taken from each reaction in volumes adjusted according to the initial concentration, such that all final samples are approximately equal in concentration. The samples were diluted in acetonitrile, to denature the enzyme. After centrifuging, the samples were injected on HPLC columns using reverse phase mode.

The ^{1}H- and ^{13}C-NMR spectra were recorded on a Bruker spectrometer operating at 400 MHz. High performance liquid chromatography analyses were developed on Agilent 1200 instrument using Phenomenex LUX Cellulose-2 column for examination of enantiomeric excess, Fig. 1., and Agilent Zorbax XDB-C8 (both 150 × 4,6 mm) for the conversion rates. In the case of *rac*-**2b** the *O*-acylated form of the reaction product was used for enantiomer purity determination on ASTEC Chiraldex B-DM column.

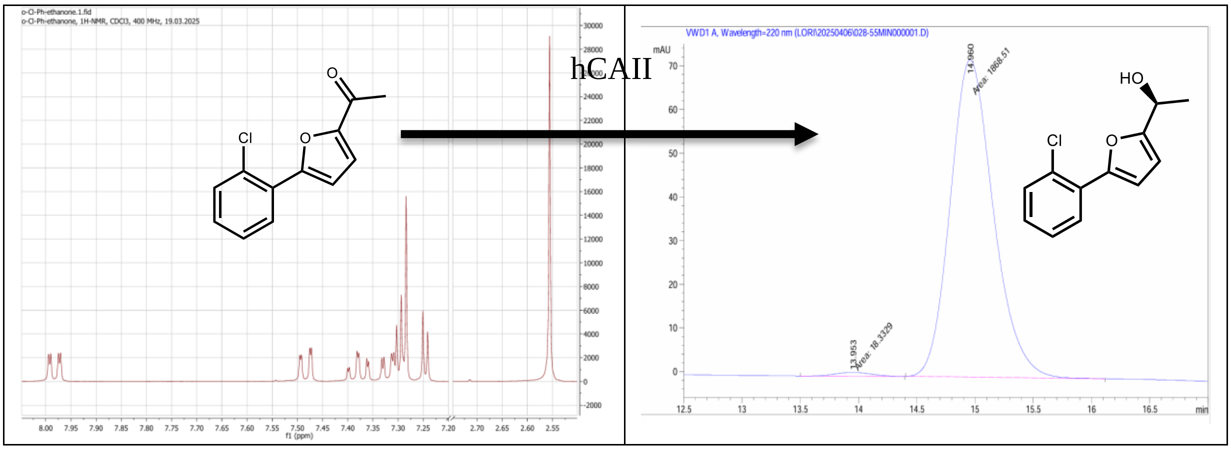

Fig. 1. Biotransformation of **1a** into (S)-**2a**. **Panel A**: ^{1}H- spectra of **1a**. **Panel B**: enantiomeric excess of the produced (S)-**2a**.

Conclusions

hCAII demonstrated tolerance toward bulkier, biphenyl-like substrates while maintaining its selectivity, underscoring its suitability for the investigated reaction.

Acknowledgements

This work was supported by the project "Renewable Enzyme Immobilization - RENZI" funded by European Union – NextGenerationEU and the Romanian Government, under National Recovery and Resilience Plan for Romania, contract no 760241/28.12.2023, cod PNRR-C9-I8-CF87/31.07.2023, through the Romanian Ministry of Research, Innovation and Digitalization, within Component 9, Investment I8"
N.L. is grateful for grant from the Sapientia Hungariae Foundation.

References

[1] P. Ji, J. Park, Y. Gu, D.S. Clark, J.F. Hartwig, Nat. Chem. 13(4) (2021) 312.
[2] L.C. Bencze, C. Paizs, M.I. Toșa, F.D. Irimie, Tetrahedron: Asymmetry 21(3) (2010) 356.
[3] D.C. Stewert, J.H.R. Snyder, 1-(5-Substituted)Furfurylideneamino Hydantoins and Imidazolidinones. US3415821A, December 10, 1968. https://patents.google.com/patent/US3415821/en (accessed 2025-05-12).

Bio-Based 5-Hydroxymethylfurfural is a Remarkable Substrate for Preparative-Scale Transaminase - Human Carbonic Anhydrase Enzymatic Cascades

Laura E. Barabás, Monica I. Toşa, Csaba Paizs*
Babeş-Bolyai University, Faculty of Chemistry and Chemical Engineering, Enzymology and Applied Biocatalysis Research Center, Arany János 11, 400028, Cluj-Napoca, Romania
**Corresponding author: csaba.paizs@ubbcluj.ro*

A bi-enzymatic transaminase from *Pseudomonas psychrotolerans* (*PpS*-TA) - human carbonic anhydrase II (hCAII) cascade for the efficient conversion of various (±)-1-phenylethan-1-amines [(±)-**1a-d**] into the corresponding enantiopure (*R*)-amines and (*S*)-1-phenylethan-1-ols was developed in HEPES-DMSO as suitable reaction medium for both enzymes. Instead of pyruvate [1], the natural amino acceptor of ω-transaminases, hydroxybenzaldehydes **4a**,**b** and hydroxymethylfurfural (HMF) **4c** were used successfully as co-substrates for the *PpS*-TA mediated kinetic resolution of the racemic amines. In the first stage the total transformation of the reactive stereoisomer of (±)-1-phenylethan-1-amine (up to 20 mM) as model compound [(±)-**1a**] to acetophenone (**2a**) occurred in presence of equimolar amounts of the amino acceptor hydroxyl-aldehydes **4a-c** with soluble *PpS*-TA. This was followed by the investigation of the simultaneous reduction of the previously formed acetophenone (**2a**) into (*S*)-1-phenylethan-1-ol [(*S*)-**3a]** and of the unreacted hydroxyl-aldehydes **4a-c** into **5a-c** in presence of hCAII using phenylsilane ($PhSiH_3$) as hydride ion source [2]. Since all **4a,b** and **5a,b** hydroxylbenzyl alcohol were strong inhibitors of hCAII, further investigations were performed only with HMF (**4c**) used as amino acceptor in the transamination reaction. Compared to procedure with soluble enzymes, the cellular cascade showed improved performance, as both biotransformations were been carried out with improved efficiency even at higher substrate concentrations using phosphate buffer DMSO mixture as reaction medium. Maintaining the activities and selectivities of the enzymes, the cellular cascade allowed the complete gram-scale conversion of (±)-**1a** into the enantiopure (*R*)-**1a** and (*S*)-**2a**, and of HMF (**4c**) into [5-(aminomethyl)furan-2-yl]methanol (**5c**) and 2,5-di-(hydroxymethyl)furan (**6c**) which were all isolated in higher than 90 % yield.

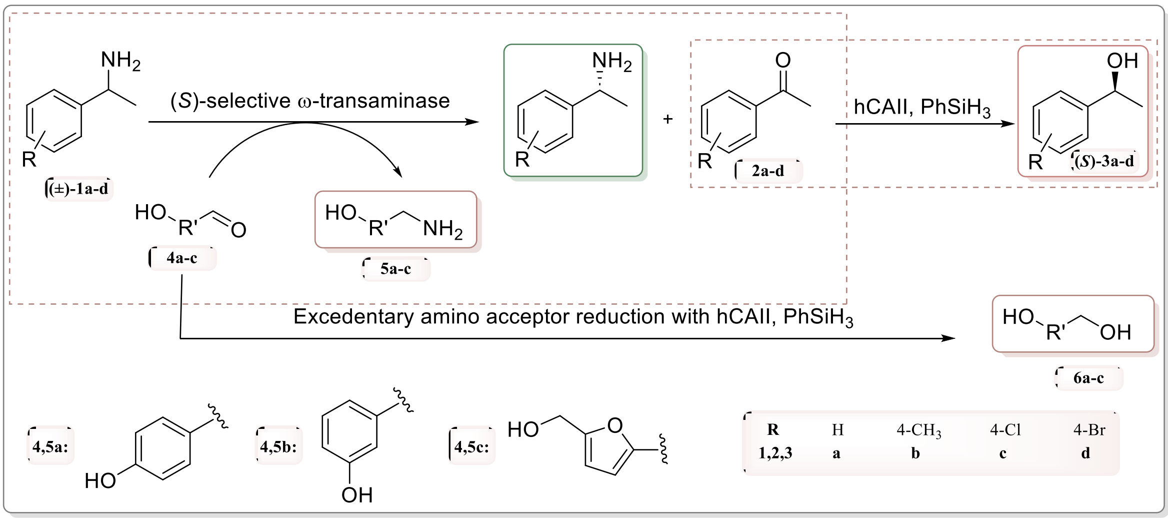

Scheme 1. *PpS*-TA–hCAII bi-enzymatic cascade for the production of enantiomerically pure amines and alcohols, as well as of achiral amino-alchols and diols from cheap starting materials.

Acknowledgements

This work was supported by the project "Renewable Enzyme Immobilization - RENZI" funded by European Union – NextGenerationEU and the Romanian Government, under National Recovery and Resilience Plan for Romania, contract no 760241/28.12.2023, cod PNRR-C9-I8-CF87/31.07.2023, through the Romanian Ministry of Research, Innovation and Digitalization, within Component 9, Investment I8".

References

[1] L.E Barabás, D.M. Scrob, A. Varga, L. Kiss, M.I. Toşa, C. Paizs, React. Chem. Eng. 8 (2023) 2001.
[2] J. Pengfei, P. Jeeyoung, G. Yang, S.C. Douglas, F.H. John, Nat. Chem. 13 (2021) 312.

Enhanced Enzyme Immobilization on Functionalized Polymeric Beads for Efficient Microfluidic Biocatalysis

Matild Pap[1*]*, Gabriel Katona[1], Csaba Paizs[1], Melinda-Emese László[1], László Poppe[1,2]
[1]*Enzymology and Applied Biocatalysis Center, Faculty of Chemistry and Chemical Engineering, Babeș-Bolyai University, 400028 Cluj-Napoca, Romania*
[2]*Department of Organic Chemistry and Technology, Budapest University of Technology and Economics, Rakpart street no.3, 1111 Budapest, Hungary*
**Corresponding authors: matild.pap@ubbcluj.ro*

Introduction

Microreactors are compact devices designed to carry out chemical reactions within a small, controlled space. Their configuration is optimized to improve reaction efficiency and product yield [1]. They can operate in both batch and continuous flow systems, with continuous flow being especially useful in biocatalysis. Enzymes, either free or immobilized, can be placed in the reactor's internal channels to catalyze reactions as substrates pass through, allowing for precise control of reaction parameters [2]. In this study, lipase B from *Candida antarctica* (CaL-B) was immobilized on an Immobead T2-150 (IB) carrier with epoxy groups [3]. Before immobilization, the carrier was modified using various diamino-alkyl derivatives and glycerol diglycidyl ether to introduce spacers of varying lengths, to improve the enzyme's activity.

Experimental

In the first step, the pristine Immobead T2-150 carrier was derivatized with various diamino-alkyl derivatives and glycerol diglycidyl ether (GDE) through covalent ring-opening reactions, Fig. 1. This process introduced spacers of varying lengths between the carrier surface and the enzyme, while preserving the original epoxy functional groups. The resulting biocatalysts were tested for activity and selectivity in acylation reactions of racemic aryl-alcohol derivatives, using a custom-designed aluminum microchip as the catalyst holder in a continuous flow microfluidic system.

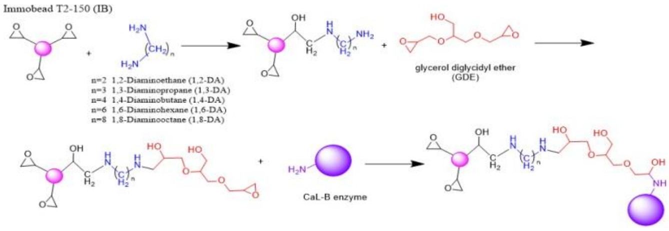

Fig. 1. Schematic representation of Immobead T2-150 based biocatalyst preparation.

Results and discussion

Surface modification of the Immobead T2-150 (IB) carrier with various diamino-alkyl groups was confirmed by elemental analysis, as the unmodified carrier contains no nitrogen. Each sample was analyzed in triplicate, and the mean values are provided in Table 1. The synthetic activity of the resulting biocatalysts was assessed via the acylation of *n*-butanol with vinyl acetate using the MBTH (3-methyl-2-benzothiazolinone-hydrazone-hydrochloride-hydrate) assay. To evaluate the retention of CaL-B activity after immobilization, the biocatalysts were also tested in the enzymatic resolution of *rac*-1-phenylethanol with vinyl acetate, under both batch, Fig. 3, and continuous flow conditions, Fig. 2. To assess the selectivity and activity of the enzyme upon immobilization, acylation of *rac*-1-phenylethanol with vinyl acetate was carried out at room temperature and at 30°C, respectively, using diethyl ether as solvent. Additionally, the acylation reaction was performed in batch mode under the same conditions at room temperature (optimized conditions: substrate/acylating agent *ratio* 1:2 *v/v*%, diethyl ether as solvent, 30 °C, and 50 mg of biocatalyst). The IB-1,4-DA-CaL-B biocatalyst was further evaluated for the enzymatic resolution of various racemic phenylethanol (PE) derivatives in a continuous flow microfluidic system. Reaction products were analyzed using gas chromatography (GC) and high-performance liquid chromatography (HPLC).

Table 1. Elemental analysis results of the carriers.

Entry	Content	Biocatalyst					
		IB	IB-1,2-DA	IB-1,3-DA	IB-1,4-DA	IB-1,6-DA	IB-1,8-DA
1	N (%)	0.02	2.55	1.55	1.52	1.53	1.58
2	C (%)	61.06	55.73	60.96	59.78	60.18	62.14
3	H (%)	7.51	7.77	7.86	7.71	7.76	8.01

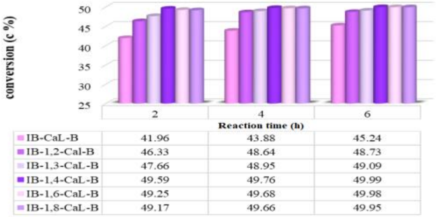

	2	4	6
IB-CaL-B	41.96	43.88	45.24
IB-1,2-Cal-B	46.33	48.64	48.73
IB-1,3-CaL-B	47.66	48.95	49.09
IB-1,4-CaL-B	49.59	49.76	49.99
IB-1,6-CaL-B	49.25	49.68	49.98
IB-1,8-CaL-B	49.17	49.66	49.95

Fig. 2. Conversion variation in time (flow); Q_v= 0.2 μL·s^{-1}

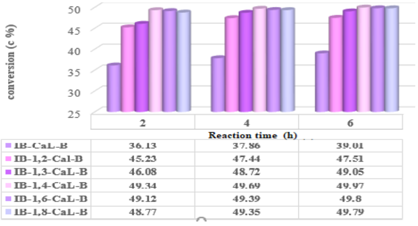

	2	4	6
IB-CaL-B	36.13	37.86	39.01
IB-1,2-Cal-B	45.23	47.44	47.51
IB-1,3-CaL-B	46.08	48.72	49.05
IB-1,4-CaL-B	49.34	49.69	49.97
IB-1,6-CaL-B	49.12	49.39	49.8
IB-1,8-CaL-B	48.77	49.35	49.79

Fig. 3. Conversion variation in time (batch mode)

Conclusions

CaL-B enzyme was immobilized on a chemically modified Immobead T2-150 carrier using diamino-alkyl groups and glycerol diglycidyl ether, as confirmed by elemental analysis. The resulting biocatalysts were tested in the acylation of *rac*-1-phenylethanol with vinyl acetate under optimized reaction conditions in batch and continuous flow. The IB-1,4-DA-CaL-B variant showed higher conversion, indicating improved activity due to the longer spacer arm. This biocatalyst was also effective with five phenylethanol derivatives, achieving high conversion in toluene after 6 h in continuous flow microfluidic system.

Acknowledgements

This work was supported by the project “Renewable Enzyme Immobilization - RENZI” funded by European Union – Next Generation EU and the Romanian Government, under National Recovery and Resilience Plan for Romania, contract no 760241/28.12.2023, cod PNRR-C9-I8-CF87/31.07.2023, through the Romanian Ministry of Research, Innovation and Digitalization, within Component 9, Investment I8.

References

[1] T. Illg, P. Löb, V. Hessel, Bioorg. Med. Chem. 18 (2010) 3707.
[2] J. Coloma, Y. Guiavarc’h, P.-L. Hagedoorn, U. Hanefeld, Chem. Commun. 57 (2021) 11416.
[3] M. Abdelmageed Othman, M. Ángeles Sanromán, D. Moldes, Enzyme Microb. Technol. 150 (2021) 1.

Modified Titanium Dioxide for Photocatalytic Degradation of Textile Dyes under Visible Ligh

Daniela Negoescu[1], Mihaela Gherendi[2], Florica Papa[1], Simona Petrescu[1], Veronica Bratan[1], Viorica Parvulescu[1]*
[1]*Institute of Physical Chemistry "Ilie Murgulescu", Romanian Academy, 060021 Bucharest, Romania*
[2]*National Institute for Lasers, Plasma and Radiation Physics, 077125 Magurele-Ilfov, Romania*
**Corresponding author: vpirvulescu@icf.ro*

Introduction

Nanoparticles of various semiconductors that have photocatalytic properties, such as TiO_2, have been widely used for the removal of organic pollutants from wastewater [1]. However, as a wide band gap semiconductor, the application of TiO_2 is practically limited for UV irradiation. Therefore, its doping with various transition metals and transition metal oxides has been pursued as a means to generate photoactivity for TiO_2 under visible light and to prevent the recombination of charge carriers [2,3]. Here, the photocatalysts with Ag or FeOx supported on TiO_2 were used in degradation of Congo Red (CR) and Crystal Violet (CV) dyes from water under visible light. The effect of composition on the activity and mechanism of reactions was studied.

Experimental

TiO_2 with and without activated carbon with P (CP) supports were obtained by sol-gel method in prezence of Brij58 surfactant and were impregnated with aqueous solutions of $AgNO_3$ and/or $Fe(NO_3)_3$, respectively. The obtained materials were dried at 80 °C and calcined in air at 450 °C. Names of the obtained samples, with 1% of each metal are: Ag/TiO_2, Ag/TiO_2-CP, Fe/TiO_2-CP, $AgFe/TiO_2$-CP. The morphology of these samples were explored by scanning electron microscopy (SEM), the surface composition by X-ray photoelectron spectroscopy (XPS), the reduction properties by H_2-Thermoprogramed reduction (TPR) and optical properties by UV-Vis spectroscopy. The photocatalytic activity of the samples was quantitatively evaluated by determining the efficiency of dyes (CR, CV) degradation.

Results and discussion

SEM iamges showed a spherical morphology for all the samples. The presence on the surface of TiO_2 and Ti sub oxide phses were evidenced by XPS spectra. Also, the XPS spectra confirmed the presence of sp2 graphitic carbon, C–O and Ti–O–C bonds, P–O, Ti–O–C and P–C bonds. The Ag3d spectra display two peaks attributed to the Ag^+ species and metallic Ag^0. Ag^0/Ag^+ ratio increases in the presence of activated carbon and decreased significant for $AgFe/TiO_2$-CP sample. Fe^0/Fe^{2+} ratio, was 0.4 for sample Fe/TiO_2-CP and 0.3 for sample with Ag and Fe ($AgFe/TiO_2$-CP). When iron and silver oxides are immobilized through the simultaneous impregnation of their precursors, a competition was created between the reduction of Fe^{3+} to Fe^{2+} and Ag^+ to Ag^0. Therefore, unreduced Fe^{3+} species remain in this sample. The presence of iron oxides and Ag_2O was also confirmed by H_2-TPR. An additional absorption band in the visible range was attributed to the local plasmon surface resonance (PSR) effect induced by Ag nanoparticles. PSR effect was evidenced especially for sample Ag/TiO_2. When CP was added, the plasmon corresponding absorption was strongly diminished. These findings are in agreement with the XPS data which indicated a high Ag^0/Ag$^+$ ratio in absence of activated carbon. Fig. 1 shows that in CV photodegradation all samples with CP present similar behavior.

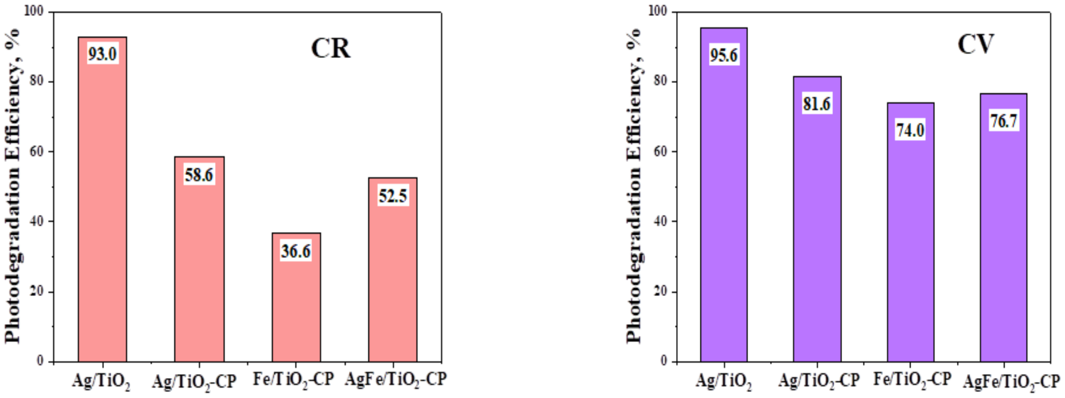

Fig. 1. The avriation of CR and CV degradation with the photocatalysts composition.

The highest efficiency was also obtained for Ag/TiO$_2$ sample. On the contrary, CR degradation was strongly influenced by the composition of photocatalysts. Thus, it can be seen that silver considerably enhances the reaction efficiency, which varies in the following order Fe/TiO$_2$-CP < AgFe/TiO$_2$-CP < Ag/TiO$_2$-CP < Ag/TiO$_2$. Under irradiation, both the e$^-$ from valence band of iron or silver oxides are activated. These electrons, as well as those generated by plasmonic resonance, are transferred by metallic Ag and AC to the oxygen and water adsorbed on the surface, generating •O^{2-} and •OH radicals. These active species cause the degradation of dyes.

Conclusions

The XPS and TPR results of the obtained photocatalysts revealed the effect of interaction between Ag and Fe on their reducibility. In the sample containing both Ag and Fe, two iron oxide species (Fe_2O_3 and FeO) were identified, which were reduced at different temperatures. In contrast, the sample containing only Fe exhibited FeO. The activity of photocatalysts decreases in the presence of activated carbon and by the association of silver with iron on the TiO$_2$-CP support. Compared to results published in the literature for similar reactions, the results obtained in the photo degradation of the CV dye can be considered to be among the best.

References

[1] M. Bhaumik, B.I. McCrindle, A. Maity, Chem. Eng. J. 260 (2015) 716.

[2] M.T. Islam, M.N.P. Roni, M.Y. Ali, M.R. Islam, M.S. Hossan, M.H. Rahman, A.A.S.M. Zahid, M.N.E. Alam, M.A. Hanif, M.S. Akhtar, Molecules 28 (2023) 6834.

[3] D. Negoescu, I. Atkinson, M. Gherendi, D.C. Culita, A. Baran, S. Petrescu, B. Trica, D. Pelinescu, R. Ionescu, V. Bratan, V. Parvulescu, J. Alloys Compd. 931 (2023) 167528.

Effect of the Synthesis Conditions on Properties of W/TiO_2-CeO_2-CP Nanocomposite Photocatalysts

Gabriela Petcu, Elena Maria Anghel, Florica Papa, Irina Atkinson, Simona Petrescu, Adriana Baran, Viorica Parvulescu*
Institute of Physical Chemistry "Ilie Murgulescu", Romanian Academy, 060021 Bucharest, Romania
**Corresponding author: vpirvulescu@icf.ro*

Introduction

The synthesis method strongly influences the properties of TiO_2 photocatalysts. Thus, the sol-gel method is widely used due to its low cost, mild conditions, and ability to produce homogeneous and pure TiO_2, while the hydrothermal method, though less common, is gaining attention for its potential to yield highly crystalline materials [1]. Also, significant research endeavors have been directed toward the modification of TiO_2, to enhance its photocatalytic performance and expand its spectral responsiveness into the visible-light range. The photocatalyst Ce-doped TiO_2 frequently has a lower band gap than TiO_2, depending on the Ce content and the method of synthesis [2,3]. The photocatalytic efficiency of these materials increased by immobilization of WO_3 resulting promising materials for photocatalytic applications [4]. Here, the properties of composite materials containing W/TiO_2-CeO_2-activated carbon, obtained by the sol-gel method and hydrothermal treatment, are comparatively presented.

Experimental

TiO_2-CeO_2-CP nanocomposite supports were obtained by sol-gel and hydrothermal method in the presence of Brij 58 and activated carbon with phosphourus as soft and hard templates, respectively. The obtained materials were calcined at 450 °C, impregnated with $(NH_4)_{20}H_2W_{12}O_{42}$ aqueous solution to obtain photocatalysts with 1% WO_3. After impregnation, the samples were calcined at 450 °C and named TCgW and TChW. The obtained samples, before and after tungsten immobilization, were characterized by X-Ray diffraction, SEM microscopy, H_2-TPR, Raman, photoluminiscence and UV-Vis spectrocopy. The photocatalytic properties were evaluated in degradation of dyes (Congo Red -CR, Crystal Violet-CV) as pollutants from water.

Results and discussion

X-ray diffractogram of TCh sample obtained by hydrothermal treatment, before and after W oxide immobilization, evidenced only the presence of anatase while for samples based on TiO_2-CeO_2-CP composite support, obtained by the sol-gel method, was obtained amorphous phase. UV-Raman spectra of TCh samples evidenced also sp2 hybridized carbon and anatase polymorph (~400, 512 and ~637 cm^{-1}). A band at ~760 cm^{-1} was attributed to peroxo-species, O_2^{2-} from the sample surface.

The H_2-TPR profiles of prepared solids are displayed in Fig. 1. Compared to TiO_2, a decrease in H_2 consumption can be observe for samples with cerium oxide after immobilization of tungsten oxide species, Fig. 1. The first peck was attributed to the reduction of surface oxygen of CeO_2 whereas, the peak centered at 580 °C correspond to the reduction of cerium species from Ce^{4+} to Ce^{3+}. The reduction of tungsten species occurs at higher temperature in the presence of Ce (around 800 °C). This confirms the existence of strong interactions between cerium and tungsten species. The hydrogen consumption is significantly higher for TCgW sample as result of high quantity of oxygen species from surface. The valence states and environment coordination of Ce and W species at TiO_2

surface were examined via Diffuse-Reflectance UV-vis spectroscopy and the results are illustrated in Fig. 2.

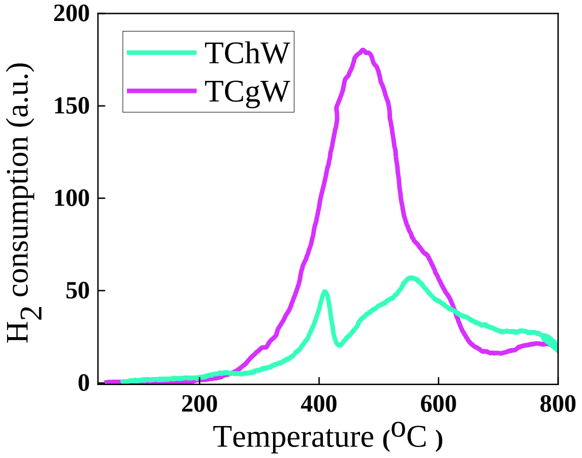

Fig. 1. UV-Vis absorption spectra of photocatalysts.

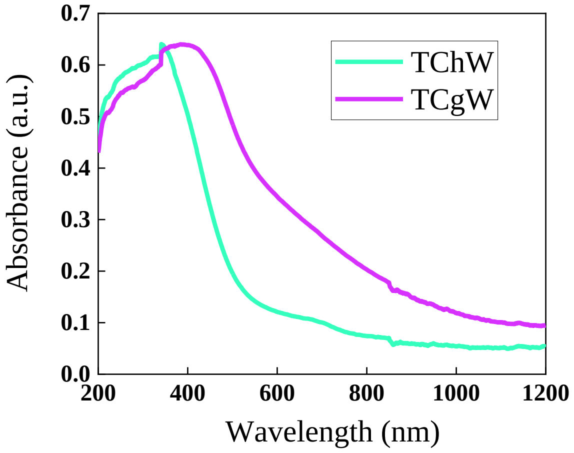

Fig. 2. H_2-TPR profiles of the synthesized photocatalysts.

The typical absorption band in the 200-400 nm range corresponds to $O^{2-} \rightarrow Ti^{4+}$ charge transfer transitions in tetrahedrally coordinated Ti^{4+}, octahedrally coordinated Ti^{4+} and TiO_2 anatase phase. The typical absorption bands of tungsten species are usually observed in the 210-270 nm range for the isolated tetrahedral W^{6+} and oligomerized W species and between 300 and 375 nm for the polymeric octahedral W^{6+} species. Additional band appear at λ>450 nm in the UV-Vis spectra of sample obtianed by sol-gel method indicating the possibility of WO_3 presence. A high efficiency of CV degradation (97.5%) was obtained in the visible light for the TChW sample and of CR degradation (99%), using the TCgW photocatalyst.

Conclusions

A significant effect of the synthesis method of W/TiO_2-CeO_2-activated carbon photocatalysts on structure, oxido-reduction, optical and photocatalytic properties was evidenced.

References

[1] L. Cano-Casanova, A. Amorós-Pérez, M.Á. Lillo-Ródenas, M.D.C. Román-Martínez, Materials 11 (2018) 2227.

[2] G.B. Vieira, H.J. Humberto Jorge José, M. Peterson, V.Z. Baldissarelli, P. Alvarez, R.de Fátima Peralta Muniz Moreira, J. Photochem. Photochem. A: Chem. 353 (2018) 325.

[3] M. Malekkiani, F. Ravari, A.H.J. Magham, M. Dadmehr, H. Groiss, H.A. Hosseini, R. Sharif, ACS Omega 7 (2022) 30601.

[4] X. Gu, S. Lin, K. Qi, Y. Yan, R. Li, V. Popkov, O. Almjasheva, Sep. Purif. Technol. 345 (2024) 127299.

Lanthanide-Doped TiO_2 Photocatalysts Used for the Photodegradation of Antibiotics in Water

Bogdan Cojocaru[1,2], Rodica Zăvoianu[1,2],Vasile I. Parvulescu[1,2]*, Octavian D. Pavel[1,2]*
[1]University of Bucharest, Faculty of Chemistry, Departrment of Inorganic Chemistry, Organic Chemistry, Biochemistry and Catalysis, 4-12 Regina Elisabeta Blv, 030018 Bucharest, Romania;
[2]Research Center for Catalysts & Catalytic Processes, Faculty of Chemistry, University of Bucharest, 4-12 Regina Elisabeta Blv., Bucharest 030018, Romania
**Corresponding authors: vasile.parvulescu@chimie.unibuc.ro, octavian.pavel@chimie.unibuc.ro*

Introduction

The generation of hazardous industrial effluents is a major problem facing all nations around the world. Photocatalytic degradation of the antibiotics is still an effective approach used to remove them from the water systems. The limitations of "classical" catalytic systems, for example TiO_2, are mainly related to the band-gap value which is large. Doping TiO_2 with lanthanides is an attractive approach to improve its photocatalytic performance due to the synergistic effects that occur as a result of this process [1]. The objective of this work was to evaluate from a physico-structural point of view the modification of TiO_2 with lanthanides as well as the evaluation of the catalytic activities of the solids obtained in the photocatalytic degradation reaction of two important antibiotics, e.g., amoxicillin, ampicillin, under visible light irradiation.

Experimental

The synthesis of doped Ln-TiO_2 (wt., 1 or 5%) type catalysts was carried out by sol-gel method (Ln=Yb^{3+}, Er^{3+}, Dy^{3+}, Pr^{3+}). Also, TiO_2 synthesized by sol-gel was impregnated with lanthanides (1% - Dy^{3+}, Pr^{3+}). The samples were calcined at 500 or 750 °C. The solids were characterized by several techniques. The catalysts were tested in the photo-degradation of ampicillin or amoxicillin (0.15 mM) under visible irradiation.

Results and discussion

X-ray patterns are typical to TiO_2 anatase or rutile, depending of their calcination temperature. One of the known effects of Ln doping of TiO_2 is the inhibition of anatase-rutile transformation. The X-ray paterns revealed that after calcination at 750 °C, the samples contain majority anatase (>85%), compared with bare TiO_2 which is 100% rutile. The size of rutile crystallites decreases after doping below 40 nm compared to 59 nm for un-doped TiO_2. The size of anatase crystallites was below 30 nm. No major differences were observed in the band-gap size after the introduction of lanthanides regardless of the preparation method (doping or impregnation), although a tendency to decrease it was observed with increasing calcination temperature, a fact explained by the transition from the anatase to the rutile phase. However, a slightly larger band gap is observed for impregnated samples, quite close to that of the un-doped TiO_2 sample. As expected, TiO_2 showed lower activity in the degradation reaction of amoxicillin under visible irradiation compared to the doped samples, Fig. 1.

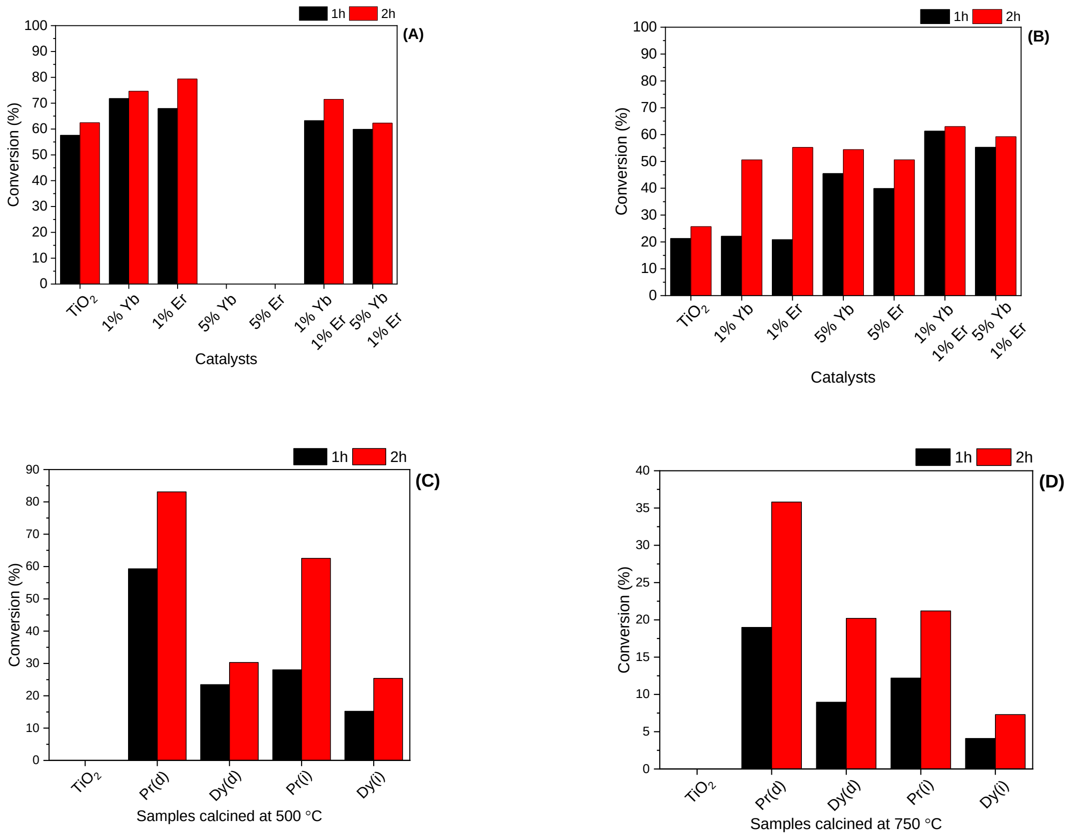

Fig. 1. Amoxicillin (0.15mM) removal by Ln-TiO_2 calcined (A) at 500 °C and (B)at 750 °C, as well as ampicillin removal by Ln-TiO_2 calcined (C) at 500 °C and (D) at 750 °C.

In the case of samples calcined at 750 °C, although the conversion decreases significantly in the case of samples containing 1% Yb, respectively 1% Er, for co-doped samples this decrease is very small. The higher activity of Pr-containing samples compared to Dy-containing samples is in line with the literature, Pr^{3+} being a more efficient volume dopant compared to Dy^{3+}.

Conclusions

Doping titanium dioxide with lanthanides, broadening the light absorption range and generating defects in the TiO_2 lattice contributed to a relatively high activity toward degradation of antibiotics under visible light irradiation.

Acknowledgements

Funding from the Romanian Ministry of Research, Innovation and Digitalization is acknowledged within the project PNRR-III-C9-2022-I5-18 (contract 760010/2022).

References

[1] F.B. Li, X.Z. Li, M.F. Hou, K.W. Cheah, W.C.H. Choy, Appl. Catal A: Gen. 285 (2005) 181.

Integrated Catalytic and Biocatalytic Approaches for the Sustainable Valorisation of Vegetable Oil-Based Feedstocks

Iunia Podolean, Mihai Bordeiasu, Madalina Tudorache, Simona M. Coman*
Department of Inorganic, Organic, Biochemistry and Catalysis, Faculty of Chemistry, University of Bucharest, Bdul Regina Elisabeta 4-12, Bucharest 030018, Romania
**Corresponding author:* simona.coman@chimie.unibuc.ro

Introduction

Due to their biodegradability, low ecotoxicity, and availability from diverse sources, vegetable oils (VOs) are considered highly valuable biomass resources [1]. Common types such as sunflower, soybean, castor, palm, and algal oils can serve as renewable starting materials. A particular category is represented by waste cooking oil (WCO) [2], which is increasingly utilized for the production of chemicals used in industrially important biomaterials, including plasticizers, biofuels, biolubricants, packaging materials, adhesives, printing inks, paints, and coatings [3]. The two main valorization pathways for VOs and WCO are transesterification - for biodiesel production and epoxidation of double bonds as an intermediate step toward plasticizer synthesis. Although numerous catalytic and biocatalytic systems have been explored for these reactions over recent years, the field remains highly active. The scientific community continues to seek advanced catalysts, such as Metal–Organic Frameworks (MOFs), to enhance yields and address challenges like low selectivity, mass-transfer limitations, and poor stability. Additionally, relatively few studies have focused on real WCO as a feedstock. In this context, the present study explores various strategies for the production of both biodiesel and epoxidized oils from VOs and WCO, aiming to identify the most effective approaches and catalytic systems.

Experimental

Transesterification and epoxidation reactions were studied using various vegetable oils (VOs) with different unsaturation levels, including fresh, adulterated, and used WCO (deep-fried) samples.

Zeolite Imidazolate Framework (ZIF) catalysts were synthesized in methanol by reacting varying ratios of $CaCl_2$ or $Cu(NO_3)_2.3H_2O$ with $Zn(NO_3)_2 \cdot 6H_2O$ and 2-methylimidazole. The resulting materials were characterized by ICP-OES, XRD, and FTIR-ATR analyses.

Epoxidation were conducted chemically using organic acids as peracid precursors and 30% H_2O_2. For catalytic and biocatalytic epoxidation, 0.5–2.5 wt.% of ZIFs or Novozyme 435 (Merk) were employed. For biodiesel synthesis, oil samples were refluxed with varying methanol-to-oil ratios. As catalysts, 1.5–2.5 wt.% of commercially available zeolites and metal oxides, as well as the synthesized and characterized ZIFs, were used. Physico-chemical characterization of the resulting products was carried out according to standard methodologies. Additional analyses included NMR spectroscopy, HPLC and FTIR-ATR.

Results and discussion

In the oil epoxidation process, Fig. 1, organic acids, ZIFs, and immobilized lipase were successfully tested as catalysts. Among them, biocatalytic epoxidation provided the most promising results, achieving high conversion while minimizing the safety risks typically associated with high-pressure systems. Under optimized conditions (molar ratio H_2O_2:double bonds:peracid agent = 1:1:0.5, with 1.5 wt.% biocatalyst), sunflower WCO was selectively epoxidized with approximately 90% conversion at a low temperature (30 °C) and within a relatively short reaction time (12 h). The acid value of the sample was 4 mg $KOH \cdot g^{-1}$.

Octanoic acid was identified as the most effective peracid agent, offering both enhanced safety and superior substrate compatibility for the enzyme compared to shorter-chain organic acids. The applicability of the developed system to five different oil samples demonstrated its versatility; however, the best results were obtained with WCO, likely due to the higher concentration of oxidized species formed during the deep-frying process.

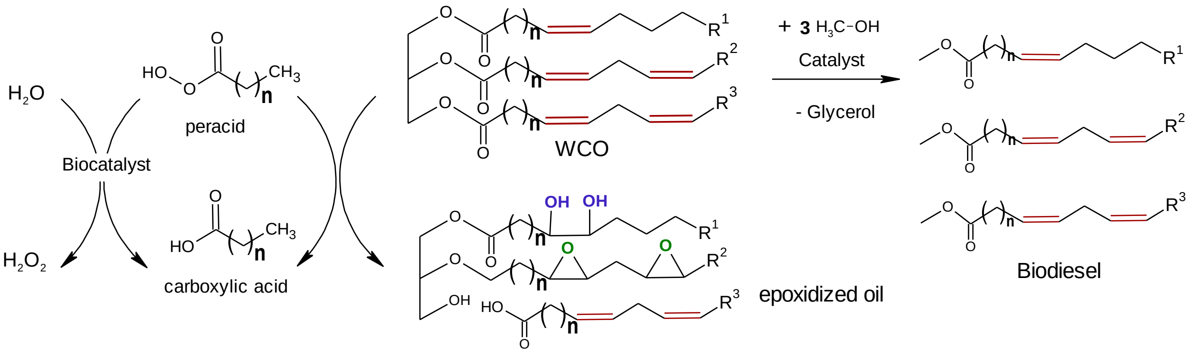

Fig. 1. Strategies for VOs and WCO valorisation.

In contrast to epoxidation, the use of biocatalysts in biodiesel synthesis yielded poor results. Experiments conducted with various commercial catalysts at 70 °C for 6 h showed that CaO achieved the highest conversion (98%) for both VOs and WCO. However, the resulting biodiesel exhibited elevated acidity and significant levels of leached metal, which do not comply with current biodiesel quality standards. Therefore, a catalytic pre-treatment step is necessary to esterify free fatty acids, especially in the case of WCO, along with additional washing steps to partially remove residual calcium. In this context, the synthesized ZIF-based catalysts offer a promising alternative. These catalysts enabled near-complete oil conversion regardless of the metal ratio used. Although they required longer reaction times (20-24 h), the ZIFs resulted in reduced soap formation, minimal metal leaching, and lower acidity in the final biodiesel.

Conclusions

This study highlights the potential of vegetable oils and waste cooking oil as renewable feedstocks for both epoxidized oil and biodiesel production. Biocatalytic epoxidation proved highly efficiency under mild conditions, while ZIF-based catalysts emerged as promising alternatives for biodiesel synthesis, offering improved product quality.

Acknowledgements

The Romanian Ministry Research and Digitalization is acknowledged for funding within the grant PNRR-III-C9-2022-I5-18, *ResPonSE* - Project, No. 760010/2022.

References

[1] G. Bhukya, S.S. Kaki, Vegetable Oil Seeds as Biomass Resource for Potential Applications in Biofuel and Biomaterials, in: S. Kumar, S. Sundaramurthy, D. Kumar, A.K. Chandel (Eds.), Springer Nature Singapore, Singapore (2024), pp. 79-99.

[2] I. Podolean, M. Tudorache, Materials 17 (2024) 4518.

[3] G. Karmakar, P. Ghosh, K. Kohli, B.K. Sharma, S.Z. Erhan, Innovative Uses of Agricultural Products and Byproducts, Chapter 1 (2020) 1-31.

Biocatalytic Transformation of α-Halo-Ketones by Human Carbonic Anhydrase II for the Enantioselective Synthesis of Alcohols and Epoxides

Diana M. Scrob*, Csaba Paizs
[1]*Enzymology and Applied Biocatalysis Center, Faculty of Chemistry and Chemical Engineering, Babeș-Bolyai University, Cluj-Napoca, Romania*
**Corresponding author: diana.scrob@ubbcluj.ro*

Introduction

Enantiopure halohydrins and epoxides are highly valuable in the pharmaceutical and natural product industries due to their significant reactivity, which enables the synthesis of a wide range of compounds. Enantiopure halohydrins serve as versatile intermediates in the production of various bioactive molecules, including natural products, agrochemicals, and pharmaceuticals [1]. The importance of chiral α-halohydrins lies in their wide applicability as chiral intermediates, for instance, α-halohydrins can be transformed into their corresponding chiral epoxides.

Enantiopure halohydrins can be easily obtained through the catalytic asymmetric reduction of α-halo-ketones using human carbonic anhydrase II (hCAII) as a biocatalyst and silanes as hydride source. Recently, human carbonic anhydrase II (hCAII) has been shown to display excellent catalytic activity and enantioselectivity in the asymmetric reduction of ketones using silanes as reducing agents. Additional benefits, such as a wide substrate range, mild reaction conditions, and the elimination of the need for cofactor regeneration, position hCAII as a promising enzyme for applications in the synthesis of chiral alcohols [2].

Experimental

In this study, we present a novel sequential biotransformation reaction of α-halo-ketones when the hCAII catalyzed enantiotop selective reduction is followed with the enzyme catalyzed *in situ* ring closure of the halohydrins, leading to the formation of the corresponding epoxides. The substrate scope of hCAII and the optimal reaction conditions were investigated as a prerequisite for the preparative scale production of both reaction products, Fig. 1.

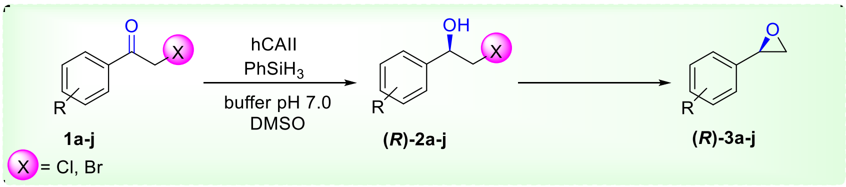

	a	b	c	d	e	f	g	h	i	j
R	H	2-Cl	3-Cl	4-Cl	2-Br	3-Br	4-Br	3-OMe	4-OMe	4-CN

Fig. 1. Enzymatic reduction of α-halo-ketones (**1a-j**) to enantiopure halohydrines **(*R*)-2a-j** followed by ring closure **(*R*)-3a-j**.

Results and discussion

Regarding the enantiomeric excess of the epoxide, values exceeding 99% were obtained in all experiments. However, significant variations were observed in the enantiomeric excess of the (*R*)-halohydrin with values exceeding 90% for those derived from the substrates 2-bromo-1-phenylethan-1-one, 2-chloro-1-phenylethan-1-one, and 2-bromo-1-

(3-methoxyphenyl)ethan-1-one. Various buffers were also tested, with 50 mM and 100 mM HEPES at pH 8 proving to be the most suitable. A significant influence of temperature was observed on both the reaction rate and the ratio of the two products formed in the reaction mixture. Lowering the temperature disfavored epoxide formation, while increasing the temperature had the opposite effect, promoting efficient epoxide ring closure. The optimal temperature range for this process was found to be between 20 and 45 °C. The substrate concentration was also varied to investigate the catalytic performance of the enzyme, ranging from 10 mM to 200 mM.

Conclusions

An innovative sequential biotransformation protocol was developed using hCA II, aimed at the synthesis of enantiopure epoxides and alcohols with high synthetic value. Optimal reaction conditions were investigated as essential steps toward the preparative-scale production of both reaction products. Remarkable enantiomeric excesses were obtained for all epoxides, using variable substrate concentrations ranging from 10 to 200 mM. For the determination of conversion and enantiomeric excess, high-performance liquid chromatography (normal-phase HPLC) methods were developed, employing various chiral columns to achieve effective separation.

Acknowledgements

This work was supported by the project “Advanced (multi)-enzymatic synthesis and purification processes for bio-based furan derivatives – ASPIRE” funded by European Union – NextGenerationEU and the Romanian Government, under National Recovery and Resilience Plan for Romania, contract no 760042/23.05.2023, cod PNRR-C9-I8-CF25/14.11.2022, through the Romanian Ministry of Research, Innovation and Digitalization, within Component 9, Investment I8”.

References

[1] F. Xue, C. Li, Q. Xu, Appl. Microbiol. Biotechnol. 105 (2021) 3411.
[2] P. Ji, J. Park, Y. Gu, D.S. Clark, J.F. Hartwig, Nature Chem. 13 (2021) 312.

Sustainable Biocatalysis for the Synthesis of Functional Puerarin esters Using Immobilized Lipase from *Candida antarctica* B

Liga Sergio, Cristina Paul, Francisc Péter*
Department of Applied Chemistry and Engineering of Organic and Natural Compounds, Faculty of Chemical Engineering, Biotechnologies and Environmental Protection, Politehnica University Timisoara, Vasile Pârvan No. 6, 300223 Timisoara, Romania
**Corresponding author: francisc.peter@upt.ro*

Introduction

Puerarin is a naturally occurring O-glycoside isoflavone recognized for its wide range of therapeutic properties, including antioxidant, anti-inflammatory, neuroprotective, and cardioprotective effects [1]. However, its industrial application is significantly hindered by low bioavailability, primarily due to poor solubility in both aqueous and lipid environments, as well as limited stability. To address these limitations, enzymatic esterification was employed as a strategy to enhance its physicochemical characteristics [2,3]. In this study, Puerarin was esterified with natural acids-hexanoic acid and octanoic acid-using a lipase-catalyzed reaction (lipase from *Candida antarctica* B). The enzymatic synthesis conditions were optimized, and the resulting Puerarin esters were analyzed using high-performance liquid chromatography (HPLC), with DAD detection performed at 260 nm. The high conversion efficiencies achieved underscore the potential of this method for improving the solubility and stability of Puerarin, thereby paving the way for further pharmaceutical and functional investigations.

Experimental

A variety of experiments have explored the synthesis of flavonoid esters using different active donors, including both aromatic and aliphatic natural acids. Among these, natural acids have been particularly valuable due to their ability to enhance lipid solubility (lipophilicity). In this study, hexanoic (caproic) acid and octanoic (caprylic) acid were employed as natural acyl donors, with octanoic acid showing the highest reactivity toward Puerarin. To favor esterification over hydrolysis, an excess of the acyl donor was necessary.

Consequently, the impact of varying molar ratios of Puerarin to carboxylic acid (1:3, 1:25, and 1:50) was examined. Reactions were catalyzed by immobilized lipase from *Candida antarctica* B (GenoFocus, Republik of Korea) at 50 °C, under agitation at 1000 rpm for 120 minutes. The conversion values of Puerarin were calculated by HPLC analysis of samples taken at different reaction times.

Results and discussion

In the initial stage of this experimental study, the influence of the molar ratio between Puerarin and hexanoic acid on esterification efficiency was evaluated. An appreciable increase in conversion was observed, rising from 49.2% to 70.5% as the molar ratio increased from 1:3 to 1:25, based on values obtained after 2 h of reaction. However, further increasing the ratio to 1:50 resulted in a slight decrease in conversion efficiency. These results suggest that a molar ratio of 1:25 represents the optimal condition for the esterification of Puerarin with hexanoic acid, with a corresponding reaction time of 2 h.

Similarly, when octanoic acid was employed as the acyl donor, a marked improvement in conversion was noted. The conversion increased significantly from 20.2% to 68% as the molar ratio was raised to 1:50 under identical reaction conditions. Accordingly, the optimal molar ratio for the esterification of Puerarin with octanoic acid was determined to be 1:50, with a reaction time of 2 h.

Conclusions

Based on the experimental investigation of the enzymatic esterification of Puerarin with natural fatty acids *i)* tetrahydrofuran (THF) was confirmed to provide the highest solubility for Puerarin and was therefore selected as the optimal reaction solvent; *ii)* the enzymatic biocatalysis of Puerarin with natural acids demonstrated high efficiency, achieving conversion rates exceeding 70% within a 2 h reaction period; *iii)* the products were successfully identified using high-performance HPLC, the chromatograms indicating the formation of a single esterification product under the selected conditions; *iv)* high excess of carboxylic acid is needed, as the optimal molar ratios for maximum conversion of Puerarin were 1:25 for the reaction with hexanoic acid and 1:50 for the reaction with octanoic acid.

References

[1] S. Liga, C. Paul, Int. J. Mol. Sci. 25 (2024) 5222.
[2] L. Mo, G. Zhao, X. Li, X. Xiao, N. He, H. Xu, Y. Yu, J. Drug Deliv. Sci. Technol. 67 (2022) 102882.
[3] S. Lee, H. Shin, J. Bae, T. Lee, M. Kim, H.B. Jeon, K.H. Lee, H.Y. Yoo, C. Park, Int. J. Mol. Sci. 25 (2024) 709.

Sustainable Synthesis of Enantiopure Chiral Alcohol Mediated by the *R*-Selective Alcohol Dehydrogenase from *Lactobacillus kefir*

Aishwarya Singh[1,*], Anca Elena Anghel[1], Soud-Diana Tork[1], Monica Ioana Toşa[1], Csaba Paizs[1], László Poppe[1,2]
[1]*Enzymology and Applied Biocatalysis Center, University of Babes-Bolyai, Faculty of Chemistry and Chemical Engineering, Romania*
[2]*Budapest University of Technology and Economics, Hungary*
**Corresponding author:* *aishwarya.singh@ubbcluj.ro*

Introduction

Alcohol dehydrogenases (ADH), also known as carbonyl reductases or ketoreductases (CREDs/KREDs), are efficient and selective enzymes to synthesize chiral alcohols [1]. The enzyme-catalyzed reaction generally uses NADH or NADPH as a cofactor. These enzymes are significant because they play a crucial role in the preparation of bio-active compounds through various metabolic pathways [2].

Experimental

The glycerol stock of ADH from *Lactobacillus kefir* was used as inoculum to prepare the pre-culture with carbenicillin resistance, and then inoculated with 1% v/v to overexpress the cells in secondary culture with 0.2 mM IPTG induction. The overexpressed cells were harvested and lysed, the protein was purified through Ni-NTA affinity chromatography using a 250 mM imidazole solution in potassium phosphate buffer at pH 6 elution. The enzyme concentration was estimated using the Bradford assay, and the specific activity of *Lk*ADH was determined by monitoring the depletion of cofactor after 10 minutes at 340 nm in an Epoch 2 Biotek microplate reader. Furthermore, a set of enzyme-catalysed reactions was performed on acetophenone as model substrate using various concentrations of isopropanol to investigate the production of chiral alcohol. The reaction mixtures were analysed through HPLC using an NX C-18 column and ACN - H_2O (30:70, v/v) as mobile phase at 20 °C and a flow rate of 1 $\mathrm{mL \cdot min^{-1}}$, monitoring the reaction mixture at 210 nm (both, the synthesised product and the untransformed substrate)

Results and discussion

The presence of *Lk*ADH in the eluted fractions was confirmed using SDS-PAGE. All fractions display a band corresponding to a molecular weight between 25-35 kDa, while the molecular weight of the *N*-terminal, 10×His-tagged *Lk*ADH is approximately 31 kDa. The specific activity of *Lk*ADH was 0.464 $\mathrm{\mu mole \cdot mg^{-1} \cdot min^{-1}}$, but according to the literature, it could be higher in the presence of the NADH, the enzyme's preferred cofactor.

Conclusions

The enzyme prefers salt buffers in the 6-7 pH range and is able to transform in 2-4 h the acetophenone into the corresponding *R*-ethanol with 80-90% conversion at 30 °C.

Acknowledgements

This work was supported by the project "Renewable Enzyme Immobilization - RENZI" funded by European Union – NextGeneration EU and the Romanian Government, under National Recovery and Resilience Plan for Romania, contract no 760241/28.12.2023, cod PNRR-C9-I8-CF87/31.07.2023, through the Romanian Ministry of Research, Innovation and Digitalization, within Component 9, Investment I8"

References

1. A. Rudzka, B. Zdun, N. Antos, et al., Commun. Chem. 6 (2023) 217 .
2. J.W. Hilborn, Z.-H. Lu, A.R. Jurgens, Q.K. Fang, P. Byers, S.A. Wald, et al. Tetrahedron Lett. 42 (2001) 8919.

Platinum@Styrene-Divinylbenzene Heterogenous Catalyst in the Hydrosilylation Reactions

Alexandru-Constantin Stoica, Madalin Damoc, Mihaela Dascalu, Maria Cazacu
Department of Inorganic Polymers, "Petru Poni" Institute of Macromolecular Chemistry, Iasi, Romania
**Corresponding author: stoica.alexandru@icmpp.ro*

Introduction

Platinum-based catalysts play a major role in a variety of technological areas, including electrochemical energy conversion such as water electrolysis or fuel cells [1]. However, hydrosilylation is by far their widely known application. Hydrosilylation, consisting of Si-H addition to multiple covalent bonds, is a highly applicative reaction, both at the laboratory level and at the industrial scale, in production of silicone polymers and other related structures [2,3]. Nevertheless, most of the studies and applications related to this reaction use homogeneous systems, which make the catalyst separation/recovery from the reaction mixture/product very challenging [3]. A new approach is introduced here to generate heterogeneous Pt catalysts by immobilizing the precursor H_2PtCl_6 on macroporous styrene-divinylbenzene copolymer (SDVB) support with subsequent reduction of Pt(IV) to Pt(0) with a hydrophobic, permethylated agent, 1,1,3,3-tetramethyldisiloxane (TMDS). The catalytic performance of the obtained Pt/SDVB system was preliminarily evaluated in the hydrosilylation reactions of 1,3-bis(vinyl)tetramethyldisiloxane (DVTMDS) with TMDS.

Experimental

Platinum heterogenization, SDVB-Pt

Over 3 g of microporous SDVB copolymer, 10 ml of 2.07% H_2PtCl_6 solution in isopropanol (i-PrOH) were added. The mixture was kept in a closed system for 24 h at room temperature, after which the system was opened and the solvent was slowly evaporated, resulting in the SDVB-Pt sample. After complete evaporation of the solvent, the SDVB-Pt was dried in vacuum at 40 °C for 6 h. The product was investigated by SEM and EDX and the degree of platinum loading was determined by atomic absorption spectrometry (AAS) analysis.

Platinum reduction and hydrophobization, SDVB-Ptx (x=1a, 1b, 2, 3)

Four variants of SDVB-based platinum catalysts were prepared. For this, SDVB-Pt microspheres (1 g) were further treated as follows:

a) with a solution of TMDS (0.2 mL in 5 mL i-PrOH) and subsequently the mixture was left to stand for 2 h; in this process, platinum was reduced, the spheres were filtered and washed with i-PrOH, dried in vacuum at 40 °C for 6 h (**SDVB-Pt1a**).

b) similar to the SDVB-Pt1a variant, except that 10 μL MTMS was added, and the filtered spheres were not washed with solvent, thus ensuring an oligomeric layer on the surface (**SDVB-Pt1b**).

c) with 5 mL of a solution in i-PrOH consisting of 0.2 mL TMDS, 0.5 g PDMHS, 10 μL MTMS and a drop of DBTDL; the resulting mixture was kept at room temperature for 3 hours, then filtered, and the spheres were dried under vacuum at 40 °C for 6 h (**SDVB-Pt2**).

d) 0.2 mL of TMDS and 10 μL of methyltrimethoxysilane, MTMS in 3 mL of THF, immediately filtered and treated with a solution of polydimethylmethylvinylsiloxane, PDMVS (0.5 g of THF in 3 mL); the system was closed and left at RT overnight, the next day the spheres were filtered and dried at RT (**SDVB-Pt3**).

The samples thus obtained were visualized by SEM, and analyzed by XPS to highlight the reduction of platinum, and DVS to evaluate the hydrophobicity.

Hydrosilylation reactions, HVS=Ptx (x=1a, 1b, 2, 3)

SDVB-Ptx samples (x=1a, 1b, 2, 3) were tested in the hydrosilylation reaction of divinyltetramethyldisiloxane (DVTMDS) with TMDS in a molar ratio of 1.00:1.05, carried out in toluene solution at 65 °C in normal atmosphere. Amounts of SDVB-Ptx were used to ensure platinum concentrations according to the values in Fig. 1a and the kinetics of the reactions were monitored by IR spectroscopy. Upon completion of the reaction, the catalyst was separated by filtration and was suitable for reuse.

Results and discussion

The hydrosilylation reactions of DVTMDS with TMDS with the four catalysts (HVS-Ptx reactions) were monitored by IR spectroscopy, following the changes in the intensities of the absorption bands at 2135 cm^{-1} corresponding to the Si–H bond in relation to that of the Si–CH_3 bond at 1261 cm^{-1}, selected as a reference. The time-varying curves of the Si–H conversion values calculated for HVS-Ptx (x = 1a, 1b, 2, 3) are shown in Fig. 1b.

a)

Catalyst	μgPt·mmol^{-1} TMDS	t(min) for 50% SiH conversion	Conv.$_{max}$ (%)
HVS-Pt1a	0.0251	16.0	100
HVS-Pt1b	0.0147	3.12	99.74
HVS-Pt2	0.0140	73.32	88.86
HVS-Pt3	0.261	45.24	86.7

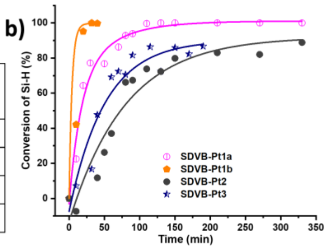

Fig. 1. (a) The Pt catalyst amounts in μg Pt/mmol TMDS used and conversion values estimated by IR study; (b) Ehe evolution of conversion in time.

Other model reactions, namely the hydrosilylation of allylic alcohol with TMDS, as well as the hydrosilylation of 1-hexene with triethoxysilane of great industrial interest mainly for obtaining coupling agents [4], have also been previously addressed [5].

Conclusions

By reducing platinum deposited on SDVB support with TMDS, when simultaneously with the reduction of platinum it is also hydrophobized in a single step, suitable catalysts for conducting the hydrosilylation reaction in a heterogeneous system can be obtained. This allows the obtaining of catalyst-free compounds.

Acknowledgements

This work was financially supported by a grant from the Ministry of Research, Innovation and Digitization, project no. PNRR-III-C9-2023-I8-99 within the National Recovery and Resilience Plan.

References

[1] F. Li, J.-B. Baek, Nature Catalysis 2 (2019) 477.
[2] P.B. Kettler, Org. Process. Res. Dev. 7 (2003) 342.
[3] W. Agata, M. Hieronim, F. Ryszard, Apple Academic Press (2015)
[4] S. Shi, et al., Chem. Asian J. 12 (2017) 2404.
[5] A.-C. Stoica et al., Appl. Organomet. Chem. 36 (2022) e6485.

Sustainable Glyceric Acid Production *via* Immobilized Laccase Biocatalysis

Andreea Petrovici, Ioan Bîtcan, Francisc Péter, Anamaria Todea*
University Politehnica Timisoara, Faculty of Industrial Chemistry and Environmental Engineering, 300001, C. Telbisz 6, 300001 Timisoara, Romania
**Corresponding author: anamaria.todea@upt.ro*

Introduction

The surplus of glycerol from biodiesel production has sparked interest in converting it into valuable chemicals like glyceric acid, used in food, medicine, and cosmetics [1]. While traditional chemical oxidation is effective, it lacks selectivity and is costly. Biocatalytic methods using laccases offer a greener alternative but struggle with enzyme stability and reuse [2]. This study investigates glycerol oxidation using four commercial laccases—especially Trametes versicolor and Aspergillus sp.—and introduces Ni-Zn ferrite as a novel immobilisation support, improving enzyme performance, reusability, and glyceric acid yield.

Experimental

The screening involved four native laccases combined with five mediators, focusing on glycerol oxidation efficiency. The two top-performing enzymes (*T. versicolor* and *Aspergillus sp.*) were covalently immobilized onto six functionalized supports: three magnetic (Fe_3O_4, Ni-Zn, and Ni-Zn-Co ferrites) and three polymethacrylate-based Lifetech™ resins with amino and epoxy functional groups. Immobilization was carried out via glutaraldehyde-mediated crosslinking, followed by $NaBH_4$ reduction to stabilize Schiff bases. Enzymatic activity was assessed using 2,6-dimethylphenol assays, while glycerol oxidation was monitored by HPLC over 96 h under optimized pH and temperature conditions. Comprehensive characterizations, including XPS and SEM, validated enzyme attachment and assessed stability.

Results and discussion

Trametes versicolor laccase immobilized on Ni-Zn ferrite particles (MG-Zn2) and on epoxy-butyl polymethacrylate resin demonstrated superior catalytic performance, retaining high activity across a broad pH and temperature range (optimal at pH 6.5 and 50 °C). Covalent immobilization enhanced reusability, with the magnetic biocatalyst retaining ~80% activity after five cycles post-$NaBH_4$ treatment. The glycerol oxidation yield reached 50% conversion to glyceric acid within 72-96 h — substantially outperforming previous reports (typically below 10% for covalent immobilization). SEM and XPS confirmed stable enzyme layers (~3-4 nm) post-reaction cycles without morphological degradation. Comparative tests revealed that the epoxy-butyl spacer group significantly improved operational stability relative to other resin supports.

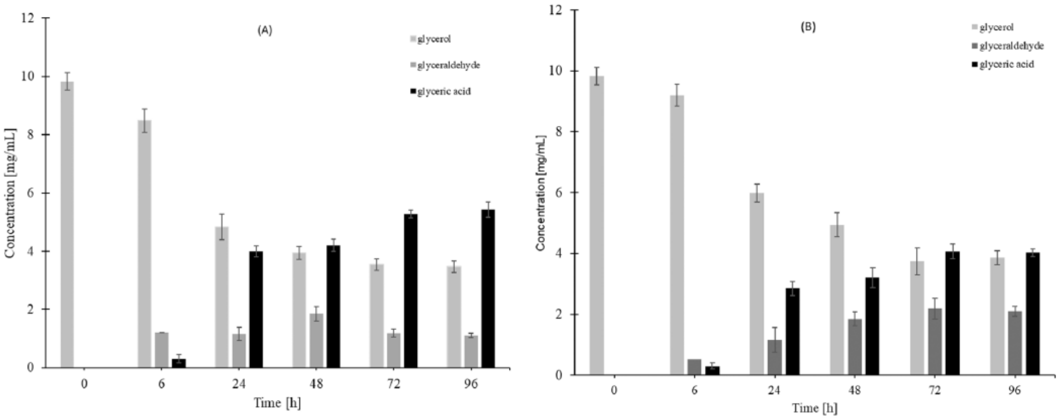

Fig. 1. Concentration values of glycerol, glyceraldehyde and glyceric acid over time in the presence of immobilized *T. versicolor* laccase on (A) Ni-Zn ferrite magnetic support (TvL@MG-Zn2) and (B) on methacrylic resin functionalized with epoxy butyl groups (RS EPX-Butil), at 50 °C, using 20 mg·mL^{-1} immobilized enzyme.

Conclusions

This study presents a robust biocatalytic system for glycerol valorization using immobilized laccases. The innovative use of Ni-Zn ferrite supports combined with covalent immobilization strategies yielded biocatalysts with excellent stability, reusability, and conversion efficiency. The approach addresses longstanding challenges in laccase applications, making it a promising pathway for sustainable glyceric acid production. Further optimization and scale-up studies are encouraged, especially to integrate this system within biorefinery frameworks.

Acknowledgements

This work was supported by a grant of the Romanian Ministry of Education and Research, CNCS – UEFISCDI, project number PN-III-P1-1.1-TE-2019-1573, within PNCDI III, contract number TE 101. Additional financial support was provided by the project “Network of excellence in applied research and innovation for doctoral and post-doctoral programs / InoHubDoc” (POCU/993/6/13/153437) and by project PN-III-P4-ID-PCE-2020-2177, contract number PCE 157/2021. The authors also acknowledge Dr. Simona Șerban from Purolite Ltd. for the generous donation of functionalized polymethacrylate resin supports.

References

[1] N.M. Kosamia, M. Samavi, B.K. Uprety, S.K. Rakshit, Catalysts 10(609) (2020) 1,
[2] Z. Shokri, F. Seidi, S. Karami, C. Li, M.R. Saeb, H. Xiao, Carbohydr. Polym. 262 (2021) 117963.

Optimizing Furfural Condensation: A Factorial Approach with Polymer-Bound DMAP

Souad-Diana Tork, Anca Anghel, Monica Ioana Toşa, László Csaba Bencze
Enzymology and Applied Biocatalysis Research Center, Faculty of Chemistry and Chemical Engineering Babeş-Bolyai University, RO-400028 Cluj-Napoca, Arany János 11, Romania
**Corresponding author: souad.tork@ubbcluj.ro*

Introduction

Furfural, a versatile and renewable platform chemical derived from lignocellulosic biomass, holds significant potential as a starting material for the synthesis of various bio-based compounds [1,2]. While chemoenzymatic strategies have been extensively explored for furfural valorization, its application in the synthesis of non-proteinogenic amino acids remains a relatively underexplored area. Specifically, the efficient chemical condensation of furfural to generate key intermediates like furylacrylic acid is a crucial step in such routes [3,4]. To address this, our study focuses on optimizing the Knoevenagel-Doebner condensation of furfural using a readily separable and reusable polymer-bound 4-dimethylaminopyridine (DMAP) catalyst to synthesize 3-(2-furyl)acrylic acid, a direct precursor for the enzymatic synthesis of enantiomerically enriched l-3-(2-furyl)alanine. This work highlights the critical optimization of the chemical condensation step through a systematic factorial design approach, aiming to enhance the efficiency and sustainability of this key transformation within a preparative-scale chemoenzymatic pathway.

Experimental

The chemical synthesis of 3-(2-furyl)acrylic acid was performed via Knoevenagel-Doebner condensation of furfural with malonic acid in DMSO. A fractional 2^3 factorial design was employed to optimize the reaction conditions, investigating the impact of three key factors: reaction temperature, equivalents of polymer-bound DMAP catalyst, and reaction time. The progress of the reaction and final conversion to 3-(2-furyl)acrylic acid were monitored and quantified using HPLC. The effects of the individual factors and their interactions on the reaction conversion were statistically analyzed using Minitab software, employing a first-order model with interaction terms and a significance level of $p<0.05$. The subsequent enzymatic hydroamination step [5,6], utilizing phenylalanine ammonia lyase from *Arabidopsis thaliana* (*At*PAL) expressed in *E. coli* cells, was performed in a one-pot procedure with optimized conditions (30 °C, 200 mM furylacrylic acid, 3 M ammonium carbamate). The chemoenzymatic procedure was successfully scaled up to gram-level synthesis starting from 500 mg.

Results and discussion

The factorial design analysis revealed that reaction time, and the interaction effects of temperature × time and time × DMAP equivalents, were the most significant factors ($p\leq0.05$) influencing the Knoevenagel-Doebner condensation of furfural. The regression analysis indicated a positive correlation between DMAP catalyst concentration and conversion, with a maximum analytical-scale conversion of 82.05% achieved after 24 h at a low temperature (60 °C) and a high DMAP equivalent (0.1%). Further optimization in a second factorial experiment led to a slight increase in conversion to 86.55% under slightly modified conditions (60 °C, 0.12 equivalents of polymer-bound DMAP). Notably, the optimized chemical step (1 eq. furfural, 0.98 eq. malonic acid, 0.2 eq. polymer-bound DMAP, 70 °C, DMSO) achieved a high conversion of 98% at the preparative scale (starting from 0.5 g furfural) after 24 h. This chemically synthesized furylacrylic acid was successfully coupled in a one-pot procedure with the enzymatic hydroamination by *At*PAL, yielding l-3-(2-furyl)alanine with a 98% conversion in the enzymatic step, Fig. 1. The targeted amino acid was subsequently isolated via ion-exchange chromatography.

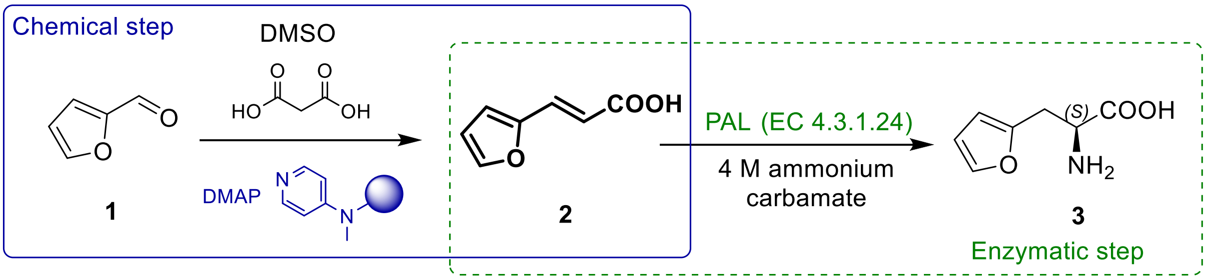

Fig. 1. The chemoenzymatic one-pot synthesis of enantiomerically enriched L-3-(2-furyl)alanine.

Conclusions

Based on our systematic optimization of the Knoevenagel-Doebner condensation using a readily recoverable polymer-bound DMAP catalyst, we have established an efficient chemical route for the synthesis of 3-(2-furyl)acrylic acid. Furthermore, the successful one-pot coupling of this intermediate with enzymatic hydroamination by *At*PAL yielded enantiomerically enriched l-3-(2-furyl)alanine. These findings underscore the potential of integrating optimized chemical catalysis with biocatalysis for the sustainable production of non-proteinogenic amino acids from renewable resources like furfural.

Acknowledgements

This work was supported by the project “Advanced (multi)-enzymatic synthesis and purification processes for bio-based furan derivatives – ASPIRE” funded by European Union – NextGenerationEU and the Romanian Government, under National Recovery and Resilience Plan for Romania, contract no 760042/23.05.2023, cod PNRR-C9-I8-CF25/14.11.2022, through the Romanian Ministry of Research, Innovation and Digitalization, within Component 9, Investment I8”.

References

[1] K.J. Yong, T.Y. Wu, C.B.T.L. Lee, Z.J. Lee, Q. Liu, J.M. Jahim, Q. Zhou, L. Zhang, Biomass Bioenergy 161 (2022) 106458.
[2] Y.M. Huang, G.H. Lu, M.H. Zong, W.J. Cui, N. Li, Green Chem. 23 (2021) 8604.
[3] G.H. Lu, M.H. Zong, N. Li, ACS Catal. 13 (2023) 1371.
[4] R. Cang, L.-Q. Shen, G. Yang, Z.-D. Zhang, H. Huang, Z.-G. Zhang, Catalysts 9 (2019) 526.
[5] J. Rétey, C. Paizs, M. Tosa, L.C. Bencze, J. Brem, F.D. Irimie, Heterocycles 82 (2010) 1217.
[6] S.T. Ahmed, F. Parmeggiani, N.J. Weise, S.L. Flitsch, N.J. Turner, ACS Catal. 8 (2018) 3129.

Biocatalytic Alternative of Lignin Valorization Based on the Carboxymethylation Process

Sabina Ion, Vasile I. Parvulescu, Madalina Tudorache*
Department of Organic Chemistry, Biochemistry and Catalysis, University of Bucharest, Soseaua Panduri 90, sector 5, 050663 Bucharest, Romania
**Corresponding author: madalina.sandulescu@g.unibuc.ro*

Lignin is a complex heterogeneous 3D polymer of the biomass. So that, lignin can be an alternative raw material with enormous potential to replace fossil-based resources for the sustainable production of many chemicals and materials. It is one of the most abundant natural bio-polymers with strong intra/inter-molecular hydrogen interactions, conserved/modified during the pulping process leading to variation of the lignin properties. For tailing lignin properties such as composition/ functional groups, key enzymes can be used for developing biocatalytic processes leading to new polymers with predictable properties [1].

In this study, we investigated biocatalytic routes for the addition (grafting) of functional groups in the lignin. A proposed alternative is to graft the lignin with dimethyl carbonate (DMC). The process is assisted by lipase enzyme as biocatalyst. In this way new polymeric structure is achieved with properties (e.g. conductivity, acidity/basicity, thermostability) [2,3].

The derivatization alternative was evaluated during the enzyme (lipase) screening step. The derivatized lignins (CML) were characterized in order to identify the modifications of the chemical structure and the direct effect on the lignin properties. Thus, the carboximethylation process was demonstrated based on the ^{13}C-NMR analysis. The results supported the success of lignin carboxymethylation, where carbonate carbonyl carbons were detected at 154 ppm. The FTIR spectra collected before and after the carboxymethylation process evidenced as well the lignin modification. Additionally, CML product was characterized using conductivity measurements, gel permeation chromatographic analysis (GPC), thermogravimetric analysis (TGA), temperature-programmed desorption (TPD-NH_3/CO_2), scanning electron microscopy (SEM), and nuclear magnetic resonance (NMR) analyses. All these characterizations provided clearly evidences of the lignin modeling properties as direct effect of the biocatalytic modification of lignin structure.

So that, new biocatalytic strategy of lignin derivatization has been developed for carboxymethyl of lignin. The derivatized lignin afforded suitable characteristics for industrial applications, such as ion-exchange resins, cationic surfactants, flocculants, coagulants, heavy metal adsorbents or support for protein immobilization [4].

Acknowledgements

This work was financially supported by UB project, contract no. 143.

References

[1] R. Weiss, G.M. Guebitz, A. Pellis, G.S. Nyanhongo, Trends Biotechnol. 38(11) (2020) 1215.
[2] S. Ion, C. Opris, B. Cojocaru, M. Tudorache, I. Zgura, A. Galca, A. Bodescu, M. Enache, G. Maria, V.I. Parvulescu, Front. Chem. 6 (2018) 124.
[3] S. Ion, T. Brudiu, A. Hanganu, F. Munteanu, M. Enache, G.M. Maria, M. Tudorache, V. Parvulescu, Molecules 25(21) (2020) 4921.
[4] C. Lite, S. Ion, M. Tudorache, I. Zgura, A.C. Galca, M. Enache, G.M. Maria, V.I. Parvulescu, Catal. Today 379 (2021) 222.

Industry

High resolution gas and vapor sorption systems for catalyst analysis

Valentin Cânpean*, Mircea Armenean
SC Nanoteam SRL, Cluj-Napoca, Romania
**Corresponding author: valentin_canpean@nanoteam.ro*

The importance of catalysts stretches over a wide range of applications, ranging from automotives to biological systems, and much more. Thus, understanding catalysts is of utmost importance for future applications. However, understanding catalysts is highly dependent on the accuracy and reproducibility of experimental instruments we use. High-quality instruments must provide accuracy to detect catalysts behavior, sensitivity to detect minor variations in the sorption or reaction rates, while ensuring the reproducibility of the results under the same conditions.

Hidden Isochema is a world leader in the design and manufacture of sorption instruments for research, development and production applications in materials science and related fields. It offers a range of fully automated gravimetric and manometric instruments, with high sensitivity, accuracy and reproducibility, for determining the equilibria and kinetics of gas and vapor sorption by solid and liquid materials, making them ideal for catalyst characterization, material science, and adsorption studies. Hidden Isochema also offers dynamic vapor sorption (DVS) analyzers and breakthrough analyzers to study real-time sorption behavior and catalytic performance. Fig. 1 outlines the product overview of Hidden Isochema.

Fig. 1. Hidden Isochema product overview.

Fig. 2 shows the kinetics of hydrogen absorption by Pd, at 303K and 40 mbar during a period of 60 h, measured using the XEMIS sorption analyzer. The orange trace represents the same system, but with no sample loaded, showing minimal weight change over the experiment duration, demonstrating the high balance stability, representing a highly stable baseline reading above which kinetic processes can be accurately characterized.

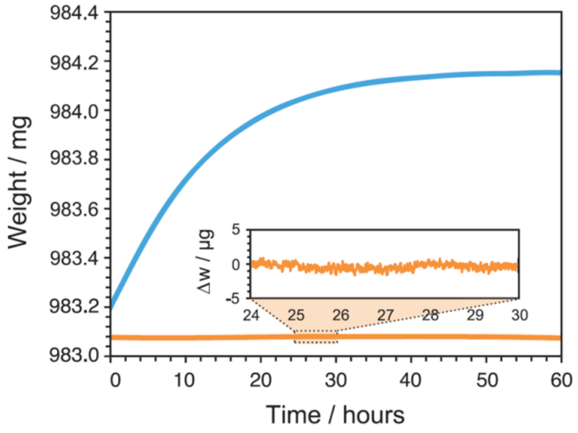

Fig. 2. H_2 absorption by Pd [1].

Fig. 3a shows CH_4 adsorption isotherms on alum shale, at five temperatures points in the range 298-358 K. Due to the extremely low uptake, shale poses great difficulties for running measurements and getting accurate results. However, the XEMIS sorption analyzer accurately measured the sorption processes, demonstrating its ability to perform high accuracy measurements in the μmol/g range, even for samples exhibiting extremely low uptakes.

Fig. 3b shows SO_2 adsorption-desorption isotherms on a MOF (Metal–Organic Framework), NOTT-300 [2,3], at five temperature points in the range 298-348 K. The isotherms exhibit excellent reversibility, demonstrating both the excellent long-term stability of the XEMIS microbalance and its compatibility with corrosive species.

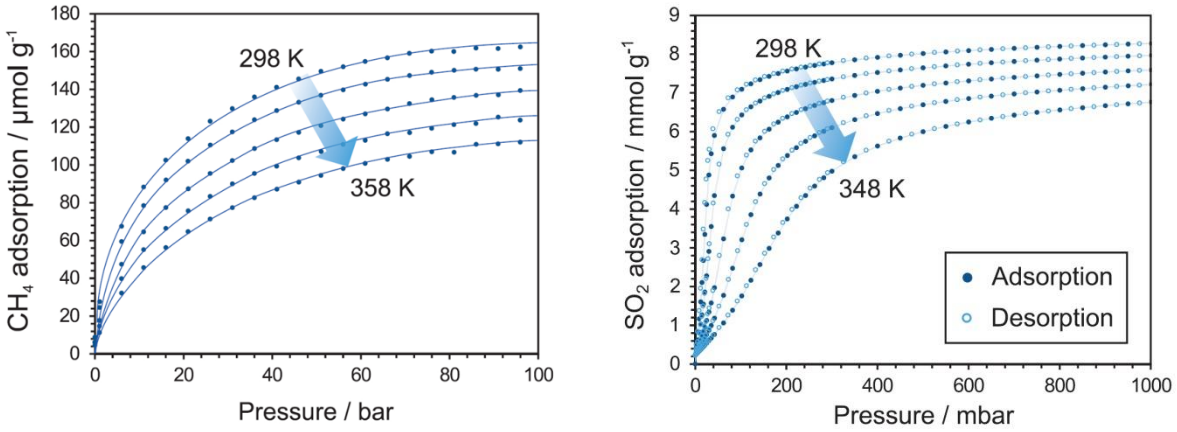

Fig. 3. a) CH_4 adsorption on alum shale; b) SO_2 sorption isotherms on NOTT-300 [1,2].

References

[1] https://hidenisochema.com/content/uploads/2017/01/Hiden-Isochema-XEMIS-Brochure.pdf
[2] https://hidenisochema.com/content/uploads/2016/04/Hiden-Isochema-Application-Note-130.pdf
[3] S. Yang, J. Sun, A.J. Ramirez-Cuesta, S.K. Callear, W.I.F. David, D.P. Anderson, R. Newby, A.J. Blake, J.E. Parker, C.C. Tang, M. Schröder, Nat. Chem. 4 (2012) 887.

Catalytic processes – useful analytical techniques and instruments

G. Birda*
SC Muso SRL, Bucharest, Romania
**Corresponding author: office@muso.ro*

Alfabetical Index of Authors